# nano bio & med 2022

nov. 22-24, barcelona (Spain)

www.nanobiomedconf.com

# abstracts book

## Organisers

IBEC Institute for Bioengineering of Catalonia — Excelencia Severo Ochoa

Phantoms foundation

ICN2 Institut Català de Nanociència i Nanotecnologia — Excelencia Severo Ochoa

NANOMED SPAIN

BOKU Universität für Bodenkultur Wien
University of Natural Resources and Applied Life Sciences, Vienna


Share your conference pics and stories
#nanobiomedconf

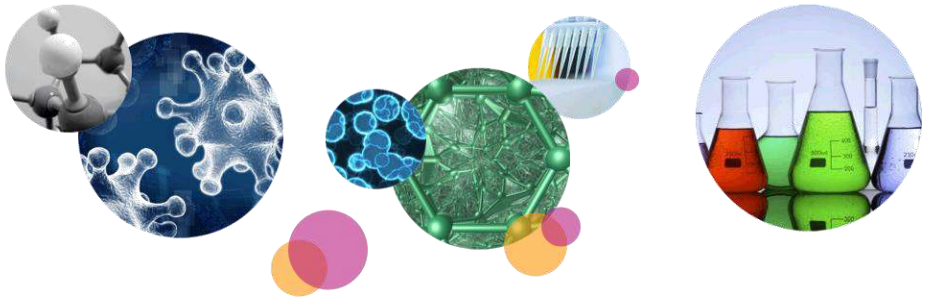

# Index



On behalf of the Organising Committee, we take great pleasure in welcoming you to Barcelona (Spain) for the nanoBio&Med2022 International Conference after 2 years break due to COVID.

This event, after successful editions organised within ImagineNano in Bilbao 2011 & 2013, and in Barcelona in 2014, 2015, 2016, 2017, 2018 & 2019, is going to present again in-person the most recent international developments in the field of Nanobiotechnology and Nanomedicine and will provide a platform for multidisciplinary communication, new cooperations and projects to participants from both science and industry. Emerging and future trends of the converging fields of Nanotechnology, Biotechnology and Medicine will be discussed among industry, academia, governmental and non-governmental institutions.

nanoBio&Med2022 will be the perfect place to get a complete overview into the state of the art in those fields and also to learn about the research carried out and the latest results. The discussion in recent advances, difficulties and breakthroughs will be at his higher level.


We are indebted to the following Companies and Scientific Institutions for their support: Institute for Bioengineering of Catalonia (IBEC), NanomedSpain and American Elements.

In addition, thanks must be given to the staff of all the organising institutions whose hard work has helped planning this conference.


NanobioMed2022 Organising Committee

# Organising committee

- Antonio CORREIA

  President of the Phantoms Foundation (Spain)

- Arben MERKOÇI

  ICN2 / ICREA (Spain)

- Dietmar PUM

  Deputy Head of the Biophysics Institute – BOKU (Austria)

- Josep SAMITIER

  Director of the Institute for Bioengineering of Catalonia – IBEC
  Coordinator of the Spanish Nanomedicine Platform - NanomedSpain (Spain)

# Sponsors

# Supported by

# General info

**Free Wifi:**
PCBGuest network
Username: nanobiomed-guest
Password: 3J4KfeXD

**Cocktail Lunch:**
Offered by nanoBioMed2022 Organisers
Tuesday November 22 (13:00)

**Conference Dinner:**
Restaurant CAN CORTADA
Tuesday November 22 (21:00)


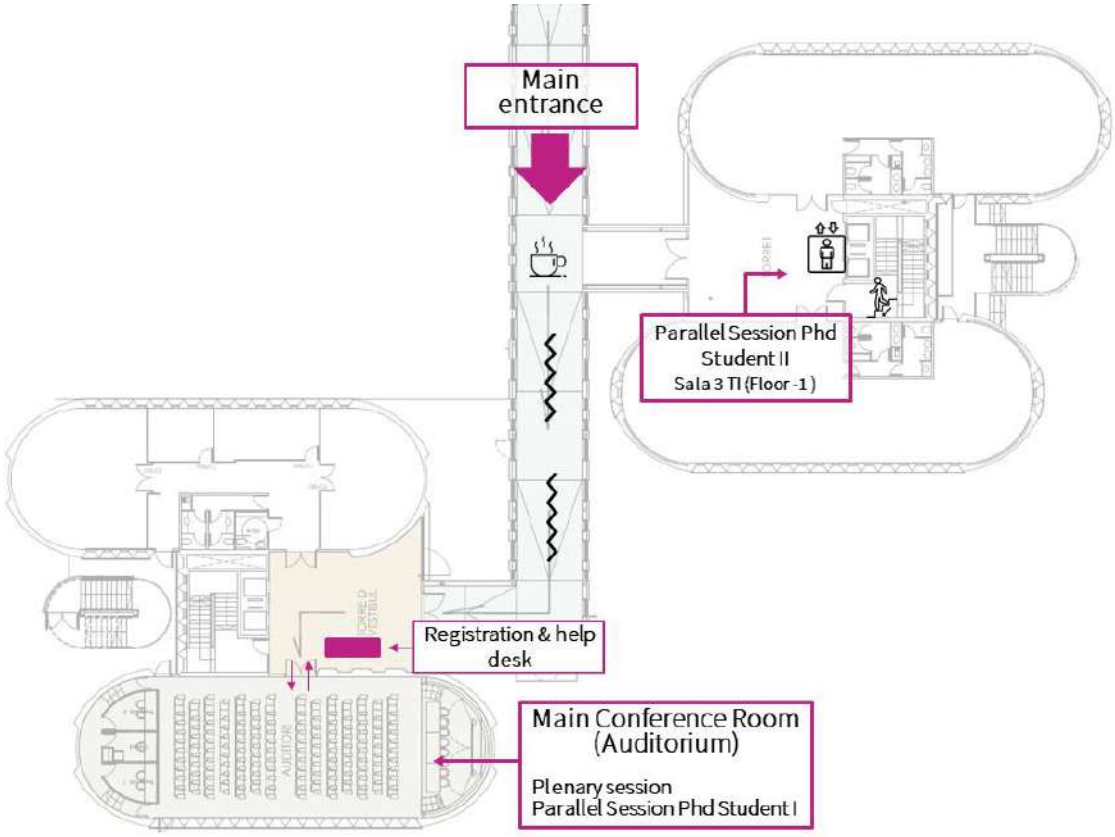

# Programme

## Tuesday November 22, 2022

| | | |
|---|---|---|
| 08:45 | | Opening Ceremony |
| 09:00 | | Nanobots going in vivo |
| *Keynote* | | Samuel Sanchez (IBEC, Spain) |
| 09:30 | | Bioengineering enzyme-powered nanobots: towards programmable design and functionality |
| *Keynote* | | Tania Patiño Padial (Eindhoven University of Technology, The Netherlands) |
| 10:00 | | Light-Triggered Vapor Nanobubbles and Nanomotors for Drug Delivery Applications |
| *Invited* | | Juan Fraire (IBEC, Spain) |
| 10:20 | | Coffee Break & Poster Session |
| 11:00 | | Biomedical applications of sperm-hybrid micromotors |
| *Keynote* | | Mariana Medina Sánchez (IFW Dresden, Germany) |
| 11:30 | | Using Nature's engineering principles to design biointerfaces and synthetic cells for nanomedicine |
| *Keynote* | | César Rodriguez-Emmenegger (IBEC, Spain) |
| 12:00 | | Evaluating the collective dispersion of magnetic-enzymatic nanomotors |
| *Oral* | | Anna Bakenecker (Institute for Bioengineering of Catalonia (IBEC), Spain) |
| 12:15 | | Poster Session |
| 13:00 | | Cocktail Lunch & Poster Session |
| 14:00 | | Title to be defined |
| *Keynote* | | Kostas Kostarelos (The University of Manchester, UK) |
| 14:30 | | Monolayer Graphene on polymer as a material for combining therapy and diagnostic in-vivo: from basic science to medical applications |
| *Keynote* | | Vincent Bouchiat (Grapheal, France) |
| 15:00 | | How to Transform a Novel 2D Nanomaterial in 'Medical Grade' |
| *Invited* | | Neus Lozano (ICN2, Spain) |
| 15:20 | | The phenotypic association theory and its application in nanomedicine design |
| *Keynote* | | Giuseppe Battaglia (IBEC, Spain) |
| 15:50 | | A new Paradigm to identify brain targeting peptides |
| *Oral* | | Daniel Gonzalez Carter (IBEC, Spain) |
| 16:05 | | Advancing a new nanomedicine for Fabry disease treatment towards clinical translation |
| *Oral* | | Elisabet González Mira (Institute of Materials Science of Barcelona, CSIC, Spain) |
| 16:20 | | Antibiofilm and antibacterial activity of Ag-intercalated $Tm^{3+}/Er^{3+}$ co-doped layered perovskites and their exfoliated 2D nanosheets |
| *Oral* | | Zeynep Firtina Karagonlar (Izmir University of Economics, Turkey) |
| 16:35 | | Hydrogen-Bonding and Long-Range Interactions Involved in the Initial Attachment of Biofilm-Dispersed Escherichia coli and Bacillus subtilis |
| *Oral* | | F. Pinar Gordesli Duatepe (Izmir University of Economics, Turkey) |
| 16:50 | | Coffee Break & Poster Session |
| 17:20 | | Molecular Electronics with DNA towards DNA Detection |
| *Keynote* | | Danny Porath (The Hebrew University of Jerusalem, Israel) |
| 17:50 | | Engineering a model cell with DNA nanotechnology |
| *Keynote* | | Kerstin Göpfrich (Max Planck Institute for Medical Research, Germany) |
| 18:20 | | Nano-omics: nanotechnology-enabled harvesting of blood-circulating biomarkers |
| *Invited* | | Marilena Hadjidemetriou (University of Manchester, UK) |
| 18:40 | | Detection of short nucleotides with DNA nanopores |
| *Oral* | | Juan Elezgaray (CRPP, CNRS UMR 5130, France) |

21:00 Conference Dinner - Restaurant CAN CORTADA, Barcelona – Spain
5 minutes walking distance from the underground stop "Valldaura" (green line nº03)

# Wednesday November 23, 2022

09:00 Genetic code expansion in biosensing and tissue engineering
*Keynote* **Lital Alfonta** (Ben-Gurion University, Israel)

09:30 Nanoengineered Surfaces for modulating cellular responses and sensing applications
*Invited* **Akash Bachhuka** (University Rovira i Virgili, Spain)

09:50 Nanobiosensor devices for environmental quality assessment as containment systems
*Oral* **Alejandro Hernández-Albors** (ITENE, Spain)

10:05 $MoS_2$ Defect Healing for High-Performance Sensing of Polycyclic Aromatic Hydrocarbons and Mercury Ions
*Oral* **Sara Gullace** (Université de Strasbourg- ISIS, France)

10:20 Coffee Break & Poster Session

## Parallel Session Phd Student I
Topics: Bio-Inspired nanotechnologies, Bioelectronics, Drug Delivery, Integrated Systems / Sensors

11:00 Porated liposomes: towards new nanomotors model
*Oral* **Bárbara Borges Fernandes** (Institute for Bioengineering of Catalonia (IBEC), Spain)

11:10 Novel piezoelectronic microdevice for electrical cell stimulation
*Oral* **Marc Navarro Pons** (Institute of Microelectronics of Barcelona (IMB-CNM, CSIC), Spain)

11:20 Different size microdevices with nanostructured ZnO integrated for electrical cell stimulation
*Oral* **Laura Lefaix Fernández** (Microelectronics Institute of Barcelona (IMB-CNM, CSIC), Spain)

11:30 Design of targeted PLGA-$SO_3$ Nanoparticles encapsulating PARP and PD-L1 Inhibitors for BRCA-mutated breast cancer therapy
*Oral* **Daniel Rodríguez Ajamil** (Tel Aviv University, Israel)

11:40 Inhaled amorphous drug nano- particle formulations of BTZ043 to improve tuberculosis treatment
*Oral* **Feng Li** (University of Vienna, Austria)

11:50 4D-printed multifunctional microcarriers for passive and active cargo delivery
*Oral* **Fatemeh Rajabasadi** (IFW dresden, Germany)

12:00 Towards a universal biosensing platform based on graphene/pyrene surfaces for neurotransmitters
*Oral* **Marta Delga Fernandez** (Catalan Institute of Nanoscience and Nanotechnology, Spain)

12:10 Tailoring carriers for specific applications by unveiling the role of individual components in pBAE/polynucleotide polyplexes: on road to rational formulations
*Oral* **María Navalón** (Quimic de Sarrià (IQS), Universitat Ramon Llull (URL), Spain)

12:20 A low cost, versatile and portable impedimetric biosensor for SARS-CoV-2 detection
*Oral* **Soroush Laleh** (IFW dresden, Germany)

## Parallel Session Phd Student II
Topics: Nanobioanalysis in vitro, NanoBioSensors, Nanomaterials for Bio & Medical Applications, NanoMaterials for Medicine

11:00 Bioactivity of PDGF-BB-loaded NLCs after sterilization with gamma or beta radiation
*Oral* **Jorge Ordoyo** (University of the Basque Country (UPV/EHU), Spain)

11:10 Upgrading nanobiosensing platforms: comparison between different inkjet printed biosensors for detection of Neutrophil Gelatinase Associated Lipocalin-2 (NGAL)
*Oral* **Massimo Urban (**Catalan Institute of Nanoscience and Nanotechnology (ICN2), Spain)

11:20 Nanobiosensing of Small Molecules: Challenges and Prospects for Molecular Imprinting
*Oral* **José Marrugo-Ramírez** (ICN2, Spain)

11:30 Challenges of printing on Mussel-Inspired free-standing films as Artificial biosensing Skin
*Oral* **Gabriel Maroli** (Catalan Institute of Nanoscience and Nanotechnology (ICN2), Spain)

11:40 Aptamer displacement Lateral Flow assay for Phenylketonuria monitoring
*Oral* **Celia Fuentes Chust** (Institut Català de Nanociència i Nanotecnologia, Spain)

11:50 Protein-stabilized nanomaterials as novel MRI contrast agents
*Oral* **Gabriela Guedes** (CIC biomaGUNE, Spain)

12:00 Encapsulation of magnetic nanocubes in core shell polymeric nanoparticles for their application in hyperthermia
*Oral* **Ivana Cavaliere** (Catalan Institute of Nanoscience and Nanotechnology (ICN2), Spain)

12:10 Biomimetic Nanoparticles for Cancer Target Immunotherapy
*Oral* **Clara Baldari** (Universita´ del Salento, Italy)

12:20 Anticancer properties of selenium nanoparticles encapsulated by oncolytic virus capsids
*Oral* **Cláudio Ferro** (University of Lisbon, Portugal)

| | Plenary |
|---|---|
| 12:30 | Effect of $CeO_2$ NPs of varying $Ce^{3+}$ and $Ce^{4+}$ content on Chlamydomonas reinhardtii under high light stress |
| *Oral* | **Shabnam Nisha** (Palacký University, Czech Republic) |
| 12:45 | NanoQSAR models on the toxicity of quantum dots |
| *Oral* | **Salvador Moncho Escriva** (ProtoQSAR , Spain) |
| 13:00 | In Vitro Cytotoxicity of Upconverting Tm/Er Co-Doped Layered Perovskite and their Nanosheets |
| *Oral* | **Özge Sağlam** (İzmir University of Economics, Turkey) |
| 13:15 | Guefoams: A new concept of filter media for water bacterial removal |
| *Oral* | **Lucila Maiorano** (University of Alicante, Spain) |
| 13:30 | Lunch |
| 14:45 | Tamm resonances in nanoporous anodic alumina photonic structures for sensing applications |
| *Keynote* | **Lluis F. Marsal** (Universitat Rovira i Virgili, Spain) |
| 15:15 | Layered carbon-stabilised porous silicon nanostructures to build electrochemical sensors |
| *Keynote* | **Beatriz Prieto-Simon** (ICREA/URV, Spain) |
| 15:45 | Inkjet printing of nanobiosensors: limits, challenges, and opportunities |
| *Invited* | **Giulio Rosati** (ICN2, Spain) |
| 16:05 | Gold nanoshells with silica-coated magnetic cores for multimodal imaging and sensing |
| *Oral* | **Ondrej Kaman** (FZU - Institute of Physics of the Czech Academy of Sciences, Czech Republic) |
| 16:20 | Controlling cell signaling using magnetic nanoparticles and alternating magnetic fields |
| *Keynote* | **Dekel Rosenfeld** (Tel Aviv University, Israel |
| 16:50 | Coffee Break & Poster Session |
| 17:30 | Opportunities and Challenges of Graphene Neurotechnology in Neuroscience and Medical Applications |
| *Keynote* | **Jose Antonio Garrido** (ICREA/ICN2, Spain) |
| 18:00 | AI-Guided Optical Sensors for The Early Detection of Gynecologic Cancers |
| *Keynote* | **Zvi Yaari** (The Hebrew University of Jerusalem, Israel) |
| 18:30 | 3D sensing platform for single cell extracellular pH mapping in time and space: a pre-clinical model to |
| *Oral* | study tumor microenvironment and drug screening |
| | **Loretta del Mercato** (Institute of Nanotechnology (CNR-Nanotec), Italy) |
| 18:45 | Innovative 3D microfluidic brain tumor-on-a-chip systems: design, characterization, and preliminary |
| *Invited* | testing with chemotherapy drug-loaded nanocarriers |
| | **Attilio Marino** (IIT, Italy) |
| 19:05 | Safe and efficient modular nanovectors for gene/drug delivery in precision medicine |
| *Oral* | **Ilaria Elena Palamà** (CNR-Institute of Nanotechnology, Italy) |

## Thursday November 24, 2022

| | | |
|---|---|---|
| 09:00 | Plasma Engineered Nanomaterials for Bio & Medical Applications | |
| *Invited* | **Behnam Akhavan** (University of Newcastle, Australia) | |
| 09:20 | Radical-based Nanoparticles with Advanced Optical Properties for Biological Applications | |
| *Invited* | **Inma Ratera** (ICMAB, Spain) | |
| 09:40 | Novel nanostructured materials accelerating osteogenesis | |
| *Oral* | **Margarita Apostolova** (Roumen Tsanev Institute of Molecular Biology - BAS, Bulgaria) | |
| 09:55 | Return of the Jedi: Fighting Antimicrobial Resistance with Nanobiotics | |
| *Oral* | **Iris Batalha** (Institute for Bioengineering of Catalonia (IBEC), Spain) | |
| 10:10 | Coffee Break & Poster Session | |
| 10:45 | Novel application of lipid nanoemulsions in breast cancer | |
| *Oral* | **Ana Belen Davila Ibañez** (Joint Unit Roche-Chus, Spain) | |
| 11:00 | MRI tumour detection using metal-free radical dendrimers as contrast agents | |
| *Oral* | **Vega Lloveras Monserrat** (ICMAB CISC: Institut de Ciencia de Materials de Barcelona, Spain) | |
| 11:15 | Spatial mapping of biophysical properties in human cells and tissues by scanning probe microscopy (SPM) | |
| *Oral* | **Annalisa Calo** (IBEC-UB, Spain) | |
| 11:30 | Boron clusters-based systems for molecular imaging and BNCT | |
| *Oral* | **Rosario Núñez** (Instituto de Ciencia de Materiales, Spain) | |
| 11:45 | PERsistent Luminescence (PERL) nanoparticles for small animal in vivo bioapplications | |
| *Keynote* | **Aurelie Bessiere** (University of Montpellier, France) | |
| 12:15 | Nanocasting template synthesis of porous persistent luminescent nanoparticles for PDT | |
| *Oral* | **Mathilde Menard** (ICGM, France) | |
| 12:30 | Structure-Function Guided Fabrication of Biodegradable RNA-Binding Polymers | |
| *Keynote* | **Moran Frenkel-Pinter** (The Hebrew University of Jerusalem, Israel) | |
| 13:00 | Piezoelectric membranes to enhance skin regeneration | |
| *Oral* | **Andreu Blanquer Jerez** (Universitat Autònoma de Barcelona, Spain) | |
| 13:15 | Intranasal Administration of Novel Nanocarriers for Glioblastoma treatment | |
| *Keynote* | **Daniel Ruiz-Molina** (ICN2-CSIC, Spain) | |
| 13:45 | Concluding remarks | |

SCAN THE QR TO ACCESS THE LATEST UPDATED PROGRAMME

www.nanobiomedconf.com/FILES/NanoBioMed2022_program.pdf

# Speakers/Orals/Posters list

## Authors

## Authors

## Authors

# Genetic code expansion in biosensing and tissue engineering

**Lital Alfonta**
Itay Algov, Liron Amir, Eden Ozer, Yonatan Chemla, Orr Schlesinger, Mor Pasi, Aviv Feiretag,

Ben-Gurion University of the Negev, POBOX653, Beer-Sheva 8410501, Israel

alfontal@bgu.ac.il

Abstract

Genetic code expansion is a robust technology that enables the site-specific modification of proteins theoretically at will, with more than 300 unnatural amino acids. This ability enables the modification of proteins with biorthogonal chemical handles (Nobel Award in Chemistry (2022) was awarded for the development of Biorthogonal Chemistry), biophysical probes, and redox-active amino acids that do not exist in nature as amino acids, among other possibilities. In the past several years we have expanded the genetic code of several microorganisms: *Synechococcus sp. Cyanobacteria, [1] Pseudomonas aeruginosa,[2] Vibrio natriegens, [3] and Chlamydomonas reinhardtii*. Thus, we now have a set of molecular tools that allow us to modify proteins in these microorganisms in addition to doing so in *E. coli*. In those different microorganisms, proteins and enzymes were modified with unnatural amino acids to tether them site-specifically to electrodes to allow direct electron transfer between the enzyme active site and an electrode. [4-8] Enzymes were both oxidative enzymes where the electrons flow to the electrode as well as reducing enzymes where electrons were effectively injected to the enzyme active site. In addition, we use this technology to express novel peptides with incorporated unnatural amino acids that give these peptides novel chemistries, these peptides can serve as scaffolds and adhesive materials in tissue engineering applications. Uses and characterization of these enzymes and peptides will be discussed.

## References

[1] Yonatan Chemla, Mor Friedman, Mathias Heltberg, Anna Bakhrat, Elad Nagar, Rakefet Schwarz, Mogens Høgh Jensen, Lital Alfonta, *Biochemistry*, 56 (2017) 2161

[2] Eden Ozer, Karin Yaniv, Einat Chetrit, Anastasya Boyarski, Michael M. Meijler, Ronen Berkovich, Ariel Kushmaro, Lital Alfonta, *Science Advances,* 7 (2021) eabg8581.

[3] Eden Ozer**,** Lital Alfonta, *Front. Bioeng. Biotechnol.* 9 (2021) 594429

[4] Liron Amir, Stewart A. Carnally, Josep Rayo, Shaked Rosenne, Sarit Melamed Yerushalmi, Orr Schlesinger, Michael M. Meijler, Lital Alfonta, *J. Am. Chem. Soc.* 135 (2013) 135, 70

[5] Orr Schlesinger, Mor Pasi, Rambabu Dandela, Michael M. Meijler, Lital Alfonta, *Phys. Chem. Chem. Phys.* 20 (2018) 6159

[6] Itay Algov, Aviv Feiretag, Lital Alfonta, *Biosens. Bioelectron.* 180 (2021), 113117

[7] Itay Algov, Aviv Feiertag, Rafi Shikler, Lital Alfonta, *Biosens. Bioelectron.* 210 (2022) 114264

[8] Itay Algov, Lital Alfonta, *ACS measurement Science Au*, 2, (2022) 78

## Figures

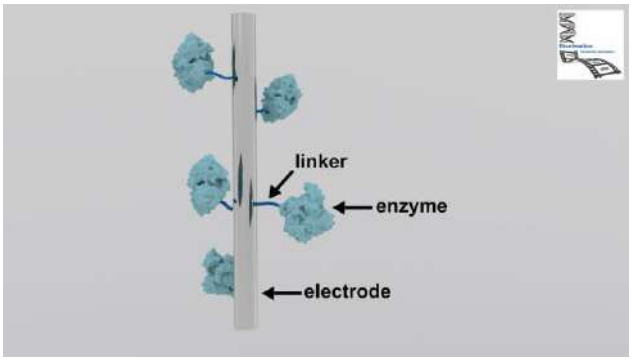


**Figure 1.** Site-specific wiring and orientation of enzymes to electrodes

# The phenotypic association theory and its application in nanomedicine design

**Giuseppe Battaglia**[1,2],

[1]Catalan Institution for Research and Advanced Studies (ICREA), Barcelona, Spain
[2]Institute for Bioengineering of Catalonia - Barcelona Institute of Science and Technology, Barcelona Spain
gbattaglia@ibecbarcelona.eu (Arial 9)

The central dogma in biological interactions and its application to drug design states that the higher the drug or ligand affinity (i.e. the most negative binding energy) to its cognate receptor, the higher its ability to target cells or tissues expressing the same receptor. However, such a maximal selectivity at the single molecules imposes that high-affinity ligands target indiscriminately any cells expressing the given receptor. The chemical nature of biological units extends beyond single molecules. As biomolecules combine into single cells, the number of configurations increases so much that we can confidently say that each cell of our body is different from the other. We may not need to dissect the complexity of the single cell down to the quantum level to create more selective drugs. Still, we need to upgrade our molecular design to include more holistic effects to distinguish biological targets more precisely. In the last decade, we have assessed biological targets' internal state energetic configurations matching them with complementary multivalent units to favour selective associations based on multiple bonds. We have borrowed statistical and soft matter physics tools to address this challenge.

We know from the super-selectivity theory (SST) [2] that multivalent units interact via the collective effect of the single affinities (or avidity) and association changes with receptors or ligand numbers, not linearly, giving rise to entropy-driven interactions. This unique nature means that if we combine low-affinity ligands, we can have association only when receptors are high in numbers, effectively targeting cells that overexpress the desired receptor. We have proven SST experimentally [3-5] and demonstrated that the overall interaction combines the specific ligand/receptor bonds with mean-field repulsive potential arising from steric effects. Borrowing similar nomenclature used in quantum physics to handle the multidimensional nature of the problem, I here define the different states that characterise a cell phenotype and the multivalent unit to target using a vector of features, one that defines the cell phenotype as $|\varphi_j\rangle$ representing the specific cell receptors compositions and is the mean-field steric potentials. We can define a multivalent unit vector of features is defined as $\langle\nu_j|$ and state that two are complementary if

$$\langle\nu_i|\boldsymbol{\Theta}|\varphi_j\rangle = \delta_{ij} = \begin{cases} 1, & \text{if } i \equiv j \\ 0, & \text{if } i \not\equiv j \end{cases} \quad (1)$$

The *ith* multivalent unit, the *jth* cell phenotypes are complementary via the hierarchical operator $\boldsymbol{\Theta}$ defined in **fig.1**. Using such a formalism, I will show that we can adapt molecular engineering tools to design highly selective drugs.

## Figures

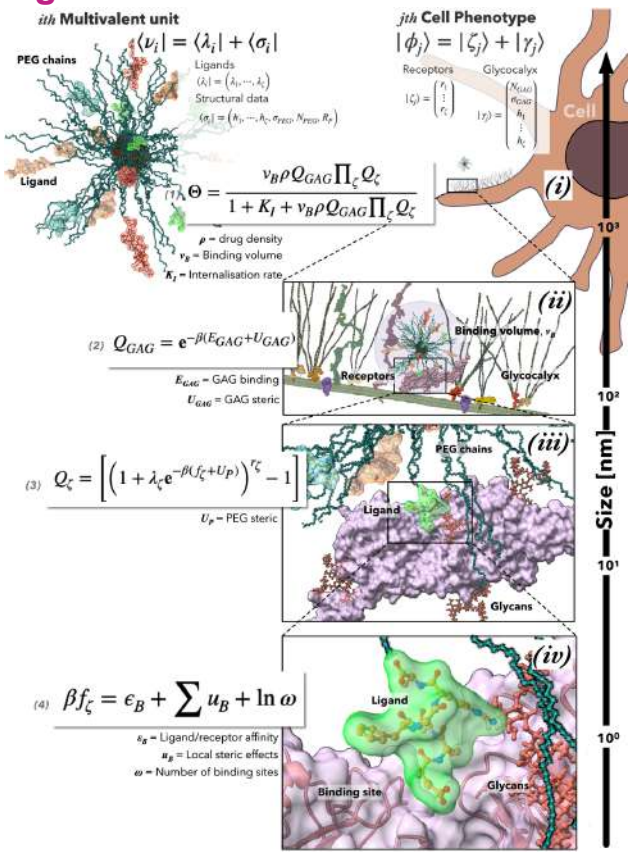


**Figure 1.** Schematics of the interaction between a given jth cell characterised by a unique phenotype and its complementary multivalent unit9)

## References

[1] P. Ehrlich, F. Himmelweit, and M. Marquardt, *The collected papers of Paul Ehrlich*. 1957, London: Pergamon Press.

[2] F.J. Martinez-Veracoechea and D. Frenkel, 'Designing super selectivity in multivalent nano-particle binding'. *PNAS*, **108**, 10963 (2011)

[3] X. Tian, S. Angioletti-Uberti, and G. Battaglia, 'On the design of precision nanomedicines'. *Sci. Adv.*, 2020. **6**, eaat0919.

[4] M. Liu, A. Apriceno, A., M. Sipin, E. Scarpa, L. Rodriguez-Arco, A. Poma, G. Marchello, G. Battaglia and S. Angioletti-Uberti 'Combinatorial entropy behaviour leads to range selective binding in ligand-receptor interactions. *Nat Commun.* **11**, 4836 (2021)

[5] S. Acosta-Gutiérrez, D. Matias, M. Avila-Olias, V. M. Gouveia, E. Scarpa, J. Forth, C. Contini, A. Duro-Castano, L. Rizzello, and G. Battaglia 'A Multiscale Study of Phosphorylcholine Driven Cellular Phenotypic Targeting' *ACS Cent. Sci.* 8, 7, 891–904 (2022)

# PERsistent Luminescence (PERL) nanoparticles for small animal *in vivo* bioapplications

**A. Bessière**[1], D. Gourier,[2] B. Viana,[2] K.R. Priolkar,[3] S.K. Sharma,[2] N. Basavaraju,[3] A.J.J Bos,[4] P. Dorenbos,[4] T. Maldiney,[5] C. Richard,[5] D. Scherman,[5] J.-O. Durand[1]

[1] ICGM, Univ. Montpellier,CNRS, ENSCM,France
[2] IRCP, Chimie ParisTech, CNRS, Paris, France
[3] Department of Physics, Goa Univ., India
[4] UTCPBS, CNRS, Univ. Paris Descartes, Paris, France
[5] Faculty of Applied Sciences, Delft Univ. of Technology, The Netherlands

Aurelie.bessiere@umontpellier.fr

Chemists have a wide toolbox to prepare inorganic luminescent nanoparticles that can serve as highly efficient non-bleaching optical probes. However, the weak penetration of light across the living tissues appears as a major hindrance to the use of such luminescent nanoparticles *in vivo*. First, the luminescent nanoparticles cannot be excited in the UV or visible range across the tissues and, second, their photoluminescence signal is then hidden by the tissues autofluorescence yielding a poor signal/noise ratio. Outside the UV-visible range, X-rays penetrate the tissues and *radioluminescent* nanoparticles represent an option to convert X-rays into visible/infrared light. However, their use is limited by the maximum tolerable dose. Alternatively, some infrared radiation falls into the tissues transparency windows. *Up-converting* nanoparticles, that convert 980 nm laser light into UV-visible therefore seem attractive, but they require intense laser power that causes detrimental heating to living animals. PERsistent Luminescence (PERL) nanoparticles, i.e. optical batteries, represent an exciting third option.

A PERL material is an inorganic crystalline host doped with a luminescent ion and a point defect has been introduced in a controlled manner. When illuminated by an external radiation (X-ray, UV, visible) the excitation energy is stored in the material in the form of electrons/holes trapped at point defects ("charging"). Once excitation is stopped, the ambient temperature (or the temperature of the animal body) triggers the progressive release of trapped electrons/holes, which then continuously feeds the luminescent center and yields a slowly decaying luminescence (minutes/hours).

In 2011, we pioneered $ZnGa_2O_4$:Cr (ZGO) as a near-infrared-emitting PERL material suitable for *in vivo* small animal imaging [1]. Thanks to several spectroscopies (optical, EPR, EXAFS/XANES) we elucidated the PERL mechanism of ZGO, i.e. a localized charge trapping process at antisite defects of the spinel host matrix around $Cr^{3+}$ ions [2] [3]. This special feature confers ZGO the unique capacity of being charged not only by UV radiation but also with orange-red light. Hence, prepared by suited hydrothermal routes, 40-60 nm large ZGO nanoparticles are highly performant for small animal *in vivo* tumor imaging [4]. As the excitation is delayed relative to the emission, the technique avoids the excitation of the animal tissues and suppresses autofluorescence, yielding an excellent signal/noise ratio for optical imaging. Further, as the ZGO nanoparticles can be re-charged *in vivo* by orange/red light, the PERL signal is followed over days.

In the last decade, ZGO-based PERL nanoparticles have boomed as bioprobes in the field of small animal *in vivo* imaging and have been conveniently coupled to therapeutic agents to become outstanding theranostic nano-platforms. Notably, ZGO nanoparticles have been associated to photosensitizers (for ex. phtalocyanines) to serve as internal light sources to realize photodynamic therapy (PDT) in deep-seated tumors [5].

## References

[1] Bessiere, A. et al. ZnGa2O4:Cr3+: a new red long-lasting phosphor with high brightness. *Opt. Express* 19, 10131-10137 (2011).

[2] A. Bessiere, S. K. Sharma, N. Basavaraju, K. R. Priolkar, L. Binet, B. Viana, A. J. J. Bos, T. Maldiney, C. Richard,D. Scherman and D. Gourier, Chem. Mater., 2014, 26,1365–1373.

[3] D. Gourier, A. Bessiere, S. K. Sharma, L. Binet, B. Viana, N. Basavaraju and K. R. Priolkar, J. Phys. Chem. Solids, 2014, 75, 826–837.

[4] T. Maldiney, A. Bessiere, J. Seguin, E. Teston, S. K. Sharma, B. Viana, A. J. J. Bos, P. Dorenbos, M. Bessodes, D. Gourier, D. Scherman and C. Richard, Nat. Mater., 2014, 13, 418–426

[5] A. Bessière, J.O. Durand, C. Noûs, Persistent luminescence materials for deep photodynamic therapy, Nanophotonics 10 (2021) 2999–3029

## Figures

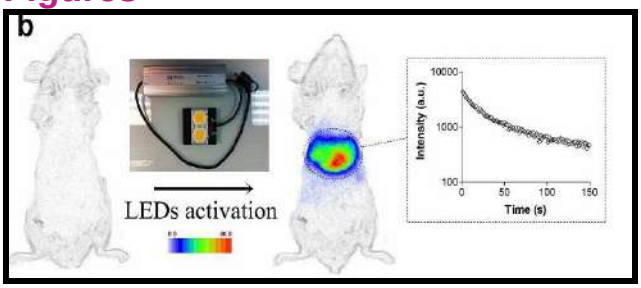


**Figure 1.** The detection of ZGO PERL nanoparticles after in vivo activation. Nanoparticles were first excited by UV and intravenously injected to monitor short-time biodistribution. After complete extinction of the PERL signal (in this case 15 h after the initial excitation), PERL was activated through living tissues following a 2 min orange/red LED excitation, and immediately acquired for 3 min under the photon counting system. The inset shows a persistent luminescence decay curve corresponding to the signal from the liver.

# Monolayer Graphene on polymer as a material for combining therapy and diagnostic in-vivo: from basic science to medical applications

**Vincent BOUCHIAT** [1,2]

[1]Grapheal SAS, 38042 Grenoble, France
[2]On leave from Institut Néel, CNRS-Grenoble, France.

info@grapheal.fr

After a more than a decade and tens of thousands of publications, graphene produced by chemical vapour deposition on copper foils still remain at the sweet spot regarding cost, speed and quality for large scale production of monolayers on insulators. I will briefly recall the principle of these technique and then present the use of this technology for biological (1) and medical applications from both the academic and industrial point of view. In particular, I will be insisting on the possibility to combine therapeutics (biostimulation, such as stimulated wound healing) and diagnostics (biosensing) features in the same device and using graphene on polymer as the unique material.

To explore more that possibility, I will show results of in-vitro cellular growth (neurons and skin fibroblasts) on graphene-covered glass which shows the stimulation of growth (1) and migration of cells promoted by the graphene substrate together with the possibility of probing their activity (2,3) down to the sub-cellular scale (2) . I will present the preclinical results on animal studies and the perspectives of their commercial use (4) for wound-care, in particular the treatment and diagnostics of chronic wounds (5) that affect the diabetics and elderly.
I will also present more recent works on the realization of in vitro diagnostics based on the same material (6,7) . we are developing a concept of an electronic strip based on a new material for medicine, graphene, whose maturity finally allows its introduction on an industrial scale. The implementation of synthesis techniques of this material from microelectronics allows to produce it in mass at low cost. These sensors powered by a simple smartphone will be coupled with a digital monitoring solution via the smartphone that will improve the diagnosis in the field and the monitoring of chronic diseases. I will detail the functioning of the testNpass (figure 1) , for the detection of the SARS-CoV-2 virus, in particular the process of conversion of the biochemical signal into an electrical signal. Finally, I will show that a myriad of other use cases of this technology exists beyond the detection of pathogens in the field.

## References

[1] Impact of crystalline quality on neuronal affinity of pristine graphene. F. Veliev et al. Biomaterials. 86, 33-41, (2016).
[2] Sensing ion channels in neuronal networks with graphene transistors , Farida Veliev et al. 2D Mater. Vol. 5 045020 (2018).
[3] Recordings of spontaneous spikes evoked in hippocampal neurons by flexible and transparent graphene transistors, Farida Veliev, Frontiers in Neurosci. doi: 10.3389/fnins.2017.00466 (2017).
[4] https://www.grapheal.com
[5] Monolayer graphene-on-polymer dressings promote healing and stabilize skin temperature on acute and chronic wound models. DOI : 10.1101/2021.05.16. 444337;
[6] Mishyn, Vladyslav, et al. "Catch and release strategy of matrix metalloprotease aptamers via thiol–disulfide exchange reaction on a graphene based electrochemical sensor." *Sensors & Diagnostics* 1.4 (2022): 739-749.
[7] Mishyn, Vladyslav, et al. "Catch and release strategy of matrix metalloprotease aptamers via thiol–disulfide exchange reaction on a graphene based electrochemical sensor." *Sensors & Diagnostics* 1.4 (2022): 739-749.

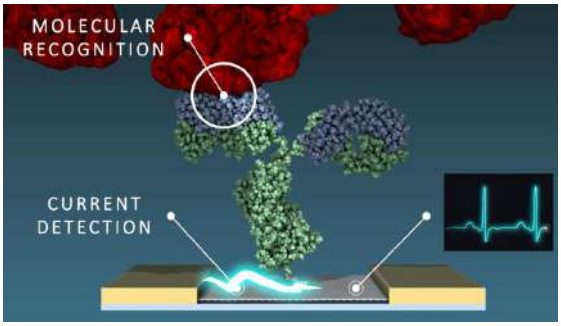


**Figure 1.** Detection principle of graphene Field effect transistor coated with a monolayer of antibodies. The biomolecular affinity with an antigen is influencing the local charge on the graphene surface which changes its global electrical conductance .

**Figure 2.** Graphene biosensors printed on polymer .

# Structure-Function Guided Fabrication of Biodegradable RNA-Binding Polymers

**Moran Frenkel-Pinter** [1,2], Jay W. Haynes [2,3], Anton S. Petrov [2,3], Ramanarayanan Krishnamurthy [4], Nicholas V. Hud [1,2], Loren Dean Williams [2,3] and Luke J. Leman [4]

[1]Institute of Chemistry, The Hebrew University of Jerusalem, Israel 91904
[2]NASA Center for the Origins of Life, Georgia Institute of Technology, Atlanta, GA (USA)
[3]School of Chemistry & Biochemistry, Georgia Institute of Technology, Atlanta, GA (USA)Arial 9)
[4]Department of Chemistry, The Scripps Research Institute, La Jolla, CA (USA)

moran.fp@mail.huji.ac.il

Abstract

Development of biodegradable polymers that bind and stabilize RNA is of high importance for various pharmaceutical and biotechnological applications. For instance, the ability to control the degradation rates of RNA is crucial for development of RNA-based vaccines (such as latest developments of coronavirus vaccines). Depsipeptides, which contain both peptide and ester bonds, have been widely studied as biodegradable polymers and as natural products, and are known to synergize from the properties of both peptides and polyesters. While interactions between RNA and positively charged peptides have been previously investigated, no comparable studies on interactions between positively charged depsipeptides and RNA have been reported. To study the structure-function relationship of depsipeptide interactions with RNA, we synthesized a library of positively charged depsipeptides and peptides. The sequences varied in the side chains and in the number and location of ester linkages within the depsipeptide backbone. We demonstrated that positively charged depsipeptides significantly increased the thermal stability of folded RNA structures. In turn, RNA can reduce the rate of hydrolysis of positively charged depsipeptide ester bonds by >30-fold. These results suggest that rational design of positively charged depsipeptides can allow tremendous control over the mode of interaction and stability of RNA-peptide complexes.

## References

[1] Frenkel-Pinter M, Haynes JW, Mohyeldin AM, C M, Sargon AB, Petrov AS, Krishnamurthy R, Hud NV, Williams LD* and Leman LJ* (2020). Mutually Beneficial Interactions Between Proto-Peptides and RNA. *Nature communications*; 11(1):3137. doi: 10.1038/s41467-020-16891-5.

[2] Proteinaceous over Non-Proteinaceous Cationic Amino Acids in Model Prebiotic Oligomerization Reactions. *Proceedings of the National Academy of Sciences*; 116(33):16338-16346

## Figures

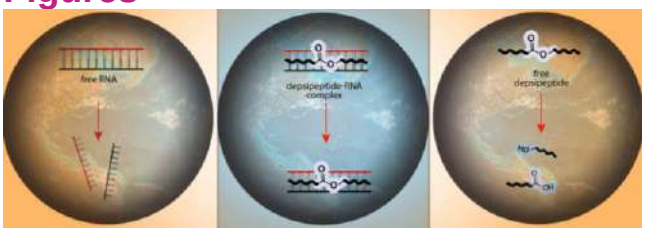

**Figure 1.** Molecules in Mutualism: Prebiotic Mixtures of Cationic Depsipeptides and RNA.

# Engineering a model cell with DNA nanotechnology

**Kerstin Göpfrich**[1,2], Kevin Jahnke[1,2], Tobias Abele[1,2], Yannik Dreher[1,2], Tobias Walther[1,2], Mai P. Tran[1,2]

[1]ZMBH, Center for Molecular Biology, Heidelberg University, Heidelberg, Germany
[2]Max Planck Institute for Medical Research, Heidelberg, Germany

k.goepfrich@zmbh.uni-heidelberg.de

Abstract

Can we construct a cell from non-living matter? In search for answers, bottom-up synthetic biology has successfully encapsulated functional sets of biomolecules inside lipid vesicles, yet a “living” synthetic cell remains unattained.

Instead of relying exclusively on biological building blocks, the integration of new tools can be a shortcut towards the assembly of a synthetic model cell. This is especially apparent when considering recent advances in 3D laser printing and DNA nanotechnology.

With 2-photon 3D laser printing we were able to print structures on the inside of giant unilamellar lipid vesicles (GUVs) (**Fig. 1**) [1].

DNA nanotechnology allowed us to engineer various functional parts for synthetic cells, which, meanwhile have found early applications as biophysical probes in cell biology [2]. Recently, we engineered functional DNA-based mimics of a cytoskeleton. These cytoskeletons are capable of stimuli-responsive reversible assembly [3], cargo transport (**Fig. 2**) [4], mechanochemical signal transduction [5] and can deform GUVs from within [6].

We further demonstrate the division of DNA-containing GUVs based on phase separation [7] or spontaneous curvature increase [8] and osmosis rather than the biological building blocks of a cell’s division machinery. We derive a parameter-free analytical model which makes quantitative predictions that we verify experimentally. The osmolarity increase can be triggered by enzymatic reactions or by light-triggered release of caged compounds.

Ultimately, by coupling GUV division to their informational content and their function, we aim for a prototype of a synthetic cell capable of evolution.

## References

[1] Abele, T., Messer, T., Jahnke, K., Hippler, M., Bastmeyer, M., Wegener, M., & Göpfrich, K., Advanced Materials, 2106709 (2021).
[2] Schönit, A., Giudice, C., Hagen, N., Olleg, D., Jahnke, K., Göpfrich, K. & Cavalcanti-Adam, A., Nano Letters 22 (2021), 302-310
[3] Jahnke, K., Ritzmann, N., Fichtler, J., Nitschke, A., Dreher, Y., Abele, T., Hofhaus, G., Platzman, I., Schröder, R., Müller, D. J., Spatz, J. P. & Göpfrich, K., Nature Communications 12 (2021), 3967.
[4] Zhan, P., Jahnke, K., Liu, N. & Göpfrich, K. Nature Chemistry 14 (2022), 958–963.
[5] Jahnke, K., Illig, M., Scheffold, M., Tran, M.P., Mersdorf, U. & Göpfrich, K. bioRxiv 2022.04.26.489423 (2022).
[6] Jahnke, K., Huth, V., Walther, T., Schönit, A., Mersdorf, U., Liu, N. & Göpfrich, K., ACS Nano 16 (2022), 7233–7241.
[7] Dreher, Y., Jahnke, K., Bobkova, E., Spatz, J. P. & Göpfrich, K. Angewandte Chemie Int. Ed., 60 (2020), 10661.
[8] Dreher, Y., Jahnke, K., Schröter, M. & Göpfrich, K., Nano Letters 21 (2021), 5952–5957.

## Figures

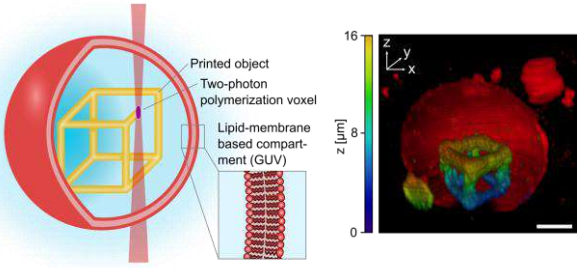


**Figure 1.** 2-photon 3D laser printing inside of lipid vesicles (GUVs) [1].

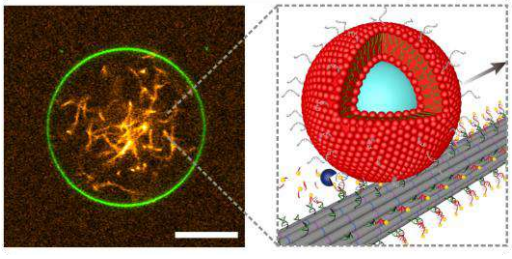

**Figure 2.** DNA cytoskeletons in GUVs (left) and illustration of transport of vesicular cargo (right) [4]. Scale bar: 10um.

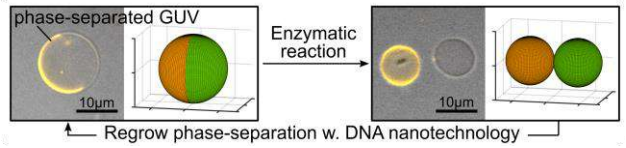


**Figure 3.** Experimental demonstration and theoretical model of GUV division [6].

# *Tamm resonances in nanoporous anodic alumina photonic structures for sensing applications*

**Lluis F. Marsal**
A. Rojas, L.K. Acosta

Universitat Rovira I Virgili, *Departament d'Enginyeria Electrònica, Elèctrica i Automàtica, Universitat Rovira i Virgili, Avinguda Països Catalans 26, 43007*, Tarragona, Spain

lluis.marsal@urv.cat

Nanoporous anodic alumina (NAA) is a versatile and promising nanoporous material obtained by the electrochemical anodization of aluminum. It is based on a cost effective technology, and is fully scalable, and compatible with conventional micro and nanofabrication processes. Under specific conditions of fabrication, we can get a self-ordered hexagonal distribution of nanopores and well-defined cylindrical nanopores with high aspect ratio and diameters between 10 and 400 nm [1-4]. The precise control over the diameter of the nanopore allows to create periodic variations of nanopore's diameter in deep and obtain different photonic structures, e.g.., photonic crystals, microcavities, Distributed Bragg Reflectors, etc.

The optical and photonic properties of NAA depend on intrinsically on its nanoporous structure and as well its surface functionalization. NAA can also be applied to develop new hybrid photonic structures by gold coating on nanoporous anodic alumina photonic structures (photonic crystal) [5]. In this metal-dielectric photonic structure, can be observed effects of an enhancement of the surface plasmon resonance due to absorption of the light at the interface of metallic layer and the NAA photonic crystal. This type of surface plasmon resonances is called Tamm plasmon resonances (TPR).

Figure 1 shows an example of the reflectance spectrum for a Tamm–photonic crystal structure. The spectrum shows the photonic bandgap and the absorption narrow-line associated with the strong resonant recirculation of light within the plasmon-photonic system [6].

Tamm plasmon resonance can be precisely tuned by engineering the properties and characteristics of the metal film and the porous photonic structure, providing new opportunities to achieve unique plasmonic−photonic structures for different applications (optical switching, lasing, light emission, surface-enhanced spectroscopy and sensing). One promising application of TPR is the use as a sensing platform taking advantage of its exceptional optical properties to confine/amplify the light-matter interactions [7].

In this work, we analyze the influence of the structural properties of the photonic crystal and the thickness of the gold layers coated by sputtering on reflectance spectra. Also, we performed sensing experiments by analyzing spectral shifts in the position of the TPR due to the variation of the effective medium (infiltration of different analytical solutions). TPR based on nanoporous anodic alumina offers an opportunity to explore new platforms for developing more sensitive sensor systems.

Acknowledgments
This work was supported by the Spanish Ministerio de Ciencia e Innovación (MICINN/FEDER) PDI2021-128342OB-I00, by the Agency for Management of University and Research Grants (AGAUR) ref. 2017-SGR-1527, COST Action 20126 - NETPORE and by the Catalan Institution for Research and Advanced Studies (ICREA) under the ICREA Academia Award.

## References

[1] J. Ferre-Borrull, J. Pallares, Macías G, L.F. Marsal, Materials. 7 (2014). 5225-5253
[2] G. Macias, L.P. Hernández-Eguía, J. Ferré-Borrull, J. Pallares, L.F. Marsal, ACS Appl. Mater. Interfaces, 5 (2013) 8093.
[3] A Santos, J Ferré-Borrull, J Pallarès, L.F. Marsal, physica status solidi (a) 208 3, (2011) 668-674
[4] A. Santos, L. Vojkuvka, M. Alba, V.S. Balderrama, J Ferré-Borrull, et al. Physica Status Solidi (a) 209 10, (2012) 2045-2048.
[5] Laura K. Acosta, Francesc Bertó-Roselló, E. Xifre-Perez, Abel Santos, J. Ferre-Borrull, L.F. Marsal. ACS Appl. Mater. Interfaces, 11, (2019). 3360-3371
[6] B. Oleksandr, B. Alexandr, R., Victor, E. Dean R. and F., Vassili Nanophotonics, vol. 9, no. 4, (2020), pp. 897-903.
[7] H. Nguyen Que Tran, N.Dang Ai Le, Q. Ngoc Le, C. Suwen Law, S. Yee Lim, A. D. Abell, and A. Santos. ACS Applied Materials & Interfaces (2022) 14 20, 22747-22761

## Figures

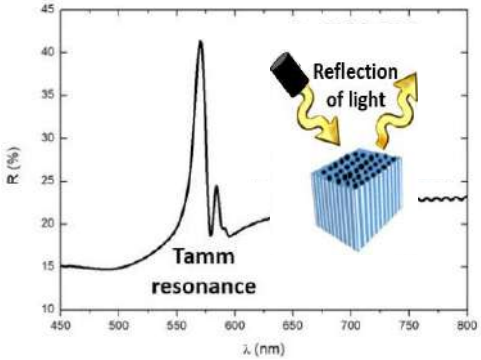


**Figure 1.** Reflectance spectrum of NAA-Photonic Crystal coated with gold showing the characteristic dip corresponding to a Tamm resonance signal.

# Biomedical applications of sperm-hybrid micromotors

**Mariana Medina-Sánchez**

[1]Institute for Integrative Nanosciences, Leibniz Institute for Solid State and Materials Research (IFW Leibniz, Dresden), Germany
[2]Center for Molecular Bioengineering (B CUBE), Dresden University of Technology, Germany

m.medina.sanchez@ifw-dresden.de

Among the various reported medical microrobots, those based on physical and biological propulsion are promising for various biomedical tasks in living organisms. In particular the ones based on motile cells or microorganisms possess the ability to swim efficiently in complex environments, interacting with other biological tissues, and performing a variety of functions. Moreover, by incorporating engineered microparts to those biological components, it is possible to create unique medical tools capable of performing theragnostic operations non-invasively. Such microparts could be designed for instance to perform micromanipulation, local sensing, to enhance imaging contrast, or can be combined with already medically-approved nanomedicines for combinatory and targeted therapy.

In particular, our group have developed different types of such physical and biohybrid micromotors. We have successfully demonstrated the guidance and transport of motile and immotile sperm by magnetic microcarriers, actuated by weak external magnetic fields, in vitro, employing biological-relevant fluids. These sperm-hybrid microrobots have also been used as drug carriers towards gynecological cancer treatment. Moreover, we succeeded in the transport and release of multiple viable and mature sperm, being a crucial step to achieve the egg fertilization in vivo or to control drug dose in the case of cancer therapy. We have also evaluated their performance under blood stream and exploited their cargo-delivery functionality by functionalizing the carriers with heparin-loaded nanoliposomes. Finally, in order to translate these technologies to pre-clinical trials, we have reported the successful tracking of magnetically-driven micromotors in phantom, ex-vivo and in living mice with high spatial and temporal resolution employing ultrasound and photoacoustic imaging.

## References

[1] F. Rajabasadi, S. Moreno, K. Fichna, A. Aziz, D. Appelhans, O.G. Schmidt, M. Medina-Sánchez* (2022), Adv Mater., https://doi.org/10.1002/adma.202204257

[2] L. Schwarz, D.D. Karnaushenko, F. Hebenstreit, R. Naumann, O.G. Schmidt, and M. Medina-Sánchez* (2020) A rotating spiral micromotor for non-invasive zygote transfer. Adv. Sci., 7(18), 2000843.

[3] H. Xu*, M. Medina-Sánchez*, M.F. Maitz, C. Werner, and O.G. Schmidt (2020) Sperm micromotors for cargo delivery through flowing blood. ACS Nano, 14(3), 2982

[4] M. Medina-Sánchez* and O. G. Schmidt* (2017) Medical microbots need better imaging and control. Nature, 545, 406.

[5] M. Medina-Sánchez*, L. Schwarz, A. K. Meyer, and F. Hebenstreit, O. G. Schmidt (2016) Cellular Cargo Delivery: Toward Assisted Fertilization by Sperm-Carrying Micromotors. Nano Lett. 16 (1), 555.

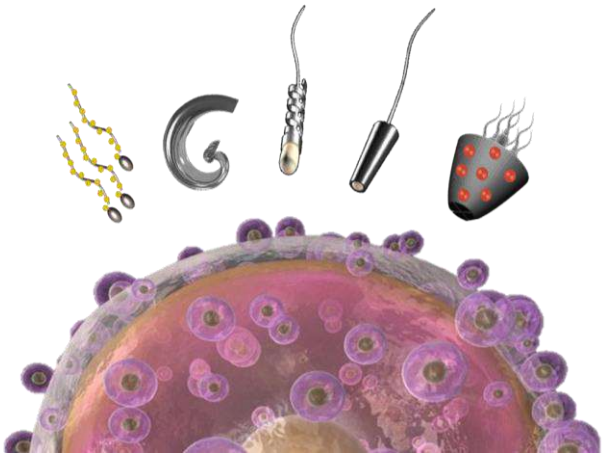

## Figures

**Figure 1.** Sperm-based micromotors for gynecological healthcare applicaitons

# Bioengineering enzyme-powered nanobots: towards programmable design and functionality

**Tania Patiño Padial**[1]

[1]Biomedical Engineering Department, Biomedical Engineering, Institute for Complex Molecular Systems
Eindhoven University of Technology
Het Kranenveld 14, 5612 AZ Eindhoven, The Netherlands

t.patino.padial@tue.nl

In the last years, researchers have found inspiration in the rich multifunctionality of biological systems to engineer "intelligent" artificial active nanosystems able to move, interact, communicate and perform complex tasks at the nanoscale. While the self-propulsion of micro- and nanomachines may not be enough to ride above the blood flow, they may find promising applications in overcoming some of the biological barriers that limit the diffusion of traditional "passive" nanoparticles, which is a main challenge in nanomedicine.

Recently, artificial nanomachines that harness chemical energy from enzyme catalysis and convert it into active motion have been developed. These motor-fuel complexes hold a great potential towards nanomedicine thanks to their versatility, bioavailability and full biocompatibility. Although the field is still in its infancy, several milestones have been reached, such as enhanced anti-cancer drug delivery [1] specific targeting and penetration in 3D bladder cancer spheroids [2] and swarming behaviour within the bladder *in vivo* [3].
However, when biomedical applications are envisaged, several fundamental questions need to be resolved: what are the optimal design features of enzyme-powered nanomachines? How to integrate multiple and smart functionalities? How to achieve full biocompatibility?

In this talk, I will focus on the recent work carried out by our group on understanding the fundamental aspects behind the design of enzyme-propelled nanobots [4-7] and our last results towards the design of next generation nanobots, with safe and programmable design and actuation. We exploited the unique tunability and programmability of synthetic DNA to address these challenges. First, we designed hybrid DNA-enzyme micromotors with the capability to sense and monitor their own activity [8]. Moreover, we used synthetic DNA as building blocks to engineer nanobots with controlled enzyme binding, and studied the effect of enzyme density on the motion behavior. The unique programmability and biocompatibility of DNA could pave the way towards overcoming current challenges on the development of synthetic self-propelled nanomachines.

## References

[1]Hortelao A. *et al*. *Adv. Funct. Mater*., 2018, 1705086.

[2]Hortelao A. *et al*. *ACS Nano*, 2018 acsnano.8b06610.

[3]Hortelao A., *et al. Science robotics*, 2021, 52, 6, eabd2823.

[4]Arqué et al. *Nat. Commun.* 2019, 10, 1- 12.

[5]Patino et al. *Acc. Chem. Res.* 2018, 51, 2662-2671.

[6]Patino et al. *J. Am. Chem. Soc.* 2018, 140, 7896-7903.

[7]Patino et al. *ChemRxiv.* 2021.

[8]Patino et al. *Nanoletters*, 2019, 3440-3447.

# Layered carbon-stabilised porous silicon nanostructures to build electrochemical sensors

**Beatriz Prieto Simón**

[1]Universitat Rovira i Virgili, Av. Països Catalans 26, 43007 Tarragona, Spain
[2]ICREA, Pg. Lluís Companys 23, 08010, Barcelona, Spain

beatriz.prieto-simon@urv.cat

Advances in the design of electrochemical biosensors based on nanostructured materials have paved the way towards the next generation of diagnostic tools. Building biosensors from nanostructured transducers which morphological and electrochemical properties can be easily tuned is key to maximise their analytical performance.

While the incorporation of carbon-based nanomaterials within the design of electrochemical sensors has opened new avenues, in some cases the advantages are overshadowed by large background currents, poor stability, or long and costly fabrication processes. To overcome those limitations, our research has focused over the last few years on exploring carbon-stabilised porous silicon (pSi), a new class of nanostructured material which can be straightforward fabricated, shows great versatility in terms of both structural features and surface chemistry, and is highly effective as electrochemical transducer (Figure 1). We previously reported electrode architectures based on pSi carbon-stabilised via *in situ* thermal decomposition of acetylene gas [1-3]. Such carbonisation method forms a conformal conductive ultrathin carbon layer on pSi, delivering two types of electrochemical transducers depending on the temperature selected for carbonisation: thermally hydrocarbonised pSi (THCpSi) and thermally carbonised pSi (TCpSi). Recently, we envisaged a new approach to generate a carbon layer on pSi, and thus produce another type of high-performing pSi-based electrochemical transducers. We followed a previously reported method of thermally carbonising furfuryl alcohol (FA)-coated pSi. FA is first infiltrated within a pSi template, then polymerised, and finally subjected to extensive pyrolysis. Polyfurfuryl alcohol-modified pSi (PFApSi) adds to the already reported THCpSi and TCpSi, complementing their physicochemical properties, and thus broadening the suite of available carbon-stabilised pSi electrochemical transducers.

The potential of these novel materials to design new electrochemical sensing strategies is herein exemplified by a double-layer pSi nanostructure fabricated via a two-step electrochemical anodisation process [4]. The pore morphological features (e.g. pore size, depth) at each pSi layer are precisely defined by simply varying the anodisation parameters. Next, different types of carbon with tailored wettability and surface chemistry are formed *in situ* on the pore walls of each layer via stepwise temperature-controlled acetylene decomposition. Double-layer structures with distinct functionalities on each layer are harnessed for site-specific modification of bioreceptors. These platforms not only feature remarkable geometrical properties, but also excellent electrochemical performance, underpinned by their fast electron-transfer kinetics, low double-layer capacitance and high sensitivity. The potential of carbon-stabilised pSi double-layer structures as novel highly performing biosensors is here demonstrated through a voltammetric sensor for the detection of key nucleic acid biomarkers.

## References

[1] K. Guo, A. Sharma, R. Toh, E. Alvárez de Eulate, T.R. Gengenbach, X. Cetó, N.H. Voelcker, B. Prieto-Simón. Adv. Funct. Mater., 29 (2019) 1809206

[2] K.-S. Tücking, R.B. Vasani, A.A. Cavallaro, N.H. Voelcker, H. Schönherr, B. Prieto-Simón. Macromol. Rapid Commun., (2018) 1800178

[3] M. Alba, M. Robin, D. Menzies, T.R. Gengenbach, B. Prieto-Simón, N.H. Voelcker. Chem. Comm., 55 (2019) 8001–8004

[4] K. Guo, M. Alba, G.P. Chin, Z. Tong, B. Guan, M. J. Sailor, N.H. Voelcker, B. Prieto-Simón. ACS Appl. Mater. Interfaces, 14 (2022) 15565–15575

## Figures

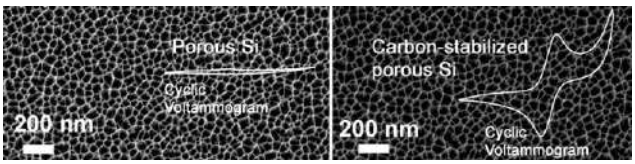


**Figure 1.** Scanning electron microscopy images and cyclic voltammograms of a pSi substrate prior and after carbon stabilisation

# Radical-based Nanoparticles with Advanced Optical Properties for Biological Applications

**I. Ratera,**[1,2] D. Blasi,[1,5] N. Gonzalez-Pato,[1,2] P. Mayorga,[1] X. Rodriguez-Rodriguez,[1] S. Sumithra,[1] N. Camarero,[3] O. Esquivias,[1] J. Guasch,[1,2,4] A.G. Campaña,[6] A. Laromaine,[1] P. Gorostiza,[3,2] and J. Veciana.[1,2]

[1]Institut de Ciència de Materials de Barcelona (ICMAB-CSIC), 08193 Bellaterra, Spain.
[2]Networking Research Center on Bioengineering, Biomaterials, and Nanomedicine (CIBER-BBN), Campus UAB, Bellaterra, 08193, Spain.
[3]Institute for Bioengineering of Catalonia (IBEC), Ed. Hèlix | Baldiri Reixac 15-2, 08028-Barcelona Spain.
[4]Dynamic Biomimetics for Cancer Immunotherapy, Max Planck Partner Group, ICMAB-CSIC, Campus UAB, Bellaterra, 08193, Spain.
[5]Dipartimento di Chimica, Università degli Studi di Bari "Aldo Moro", 70125 – Bari, Italy
[6] Dept of Organic Chemistry, University of Granada, C. U. Fuentenueva, 18071 Granada (Spain)

iratera@icmab.es

Trityl-based radicals represent a unique case of organic free-radicals where a propeller-like conformation is responsible for the protection of the odd electron, mainly located in the central α-carbon. Among them, a special mention should be done for the perchlorotriphenylmethyl radical (PTM), which are particularly chemically stable due to the high steric hindrance provided by the chlorine atoms in ortho positions which protect their single unpaired electron localised on the central carbon atom. In addition to their inherent magnetic spin due to the unpaired electron, PTMs exhibit other appealing properties such as a rich electrochemistry, characteristic electronic and optical properties (absorption and emission) [1] and chirality and their derived applications which is still a field poorly exploited. Here, we review recent developments employing trityl-based radicals which include its structuration at the nanoscale as organic radical nanoparticles (OrNPs) [2] for two different applications; as efficient circularly polarized luminescence magnetic emitters [3] and as ratiomeric nanothermometers in water for biological applications.

## References

[1] a) I. Ratera, et al. J. Mater. Chem. C, 9, 1061 (2021); b) V. Diez-Cabanes, A. Gomez, M. Souto, N. Gonzalez-Pato, J. Cornil, J. Veciana, I. Ratera, J. Mater. Chem. C, 7, 7418 (2019); c) V. Diez-Cabanes, D. C. Morales, M. Souto, M. Paradinas, F. Delchiaro, A. Painelli, C. Ocal, D. Cornil, J. Cornil, J. Veciana, I. Ratera, Adv. Mater. Technol., 1800152 (2019)

[2] Blasi, D., Nikolaidou, D.M., Terenziani, F., Ratera, I., Veciana, J., Phys. Chem. Chem. Phys., 19, 9313 (2017)

[3] a) P. Mayorga, V. G. Jimenez, D. Blasi, I. Ratera, A. G. Campaña, J. Veciana, Angew. Chem. Int. Ed., 58,16282 (2019); b) P. Mayorga, V.G. Jimenez, D. Blasi, T. Parella, I. Ratera, A. G. Campaña, J. Veciana, Chem. Eur. J., 26, 3776 (2020)

## Figures

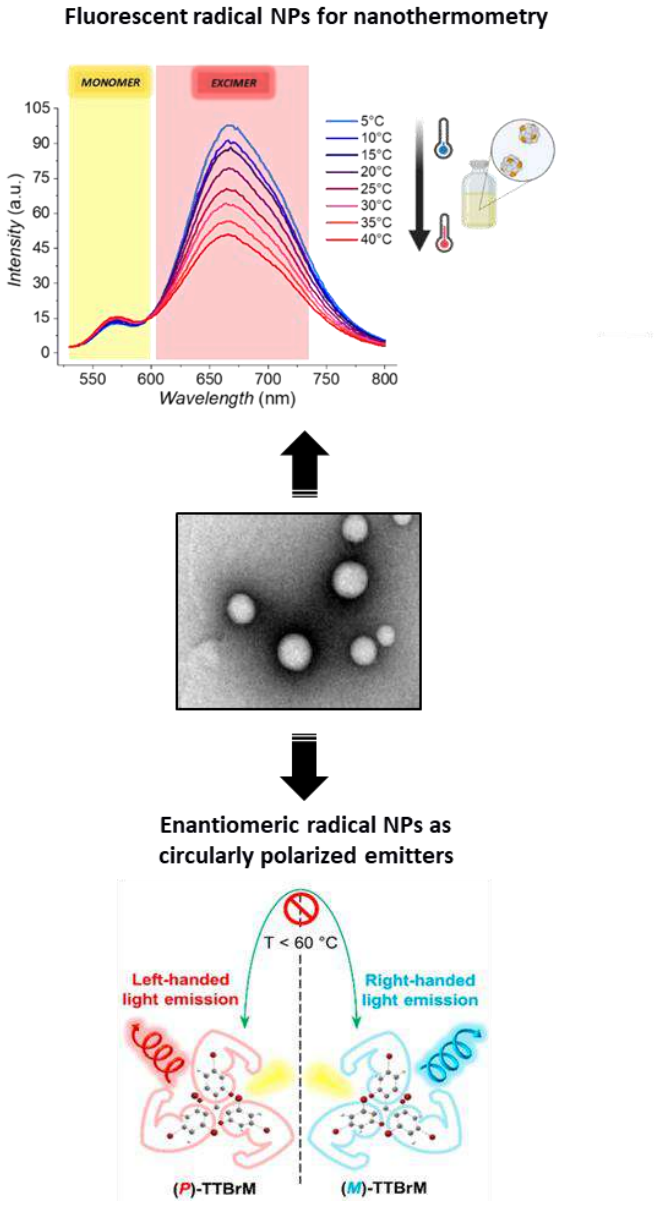


**Figure 1.** Top) Temperature-dependent fluorescence emission spectra of TTM radical doped OrNPs suspended in water; Bottom) Efficient circularly polarized luminescent magnetic emitters from enantiopure propeller-like trityl-brominated OrNPs with high racemization barrier.

# Using Nature's engineering principles to design biointerfaces and synthetic cells for nanomedicine

**César Rodriguez-Emmenegger**[1,2]

[1]*Institute for Bioengineering of Catalonia (IBEC), Barcelona, Spain,*
[2]*Institució Catalana de Reserca I Estudis Avançats (ICREA), Barcelona, Spain*

crodriguez@ibecbarcelona.eu

Nature achieves unmatched functionality by the self-assembly of (macro)molecular building blocks in a hierarchical manner. All information necessary for the function is encoded at the molecular level. Unraveling such blueprints serves as a powerful paradigm in the bio-inspired synthesis of materials that can seamlessly interface with living matter or perform non-natural functions. In this talk, I will present three examples. Firstly, I will present nanoscale coatings for blood contacting medical devices that not only do not activate coagulation but that can even direct blood to digest deadly thrombi. Such coatings find applications in membrane of oxygenators, hemodialysis, and artificial hearts.[1] Secondly, I will present our concept of Kill&Repel coatings for wound dressings.[2] These coatings combine the synergistic action of in situ assembled polymer brushes with a killing mechanism that is orthogonal to eukaryotic cells. When applied to wound dressings they were able to prevent the colonization from various pathogens. The last part of the talk will focus on the development of "quasi-living therapeutics" which are synthetic cells that exert a therapeutic action by recapitulating some biological function.[3] I will illustrate this with Phagocytic Synthetic Cells (PSC) which engulf and kill bacteria and viruses. The dual mode of action is inspired by phagocytosis. The PSCs have the potential to revolutionize the way we fight infectious diseases caused by antibiotic-resistant germs, which is one of the biggest global threats to our welfare.

## References

[1] a) J. Quandt, M. Garay-Sarmiento, L. Witzdam, J. Englert, Y. Rutsch, C. Stöcker, F. Obstals, O. Grottke, C. Rodriguez-Emmenegger, *Advanced Materials Interfaces* **2022**, DOI: 10.1002/admi.202201055; b) F. Obstals, L. Witzdam, M. Garay-Sarmiento, N. Y. Kostina, J. Quandt, R. Rossaint, S. Singh, O. Grottke, C. Rodriguez-Emmenegger, *ACS Appl Mater Interfaces* **2021**, 13, 11696.

[2] M. Garay-Sarmiento, L. Witzdam, M. Vorobii, C. Simons, N. Herrmann, A. de los Santos Pereira, E. Heine, I. El-Awaad, R. Lütticken, F. Jakob, U. Schwaneberg, C. Rodriguez-Emmenegger, *Adv. Funct. Mater.* **2021**, 32.

[3] a) A. M. Wagner, J. Quandt, D. Soder, M. Garay-Sarmiento, A. Joseph, V. S. Petrovskii, L. Witzdam, T. Hammoor, P. Steitz, T. Haraszti, Potemkin, II, N. Y. Kostina, A. Herrmann, C. Rodriguez-Emmenegger, *Adv Sci (Weinh)* **2022**, DOI: 10.1002/advs.202200617e2200617; b) A. M. Wagner, H. Eto, A. Joseph, S. Kohyama, T. Haraszti, R. A. Zamora, M. Vorobii, M. I. Giannotti, P. Schwille, C. Rodriguez-Emmenegger, *Adv Mater* **2022**, DOI: 10.1002/adma.202202364e2202364; c) A. Joseph, A. M. Wagner, M. Garay-Sarmiento, M. Aleksanyan, T. Haraszti, D. Soder, V. N. Georgiev, R. Dimova, V. Percec, C. Rodriguez-Emmenegger, *Adv Mater* **2022**, n/a, e2206288; d) N. Y. Kostina, K. Rahimi, Q. Xiao, T. Haraszti, S. Dedisch, J. P. Spatz, U. Schwaneberg, M. L. Klein, V. Percec, M. Moller, C. Rodriguez-Emmenegger, *Nano Lett* **2019**, 19, 5732.

## Figures

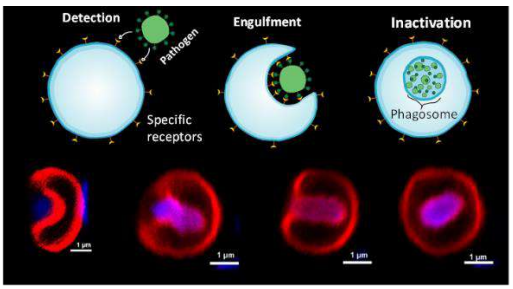


**Figure 1.** Phagocytic synthetic cells engulfing a living *E. coli* by simple physical interactions.

# Controlling cell signaling using magnetic nanoparticles and alternating magnetic fields

**Dekel Rosenfeld**[1]

[1]Department of Biomedical Engineering, Faculty of Engineering, Tel Aviv University, Tel Aviv, Israel

Dekelr@tauex.tau.ac.il

Iron oxide magnetic nanoparticles (MNPs) with diameter of 20-25 nm dissipate heat when exposed to weak alternating magnetic fields (AMFs) with amplitudes <50 mT and frequencies of 100-600 kHz. This heat can be exploited to activate cells that have thermally sensitive ion channels on their membrane via magnetothermal modulation. One example for such ion channel is the transient receptor potential vanilliod 1 (TRPV1), the capsaicin receptor, a non-selective cation channel that is calcium-permeable and can be activated by heat with temperature threshold above 42ºC. Previous studies have demonstrated the expression of TRPV1 in various peripheral organs as well as sensory neurons. AMF has high penetration rate with no deleterious effects, and therefore suitable for the activation of cells within deep organs in the body.

We exploit the magnetothermal approach to control calcium signaling in cells within deep organs and with a minimally invasive scheme. We introduce magnetically-controlled stress hormone release from adrenal glands- corticosterone and epinephrine [1], demonstrated in cell cultures and in vivo. Abnormal regulation of hormones produced within the adrenal gland have been linked to altered stress response and controlling their release is particularly relevant in psychiatric and mental disorders.

In another design, we exploit the magnetothermal approach to guide axonal growth via enhanced calcium influx in a model of sensory nerve regeneration and suggests a new mechanistic strategy to overcome the limited axonal regeneration that exists in nociceptive sensory neurons and central nervous system neurons [2].

## References

[1] D. Rosenfeld et. al, *Science Advances*, (2020) eaaz3734.

[2] D. Rosenfeld et. al, *Advanced Functional Materials*, (2022), 0224558.

## Figures

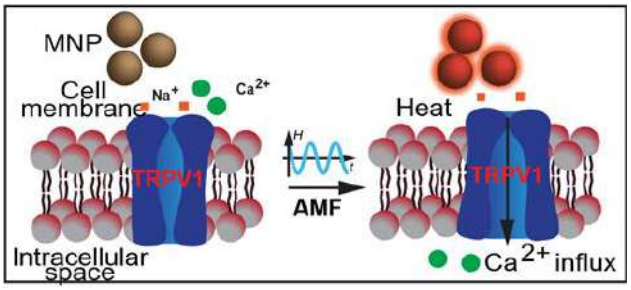


**Figure 1.** Magnetothermal approach to control calcium influx by modulating TRPV1

# Intranasal Administration of Novel Nanocarriers for Glioblastoma treatment

**Daniel Ruiz-Molina**[1], Fernando Novio[2], Jordi Bruna[3], Victor Yuste[4,5], Paula Alfonso-Triguero[1], Ana Paula Candiota[6,7,8],Julia Lorenzo[7,8]

[1] Catalan Institute of Nanoscience and Nanotechnology (ICN2), CSIC and BIST, Campus UAB, Bellaterra, 08193 Barcelona, Spain.
[2] Departament de Química, Universitat Autònoma de Barcelona (UAB), Campus UAB, Cerdanyola del Vallès 08193, Barcelona, Spain
[3] Neuro-Oncology Unit, Bellvitge University Hospital-ICO (IDIBELL), Avinguda de la Gran Via de l'Hospitalet, 199-203, L'Hospitalet de Llobregat, Barcelona, Spain
[4] Instituto de Neurociencias. Universitat Autònoma de Barcelona (UAB), Campus UAB, Cerdanyola del Vallès 08193, Barcelona, Spain
[5] Centro de Investigación Biomédica en Red Sobre Enfermedades Neurodegenerativas (C.I.B.E.R.N.E.D.), Campus UAB, Cerdanyola del Vallès, 08193 Bellaterra, Spain
[6]Centro de Investigación Biomédica en Red: Bioingeniería, Biomateriales y Nanomedicina, 08193 Cerdanyola del Vallès, Spain
[7] Departament de Bioquímica i Biologia Molecular, Universitat Autònoma de Barcelona, 08193 Cerdanyola del Vallès, Spain
[8] Institut de Biotecnologia i de Biomedicina, Departament de Bioquimica i Biologia Molecular, Universitat Autònoma de Barcelona, 08193 Cerdanyola del Vallès, Barcelona, Spain)

dani.ruiz@icn2.cat

The progressive population aging in developed countries has favored a steady prevalence increase over the years of many pathologies of the central nervous system (CNS), such as neurodegenerative diseases (e.g., amyotrophic lateral sclerosis, Alzheimer's, Parkinson's, Huntington's, and prion diseases), genetic deficiencies (e.g., lysosomal storage diseases, leukodystrophy) and brain cancer (i.e. glioblastoma multiforme).

Most of neurological diseases (ND) clearly diverge in their origin, overall population incidence and treatment though all of them share the same problem, namely the lack of efficacy of their state-of-the-art therapies originated largely by the existence of the blood-brain barrier (BBB). This barrier limits the access of most therapeutic agents to the brain area, and for those crossing requires ever-increasing drug doses increasing side effects.

Intranasal administration represents an alternative route to transport drugs from the nasal mucous membrane through the trigeminal nerve, and from there to the brain while largely avoiding the systemic dispersal of the drug and the limitations of BBB. However, as far as we know no IN products for GB are nowadays commercialized mostly due to the poor mucosa penetration of most drugs, the rapid mucociliary clearance and the enzymatic degradation.

In this sense, the use of nanotechnology-based approaches is of special interest as allows for control of the formulation, surface charge, hydrophilicity, and mucoadhesion and favors the transcellular transport to the brain as well as induce both a systemic and local immune response. In this presentation we will face the work developed at the Nanostructured Functional Materials group with this aim.

## References

[1] D.Ruiz-Molina, X. Mao, P. Alfonso-Triguero, J. Lorenzo, J. Bruna, V. J Yuste, A.-P. Candiota, F. Novio, *Cancers* **2022**, *14*, 4960.
[2] X. Mao, P. Calero-Pérez, D. Montpeyó, J. Bruna, V. J Yuste, A.-P.Candiota, J. Lorenzo, F. Novio, D. Ruiz-Molina *Nanomaterials* **2022**, *12* (7), 1221.
[3] X. Mao, S. Wu, P. Calero-Pérez, A.-P. Candiota, P. Alfonso, J. Bruna, V. J Yuste, J. Lorenzo, F. Novio, D. Ruiz-Molina *Cancers* **2022**, *14* (2), 410.
[4] J. García-Pardo, F. Novio, F. Nador, I.Cavaliere, S. Suárez-García, S. Lope-Piedrafita, A.-P.Candiota, J. Romero-Gimenez, B. Rodríguez-Galván, J.Bové, M. Vila, J. Lorenzo, D. Ruiz-Molina *ACS nano* **2021**, *15* (5), 8592.

## Figures

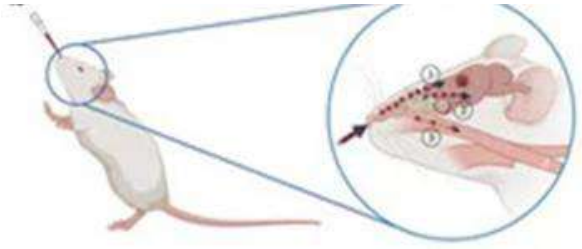

**Figure 1.** Schematic representation of the intranasal delivery of nanocarriers for Glioblastoma treatment

# Nanobots going in vivo

**Samuel Sánchez**[1],

[1]Institute for Bioengineering of Catalonia (IBEC), Barcelona, Spain
[2]Catalan Institute for Research and Advanced Studies (ICREA), Barcelona, Spain

ssanchez@ibecbarcelona.eu

One of the dreams in nanotechnology is to engineer small vehicles and machines, called here nanobots, which can eventually be applied *in vivo* for medical purposes. Yet, reaching that fascinating goal is not a trivial thing and several challenges need to be addressed. First, researchers need to incorporate efficient but also bio-friendly propulsion mechanisms into the nanobots. Our strategy comprises the use of biocatalysts such enzymes for converting biologically available fuels into a propulsive force. Secondly, nanoparticles' chassis should be generally recognized as safe (GRAS) material, biocompatible and/or biodegradable.
In my talk, I will present how we bioengineer hybrid nanobots combining the best from the two worlds: biology (enzymes) and (nano)technology (nano-micro-particles) providing swimming capabilities, biocompatibility, imaging, multifunctionality and actuation.
Besides the understanding of fundamental aspects (1), and controlling the performance of micro-nanobots (2) I will present some of the proof-of-concept applications of biocompatible nanobots such as the efficient transport of drugs into cancer cells (3) and 3D spheroids (4), sensing capabilities (5), anti-bactericidal applications (6) and the use of molecular imaging techniques like PET-CT (7) or Photoacoustic (8) for the tracking and localization of swarms of nanobots both *in vitro* and *in vivo* in confined spaces like mice bladder.

## References

[1] Arqué et al. Nat. Commun. 2019. 10, (1) 1-12.; Patino et al. Acc. Chem. Res. 2018, 51, (11) 2662-2671
[2] Patino et al. J. Am. Chem.Soc. 2018, 140 (25) 7896-7903
[3] Hortelao et al. Adv. Funct. Mat 2018, 28, 1705086
[4] Hortelao et al. ACS Nano 2019, 13, (1), 429-439
[5] Patino et al. NanoLett. 2019, 19, (6), 3440-3447
[6] Arqué et al. ACS Nano 2022, 16, 5, 7547–7558
[7] Hortelao et al. Sci. Robotics. 2021, 6, (52), eabd2823.
[8] D. Xu et al. ACS Nano, 2021, 15 (7), 11543-11554

# AI-Guided Optical Sensors for The Early Detection of Gynecologic Cancers

**Zvi Yaari** [1]

[1]School of Pharmacy, Faculty of Medicine, Hebrew University of Jerusalem, Ein Kerem Campus, Jerusalem, Israel

zvi.yaari@mail.huji.ac.il

**AI-Guided Optical Sensors for The Early Detection of Gynecologic Cancers**

Gynecologic cancers are particularly difficult to diagnose. Patient prognosis and quality of life are affected substantially by this problem. We are developing new technologies to improve cancer detection using liquid biopsy and in vivo sensor approaches. With artificial intelligence algorithms, we harnessed the unique optical properties and sensitivity of single-walled carbon nanotubes to develop intelligent optical sensors. We developed platforms to detect multiple cancer biomarkers in both patient biofluids and within the uterine cavity as implantable devices. Applying machine learning algorithms to analyze the optical response of the sensors enabled the precise detection of multiplexed biomarkers. In addition, when implanted in human uteri, the sensors detected the biomarkers and successfully differentiated between benign and malignant cases. These technologies will significantly improve diagnostics and lead to robust, point-of-care technologies for early-stage diagnosis.

## References

[1] Yaari, Z. et al., *Science Advances*, 7/47 (2021), eabj0852.
[2] Yaari, Z. et al., Nano Letters, 20/11 (2020), 7819-7827.

# Plasma Bio-Engineering: Functional Interfaces and Nanomaterials for Biomedicine Applications

**Behnam Akhavan**

School of Engineering, University of Newcastle, Callaghan, 2308 NSW, Australia
Hunter Medical Research Institute (HMRI), New Lambton Heights, NSW 2305, Australia
School of Physics, University of Sydney, Sydney, NSW 2006, Australia
The University of Sydney Nano Institute, The University of Sydney, Sydney, NSW 2006, Australia
School of Biomedical Engineering, University of Sydney, Sydney, NSW 2006, Australia
[2]Organization, Address, City, Country (Arial 9)

Behnam.Akhavan@newcastle.edu.au

Implantable medical devices are increasing in global prevalence, with hundreds of thousands of operations performed annually. However, a significant proportion of these operations experiences failure due to infection and/or poor integration with host tissues. Biomimetic functionalization of surfaces enables control over the biological response by signalling through immobilized proteins and other biomolecules. Here we present a novel approach for the fabrication of radical-rich organic coatings that are chemically and mechanically robust for surface engineering of implantable medical devices [1-5]. Our results demonstrate that multifunctional protein layers, peptide molecules, or even silver nanoparticles can be covalently immobilized on such radical-rich interfaces for improved cellular activity and enhanced antimicrobial properties. Our recent findings provide evidence on utilizing this technology for polymerization and covalent attachment of hydrogel layers [6], as well as tuning the orientation and density of immobilized molecules on surfaces by simply tuning pH or applying external electric fields during the biomolecule immobilization [7]. The plasma bio-engineering approach presented here holds great promise to create the next generation of bioactive materials and interfaces for biomedical implant applications and beyond.

## References

[1] B. Akhavan, S.G. Wise, M.M.M. Bilek, Substrate-Regulated Growth of Plasma-Polymerized Films on Carbide-Forming Metals, Langmuir 32(42) (2016) 10835-10843.
[2] C.A. Stewart, B. Akhavan, J. Hung, S. Bao, J.-H. Jang, S.G. Wise, M.M. Bilek, Multifunctional Protein-Immobilized Plasma Polymer Films for Orthopedic Applications, ACS Biomaterials Science & Engineering 4(12) (2018) 4084-4094.
[3] M. Croes, B. Akhavan, O. Sharifahmadian, H. Fan, R. Mertens, R.P. Tan, A. Chunara, A.A. Fadzil, S.G. Wise, M.C. Kruyt, A multifaceted biomimetic interface to improve the longevity of orthopedic implants, Acta Biomater. (2020).
[4] B. Akhavan, T.D. Michl, C. Giles, K. Ho, L. Martin, O. Sharifahmadian, S.G. Wise, B.R. Coad, N. Kumar, H.J. Griesser, Plasma activated coatings with dual action against fungi and bacteria, Appl. Mater. Today 12 (2018) 72-84.
[5] B. Akhavan, S. Bakhshandeh, H. Najafi-Ashtiani, A.C. Fluit, E. Boel, C. Vogely, B.C.H. van der Wal, A.A. Zadpoor, H. Weinans, W.E. Hennink, M.M. Bilek, S. Amin Yavari, Direct covalent attachment of silver nanoparticles on radical-rich plasma polymer films for antibacterial applications, J. Mat. Chem. B (2018).
[6] R. Walia, B. Akhavan, E. Kosobrodova, A. Kondyurin, F. Oveissi, S. Naficy, G.C. Yeo, M. Hawker, D.L. Kaplan, F. Dehghani, Hydrogel− Solid Hybrid Materials for Biomedical Applications Enabled by Surface-Embedded Radicals, Adv. Funct. Mater. 30(38) (2020) 2004599.
[7] L.J. Martin, B. Akhavan, M.M. Bilek, Electric fields control the orientation of peptides irreversibly immobilized on radical-functionalized surfaces, Nature Communications 9(1) (2018) 357.

## Figures

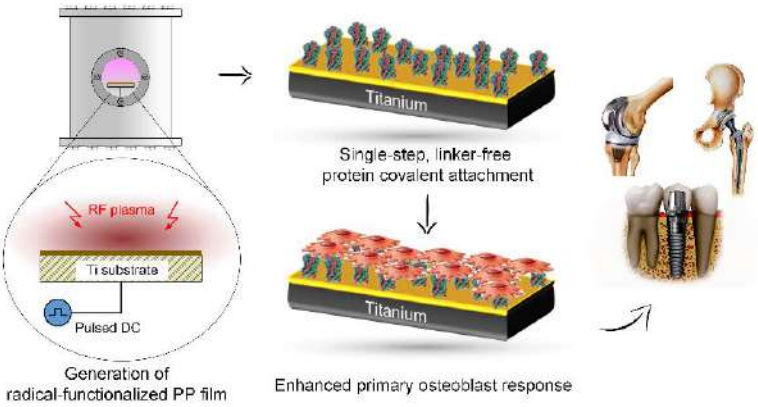

# Nanoengineered Surfaces for modulating cellular responses and sensing applications

**Akash Bachhuka**,

Department of Electronics, Electric and Automatic Engineering, Universitat Rovira I Virgili, Tarragona, Spain

Akash.bachhuka@urv.cat

## Abstract

The greatest challenge in the field of biomaterials is the understanding and the prediction of long-term biological responses in patients receiving implantable materials. Reconstructing and detailing these mechanisms may allow for more targeted approaches and highlights how immune processes are amenable to manipulation by synthetic biomaterials. The interplay between plasma polymerized thin films in combination with surface nanotopography proved to be an important factor in cell-surface interaction [1] (Figure 1). We demonstrated that the right combination of chemistry and nanotopography can be used to modulate cellular adhesion, collagen deposition, and macrophage polarization (the expression of pro-inflammatory and anti-inflammatory signals) [2-5] (Figure 2).
Furthermore, our surface engineering expertise was utilized to fabricate metal ion sensors and biosensors [6,7] (Figure 3). We anticipate that future explorations in this field of research will facilitate the rational design of biomedical implants and devices with physicochemical surface characteristics tailored at the nanoscale that will enhance utility and function and improve clinical outcomes.

## References

[1] Bachhuka A, Hayball JD, Smith LE, Vasilev K. ACS Applied Materials & Interfaces. 2015, 7, 23767-75
[2] Chen Z#, Bachhuka A#, Han S, Wei F, Lu S, Visalakshan R. M, Vasilev K, Xiao Y. ACS Nano, 2017, 11 (5), 4494-4506.
[3] Christo SN#, Bachhuka A#, Diener KR, Mierczynska A, Hayball JD, and Vasilev K. Advanced Healthcare Materials, 2016.
[4] Bachhuka A, Christo SN, Cavallaro A, Diener KR, Mierczynska A, Smith LE, Marian R, Manavis J, Hayball JD, Vasilev K. Journal of colloid and interface science. 2015, 457, 9-17.
[5] Bachhuka A, Madathiparambil Visalakshan R, Law CS, Santos A, Ebendorff-Heidepriem H, Karnati S, Vasilev K. ACS Applied Biomaterials. 2020 Feb 16;3(3):1496-505.
[6] Zuber A#, Bachhuka A#*, Tassios S, Tiddy C, Vasilev K, Ebendorff-Heidepriem H. Sensors. 2020 Jan 15;20(2):492.
[7] Bachhuka A*, Heng S, Vasilev K, Kostecki R, Abell A, Ebendorff-Heidepriem H. Sensors. 2019 Apr 17;19(8):1829.

## Figures

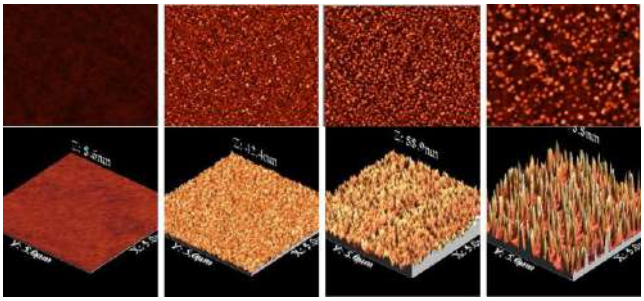

**Figure 1.** Atomic Force Microscopic images (2D and 3D) of surfaces modified with different sized gold nanoparticles.

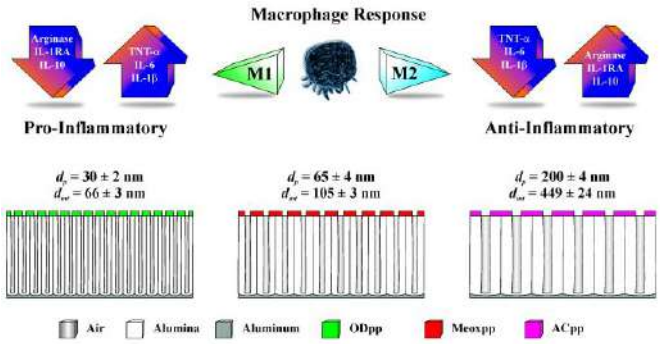


**Figure 2.** Schematic representation of macrophage polarization on nanoporous alumina surfaces.

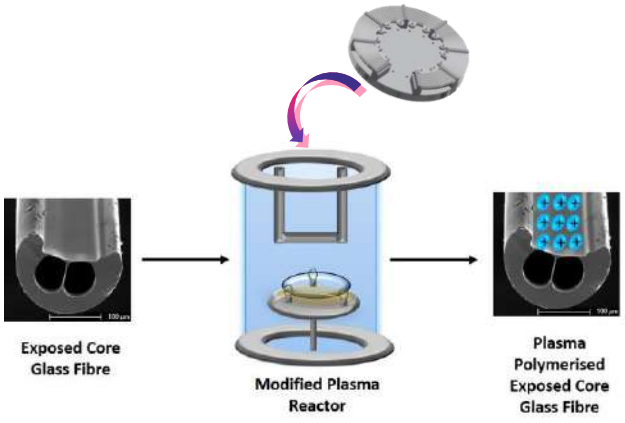


**Figure 3.** Schematic for plasma modification of exposed core fibre for metal ion sensing.

# Light-Triggered Vapor Nanobubbles and Nanomotors for Drug Delivery Applications

**Juan Fraire**[1,2], Maria Guix,[1] Ana C. Hortelao,[1] Noelia Ruiz Gonzalez,[1] Anna C. Bakenecker,[1] Pouria Ramezani,[2] Félix Sauvage,[2] Stefaan De Smedt,[2] Kevin Braeckmans,[2] Samuel Sánchez,[1,3]

[1]Institute for Bioengineering of Catalonia (IBEC), Barcelona, Spain.
[2]Laboratory for General Biochemistry and Physical Pharmacy, Ghent University, Ghent, Belgium.
[3]Catalan Institute for Research and Advanced Studies (ICREA), Barcelona, Sapin.

jfraire@ibecbarcelona.eu

Targeted drug delivery depends on the ability of nanocarriers to reach the target site, which requires the penetration of different biological barriers. Penetration is usually low and slow because of passive diffusion and steric hindrance [1]. Nanomotors (NMs) have been suggested as the new generation of nanocarriers in drug delivery due to their autonomous motion and associated mixing hydrodynamics [2], especially when acting as a swarm (emergent collective behavior) [3].

In this study, we present a unique nanotechnological approach based on the use of nanomotors with advanced photothermal effects for disruption of biological barriers (overcoming passive diffusion and steric hindrance limitations) [4]. For this, we explored the concept of urease-powered nanomotor swarms designed as such that they can exert disruptive mechanical forces upon laser irradiation. When exposed to pulsed laser light, a powerful vapor nanobubble (VNB) is formed from the nanomotors, which mechanical energy is used for the disruption of a biological barrier model based on Type I collagen fibers (model of the extracellular matrix).

In this talk I will describe the main results linked to the design of urease-powered nanomotors able to form VNBs upon irradiation with ns laser pulses and the subsequent mechanical disruption of a biological barrier model [5].
First, I will discuss the motion dynamics of individual nanomotors as well as the emergent collective behavior of swarms of these motors using optical microscopy, and the exploitation of this swarming effect for navigation on a lab-on-a-chip system.
Second, I will demonstrate the successful disruption of the collagen fibers with these nanomotors, both at the single fiber level and even with bulk measurement of the rheological properties.
Finally, I will show how the use of troops of swarms of nanomotors with different capabilities allows to overcome the limitations of passive particles for trespassing biological barriers in terms of passive diffusion and steric hindrance:

- Swarm 1: nanomotors that can induce micro-environment modifications upon irradiation.
- Swarm 2: fluorescent nanomotors acting as a reporter.

Our results show that the microenvironment modifications induced by Swarm 1 can enhance 10-fold the delivery of (Swarm 2) into a cell model.

## References

[1] Blanco, E.; Shen, H.; Ferrari, M. Nat Biotechnol., 33 (2015), 941–951.
[2] Gao, W.; Wang, J., 6 (2014), 10486–10494.
[3] Hortelao, A. C.; Simó, C.; Guix, M.; Guallar-Garrido, S.; Julián, E.; Vilela, D.; Rejc, L.; Ramos-Cabrer, P.; Cossío, U.; Gómez-Vallejo, V.; Patiño, T.; Llop, J.; Sánchez, S., Sci Robot., 6 (2021).
[4] Sauvage, F.; Fraire, J. C.; Remaut, K.; Sebag, J.; Peynshaert, K.; Harrington, M.; van de Velde, F. J.; Xiong, R.; Tassignon, M.-J.; Brans, T.; Braeckmans, K.; de Smedt, S.C., ACS Nano, 13 (2019), 8401–8416.
[5] Fraire, J.C. et al., Light triggered Mechanical Disruption of Extracellular Barriers by Swarms of Enzyme Powered Nanomotors for Enhanced Delivery, (submitted).

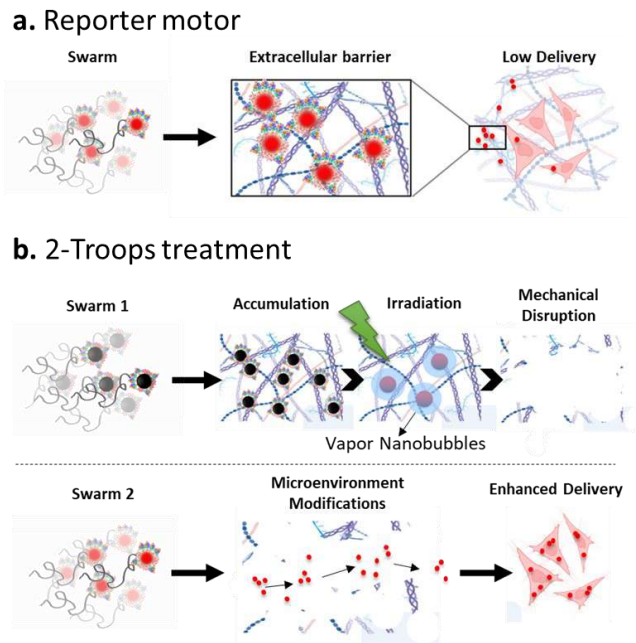


**Figure 1.** Troops of swarms of enzyme-powered NMs for enhanced delivery: a. Shielding effect of extracellular barrier model on the delivery of swarms of reporter motors. b. Swarm 1 (IONP NMs with photothermal properties) will penetrate the extracellular barriers encountered in the path to reach target cells; next, they will be irradiated, resulting in the barrier disruption due to the mechanical damage caused by the VNB formation/collapse from the IONP heated cores; microenvironment modifications generated by Swarm 1 will allow swarms of fluorescent polystyrene based motors (Swarm 2) to access the target cells (enhanced delivery).

# Nano-omics: nanotechnology-enabled harvesting of blood-circulating biomarkers

**Marilena Hadjidemetriou**

NanoOmics team, Nanomedicine Lab,
Faculty of Biology, Medicine & Health,
University of Manchester, UK

marilena.hadjidemetriou@manchester.ac.uk

Over the past decade, the development of 'simple' blood tests that enable disease screening, diagnosis or monitoring and facilitate the design of personalized therapies without the need for invasive tumour biopsy sampling has been a core ambition in cancer research.

Among liquid-biopsy analytes, proteins are the biological endpoints of cellular processes and the most clinically established biomarkers in molecular diagnostics. However, the discovery of novel protein biomarkers in blood remains notoriously difficult. This is largely due to the blood proteome analysis challenge, caused by the overwhelming masking effect of highly abundant proteins (e.g., albumin accounts for 50% of the total protein content). The extraction and mass spectrometry (MS) analysis of massively diluted amounts of disease-specific proteins in blood (at the pg/ml-ng/ml range), remain a major bottleneck for liquid biopsies to be embedded in clinical practice.

The quest for novel blood biomarkers has led to the development of nanotechnology-based blood analysis solutions. We have recently introduced the *'Nano-Omics'* paradigm,[1] to describe the nanotechnology-enabled enrichment and analysis of blood-circulating molecular biomarkers. Nano-Omics utilizes nanoparticles (NPs) as scavenging platforms to capture, enrich and isolate disease-associated analytes from biological fluids for downstream omics analyses.

Specifically for protein biomarker discovery, Nano-Omics exploits the spontaneous and untargeted adsorption of proteins onto the NP surface once in contact with biological fluids, known as *'protein corona'* formation (**Fig.1**).[2] Recovery and purification of corona-coated NPs from unbound proteins and subsequent analysis MS addresses the issue of albumin masking and offers substantial 'broadening' of the blood proteome coverage. This results in the identification of low molecular weight and low abundance proteins that cannot be directly detected by conventional proteomic analysis of blood.[3] Comprehensive comparison between *'healthy'* and *'diseased'* coronas by MS enables the identification of multiple previously unrecognized candidate biomarker proteins (**Fig.1**). Unlike other NP-based biosensing technologies designed to capture already-known disease-associated analytes, this 'blood-mining' approach has the potential to accelerate the discovery phase of the biomarker development. While the *ex vivo* corona formation (upon incubation of NPs with biofluids in a tube) has been exploited for the analysis of human clinical samples, the molecularly richer *in vivo* corona (forming upon intravenous administration of NPs and their subsequent recovery from blood) has been shown to enable the discovery of biomarkers in preclinical models.

During the past decade, we have learnt that a complex protein corona forms rapidly on the surfaces of all nanoscale materials to varying degrees, depending on their physicochemical properties and surface characteristics. More recently, the NP protein corona formation has conceptually morphed into the multi-molecular self-assembly of layers composed of proteins, lipids, polysaccharides and nucleic acids, termed the *'biomolecule corona'*. For example, we demonstrated the interaction of cfDNA with lipid-based NPs upon their incubation with human plasma samples.[4] The discovery of this additional omics dimension paves the way for further investigations of the potential exploitation of the NP biomolecule corona to enrich proteogenomic biomarkers in blood. The Nano-Omics platform technology could be deployable across a range of biomarker applications and pressing clinical challenges.

## Figures

**Figure 1. The Nano-Omics proteomics analysis workflow.** The Nano-Omics technology relies on the non-specific adsorption of disease-associated proteins onto the nanoparticle surface, once in contact with blood (known as '*protein corona'* formation). Protein corona analysis by liquid chromatography-tandem mass spectrometry (LC: MS/MS) addresses the issue of albumin masking and enables an in-depth analysis of the blood proteome.

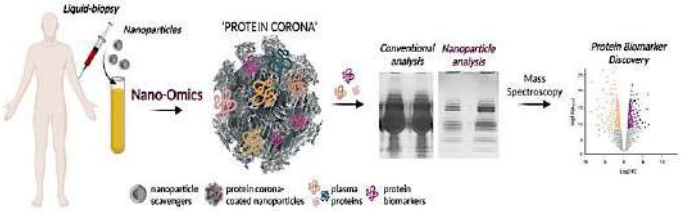


## References

[1] Gardner L, Kostarelos K, Mallick P, Dive C, Hadjidemetriou M*. Nano-Omics: Multidimensional Harvesting of the Blood-Circulating Cancer Biome. Nature Reviews Clinical Oncology, 2022; 19, 551–561.

[2] Hadjidemetriou M, Kostarelos K. Evolution of the nanoparticle corona. Nature Nanotechnology, 2017; 12 (4), 288-290.

[3] Hadjidemetriou M*, Papafilippou L, Unwin R, Clamp A, Kostarelos K. Nanoparticle-enabled cancer biomarker discovery: a proof of concept study in ovarian carcinoma patients. Nano Today, 2020; 34, 100901.

[4] Gardner L, Warrington J, Rogan J, Rothwell D, Brady G, Dive C, Kostarelos K, Hadjidemetriou M*. The Biomolecule Corona of Lipid Nanoparticles Contains Circulating Cell-free DNA. Nanoscale Horizons, 2020; 5(11), 1476-1486

# How to Transform a Novel 2D Nanomaterial in '*Medical Grade*'

**Neus Lozano**,

Catalan Institute of Nanoscience and Nanotechnology (ICN2), CSIC and BIST, Campus UAB, Bellaterra, 08193 Barcelona, Spain

neus.lozano@icn2.cat

Graphene and its derivatives have been attracting tremendous attention for over a decade, since in 2004, a single sheet of graphene was isolated and characterized by Novoselov and Geim [1]. In particular, graphene oxide (GO) - the oxidized form of graphene - has become one the most investigated materials in the biomedical field due to its hydrophilicity and improved compatibility with biological systems. It is rapidly becoming the reference 2D nanomaterial for use in medical applications.

Determination of the opportunities and limitations that GO offers in biomedicine are particularly prone to inaccuracies due to the wide variability in the preparation methodologies for the synthesis of GO. Most of the methods used are based on oxidation of graphite following a modified Hummers' protocol [2], which involves the use of oxidizing reagents and acids. However, this method yields GO with different degrees of oxidation and impurities. Additional purification steps are required to enhance the purity of the material, by isolating the purest fraction of GO in the absence of by-products or contaminants [3]. Bacterial endotoxin contamination during the synthesis process and handling, can confound toxicological testing of the materials [4], and needs to be carefully and highly considered on the production of GO for biomedical applications.

To avoid some of the pitfalls encountered with commercial GO materials, we have made a systematic bottom-up effort during the last 10 years to generate '*medical grade'* GO suspensions. These water-based suspensions were produced from graphite flakes [5] following a modified Hummers' method further improved to ensure endotoxin-free [4] suspensions of single- to few-layer GO sheets of the highest chemical purity. These materials were produced in a range of different lateral dimensions [7] to assess the impact of this parameter with respect to biological impact [6].

Furthermore, a suite of characterization techniques has been established to confirm the quality, reproducibility, and low batch-to-batch variability of each synthesis [6]. In the last decade, these GO suspensions have been used for either hazard assessment or biomedical proof-of-concept studies, to reveal the relationship between the nanomaterial structure and either their toxicological limitations or their potential utility in biomedical applications.

This talk will describe the requirements needed to be fulfilled when a novel 2D nanomaterial, such as GO, should be produced for biological applications including their toxicological evaluation. As a general consideration, GO material must be fabricated as stable aqueous suspensions, with an exhaustive reproducibility and careful control of structural, chemical, and bacterial impurities, leading to what we define as '*medical grade'* quality requirement.

More broadly, biological studies of novel nanomaterials must be performed with such '*medical grade'* quality specifications, meaning very specific and thoroughly characterized types of materials, to allow accurate and reliable assessment of hazard or potential in healthcare applications.

## References

[1] Novoselov, K. S. et al, Science 306 (2004) 666.
[2] Hummers W. S. et al., J. Am. Chem. Soc. 80 (1958) 1339.
[3] Ali-Boucetta H., Adv. Healthcare Mater. 2 (2013) 433–441.
[4] Mukherjee S. P., et al. PLoS ONE, 11 (2016) 11:e0166816.
[5] Jasim, D. A. et al., 2D Materials 3 (2016) 014006.
[6] Kostarelos, K. et al. Science 344 (2014) 261.
[7] Rodrigues A. F., et al., 2D Materials 5 (2018) 035020.

## Figures

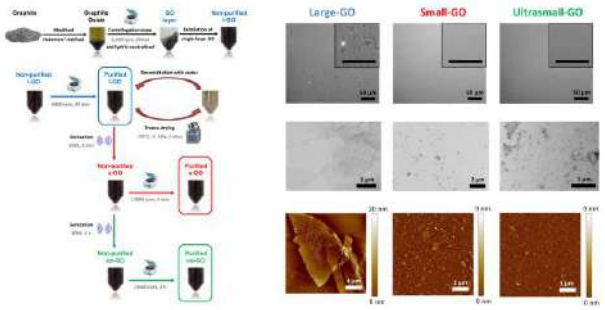


**Figure 1.** Synthesis and structural characterization of *'medical grade'* GO suspensions with three different lateral dimensions.

# Innovative 3D microfluidic brain tumor-on-a-chip systems: design, characterization, and preliminary testing with chemotherapy drug-loaded nanocarriers

**Attilio Marino**[1]
Matteo Battaglini[1]
Omar Tricinci[2]
Alessio Carmignani[1]
Gianni Ciofani[1]

[1]Istituto Italiano di Tecnologia, Smart Bio-Interfaces, Viale Rinaldo Piaggio 34, 56025 Pontedera
[1]Istituto Italiano di Tecnologia, Center for Materials Interfaces, Viale Rinaldo Piaggio 34, 56025 Pontedera

attilio.marino@iit.it

Central nervous system (CNS) tumors comprise over 100 histologically distinct subtypes and are among the most fatal cancers [1]. In children and adolescents, they represent the second cause of death (26% of cases) after leukemia (28%) [2]. Different innovative and personalized anticancer drugs, even if potentially able to treat brain tumors, have not been reached or passed the clinical trial phases due to their limited ability to reach the brain *via* systemic administration [3]. The blood-brain barrier (BBB; *i.e.*, the biological barrier characterized by vascular endothelial cells tightly connected to neurons, astrocytes, and pericytes) represents the main obstacle to the drug delivery from blood microcapillaries to the brain parenchyma. Therefore, intensive research activities have been applied in the last 10 years to the realization of *in vitro* platforms realistically reproducing the BBB to investigate drug delivery to the brain.

In this scenario, our research group designed and characterized the first 1.1 scale model of the brain microcapillaries mimicking blood flow through a fluidic system. The faithful reconstruction of the brain microcapillaries has been obtained through two-photon lithography, an innovative microfabrication approach allowing for rapid and high-resolution prototyping of 3D microstructures (Figure 1). The proposed model can be implemented in at least two configurations. A first device, simple and user-friendly, allows the single-step seeding of endothelial cells and astrocytes on the external surface of the porous micro-tubes. A second one, more biomimetic but more complex, allows the integration of multiple cell types associated with the BBB in physio/pathological conditions (*e.g.*, endothelial cells, astrocytes, pericytes, neurons, and tumor cells). In both configurations, the obtained barrier shows good performances in terms of trans-endothelial electrical resistance (TEER) and reduced molecular permeability. The smart integration of the cell cultures to the microfluidic chip can be provided by our patented solution, which allows for static magnetic field (SMF)-assisted docking and automatic assembly of the magnetized scaffolds (Figure 2). The resulting brain tumor-on-a-chip systems allowed our group to test the anticancer effectiveness of nutlin-3a and nutlin-3a-loaded lipid nanocarriers. Finally, thanks to the complexity of our multicellular model, the specificity of the anticancer effect of nutlin-3a toward glioblastoma cells compared to neural and endothelial cells has been demonstrated.

The proposed brain tumor-on-a-chip systems promise to close the gap between *in vitro* and *in vivo* testing with a pivotal impact on drug discovery. Indeed, the proposed devices will provide more reliable and repeatable results *in vitro*, thus significantly contributing to lowering the risk of both early- and late-stage failures of drug testing in clinical trials. Also, these *in vitro* platforms might produce ethical benefits by excluding drug candidates with low BBB crossing capabilities from *in vivo* tests and therefore reducing animal experimentation.

## References

[1] Miller K.D. et al., CA Cancer J Clin, 5 (2021) 71:381-406
[2] Siegel R.L. et al., CA Cancer J Clin 1 (2022) 72:7-33
[3] Soni S. et al., Adv Pharm Bull 6 (2016) 3:319-335

[4] Marino A. et al., Small, 6 (2017) 14:1702959
[5] Tricinci O. et al., Adv Mater Technol, 10 (2020) 5:2000540
[6] Application IT102019000018614, 11/10/19; PCT/IB2020/059365, 6/10/2020

## Figures

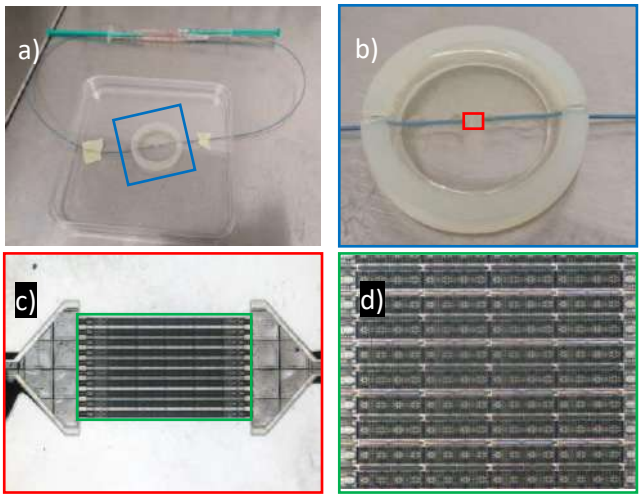


**Figure 1.** 3D microfluidic BBB system. a,b) System connected to syringes. c,d) Microscope images of the porous microtubes in parallel. Endothelial cells can be seeded inside or outside the microtubes to mimic blood microcapillaries.

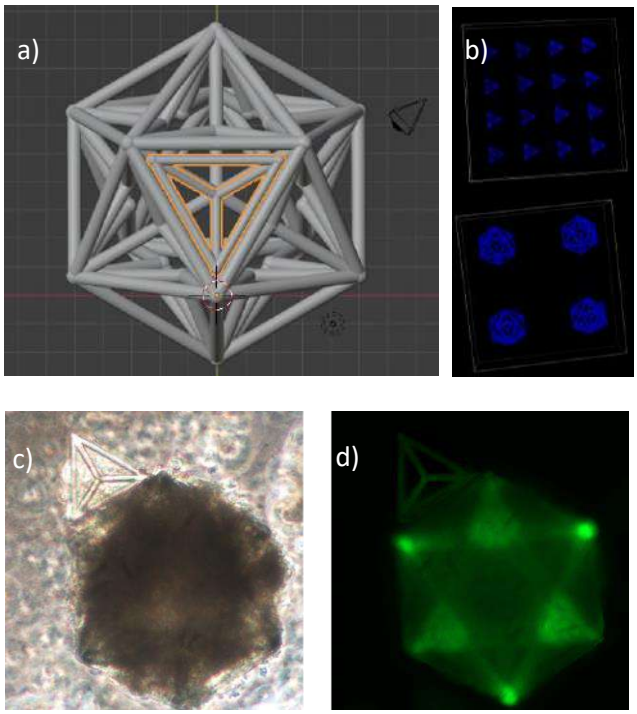


**Figure 2.** Magnetic self-assembly of cell co-cultures. a) 3D rendering of the great dodecahedron with the tetrahedron (highlighted in orange). b) 3D confocal laser scanning microscopy imaging of the tetrahedrons (top) and great dodecahedrons (bottom) fabricated by two-photon lithography. c,d) Magnetic self-assembly of the U-87 glioblastoma cells in the great dodecahedron and HCMEC endothelial cells in the tetrahedrons.

# Inkjet printing of nanobiosensors: limits, challenges, and opportunities

**Giulio Rosati**[1], Massimo Urban[1], Gustavo Dalkiranis[1,2], Gabriel Maroli[1,3], Arben Merkoçi[1,4]

[1]Institut Català de Nanociència i Nanotecnologia (ICN2), Edifici ICN2, Campus UAB - 08193 Bellaterra (Barcelona) Spain
[2]Instituto de Física de São Carlos (IFSC), Universidade de São Paulo (USP), Av. Trab. São Carlense, 400 - Parque Arnold Schimidt, São Carlos, SP, 13566-590 Brazil
[3]National Technological University (UTN-FRBA), Buenos Aires, Argentina
[4]ICREA Passeig Lluís Companys 23 08010 Barcelona, Spain

giulio.rosati@icn2.cat
arben.merkoci@icn2.cat

Electrochemical sensors, biosensors, and nanobiosensors are fundamentally composed of basic electronic components such as electrodes, conducting lines, contacts, and insulators. Therefore, it should not be surprising if the most advanced nanobiosensors are typically fabricated by standard microelectronic methods (also known as clean room based methods) such as photolithography and others.

If on one hand these methods allow for reproducible and ultra-high resolution 3D structures with a wide variety of materials, on the other hand they are very expensive. In fact, they require keeping the working environment completely dust free (possible only in specific spaces called clean rooms) and using high profile equipment.

Simple sensors and biosensors may also be fabricated with easier and out-of-the-cleanroom methods such as sputtering, screen-printing, and other additive fabrication methods. However, biosensors taking advantage of nanomaterials or nanostructures, i.e. nanobiosensors, are complicated to be fabricated with these methods without employing long and difficult decoration protocols.

Inkjet printing emerged in the past years as a promising alternative to both clean room and other printing methods for the fabrication of electrochemical nanobiosensors. This method, combined with nanomaterials-based inks (nanoparticles, 2D flakes, etc.) allows the fabrication of thin-film metal electrodes (100 nm – 1 µm) with a XY resolution in the micrometer range on both rigid and flexible substrates. The drop-on-demand strategy permits saving ink without the need of any mask and allowing for an ultra-short concept to prototype time.

Despite these appealing characteristics, inkjet printing is still struggling to permeate the biosensors market because (i) the equipment devoted to research is still very expensive, (ii) the printing performance depends on the substrate, the ink, and the printing parameters, (iii) the post-printing treatments (drying, sintering, annealing, etc.) are often complicated, time-consuming, or not compliant with many substrates such as paper, textile, and plastics.

In our group, we have proved that consumer (low-cost) inkjet printer can be successfully used for the fabrication of electrochemical biosensors on flexible plastic substrates without any post-printing treatment using metal nanoparticles-based inks [1-3], even with multi-material real-time printing. Furthermore, we have introduced a simple heater that can facilitate the printing on different substrates improving the ink adhesion and that can be printed itself with the same printer [4].

The design of the biosensors is extremely easy and can be performed on any drawing software, including MS Paint. The loading of the ink and printing are simple and straightforward as well. The perspective of our work is to be able to take not the biosensor but it's fabrication at the point of care, replacing the current paradigm of centralized fabrication to a more distributed one that we call ubiquitous printing. This will allow our society to be more resilient to supply chain disruptions (as during the COVID19 pandemic).

## References

[1] Rosati et al., Biosensors and Bioelectronics, 196 (2022) 113737.
[2] Yang et al., Biosensors and Bioelectronics, 202 (2022) 114005
[3] Rosati et al., Scientific Reports,11 (2021) 1-12
[4] Dalkiranis, Trends in Nanotechnology conference, (2022).

## Figures

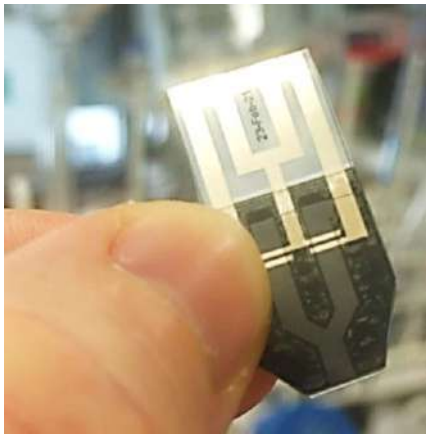

**Figure 1.** Inkjet printed differential electrochemical interdigitated impedance-based biosensor.

# Novel nanostructured materials accelerating osteogenesis

**Margarita D. Apostolova**[1], Ralitsa T. Mincheva[1], Gjorgji Atanasov[1], Sergei I. Tverdokhlebov[2], Yordan S. Handzhiyski[1]

[1]Roumen Tsanev Institute of Molecular Biology - BAS, Acad. G. Bonchev Str., Bl. 21, 1113 Sofia, Bulgaria)
[2]Tomsk Polytechnic University, 30 Lenin Avenue, 634050 Tomsk, Russian Federation)

margo@bio21.bas.bg

Osteoporosis is a disease in which the mineral density of the bone is reduced, its microarchitecture disrupted, and the expression profile of non-collagenous proteins altered. Regular fracture treatment is a complicated, multistage process, affected by cell evidence and regulated by local and systematic factors.

In osteoporotic patients, the incidence of fracture non-unions and mal-unions with poor functional outcomes is up to 20% [1], caused by poor fixation of the implant in the mechanically weak bone and progressive implant loosening at a rate faster than bone callus formation. Although the vast majority of hip fractures occur in osteoporotic patients, these fractures are fixed with implants designed for the fixation of normal healthy bone, thus ignoring the special needs of porous bone. No fracture fixation implants currently available were specifically developed for the fixation of fragility fractures. Many of these fractures, including femoral neck, proximal humerus, and knee fractures are now treated with prostheses generally fixed with bone cement. However, as acrylic fixation requires good quality cancellous bone, typically absent in the osteoporotic population, the incidence of prosthesis loosening and revision surgery is high.

The objective of the study was to develop new bioactive nanostructured materials in both acellular and autologous cell-seeded forms to enhance bone fracture fixation and healing thought creating highly porous structures, which will promote angio- and osteogenesis.

The approach to developing highly effective scaffolds for counteracting the effects of osteoporosis followed the initial lines of inquiry and involved the comparative investigation of the performance of different systems: (a) metal surfaces coated with hydroxyapatite (by micro-arc oxidation method) and/or nanodiamonds (NDs) (b) synthetic and biological polymer chemistry, by using of thermal gelling polymer and thermoplastic aliphatic polyesters, polyacrylamide, and polyethylene glycols, and copolymers; (c) genomic and proteomics analysis; (d) experiments with cell models (endothelial progenitor cells (EPS) and adult human adipose-derived cells MSCs (hADMSCs)).

The results showed that ultradispersed NDs applied on different implant materials or as UCND-coated implants can enhance the mineralization and differentiation of EPS and hADMSCs. NDs incorporated in “intelligent” gel matrixes have functioned as scaffolds attracting calcium ions and inducing hydroxyapatite crystals growth.

Further investigations demonstrated that in vitro EPS transformation to osteoblasts and long-term functions (as measured by intracellular and extracellular matrix protein synthesis and calcium-containing mineral deposition) were enhanced in an osteoprogenitor medium. In vitro and in vivo experiments of the three different micro-arc oxidation coatings prove high biocompatibility towards adult stem cells and in vivo biocompatibility.

These results provide initial evidence that synthetic nanomaterials may exhibit specific properties that are comparable to natural ones, and the nanomaterial architecture may serve as a superior scaffolding for promoting the EPS and adult stem cells differentiation and biomineralization.

We are grateful to the National Science Fund of Bulgaria (Grant Agreement KP-06-Russia/20) for their financial support

## References

[1] . Nicholson, N. Makaram, A. Simpson, JF Keating, Injury 52S2 (2021) S3–S11.

# Evaluating the collective dispersion of magnetic-enzymatic nanomotors

**Anna C. Bakenecker**[1]
Juan C. Fraire[1], Samuel Sánchez[1]

[1]Institute for Bioengineering of Catalonia (IBEC), Smart Nano-Bio-Devices, C. Baldiri Reixac 10-12, 08028 Barcelona, Spain

ssanchez@ibecbarcelona.eu, abakenecker@ibecbarcelona.eu

Many treatments are based on the systemic administration of high amounts of therapeutic drugs, which leads to side effects and limited accumulation at the target side. Therefore, methods to efficiently administer, penetrate and locally release the drugs such as smart nanoparticles (NPs) for precision medicine are highly needed. For this, NPs with self-propelling properties, which are called nanomotors, have been proposed as drug delivery systems able to overcome these limitations [1].

However, the fundamental understanding of the collective movement i.e. swarming behavior of these nanomotors is still lacking. And many nanomotor approaches are either showing high velocities or directional steering abilities, but not both at once.

Here, we present nanomotors with dual functionalities: they can be enzymatically powered and magnetically steered. These properties are being investigated as a novel strategy to deliver drugs with high precision.

**METHODS & MATERIALS**
Our nanomotors are 500 nm polymeric nanoparticles carrying superparamagnetic nanoparticles (SPIONs) on their surface giving the nanoparticles their magnetic properties. The nanoparticles were functionalized by using urease as activating enzyme [2].

To apply different magnetic field configurations, a permanent magnet array, a so called Halbach-ring, has been developed, able to apply homogeneous and gradient magnetic fields [3,4]. A magnetic particle, carrying a magnetic moment $\vec{m}$ is experiencing a force of the form

$$\vec{F} = \nabla(\vec{m} \cdot \vec{B})$$

which is pulling the nanomotors towards higher magnetic field strength $\vec{B}$. The direction of the force and therefore the direction of movement can be chosen as desired, by rotating the permanent magnet ring.

The movement behavior was analyzed using image analysis tools (Matlab) of the recorded videos of swarming nanomotors. This allows for a better understanding and quantification of the collective dispersion under different experimental conditions, such as the concentration of fuel (urea) or magnetic field configuration.

**RESULTS**
The results show swarming behaviors in the presence of the fuel for nanomotors due to their enzymatic activation, meaning they spread over a larger area and form pattern of higher and lower nanomotor concentrations. When applying a magnetic gradient field, the nanomotors showed directionality due to the presence of a magnetic force. The conducted image analysis gains an insight into these combined movement behaviors.

## References

[1] S. Sanchez et al., Chemically powered micro- and nanomotors, Angewandte Chemie - International (2015)
[2] J. C. Fraire, Light triggered Mechanical Disruption of Extracellular Barriers by Swarms of Enzyme Powered Nanomotors for Enhanced Delivery, (submitted)
[3] P. Blümler et al., Contactless Nanoparticle-Based Guiding of Cells by Controllable Magnetic Fields, Nanotechnology, Science and Applications (2020)
[4] A. C. Bakenecker et al., A concept for a magnetic particle imaging scanner with Halbach Arrays, Physics in Medicine & Biology (2020)

## Figures

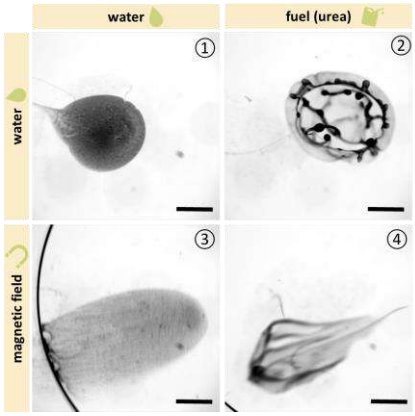


**Figure 1.** Representative snapshots from the recorded videos for each condition: 1) control, nanomotors in water show passive diffusion and sedimentation 2) fuel, nanomotors in urea show active propulsion and pattern formation 3) nanomotors in water and magnetic gradient field show directional pulling, but also sedimentation 4) fuel and magnetic field, nanomotors show active propulsion and a fast directional movement. Scale bar 2 mm.

# Biomimetic Nanoparticles for Cancer Target Immunotherapy

**Clara Baldari**[1], Gabriele Maiorano[2]; Giuseppe Gigli[1,2], Ilaria Elena Palamà[2]

1. Department of Mathematics and Physics, University of Salento, Monteroni Street, 73100 Lecce, Italy
2. Nanotechnology Institute, CNR-NANOTEC, Monteroni Street, 73100 Lecce, Italy

clara.baldari@unisalento.it

**Introduction:**
Nanotechnology gives the opportunities to target specifically cancer cells while reducing the side effects of conventional therapies through synthesis of nanoparticles (NPs) with tuneable properties (size, shape, charge, surface modifications, etc).
NPs preferably accumulate in tumor tissues due to the enhanced permeability and retention effect (EPR) allowing efficient delivery and optimal doses of therapeutic compounds to specific tissue or cell types with important applications in immunotherapy[1,2,3].

The aim of this study involves the production of polymeric nanoparticles (pNPs) able to selectively target cancer cells and simultaneously activate the immune response.
A biocompatible FDA approved polymer of particular relevance for biomedical applications is polycaprolactone (PCL) that can be easily modified to improve biomimetic features to enhance targeting properties[3,4].

**Methods:**
We develop pNPs[2,4] starting by polycaprolactone (PCL) as NPs core and cancer cell membrane as coating[5,6,7].
Morphology and size of pNPs are then characterized by DLS, SEM and TEM. pNPs uptake and homotypic binding are evaluated *in vitro* in human cancer cell lines by fluorescent microscopy and flow cytometry.

**Results:**
PCL-NPs core made with own synthetised carboxy-termined PCL, show a homogeneous distribution.
Changes in both size and surface charge confirm that nanoparticles were successfully coated with cell membranes. Also, morphological images obtained by TEM, show a distinct layer on the surface of PCL NPs verifying the correct coating with cell membrane.
The higher internalization rates of biomimetic-NPs in their source cells compared to other cell lines was confirmed by fluorescent microscopy and flow cytometry analysis, confirming the self-recognition and the preferentially interaction with cancer source cells.

**Conclusion and discussion:**

A diversity of cell types selected as membrane source allowed to develop innovative biomimetic nanoparticles that through an intrinsic strategy of self-recognition typical of cancer cell membranes (homotypic targeting) can be used to deliver drugs or genes.

On the other hand, biomimetic-NPs could be used as efficient tool in precise cancer immunotherapy for the possibility to employ patient-derived cell membranes.

**Acknowledgement:**
This study was supported by “Tecnopolo per la medicina di precisione” (TecnoMed Puglia) - Regione Puglia: DGR n. 2117 del 21/11/2018, CUP: B84I18000540002” and Progetto PON ARS01_00906 “TITAN - Nanotecnologie per l’immunoterapia dei tumori”, finanziato dal FESR nell’ambito del PON “Ricerca e Innovazione” 2014 – 2020 – Azione II – OS 1.b.

## References

[1] C. Guido, G. Maiorano, B. Cortese, S. D’Amone and I.E. Palamà, “Biomimetic Nanocarriers for Cancer Target Therapy”, Bioengineering, (2020)
[2] M. Karimia, A. Ghasemib, P.S. Zangabad, R. Rahighic, S.M.M. Basrie, H. Mirshekarig, M. Amirib, Z. Shafaei Pishabadh, A. Aslanib, M. Bozorgomidi, D. Ghoshj, A. Beyzavik, A. Vaseghil, A. R. Arefm, L. Haghanin, S. Bahramia, and M.R. Hamblino, “Smart micro/nanoparticles in stimulus-responsive drug/gene delivery systems”, Chem Soc Rev. 45(5): 1457–1501 (2016)
[3] V. Schirrmacher, “From chemotherapy to biological therapy: A review of novel concepts to reduce the side effects of systemic cancer treatment (Review)”, INTERNATIONAL JOURNAL OF ONCOLOGY 54: 407-419, (2019)
[4] B. Bahramia, M. Hojjat-Farsangic, H. Mohammadie, E. Anvarig, G. Ghalamfarsah, M. Jousefif, F. Jadidi-Niaraghe, “Nanoparticles and targeted drug delivery in cancer therapy”, Immunology Letters 190 64–83 (2017)

[5] M.J. Ramalho, E. Sevin, F. Gosselet, J. Lima, M.A.N. Coelho, J.A. Loureiro, M.C. Pereira, "Receptor-mediated PLGA nanoparticles for Glioblastoma Multiforme treatment", International Journal of Pharmaceutics (2018)

[6] Ronnie H. Fang, Che-Ming J. Hu, Brian T. Luk, Weiwei Gao, Jonathan A. Copp, Yiyin Tai, Derek E. O'Connor, and Liangfang Zhang, "Cancer Cell Membrane-Coated Nanoparticles for Anticancer Vaccination and Drug Delivery", Nano Letters, 2014, 14, 4, 2181–2188, (2014)

[7] S. Witt, T. Scheper, J.G. Walter "Production of polycaprolactone nanoparticles with hydrodynamic diameters below 100 nm", Eng Life Sci., 19:658–665, (2019)

## Figures

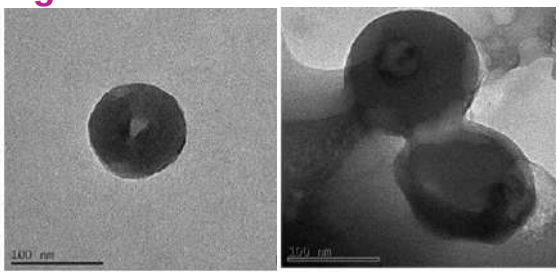

**Figure 1.** TEM images of Biomimetic NPs

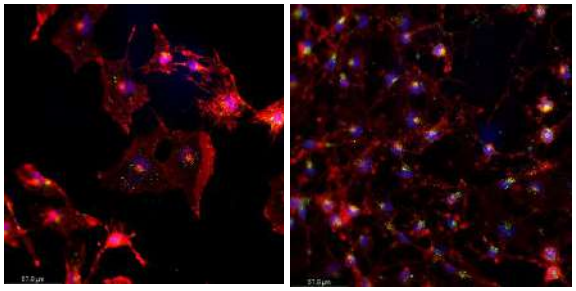

**Figure 2.** Cellular uptake of Biomimetic NPs after 24 h of treatment to fluorescent microscope. Phalloidin TRITC for beta actin, FITC for NPs and DAPI for nuclei

# Return of the Jedi: Fighting Antimicrobial Resistance with Nanobiotics

**Iris L. Batalha**[1,2,3], Audrey Bernut[4], Mark Welland[2], R. Andres Floto[3]

[1] Institute for Bioengineering of Catalonia (IBEC), Barcelona, Spain
[2] Nanoscience Centre, Department of Engineering, University of Cambridge, Cambridge, United Kingdom
[3] Molecular Immunity Unit, Department of Medicine, University of Cambridge, Cambridge, United Kingdom
[4] Université Paris-Saclay, Inserm/UVSQ, Montigny-le-Bretonneux, France.

ibatalha@ibecbarcelona.eu

Tuberculosis (TB), a mycobacterial disease that in humans can be traced back to 9,000 years ago in Atlit Yam, a city now under the Mediterranean Sea, is still today the second deadliest infection after COVID-19 [1]. Being primarily a pulmonary pathogen, the bacteria enters the respiratory tract via inhalation and is readily phagocytosed by alveolar macrophages. In the lungs, the pathogen can either be eliminated by the immune system or persist in a quiescent (latent TB) or active state [2, 3]. The World Health Organization estimates that 1/4 of the world population is infected with latent TB and 10% of those will develop active disease [4]. The discovery of antibiotics in the 40s brought hope for the eradication of the disease, but *M. tuberculosis* showed the ability to develop drug resistance through genetic mutations, not to mention that most first-line antibiotics only target replicating bacteria [2,3].

Inefficient delivery of drugs to the target site is one of the main drivers of the emergence of multi- and extensive drug resistance, as bacilli are exposed to subminimal inhibitory concentrations of drugs. Furthermore, patients must endure long treatments with multiple toxic antibiotics that have numerous side effects, which undermines patient compliance and ultimately plays a role in the rise of resistant strains. Reformulating existent antibiotics in nanocarriers (nanobiotics) is a viable solution to provide targeted drug release, reducing the dosing frequency and the overall systemic toxicity.

In particular, the conjugation of therapeutic molecules to polymers has gained significant attention from the pharmaceutical industry, as it offers the possibility to improve the aqueous solubility and stability of drugs and, consequently, extend their plasma half-life and alter their biodistribution. Such traits are particularly relevant when delivering cytotoxic drugs, which often exhibit poor solubility and rapid clearance. The main setback that the industry is facing relates to the difficulties in achieving a controlled conjugation of the therapeutic agent, which results in polydisperse polymers with wide-ranging drug loadings and sites of modification that fail to meet GMP guidelines [5].

Here, we report the synthesis of a well-defined isoniazid-based polyester with nearly quantitative loading efficiency using a fast lipase-catalysed esterification reaction, followed by hydrazone bond formation (**Figure 1**). Nanobiotics composed of isoniazid-conjugated polymer and encapsulated clofazimine presented lack of toxicity, dose responsiveness, and improved therapeutic efficacy in the treatment of mycobacterial infection in a zebrafish larval model when compared to free drugs (**Figure 2**) [6]. The main advantage of this system is the synthetic simplicity and versatility. The drug is directly conjugated to the polymer without the need for any further chemical modifications. The drug-polymer bond is acid-labile, allowing site-specific drug release, and the polymer itself is hydrolysable facilitating excretion. Polymer size can be tuned without affecting the high drug loading capacity since there is one drug conjugation site per monomeric unit of polymer.

With the slow development of new antibiotics, tunable polymeric nanobiotics offer an opportunity to deliver more effective and more tolerable combination chemotherapy using existing drugs for *M. tuberculosis* and other infectious diseases.

## References

[1] European Centre for Disease Prevention and Control – An Agency of the European Union. *Tuberculosis remains one of the deadliest infectious diseases worldwide, warns new report* (Press Release March 24th 2022).

[2] Griffiths, G., Nystrom, B., Sable, S. B. & Khuller, G. K. *Nanobead-based interventions for the treatment and prevention of tuberculosis.* Nat. Rev. Microbiol. 8, 827-834, doi:10.1038/nrmicro2437 (2010).

[3] Pai, M. *et al. Tuberculosis.* Nat. Rev. Dis. Primers 2, 16076, doi:10.1038/nrdp.2016.76 (2016).

[4] Global tuberculosis report 2021. Geneva: World Health Organization; 2021. Licence: CC BY-NC-SA 3.0 IGO.

[5] Ekladious, I., Colson, Y. L. & Grinstaff, M. W. *Polymer-drug conjugate therapeutics: advances, insights and prospects.* Nature Reviews Drug Discovery 18, 273-294 (2019).

[6] Batalha, I. L. *et al. Polymeric nanobiotics as a novel treatment for mycobacterial infections.* Journal of Controlled Release 314, 116-124 (2019).

## Figures

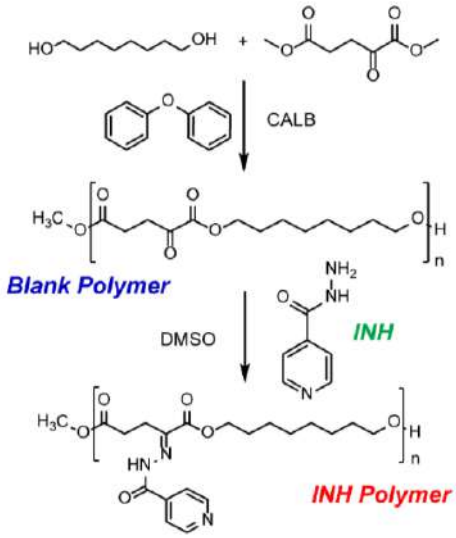


**Figure 1.** Synthesis of an α-keto polyester by (trans)esterification reaction catalysed by Lipase acrylic resin from *Candida antarctica* and conjugation to isoniazid (INH).

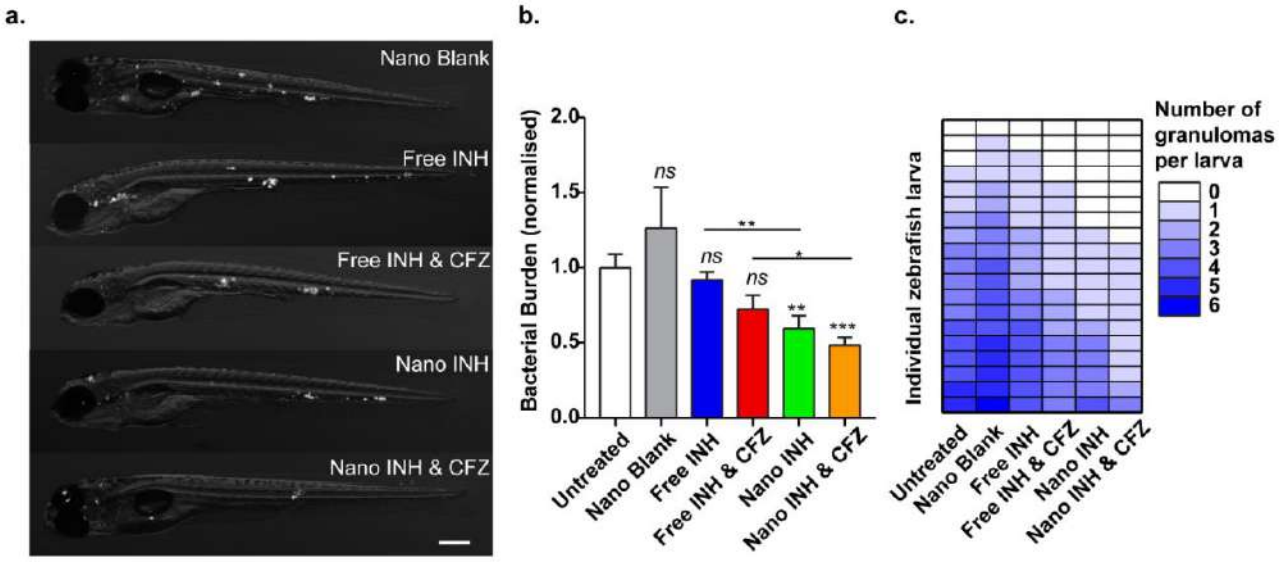


**Figure 2.** Effect of nanobiotics at 3 days post-infection on zebrafish infected with fluorescently-labelled *M. marinum*. **a.** representative images (scale bar, 200 µm). **b.** quantification of bacterial load (results plotted as mean ± SEM from 2 independent experiments; n=21). **c.** Quantification of granuloma number at 3dpi. Results are plotted as mean ± SEM from 2 independent experiments (n=19).

# Piezoelectric membranes to enhance skin regeneration

**Andreu Blanquer**[1,2], Laura Lefaix[3], Elena Filova[2], Jaume Esteve[3], Lucie Bacakova[2], Gonzalo Murillo[3]

[1]IUniversitat Autònoma de Barcelona, Campus Bellaterra, Cerdanyola del Vallès, Spain
[2]Institute of Physiology of the Czech Academy of Sciences, Videnska 1083, Prague, Czech Republic
[3]Instituto de Microelectronica de Barcelona (IMB-CNM, CSIC), C. dels Til·lers, Cerdanyola del Vallès, Spain

andreu.blanquer@uab.cat

Epithelium in healthy skin establishes and maintains a constant electrical potential. When skin layers are damaged, their electrical resistance disappears and an electric field is created locally in the injured epithelium [1]. However, it has been suggested that the endogenous electric fields, created at wound sites, are compromised or absent. In addition, diabetic skin and normal skin of aged patients evince a lower transepithelial potential, which could contribute to a delay of wound healing and to impaired microcirculation [2]. Chronic wounds affect millions of patients around the world, and it is estimated that this would increase steadily in the future due to population ageing. The prevalence of chronic wounds increases along with vascular diseases and diabetes mellitus, and along with systemic factors such as advanced age [3]. Thus, new therapeutic approaches are being developed to enhance the wound healing process. In recent years, some studies analyzed the effect of exogenous electric field to enhance wound healing [4]. Piezoelectric materials are able to create an inherent electric field when they are strained. The use of piezoelectric nanogenerators could enhance skin regeneration due to a local electrical stimulation. Here, we evaluate the biocompatibility of ZnO and polyvinylidene difluoride (PVDF) piezoelectric nanogenerators and their effect on the proliferation and differentiation of cell types involved in skin wound healing.

ZnO nanogenerators were synthesized by hydrothermal growth on an AlN thin-film layer previously deposited on glass coverslips. ZnO nanosheets with a thickness of 22 ± 2 nm were synthesized. PVDF nanofibrous membranes were deposited on Au thin-film layer by electrospinning technique, obtaining a mesh of nanofibers with 110 ± 20 nm of diameter. Human keratinocytes (HaCaT cells), fibroblasts (NHDF) and endothelial cells (HUVEC) were used for *in vitro* experiments. Keratinocytes and fibroblasts were cultured in Dulbecco's Modified Eagle's Medium (DMEM) supplemented with 10% of fetal bovine serum (ThermoFisher Scientific), and endothelial cells were cultured in Endothelial Growth Medium (EGM-2) with supplements (PromoCell). Cell viability and initial cell adhesion was analyzed after 24 h in culture using Live/Dead Kit (Invitrogen) and phalloidin staining of actin stress fibers, respectively. Cell proliferation was evaluated using resazurin assay (Sigma-Aldrich). Differentiation and stratification of keratinocytes were analyzed by immunofluorescence of cytokeratin 10 and 14. Cytokeratin 14 is presented in a basal proliferating layer, whereas cytokeratin 10 is presented in upper layers. The type I collagen synthesized by fibroblasts was immunofluorescently stained and quantified after 7 days in culture. The maturation of endothelial cells was evaluated by immunofluorescence of von Willebrand factor and platelet-endothelial cell adhesion molecule (PECAM-1, CD31).

ZnO nanogenerator arrays demonstrated to be cytocompatible for three cell types involved in skin wound healing. ZnO nanogenerators allowed cell adhesion and spreading of all three cell types, and cell viability assay showed that they were not cytotoxic (Figure 1A). In addition, the number of keratinocytes adhered to ZnO arrays was significantly higher than on glass coverslips controls. All three cell types were able to proliferate on ZnO nanogenerators. Interestingly, the proliferation rate of fibroblasts on ZnO nanogenerators was reduced during the first 3 days in culture, although on day 7 no differences were observed and even more cells were detected after 14 days in culture. Regarding endothelial cells, the number of cells was significantly higher on ZnO nanogenerators after 7 days in culture.

Keratinocyte differentiation and stratification were analyzed by cytokeratin expression. After 14 days in culture, a monolayer of basal keratinocytes and a second layer of differentiated keratinocytes was observed. The quantification of the area covered by differentiated cells showed a significantly increase of cytokeratin 10-positive cells on the ZnO nanogenerator samples. As for the fibroblasts differentiation, the collagen synthesis by cells seeded on ZnO nanogenerators was higher by 50% than by the cells growing on control samples. The maturation of endothelial cells did not show significant differences between ZnO nanogenerator and the controls.

For PVDF nanogenerator membranes, similar results regarding the cytocompatibility were obtained. Cell viability analysis did not show any cytotoxic effect of PVDF on keratinocytes, fibroblasts (Figure 1B) and endothelial cells. The cells were able to proliferate on PVDF without significant differences compared to control samples. Regarding the keratinocyte differentiation, after 7 days in culture, a basal layer of cells was positively stained for cytokeratin 14, and few cytokeratin 10-positive cells started to appear in the second layer. Endothelial cells were able to maturate on PVDF

nanogenerator membranes. Additional experiments will be performed to quantify the collagen synthesized by fibroblasts growing on PVDF membranes.

The present results are in agreement with the previous results of the positive effect of electrical stimulation on wound healing. Both piezoelectric ZnO and PVDF are considered biocompatible materials. In addition, our group previously analyzed the cytocompatibility of these two piezoelectric materials for bone healing applications, with good results in terms of viability, proliferation and cell-material interaction [5,6].

In conclusion, piezoelectric ZnO and PVDF nanogenerators allowed cell adhesion and proliferation, and proved to be cytocompatible for skin applications. Endothelial cells matured normally on both types of piezoelectric materials. Moreover, ZnO nanogenerators enhanced the collagen synthesis of fibroblasts and the differentiation and stratification of keratinocytes. The *in vitro* results indicated that ZnO and PVDF nanogenerators could be considered promising nanomaterials to enhance skin wound healing.

## References

[1] Zhao et al., Semin Cell Dev Biol, 20:6 (2009) 674-982.
[2] Nuccitelli et al., Wound Repair Regen, 19:5 (2011) 645:655.
[3] Sen et al., Wound Repair Regen, 17 (2019) 763-771.
[4] Koel, Houghton, Adv Wound Care, 3:2 (2014) 118-126.
[5] Murillo et al., Adv Mater, 29:24 (2017) 1-7.
[6] Kitsara et al., Nanoscale, 11 (2019) 9806-9817.

## Acknowledgements

This project has received funding from postdoctoral fellowship Beatriu de Pinós, funded by the government of Catalonia and European Horizon 2020 research and innovation program (grant agreement No. 801370).

## Figures

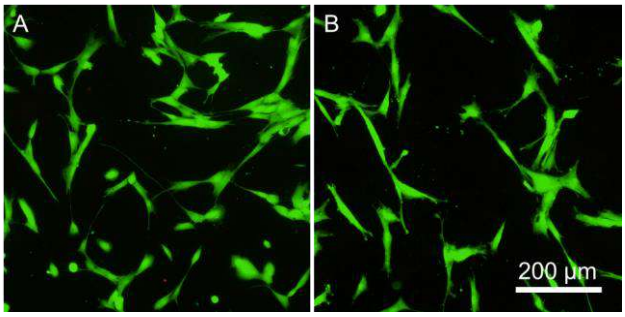


**Figure 1.** Cell viability of fibroblasts growing on ZnO (A) and PVDF (B) nanogenerators. Live (green) and dead (red) cells evaluated using the Live/Dead Kit after 24 h in culture. Olympus IX71 microscope, DP80 digital camera, obj. x 20.

# Porated liposomes: towards new nanomotors model

**Bárbara Borges Fernandes** [1,2], Azzurra Apriceno[1], Safa Almadhi[3], Subhadip Ghosh[1], Lorena Ruiz-Pérez[1], Gabriel Ing[3], Ian Williams[1,4] and Giuseppe Battaglia[1,3,5]

[1]Institute for Bioengineering of Catalonia (IBEC), The Barcelona Institute of Science and Technology (BIST), Barcelona, Spain.
[2]Department of Physics, University of Barcelona, Barcelona, Spain.
[3]Department of Chemistry and Institute for the Physics of Living Systems University College London, London, UK.
[4]Department of Physics, University of Surrey, Guildford, UK.
[5]Catalan Institution for Research and Advanced Studies (ICREA), Barcelona, Spain.

gbattaglia@ibecbarcelona.eu

Cells and microorganisms like bacteria use chemotaxis to move directly in response to concentration gradients of nutrients and toxins [1]. Likewise, synthetic delivery systems could take inspiration from nature to mimic this kind of transport. Ultimately, it could guide nanomotors in the body in a specific way, according to concentration gradients occurring physiologically [2].

Janus colloids/particles are the most studied chemotactic synthetic systems. They consist of spheres with one hemisphere covered with a catalyst, which results in a chemical gradient across its surface. This asymmetry is necessary to induce phoretic motion [3].

Envisioning therapeutical applications, proteins could be used as a catalyst in developing biocompatible motors, as their substrate and metabolites are also biocompatible and very versatile. Most of these nanomotors use proteins asymmetrically distributed on the surface of nanoparticles or nanovesicles [4]. However, these objects are unknown to the immune system. If injected intravenously, they tend to be covered with protein corona once in the blood, which can change their surface chemistry [5].

Therefore, we present a system with the basic characteristics to achieve a minimal chemotactic cell in which the enzyme is encapsulated inside a vesicle (Figure 1). It consists of an asymmetric liposome of 100 nm (made of soy phosphatidylcholine) with encapsulated glucose oxidase. The asymmetry is given by the presence of pores in the membrane, inserted by the protein alpha-hemolysin. Mass ratios of 0.075 and 0.1 Hly/lipid were used, resulting in ~2 and ~3 pores per liposome (Figure 2).

When the liposome is placed in an environment with glucose, the catalysed reaction occurs in its lumen. The products diffuse outwards through the pores, creating a local concentration gradient. The asymmetric distribution of products along its surface generates a slip velocity that moves the vesicle in response to the glucose concentration gradient (Figure 3).

The motion of the liposomes labelled with rhodamine octadecyl ester perchlorate (1%) was investigated in an Ibidi microfluidic (Figure 4). A concentration gradient of 0.05 M of glucose was established in the channel. For this particular channel, a higher concentration gradient of glucose would induce advective flow, which would hide the movement caused by chemotaxis [6].

In this experimental setup, several phenomena can be observed. The presence of the concentration gradient itself results in a difference in the interaction potential between the solute and the channel walls along the x direction. In the same way, the interaction between the solute and the vesicle's external surface will be different in the x direction, which will give rise to a slip velocity. This passive movement, called diffusioosmophoresis, happens even in inactive particles (pristine liposomes, for example).

On the other hand, active movement is related to locomotion in response to the gradient of the products generated by the enzyme-catalysed reaction. The concentration of products that is asymmetrically distributed on the surface of the liposome will result in a slip velocity that will be aligned with the concentration gradient of glucose: chemotaxis.

The movement of pristine liposomes, liposomes with encapsulated GOX with no pores (GOX-L) and with ~2/3 pores (GOX-L-Hly), was imaged with a confocal microscope and analysed with the program Trackpy.

While the pristine liposome and the one with encapsulated glucose oxidase (GOX-L) presented a velocity towards low glucose concentration, the displacement of liposomes with pores (~3) was reverted to the opposite direction. The movement of the pristine liposome and the GOX-L is due to diffusioosmophoresis. In the absence of a glucose concentration gradient, vesicles present only Brownian motion (Figure 5).

For active vesicles, the drift velocity combines diffusioosmophoresis and chemotaxis. With ~2 pores, the chemotactic rate is on the same magnitude as the diffusioosmophoresis, cancelling any drift movement. With ~3 pores, the chemotactic velocity suppresses the diffusioosmophoresis, resulting in a net drift with a speed of ~-0.7 μm/s towards high glucose concentrations (Figure 6).

In conclusion, the experiment in the microfluidic device highlights the contribution of diffusioosmophoresis and chemotaxis to the vesicle's movement. It was observed that the porated liposomes with encapsulated glucose oxidase could move in response to a glucose concentration

gradient. Its direction could be controlled according to the presence/absence of pores in its membrane.

## References


[1] G. H. Wadhams, J. P. Armitage, Nat Rev Mol Cell Biol, 5 (2004) 1024-1037.

[2] A. Joseph, C. Contini, D. Cecchin, S. Nyberg, L. Ruiz-Perez, J. Gaitzsch, G. Fullstone, X. Tian, J. Aziz, J. Preston, G. Volpe, G. Battaglia, Science Advances 3 (2017) 1-12.

[3] B. Liebchen and H. Löwen, Acc. Chem. Res. 51 (2018) 2982−2990.

[4] T. Patiño, X. Arqué, R. Mestre, L. Palacios, S. Sánchez, Acc. Chem. Res. 51 (2018) 2662−2671.

[5] C. Saraiva C. Praça, R. Ferreira, T. Santos, L. Ferreira, L. Bernardino, Journal of Controlled Release 235 (2016) 34–47.

[6] I. Williams, S. Lee, A. Apriceno, R.P. Sear, G. Battaglia, Proceedings of the National Academy of Sciences, 117 41 (2020) 25263-25271.


## Figures

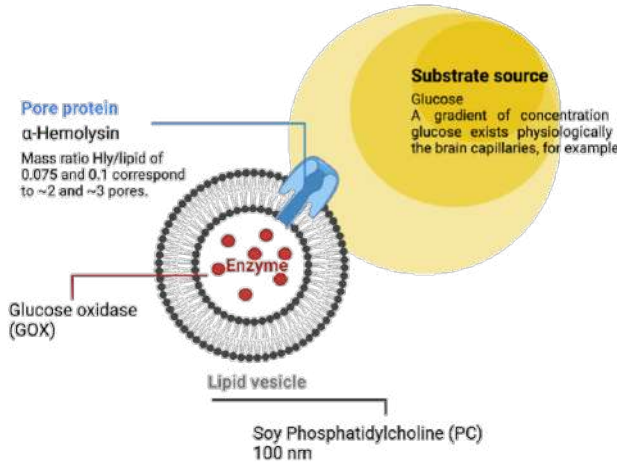


**Figure 1.** Scheme of a porated liposome with encapsulated glucose oxidase placed in an environment with a concentration gradient of glucose.

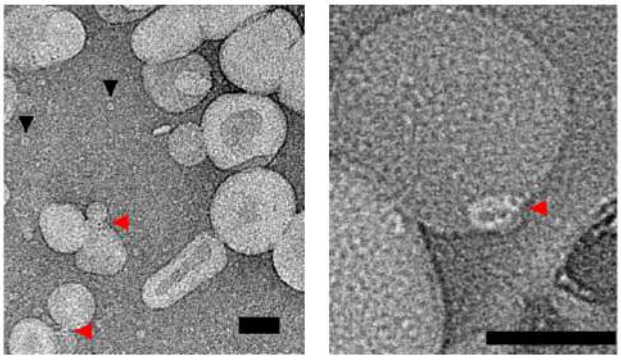

**Figure 3.** TEM micrographs of liposomes incubated with α - Hemolysin. Black and red arrows indicate Hly unbound (black) and inserted into liposomes (red), respectively. Scale bar, 50 nm.

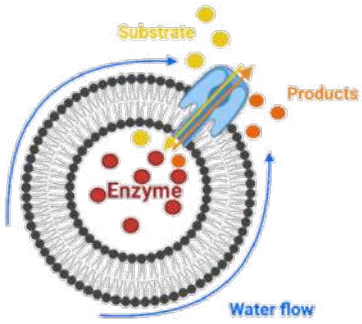


**Figure 3.** Illustration of the reaction occurring inside the porated lipid vesicle indicating the substrate and product diffusion and the generated water flow.

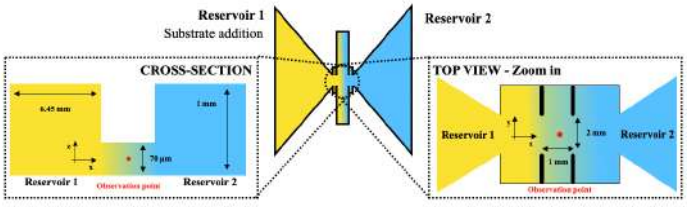


**Figure 4.** Top view of the Ibidi microfluidic device and an insert of the cross-section view.

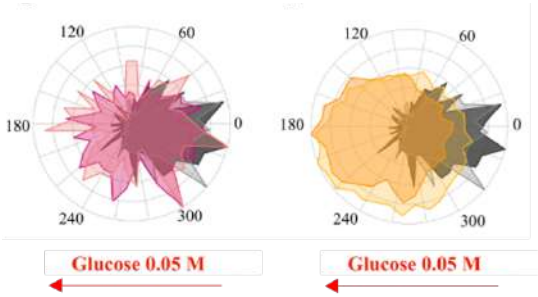


**Figure 5.** Polar histogram with displacements of pristine liposome (grey) and liposomes with 2 pores (pink) and 3 pores (orange).

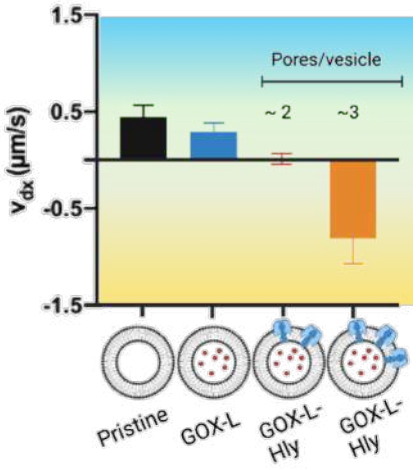


**Figure 6.** Drift velocities of pristine liposomes, GOX encapsulated liposomes without and with pores.

# Spatial mapping of biophysical properties in human cells and tissues by scanning probe microscopy (SPM)

**Annalisa Calò**[1,2], Yevgeniy Romin[3], Larissa Huetter[2], Ruben Millan Solsona[2], Gabriel Gomila[2]

[1]Universitat de Barcelona, Department of Biomedical Engineering, C/Martì I Franquès 1-11, 08028 Barcelona
[2]IBEC, Institute for Biomedical Engineering, C/Baldiri Reixac 10-12, 08028 Barcelona
[2]Memorial Sloan Kettering Cancer Center, 1275 York Avenue NY 10065

annalisa.calo@ub.edu

Illnesses can be described in terms of changes in the biophysical properties of cells and tissues, like the elasticity and the electric charge. Mechanic and dielectric properties thus can give useful information for diagnostics and therapeutics. In this work, I present the SPM as a tool to obtain multiparametric mechanic and dielectric maps at the surface of cells and tissues simultaneously. In SPM the dielectric imaging has been relatively less studied compared to the mechanical one, nevertheless its very high sensitivity makes it a valuable addition to the standard force volume mapping [3]. The objective of this research is to distinguish cell phenotypes and areas in tissue sections with heterogeneous biochemical composition at the microscale using simultaneous mechanic and dielectric mapping with SPM. This research aims to bring the SPM from the basic research and the exploration of few sample areas of nanometer-size materials with high pixel density, to the clinical contest [2,3,4], where big datasets are required for statistics, that imply testing many patients and scanning millimeter-size areas of the sample. Such data can be employed in correlative analysis using other biomedical imaging techniques and analytic techniques. Results obtained with tissue sections from patients suffering amyloidosis, as well as on fibroblasts from patients suffering different types of lung cancer, both from the Clinic Hospital in Barcelona will be shown.

## References

[1] M. Checa et al. Small Methods 5 (2021) 2100279.
[2] Calò et al, Scientific Reports, 10 (2020) 15664
[3] Tello-Lafoz et al. Immunity 54 (2021) 1037-1054
[4] Sylvie Deborde et al. Cancer Discovery 12 (2022) 1-20.

## Figures

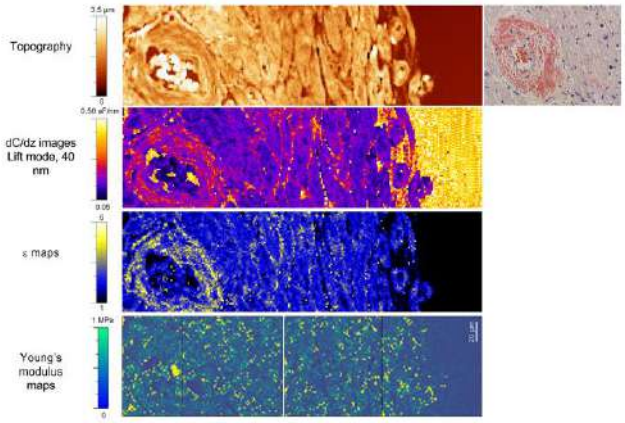


**Figure 1.** Example of multiparametric mechanical-dielectric mapping in a heart tissue section from a patient of Hospital Clinic (Barcelona) suffering from AL-λ amyloidosis.

# Encapsulation of magnetic nanocubes in core-shell polymeric nanoparticles for their application in hyperthermia

**Ivana Cavaliere**[1],
Aritz Lafuente López[1],
Alejandro Gomez Roca[1],
Josep Nogués[1],
Claudio Roscini[1],
Daniel Ruiz[1].

[1] Catalan Institute of Nanoscience and Nanotechnology (ICN2), Campus UAB, 08193 Bellaterra, Barcelona, Spain

ivana.cavaliere@icn2.cat

Cancer is still considered one of the leading causes of death worldwide. Current treatments, like surgery or chemotherapy, have the critical inconveniences of being invasive, not localized, with limited effectiveness, and leading to severe side effects for the patients [1]. Nanoparticles are a powerful tool to overcome these limitations, improving drugs' bioavailability and enhancing their stability, presenting a high loading capacity. Stimuli-responsive nanoparticles that can change their physicochemical properties under the influence of an external or internal stimulus are of particular interest [2]. In cancer therapy, nanomaterials able to generate heat under certain stimulus have gained great attention in recent decades. Indeed, hyperthermia, defined as the increase of cells' temperature above 40 °C, is considered a promising treatment used alone or in combination with other traditional ones. This increase in temperature can directly induce cancer cells' death or provoke harmful side effects, making them less resistant to the immune system or chemotherapeutic drugs. Localizing this heating effect only to the cancer region is crucial to avoid damage to healthy tissues [3]. Two main strategies can be recognized: photothermia and magnetic hyperthermia. The photothermal effect is achieved when nanomaterials, able to convert the absorbed light into heat, are used. In this case, near infrared (NIR) radiation is commonly used as the source of light because it penetrates deeper into tissues without causing side effects. Indeed, in certain NIR regions, neither water nor biomolecules absorb or scatter the light [4]. On the other side, magnetic hyperthermia is accomplished when magnetic nanomaterials are used, generating a temperature increase under an alternating magnetic field. If the amplitude and frequency of the field are low, no damage to healthy tissues is caused. Therefore, it is possible to treat tumors located deeply in the body since a magnetic field penetrates better than light, which can only reach superficial tumors [5]. In both photothermia and magnetic hyperthermia, the amplitude of the external stimulus and its time of application influence cells' death.

Among stimuli-responsive nanoparticles, biocompatible magnetic iron oxide nanoparticles (IONPs) are very promising as they respond to both NIR and magnetic fields. Moreover, they can be easily located in the tumor by guiding them with an external static magnetic field. Additionally, they can be used as a contrast agent in MRI [6]. However, parameters such as particles' composition, morphology, size, shape, and magnetic anisotropy, must be tuned to improve the heating efficiency. It has been demonstrated that cubic-shaped IONPs present a higher magnetization and heating efficiency than their spherical counterparts [7]. However, when IONPs are dispersed in water or physiological media, they drastically suffer aggregation, losing their physicochemical properties. IONPs can be coated or encapsulated with organic materials to prevent aggregation and improve their biodistribution. In addition, with IONPs, it would be possible to encapsulate biomolecules or drugs that could be delivered to the tumor. In most studies, they have been encapsulated in silica nanoparticles [8] or polymeric solid nanoparticles [9], which, due to the material rigidity might alter the properties of the magnetic nanoparticles

In this work, we have successfully encapsulated cubic superparamagnetic magnetite nanocrystals (NCs) in biocompatible polymeric nanoparticles. Furthermore, we have been able to confine NCs in the liquid core of polymeric capsules, which is made of viscous oil. This encapsulation would not only ensure NCs' stability, providing a positive effect on their biodistribution but would let the NCs to be free to rotate, preserving their excellent magneto-optic properties. The morphology of both polymeric particles (average size ~200 nm) and NCs (average size ~16 nm) has been evaluated by transmission electron microscopy (TEM). Moreover, TEM results corroborated the presence of an oil core and a polymeric shell in the case of nanocapsules, which was further demonstrated by differential scanning calorimetry (DSC). The amount of encapsulated oil was determined via nuclear magnetic resonance spectroscopy (NMR), while the quantity of encapsulated NCs was estimated by thermogravimetric analysis (TGA) and magnetometry. Finally, the efficiency of the NCs-loaded polymeric nanocapsules as a photothermal agent was demonstrated by the temperature increase of nanocapsules' suspension irradiated with a NIR light source. Interestingly, temperatures above 40 °C were reached upon NIR irradiation.

On top of that, we have induced an external anisotropy by modifying the shape of polymeric nanoparticles or nanocapsules. The resulting ellipsoidal nanoparticles containing NCs are able to orient in the direction of an applied static magnetic field. When the magnetic field is moved, the ellipsoidal NPs rotate to follow it. This system would represent a promising strategy against cancer,

acting as a powerful photothermal agent that can be easily guided and oriented.

## References


[1] Wu, M., Huang, S., Molecular and Clinical Oncology, 5 (2017) 738-746.

[2] Majumder, J., Minko, T., Expert Opinion on Drug Delivery, 2 (2021) 205-227.

[3] Mortezaee, K., Narmani, A., Salehi, M., Bagheri, M., Farhood, B., Haghi-Aminjan, H., Najafi, M., Life Sciences, 269 (2021) 119020.

[4] Chen, J., Ning, C., Zhou, Z., Yu, P., Zhu, Y., Tan, G., Mao, C., Progress in Material Science, 99 (2019) 1-26.

[5] Mehdaoui, B., Meffre, A., Lacroix, L. M., Carrey, J., Lachaize, S., Gougeon, M., Respaud, M., Chaudret, B., Journal of Magnetism and Magnetic Materials, 19 (2010), 49-52.

[6] Dürr, S., Janko, C., Lyer, S., Tripal, P., Schwarz, M., Zaloga, J., Tietze, R., Alexiou, C., Nanotechnology Reviews, 4 (2013) 395-409.

[7] Abenoja, E. C., Wickramasinghe, S., Bas-Concepcion, J., Samia A. C. S., Progress in Natural Science: Materials International, 5 (2016) 440-448.

[8] Nemec, S., Kralj, S., Wilhelm, C., Abou-Hassan, A., Rols, M.-P., Kolosnjaj-Tabi, J., *Applied. Sciences,* 20 (2020) 7322.

[9] Verma, N.K., Crosbie-Staunton, K., Satti, A., Gallagher, S., Ryan, K. B., Doody, T., McAtamney, C., MacLoughlin, R., Galvin, P., Burke, C. S., Volkov, Y., Gun'ko, Y., Journal of Nanobiotechnology, 11 (2013).


## Figures

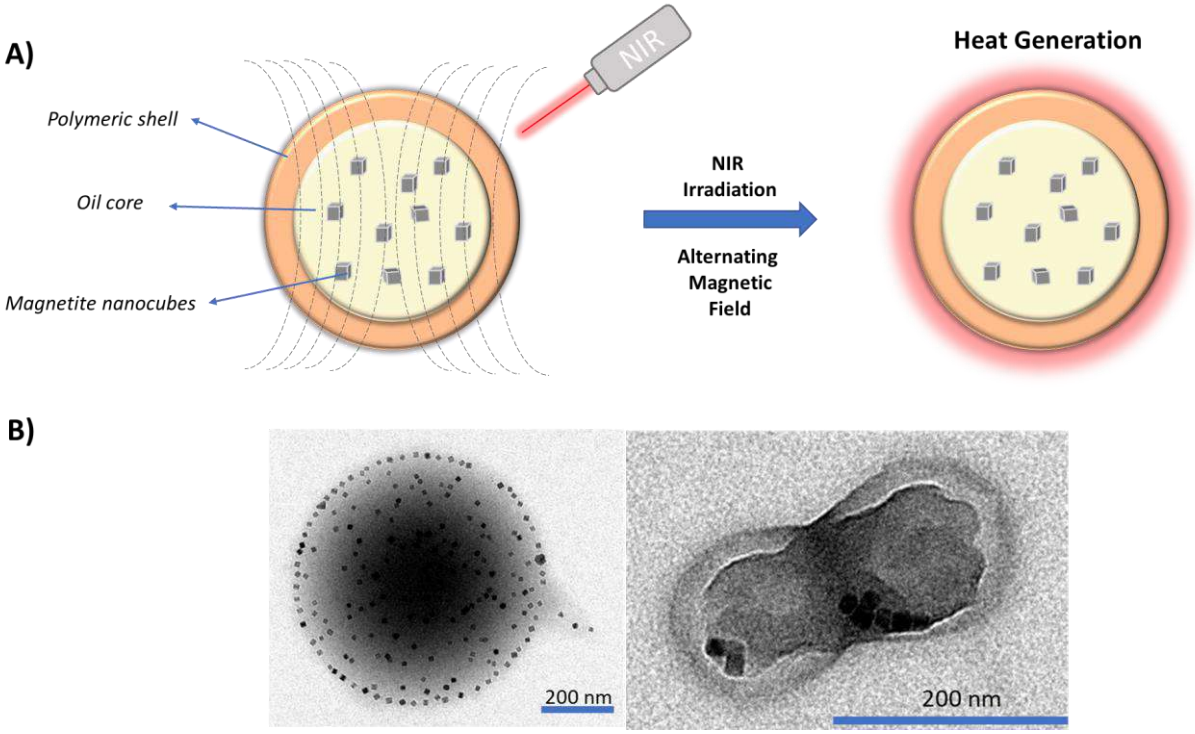


**Figure 1.** A) Schematic representation of magnetic core shell nanoparticles and heating generation after external stimuli application. B) TEM images of nanocubes encapsulated in core-shell polymeric nanoparticles.

# Novel application of lipid nanoemulsions in breast cancer

**Ana Belén Dávila Ibáñez**[1,3], N. Carmona-Ule[1], C. Abuín-Redondo[1], C. Costa[1,3], M de La Fuente[1,2,3], R. Lopez-Lopez[1,2,3].

[1]Roche-Chus Joint Unit, Translational Medical Oncology Group (Oncomet), Health Research Institute of Santiago de Compostela (IDIS), Hospital Gil Casares, Travesía da Choupana s/n, Cp:15706, Santiago de Compostela, Spain.
[2]DIVERSA Technologies S.L., 15782 Santiago de Compostela, Spain
[3.] Cancer Network Research (CIBERONC), 28029 Madrid, Spain

ana.belen.davila.ibanez@sergas.es

Metastasis is one of the main causes of cancer death, and consists of a dynamic succession of events involving the dissemination of tumor cells [1]. These cells, called Circulating Tumor Cells (CTCs), are shed from the primary tumor and travel through the blood to colonize distant organs, generating a new metastatic niche [2]. CTCs have relevance as prognostic markers in breast cancer. However, the functional properties of CTCs or their molecular characterization have not been well-studied. Thus, it is essential to culture and study these surviving cells capable of forming such metastases. The main difficult for the analysis of these cells relays in their isolation and culture ex vivo that still represents a big challenge in translational research. The main challenges of CTCs isolation and culture relate to the fact that CTCs are infrequent (1 CTC against $10^6$-$10^7$ of surrounding normal peripheral mononuclear blood cells (PBMCs)) and they are present in a slow proliferative state when isolated [3]. Moreover, CTCs show short rates of survival in the bloodstream because of their exposure to fluid shear stress. At the moment, various emerging methods have been developed for CTC enrichment, in order to improve the amount of viable material that could later be used for downstream analysis. However, robust and reliable isolation and optimized culture conditions for CTCs remain to be established.

Therefore in our laboratory we have formulated oil-in-water (O/W) Nanoemulsions (NEs) using lipids and fatty acids which have reported to influence the metabolism of cancer cells increasing the metabolic activity of cancer cells[4]. We have use them to support the culture of different CTCs samples isolated from metastatic breast cancer patients. These allowed us to perform phenotypic and gene expression analysis using RT-PCR of the cultured CTCs [5]. Finally we are working on the functionalization of these NEs in a way to target CTCs as a future tool for CTCs isolation and culture [6].
In this conference we will present the results showing the synthesis and characterization of NEs and their capability to increase the cell viability of different breast cancer cell lines. Moreover, we will present how we have generated a CTC model from breast cancer mice xenografts, to prove the ability of the NEs to facilitate their culture and expansion. Additionally, we will explain the postulated mechanism of NEs action based on their consumption by cells to use them as energy suppliers, driving proliferation.
We will also show how we use these NEs for culture supporting in isolated viable CTCs from 50 peripheral blood samples obtained from 35 patients with advanced metastatic breast cancer. We found that in 75% of samples the CTC cultures we were able to obtain a success short-term culture were cells lasted more than 23 days. Additionally we observed that the cultivability was able to predict a shorter Progression-Free Survival in these patients, independently of having 5 CTC by Cellsearch®. We also observed that CTCs before and after culture showed a different gene expression profile, concluding that the cultivability of CTCs is a predictive factor. Furthermore, the subset of cells capable of growing ex vivo showed stem or mesenchymal features and may represent the CTC population with metastatic potential in vivo.
Finally we will show our recent data when we have functionalized the nanoemulsions with two peptides, with the aim of using them as a tool for CTC isolation and culture in situ. Therefore, NEs were surface-decorated with the peptides Pep10 and GE11, which act as ligands towards the specific cell membrane proteins EpCAM and EGFR, respectively.

Therefore we will present a new methodology to support the cultivability of CTCs by the use of NEs with specific composition. We will show how the shot-term culture of CTCs could be a tool predictive factor of patient survival and how we can functionalize these NEs for future applications

## References

[1] L.A. Torre, F. Bray, R.L. Siegel, J. Ferlay, Global Cancer Statistics, 2012, 65, 2015, 87-108,
[2] https://www.cancer.gov/about-cancer/understanding/statistics (n.d.).
[3] E.E. van der Toom, J.E. Verdone, M.A. Gorin, K.J. Pienta, Technical challenges in the isolation and analysis of circulating tumor cells, Oncotarget, Oncotarget. 2016, 7, 62754-62766.
[4] N. Carmona-Ule, C. Abuín-Redondo, C. Costa, R. Pineiro, T. Pereira-Veiga,I. Martínez-Pena, P. Hurtado, R. Lopez-Lopez , M. de la Fuente, A.B. Davila Ibanez. Materials Today Chemistry, 2020, 16,100265.
[5] N. Carmona-Ule, M. González-Conde, C. Abuín, J. F. Cueva, P. Palacio, R. López-López, C. Costa, A. B. Dávila-Ibáñez, Cancers, 2021,13, 2668.
[6]. N. Carmona-Ule N. Gal, C. Abuín Redondo, M. De La Fuente Freire, R. López López, A. B. Dávila-Ibáñez, Bioengineering, 2022, 9, 380.

## Figures

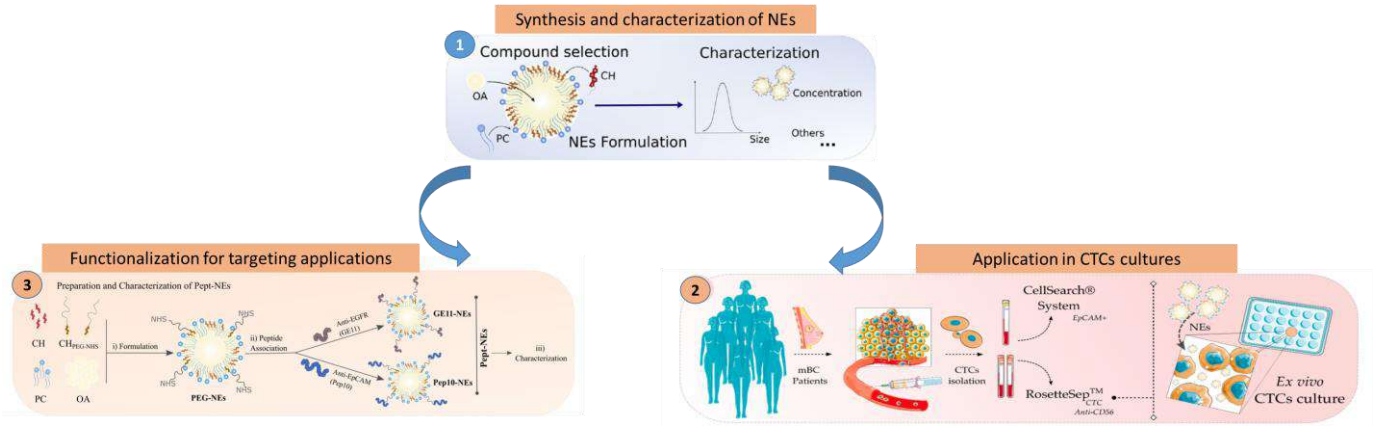


**Figure 1.** 1. Synthesis and characterizations of NEs formulated from lipid and fatty acids involved in cancer cell metabolism, 2) Use of NEs for CTCs culture and analysis of the cultured CTCs, 3) Functionalization of NEs for CTCs targeting.

# 3D sensing platform for single cell extracellular pH mapping in time and space: a pre-clinical model to study tumor microenvironment and drug screening

**Stefania Forciniti**[1], Valentina Onesto[1], Riccardo Rizzo[1], Anil Chandra[1] Saumya Prasad[1], Helena Iuele[1], Francesco Colella[1], Giuseppe Gigli[1,2], Loretta L. del Mercato[1]

[1]Institute of Nanotechnology, National Research Council (CNR-NANOTEC), c/o Campus Ecotekne, via Monteroni, 73100, Lecce, Italy;

[2]Department of Mathematics and Physics "Ennio De Giorgi", University of Salento, via Arnesano, 73100, Lecce, Italy.

Stefania.forciniti@nanotec.cnr.it

Abstract

Elevated hydrogen ion concentration accumulates in the tumor microenvironment as a result of metabolic reprogramming of cancer cells towards increased aerobic glycolysis and reduced mitochondrial oxidative phosphorylation, referred to as Warburg effect [1]. This results in spatially and temporally heterogenous acidic microenvironment which affects cancer initiation and progression as well as the efficacy of anti-cancer drug treatments [2, 3].

Therefore, monitoring the local pH metabolic fluctuations is crucial in understanding the basic biology of the tumors, and can also be used as a valid metabolic readout for cancer diagnosis and treatment [4].

Here, a method to embed silica-based ratiometric fluorescent pH sensors into a spherical 3D cell culture system, coupled with a computational method for pH spatio-temporal mapping, is presented (see figure 1) [5]. By using a confocal laser fluorescence microscopy, 3D time-lapse imaging of living cells was performed and the extracellular pH variations were monitored between 3D scaffolds with either mono or co-cultures of tumor and stroma pancreatic cells.

We obtained that the extracellular pH is cell line-specific and time-dependent. Indeed, differences in pH were detected between 3D monocultures compared to co-cultures, thus suggesting a metabolic crosstalk between tumor and stroma cells.

In conclusion, the 3D cell culture system has the potential of imaging complex 3D co-coltures in real time and of detecting their pH metabolic interplay under controlled experimental conditions, making it a suitable platform for drug screening and personalized medicine.

*The research leading to these results received funding from the European Research Council (ERC) under the European Union's Horizon 2020 research and innovation programme (grant agreement No 759959, ERC-StG "INTERCELLMED").*

## References

[1] Schwartz L, Supuran CT, Alfarouk KO. The Warburg Effect and the Hallmarks of Cancer. Anticancer Agents Med Chem. 2017;17(2):164-170;

[2] Boedtkjer E, Pedersen SF. The Acidic Tumor Microenvironment as a Driver of Cancer. Annu Rev Physiol. 2020 Feb 10;82:103-126;

[3] Zhang A, Miao K, Sun H, Deng CX. Tumor heterogeneity reshapes the tumor microenvironment to influence drug resistance. Int J Biol Sci. 2022 Apr 24;18(7):3019-3033;

[4] Parks SK, Chiche J, Pouyssegur J. pH control mechanisms of tumor survival and growth. J Cell Physiol. 2011 Feb;226(2):299-308;

[5] Rizzo R, Onesto V, Forciniti S, Chandra A, Prasad S, Iuele H, Colella F, Gigli G, Del Mercato LL. A pH-sensor scaffold for mapping spatiotemporal gradients in three-dimensional in vitro tumour models. Biosens Bioelectron. 2022 Sep 15;212:114401.

## Figures

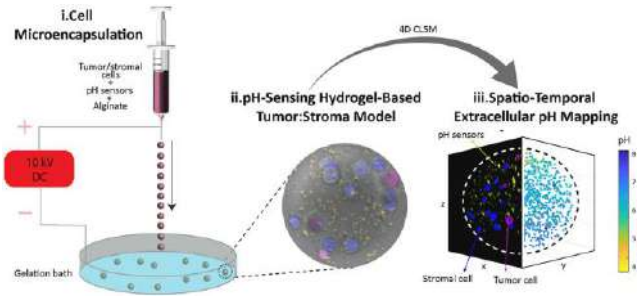


**Figure 1. Schematic illustration of the method to embed silica-based fluorescent pH sensors into alginate 3D microgels tumor models. i) Tumor/stromal cells and sensors microencapsulation in alginate to form 3D microgels tumor models; ii) pH-sensing hydrogel-based tumor/stroma model; iii) Spatio-Temporal extracellular pH mapping obtained with a specific computational analysis.**

# Towards a universal biosensing platform based on graphene/pyrene surfaces for neurotransmitters

**M. Delgà-Fernández[1]**, E. del Corro[1], Jose M. Caicedo-Roque[1], Eli Prats-Alfonso[2,3], Sergi Brosel[2], Xavi Illa[2,3], Anton Guimera-Brunet[2,3], J. A. Garrido[1,4]

[1]Catalan Institute of Nanoscience and Nanotechnology (ICN2), CSIC and the Barcelona Institute of Science and Technology (BIST), Barcelona, Spain

[2] Centro de Investigación Biomédica en Red de Bioingeniería, Biomateriales y Nanomedicina (CIBER-BBN), Madrid, Spain

[3] Institut de Microelectrònica de Barcelona, IMB-CNM (CSIC), Esfera UAB, Bellaterra, Spain

[4]Institució Catalana de Recerca i Estudis Avançats (ICREA), Barcelona, Spain

marta.delga@icn2.cat

Understanding how the human brain works is key for the development of new therapeutic treatments – such as neural stimulation - and diagnosis of neurological disorders. Implantable neural interfaces allow the recording of electrical signals to better understand the central and peripheral nervous systems[1,2]. Graphene-based field-effect transistors have been recently used as neural sensing devices, taking advantage of graphene's mechanical and electronic properties, and also open the possibility to add chemical recording capabilities, in particular for the detection of neurotransmitters.. Here, we develop a versatile graphene/pyrenebutyric acid (PyBA) platform for the detection of chemical analytes, while keeping the capability of recording electrical neural activity.

To build this platform, we perform physical evaporation of PyBA, a molecule capable to interact with the π system of graphene thanks to its aromatic nature, and to covalently interact, thanks to its carboxylic group, with an aptamer of interest through the formation of a peptidic bond.
In this work, we have optimized the PyBA evaporation conditions, aiming at forming a PyBA monolayer on single layer graphene.
Then, the binding of an aptamer that recognizes a specific analyte – thrombin is used in our particular case - is used to assess the functionality of the biosensing platform. Morphological characterization of the functionalized graphene surfaces is performed by Atomic force microscopy (AFM) and Raman spectroscopy. The presence of thrombin is detected by electrical characterization of the functionalized graphene transistors.

The thrombin biosensing experiments reveal changes in the electrical properties of graphene corresponding to each concentration tested; the obtained detection range is in good agreement with reported approaches based on in-liquid functionalization[3]. Our results demonstrate the ability of the platform to recognize the analyte of interest through binding to its specific aptamer. This graphene/PyBA universal biosensing platform is in the pipeline for the development of a new generation of multifunctional graphene-based neural implants, capable of both electrical neural sensing and neurotransmitter detection.

## References

[1] Masvidal-Codina, E., Illa, X., Dasilva, M., et al (2019) High-resolution mapping of infraslow cortical brain activity enabled by graphene microtransistors, *Nature Mater*.
[2] Garcia-Cortadella, R., Schwesig, G., Jeschke, C., et al (2021) Graphene active sensor arrays for long-term and wireless mapping of wide frequency band epicortical brain activity, *Nat Commun.*
[3] Hinnemo, M., Zhau, J., Ahlberg, P., et al (2017) On Monolayer Formation of Pyrenebutyric Acid on Graphene, *Langmuir.*

## Figures

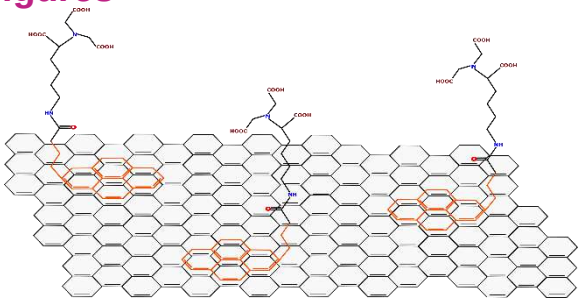

**Figure 1** Schematic representation of the PyBA-Aptamer molecules non-covalently stacked to the graphene surface. This is the base of the biosensing platform presented in this work.

## Acknowledgements

This project has been funded by MCIN/AEI/10.13039/501100011033 (project PID2020-113663RB-I00)

# Detection of short nucleotides with DNA nanopores

**Juan Elezgaray**[1],
Luyan Yang[1], Chirstophe Cullin[2]

[1] CRPP, CNRS, UMR5130, Av. Schweitzer, Pessac, France
[2]CBMN, CNRS, U. Bordeaux, Allée St Hiliare, Pessac, France

juan.elezgaray@u-bordeaux.fr

MiroRNAs (miRNA) are single strand, non-coding RNAs that play a role in the regulation of the genetic expression, through their capacity to hybridize with the 3'UTR of specific target mRNA (messenger RNA). miRNAs are known to be associated with the normal development and function of the organism, but are also involved in diseases such as cancer [1]. The attractiveness of extracellular miRNA as cancer biomarkers relies on their stability and their dysregulation in the diseased cells. However, because of their short sequence and low concentration, miRNA detection is intrinsically difficult. This paper shows how DNA nanotechnology [2,3] provides with an efficient way to detect single miRNAs in a single step process, where no amplification steps (as PCR based methods) are required. This method is based on DNA nanopores, nanometric cylindrical structures (Figure 1) that are able to perforate lipid bilayers. The geometry (width [4], length [5]) of DNA nanopores can be regulated by the interaction with short nucleotides such as miRNAs. Detection of nanopores relies on electric measurements of membrane conductance inspired from electrophysiology. We show that the presence of single nanopores with well defined conductance can be detected. Because of the close relation between geometry and conductance, this is equivalent to the detection of single miRNAs. We also describe how the same approach can be extended by the use of aptamers to the detection of small organic molecules.

## References

[1] J. Hao, F. F. Duan, Y. Wang, Curr. Opin. Genet. Dev. 46 (2017) 95103.
[2] N.C. Seeman, Annu. Rev. Biochem. 79 (2010) 6587
[3] P.W. Rothemund, Nature 2006, 440, 297302.
[4] O. Mendoza, P. Calmet, I. Alves, S. Lecomte, M. Raoux, C. Cullin, J. Elezgaray, Nanoscale 9 (2017) 97629769.
[5] L. Yang, C. Cullin, J. Elezgaray, Chem. Phys. Chem 23 (2022) e202200021.
[6] T. E. Ouldridge, A. Louis, J.P.K. Doye, J. Chem. Phys. 134 (2011) 085101

## Figures

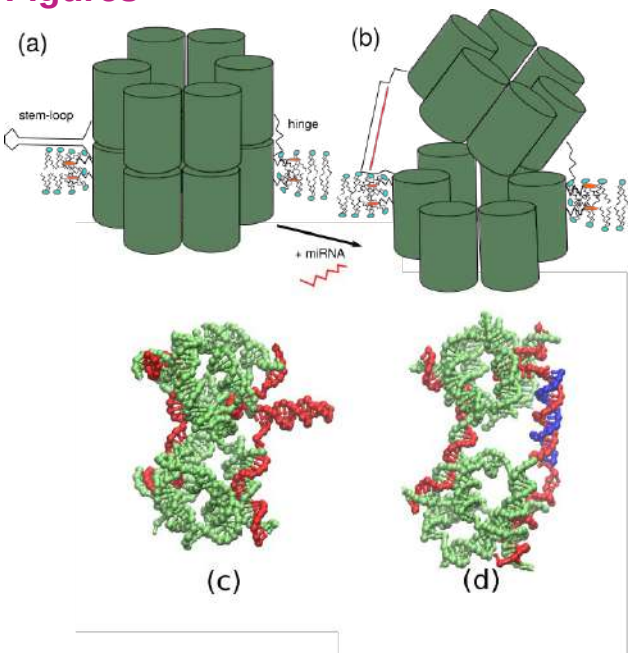


**Figure 1.** (a) and (b): schematic representation of the opening mechanism. Each cylinder represents a double helix. DNA nanopore is inserted into a lipid bilayer thanks to cholesterol modifications (orange ellipses). (a) Closed state: the stem loop imposes a short distance between two of the helices. (b) Open state: upon addition of miRNA, the stem loop unfolds giving rise to a mixed single and double stranded linker which pushes the two halves apart. (c) and (d) are oxDNA [6] simulations of closed and open conformations, respectively. Strands that form the hinge or the stem-loop locking mechanism are in red. The input signal is in blue.

# Anticancer properties of selenium nanoparticles encapsulated by oncolytic virus capsids

**Cláudio Ferro**[1,3]
Sara Feola[2], Alexandra Correia[1], Flávia Fontana[1], Vincenzo Cerullo[2], Hélder A. Santos[1,4], Helena Florindo[3]

[1] Drug Research Program, Division of Pharmaceutical Chemistry and Technology, Faculty of Pharmacy, University of Helsinki, FI-00014 Helsinki, Finland

[2] Drug Research Program, Division of Pharmaceutical Biosciences, Faculty of Pharmacy, University of Helsinki, FI-00014 Helsinki, Finland

[3] Research Institute for Medicines, iMed.ULisboa, Faculty of Pharmacy, Universidade de Lisboa, Portugal

[4] Helsinki Institute of Life Science (HiLIFE), University of Helsinki, FI-00014 Helsinki, Finland

claudio.ferro@campus.ul.pt

**Introduction**: Selenium Nanoparticles (SeNPs) have shown anticancer potential while having high biocompatibility and their functionalization using specific ligands demonstrated to have additional therapeutic effect.[1]. Viral membranes has been used to deliver anticancer cargoes [2]. Oncolytic virus (OVs), such as the chimeric adenovirus 5/3 (Ad5/3), have been studied for cancer therapy, not only by their ability to specifically target, infect and kill cancer cells while unaffecting healthy cells, but also by activating immune cells, such as Natural Killer (NK) and T cells towards the tumour itself [3,4]

**Methods**: SeNPs were produced using sodium selenite, ascorbic acid as reducing agent and bovine serum albumin as stabilizing agent, adjusting the pH reaction environment to 1. Ad5/3 virus were obtained by infecting A549 cells and further purification of the virus capsid was performed by CsCl density-gradient ultracentrifugation, after separating and lysing the cells by freeze-thaw. The SeNPs encapsulation by the virus capsids (Ad-SeNPs) was performed by both extrusion and pH-dependent encapsulation. The stability of Ad-SeNPs was performed in human plasma, cell medium, pH 7.4 and 5.5. Also, the antitumor properties were evaluated *in vitro*, including the antiproliferative potential, the internalization efficiency, the intracellular oxidative stress, and the caspase activation, using breast (4T1) and lung (A549) cancer cell lines, and a human fibroblast cell line to evaluate the systemic toxicity. The potential of Ad-SeNPs for T and NK cells polarization was also evaluated

**Results**: After the SeNPs encapsulation by viral membranes, Ad-SeNPs demonstrated a size around 100 nm, moderate polydispersity, and a negative surface charge. The nanosystem produced was stable at cell medium, human plasma, physiologic pH, although degraded at acidic pH. Ad-SeNPs presented higher anticancer properties when compared to the non-encapsulated SeNPs, increasing the SeNPs internalization into cancer cells, and therefore inducing oxidative stress, caspase-3/9 activation, and consequent cellular apoptosis. Ad-SeNPs was also able to polarize NK and T cells, proving its immunotherapeutic potential.

**Conclusion**: Our study led to the production of a nanosystem with high antitumour potential, by directly causing cancer cells apoptosis and by inducing an antitumor immunological reaction.

## References

[1] C. Ferro, H. F. Florindo, H. A. Santos, *Adv Heal. Mater.* **2021**, e2100598.

[2] T. Briolay, T. Petithomme, M. Fouet, N. Nguyen-Pham, C. Blanquart, N. Boisgerault, *Mol. Cancer* **2021**, *20*, 1.

[3] Y. Zhao, Z. Liu, L. Li, J. Wu, H. Zhang, H. Zhang, T. Lei, B. Xu, *Front. Microbiol.* **2021**, *12*, 1.

[4] S. Feola, S. Russo, E. Ylösmäki, V. Cerullo, *Pharmacol. Ther.* **2022**, *236*, DOI 10.1016/j.pharmthera.2021.108103.

## Figures

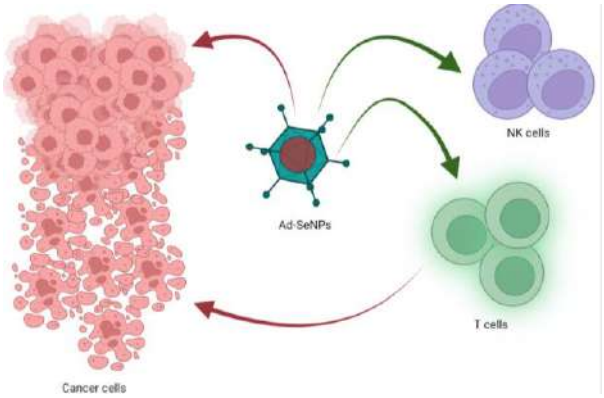


**Figure 1.** Ad-SeNPs antitumor properties are based in a 2-way mechanism, in which they induce apoptosis in cancer cells while polarizing NK and T cells

# Antibiofilm and antibacterial activity of Ag-intercalated upconverting $Tm^{3+}/Er^{3+}$ co-doped layered perovskites and their exfoliated 2D nanosheets

**Zeynep Firtina Karagonlar[1,2],**
Bensu Günay[1], Hilal Döğer[1], Özge Sağlam[1,3]

[1]Division of Bioengineering, Graduate School, İzmir University of Economics, İzmir, Turkey
[2]Department of Genetics and Bioengineering, İzmir University of Economics, İzmir, Turkey
[3]Department of Mechanical Engineering, İzmir University of Economics, İzmir, Turkey

zeynep.firtina@ieu.edu.tr

Antibiofilm and antimicrobial materials are in great demand in the medical device industry. Although Ag-based compounds are known to have high antimicrobial efficiency, rapidly released $Ag^+$ ions tend to aggregate and lose their antibacterial effect over time [1]. Thus, utilizing a new approach for using silver as an antimicrobial agent based on imparting the antimicrobial action through contact, rather than releasing $Ag^+$ ions could be beneficial. We previously demonstrated the upconversion properties of $Tm^{3+}/Er^{3+}$ co-doped Ruddlesden-Popper (RP) type perovskite $K_2La_2Ti_3O_{10}$ (KLTO) and their chemically exfoliated nanosheets [2]. In the present work, we performed Ag-intercalation of $Tm^{3+}/Er^{3+}$ co-doped KLTO layered perovskites and the nanosheets via ion-exchange process to increase their antibacterial activity. We investigated the effect of Ag-intercalated Tm/Er co-doped layered perovskites and their 2D nanosheets on the growth and biofilm formation of the human opportunistic pathogens *Escherichia coli* and *Bacillus subtilis*. Importantly, flocculation of nanosheets with $Ag^+$ ions significantly increased their antibacterial and antibiofilm activity against both species (Fig 1). Strikingly, the flocculated nanosheets demonstrated significant growth inhibitory effects at 100 µg/mL and 1000 µg/mL. At both concentrations, bacteria were not able to grow in LB broth and so no spectral readings were obtained for the 12-hour growth graph (Fig 2). In addition, the flocculated materials demonstrated low *in vitro* cytotoxicity when incubated with mammalian cell lines. Our results indicate that Ag-intercalated layered perovskites and the flocculation of the nanosheets hold great promise to be used for antimicrobial and antibiofilm purposes in biomedical engineering applications. This work was supported by the Scientific and Technological Research Council of Turkey (TÜBİTAK; Grant number 117M512).

## References

[1] Wang L, Hu C, Shao L., Int J Nanomedicine, 12 (2017) 1227

[2] Gunay B, Sarıyar E, Unal U, Karagonlar ZF, Sağlam Ö., Colloids and Surfaces A: Physicochemical and Engineering Aspects, 126003 (2021)

## Figures

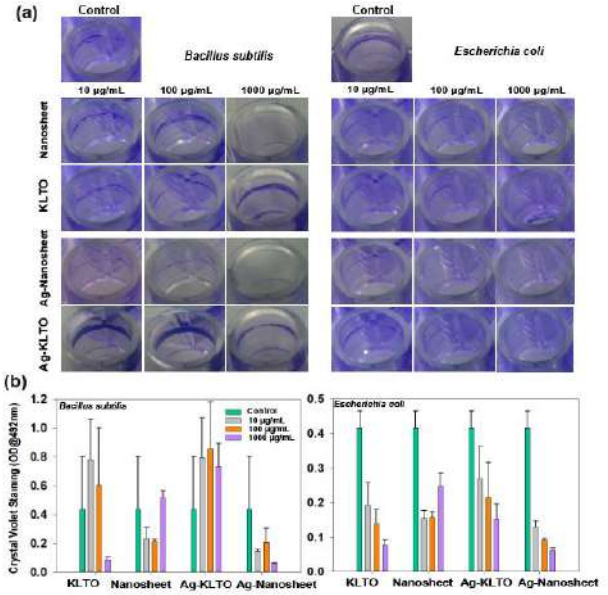


**Figure 1.** Antibiofilm properties of $Tm^{3+}/Er^{3+}$ co-doped samples before and after Ag intercalation determined by crystal violet staining.

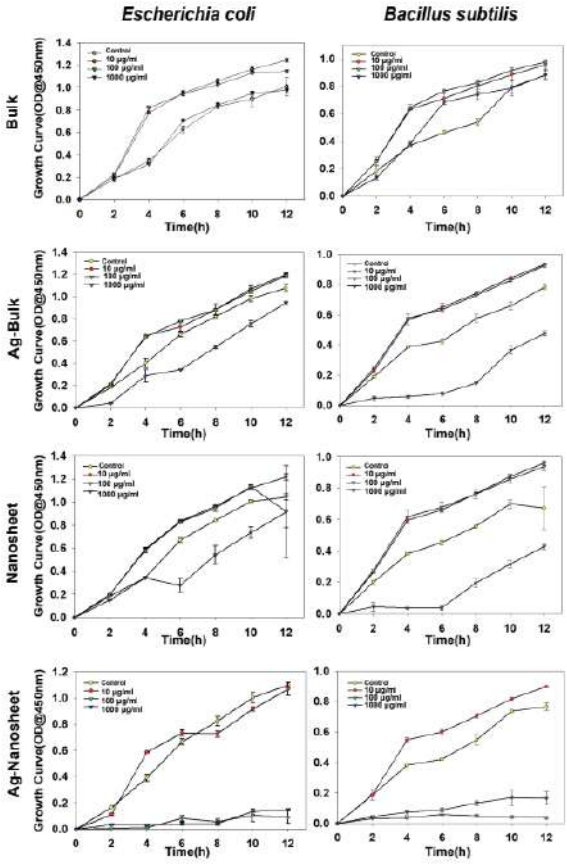


**Figure 2.** Growth curves of E.coli and B. Subtilis incubated with $Tm^{3+}/Er^{3+}$ co-doped samples before and after $Ag^+$ ions intercalation.

# Aptamer displacement Lateral Flow assay for Phenylketonuria monitoring.

**Celia Fuentes-Chust**[1], Andrea Idili[2], Claudio Parolo[3], Andrew Piper[1], Giulio Rosati[1], Arben Merkoçi[1,4].

[1]Institut Catalá de Nanociencia I Nanotecnologia (ICN2), Campus UAB, 08193 Bellaterra, Barcelona, Spain
[2]2Department of Chemical Science and Technologies, University of Rome Tor Vergata, Rome, Italy
[3]ISGlobal, Barcelona Centre for International Health Research (CRESIB), Hospital Clínic (Department of International Health), Universitat de Barcelona, Spain
[4]Catalan Institution for research and Advanced Studies (ICREA), Barcelona, Spain
arben.merkoci@icn2.cat

Phenylketonuria (PKU) is an inherited autosomal-recessive metabolic disorder that inhibits the metabolism of the amino acid phenylalanine[1]. Since 1963, it has been identified in newborns using bacterial inhibition test, a well-established screening approach. Its buildup in blood, urine, and other tissues may cause seizures, intellectual impairments, and other mental illnesses if not properly checked via diet and occasional visits to a PKU clinic. [2] Fast, robust, sensitive, and user-friendly assays are preferred for better monitoring of phenylalanine levels in PKU patients in order to enhance their quality of life. We describe a Point-of-Care aptamer lateral flow biosensor in a strand displacement format with gold nanoparticles (AuNPs) as an optical label for phenylalanine measurement in a buffer sample, which enables the identification of mild hyperphenylalaninemia, mild PKU, and classic PKU. In this work, we conjugated AuNPs to a short nucleic acid sequence that matches a segment of a previously reported aptamer that recognizes phenylalanine and printed the complex as the first line. [3] When a phenylalanine-containing buffer sample reaches the aptamer, the competition displaces the AuNP conjugate, causing the optical signal in the first line to decrease. As the AuNP conjugate flows across the rest of the lateral flow strip, it is captured by a complementary sequence in a second line, resulting in the development of a second quantifiable signal. The test is performed in 20 minutes and has a detection limit of 50 µM, which corresponds to the normal concentration of phenylalanine in the blood of healthy individuals.

## References

[1] N. Blau, F.J. Van Spronsen, H.L. Levy, Lancet., 376 (2010) 1417–1427.
[2] J. Miné, Manuèle; Chen, I. Desguerre, D. Marchant, M. Abitbol, D. Ricquier, P. De Lonlay, A. Bernard, C. Fe, Hum. Mutat. 28 (2007) 831–845.
[3] A. Idili, J. Gerson, C. Parolo, T. Kippin, K.W. Plaxco, Anal. Bioanal. Chem. 411 (2019) 4629–4635.

## Figures

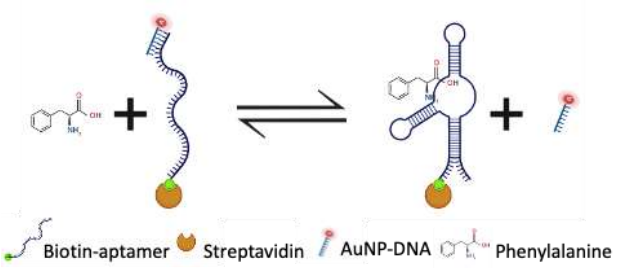


**Figure 1.** Schematic representation of the designed displacement assay.

# A New Paradigm to Identify Brain-Targeting Ligands

Giulia M. Porro[1], Italo Lorandi[1], Giuseppe Battaglia[1], **Daniel Gonzalez-Carter[1]**

[1]Institute for Bioengineering of Catalonia (IBEC), Baldiri Reixac 10-12, Barcelona, Spain

daniel.gonzalezcarter08@alumni.imperial.ac.uk

Being able to selectively deliver therapies to the brain will greatly enhance the treatment of disorders such as Alzheimer's disease by increasing therapy efficiency and decreasing detrimental side-effects.

Current brain delivery strategies employ ligands which bind targets highly expressed on the surface of the brain vasculature. However, such strategies have inherent brain-specificity limitations as the targets are not exclusively expressed on the brain vasculature, leading to increased off-target therapy accumulation in peripheral organs. Hence, alternative approaches to identify targeting ligands are required to achieve truly brain-selective therapy delivery.

We are developing a novel strategy which identifies ligands based not on their increased *binding* to the brain vasculature, but rather on their increased *retention* on the brain vasculature (scheme 1). By exploiting the particularly low rate of endocytosis of brain endothelial cells (EC) (a key aspect of the physiology of the brain vasculature[1]), we should be able to bind ligands to protein targets expressed in the vasculature of both peripheral organs and the brain, but which are endocytically removed from the former while being retained on the surface of the latter. Such ligands selectively retained on the brain vasculature would in turn serve as 'artificial targets' to increase the delivery of therapies specifically to the brain.

We have established the proof of this principle[2] by employing a biotin-conjugated ligand binding the endothelial protein PECAM-1 to deliver avidin-functionalized nanoparticles. We have shown *in vivo* that if the nanoparticles are injected shortly after administration of the anti-PECAM1 ligand, there is strongest targeting to the lung, brain, heart and pancreas, reflecting the expression levels of PECAM1 in these organs. However, as the time-interval increases, targeting to peripheral organs steadily decreases, while targeting to the brain remains constant, reflecting the differential removal of the anti-PECAM1 ligand from the various vasculature surfaces. Such differential removal leads to nanoparticle targeting solely to the brain at long time-intervals (fig. 1), indicating successful generation of artificial targets selectively on the brain vasculature.

Using phage-display technology, we have developed an *in vitro* assay based on this novel paradigm to identify candidate peptides which initially bind to liver, lung and brain EC, but are retained specifically on the surface of brain EC. We have shown that the most promising candidate peptide derived from this screening allows delivery of model proteins into brain endothelial cells.

## Figures

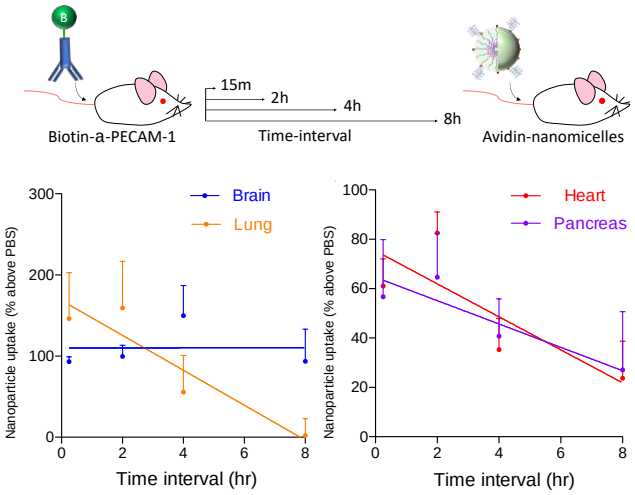


Figure 1. Brain targeting based on selective retention of ligands on the brain vasculature. Avidin-functionalized nanoparticles are targeted to the lung, brain, heart and pancreas when administered shortly after injection of a biotinylated α-PECAM1 ligand. Targeting to peripheral organs decreases with time due to removal of the α-PECAM1 ligand from the vasculature surface, leading to specific brain targeting at long time-intervals.

## References

1. Ben-Zvi et al., *Nature*, 2014; 509 (7501): 507-11.
2. Gonzalez-Carter et al, *PNAS*, 2020; 117 (32): 19141-50

**Scheme 1.** A new paradigm to identify brain-targeting ligands.

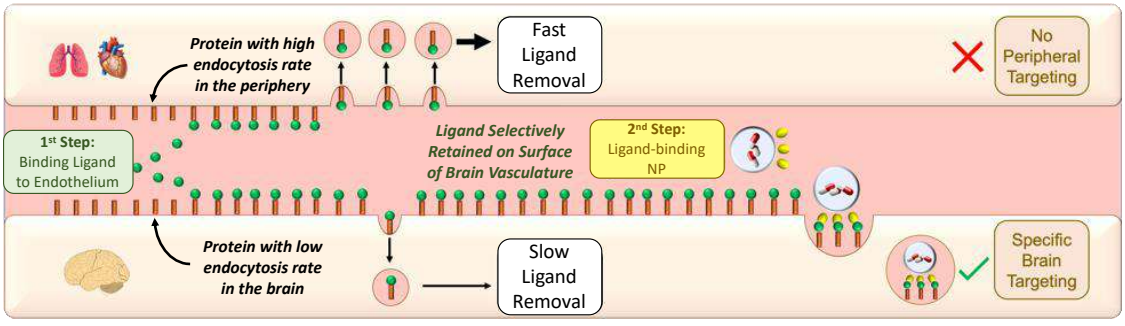

# Advancing a new nanomedicine for Fabry disease treatment towards clinical translation

**Elisabet González-Mira[1,2]**, Judit Tomsen-Melero[1,2,3], Josep Merlo-Mas[3], Edgar Cristóbal-Lecina[4,2], Vanesa Díaz-Riascos[5,2], Albert Font[6], Marc Moltó-Abad[5,2], Natalia García-Aranda[5,2], José Luis Corchero[7,2], Aida Carreño[1,2], Jannik Nedergaard Pedersen[8], Jeppe Lyngsø[8], Inbal Ionita[9], Daniel Pulido[4,2], Santi Sala[3], Jaume Veciana[1,2], Simó Schwartz Jr.[5,2], Dganit Danino[9], Jan Skov Pedersen[8], Andreu Soldevila[6], Miriam Royo[4,2], Alba Córdoba[3], Hazel Clay[10], Ibane Abasolo[5,2], Nora Ventosa[1,2]

[1] Institut de Ciència de Materials de Barcelona, ICMAB-CSIC, 08193 Bellaterra, Spain
[2] Centro de Investigación Biomédica en Red - Bioingeniería, Biomateriales y Nanoedicina, CIBER-BBN, 28029 Madrid, Spain
[3] Nanomol Technologies SL, 08193 Bellaterra, Spain
[4] Institut de Química Avançada de Catalunya, IQAC-CSIC, 08034 Barcelona, Spain
[5] Drug Delivery and Targeting and Functional Validation and Preclinical Research, CIBBIM-Nanomedicine, Vall d'Hebron Institut de Recerca (VHIR), Universitat Autònoma de Barcelona, 08035 Barcelona, Spain.
[6] Leanbio SL, 08028 Barcelona, Spain
[7] Departament de Genètica i de Microbiologia, Institut de Biotecnologia i de Biomedicina, IBB, Universitat Autònoma de Barcelona, 08193 Bellaterra, Spain
[8] Interdisciplinary Nanoscience Center, iNANO, and Departament of Chemistry, Aarhus University, DK-8000 Aarhus C, Denmark
[9] CryoEM Laboratory of Soft Matter, Faculty of Biotechnology and Food Engineering, Technion-Israel Institute of Technology, 32000 Haifa, Israel
[10] Covance Laboratories Ltd, Otley Road Harrogate, North Yorkshire HG3 1PY, United Kingdom

Contact: egonzalez@icmab.es

## Introduction

Despite advances in the development of new orphan medicines, the number of available therapies for rare diseases remains low. As few as 6% of rare diseases have an approved treatment option and if so, they come with limited effectiveness and high cost. This work addresses the need of cost-effective treatments for Fabry disease (FD), one of the most frequent Lysosomal Storage Disorders (LSD). Mutations in the alpha-galactosidase (GLA) gene, lead to the malfunction or absence of the GLA enzyme and the accumulation of globotriaosylceramide (Gb3) and similar glycosphingolipids in the lysosomes throughout the body, provoking multisystemic clinical symptoms. Of note, endothelial cells are thought to play a central role in the pathophysiology of the disease [1].

The Enzyme Replacement Therapy (ERT), which consists of the intravenous administration of an active recombinant version of the defective enzyme, is the main treatment option for patients with LSDs. However, ERT present limitations due to: (i) poor biodistribution, (ii) incapacity of enzymes to cross the Blood Brain Barrier (BBB); (iii) rapid enzyme degradation and short plasma half-life; and (iv) high immunogenicity. Consequently, frequent dosing is required (every other week) resulting in high-cost treatments.

With the aim of developing more effective ERT for FD, a nanoliposomal formulation that delivers recombinant GLA selectively to endothelial cells has been developed in the frame of the EU H2020 Smart4Fabry Project. The currently granted EU H2020 Phoenix Project pursues the transfer of this new nanomedicine to clinical phase, covering the GMP clinical lot production.

## Methods

GLA-loaded nanoliposomes (nanoGLA) functionalized with Arginine-Glycine-Aspartic acid (RGD) peptide were prepared by a one-step, green, and easy scalable method based on compressed CO2, named DELOS-susp, followed by a tangential flow filtration (TFF) procedure [2].

The relevant physicochemical/biological properties critical to product quality were identified and extensively characterized combining different techniques (e.g. DLS, cryoTEM, HPLC, 4-MUG assay). A deep optimization work based on the Quality by Design (QbD) approach was carried out to obtain a nanoformulation with optimal characteristics to scale-up and perform preclinical testing [3].

The efficacy of nanoGLA to metabolize the Gb3 accumulations was compared to the non-nanoformulated GLA, both in vitro and in vivo. In vitro, the ability of nanoGLA to reduce (hydrolyse) the Gb3 substrate was measured by using Nitrobenzoxadiazole (NBD)-Gb3 fluorescent substrate in Mouse Aortic Endothelial Cells (MAEC) derived from Fabry KO mice. This assay measures the ability of the enzyme to internalise in cells, reach the lysosomes and hydrolyse the substrate of the GLA enzyme, offering a rapid and clear assay to test both the internalisation and the efficacy of the tested compound. The in vivo efficacy of the nanoGLA was tested in Fabry KO mice [4] by comparing the Gb3 levels in animals treated with intravenous (IV) administrations of single or repeated doses of nanoGLA, free (non-entrapped) GLA or the commercialized Replagal® at 1 mg/kg. A pharmacokinetic study was also completed in rats, where plasma levels of the total GLA were assessed following IV administration of nanoGLA.

## Results

After a deep nanoformulation's optimization process, small, uniform, and mainly unilamellar GLA-loaded RGD-targeted nanoliposomes were successfully prepared by DELOS-susp, with high enzyme entrapment efficiency (>90%), enhanced enzymatic activity, and superior efficacy in cell culture [4]. Moreover, this nanoGLA has provided in vivo

evidence supporting an increase in GLA activity in plasma and higher Gb3 clearance in liver, spleen, lung, heart, kidney, skin and even brain, compared to the non-nanoformulated enzymes (included the commercially available agalsidase alpha or Replagal®) [5]. These results were consistent with an extended half-life compared to the free GLA formulation in a pharmacokinetic study in rats.

## Conclusions

DELOS-susp has emerged as a robust manufacturing technology for the preparation of GLA-loaded RGD-targeted nanoliposomes with the consistent quality for further regulatory purposes. This new liposomal formulation of GLA improves the ERT efficacy in preclinical models of FD. Based on the potential clinically relevant advantage of the nanoGLA versus authorized ERTs, the EMA has granted the Orphan Drug Designation [6]. This designation has important implications for the translation of the new therapeutic product from bench to bedside.

## Acknowledgements

Authors acknowledge the financial support from the European Commission through the H2020 programs (Smart-4-Fabry project, ID 720942, and Phoenix-OITB ID 953110), the Networking Research Center on Bioengineering, Biomaterials, and Nanomedicine (CIBER-BBN), Project MOL4BIO PID2019-105622RB-I00 funded by Agencia Estatal de Investigación- Ministerio de Ciencia e Innovación MCIN/AEI /10.13039/501100011033 and ISCIII grant program (MERIAN, PI18_00871) cofounded by the European Regional Development Fund (ERDF).

## References

[1] K Kok et al., Biomolecules. 11(2) (2021) 271.
[2] I. Cabrera et al., Adv. Healthcare Mater., 5 (2016) 829–840.
[3] J. Merlo-Mas et al., J. of Supercritical Fluids 173 (2021) 105204.
[4] T Ohshima et al., Proc. Natl. Acad. Sci. U. S. A. 94 (1997) 2540–4.
[5] J Tomsen-Melero et al., ACS Appl. Mater. Interfaces ACS Appl. Mater. Interfaces 13 (2021) 7825–7838.
[6] WO2022161990 -Liposomes and its use for enzyme delivery.
[7] European Commission. Community Register of orphan medicinal products - Designation number: EU/3/20/2396.https://ec.europa.eu/health/documents/community-register/html/o2396.htm (2021).

## Figures

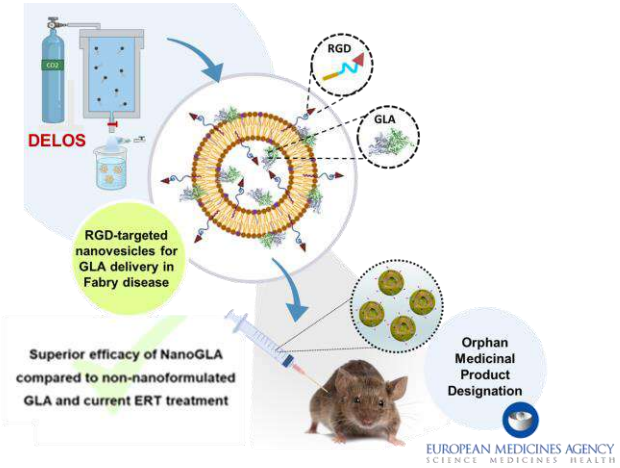


**Figure 1.** Graphical summary of the milestones achieved with the GLA-loaded nanoliposomes functionalized with the RGD peptide.

# Hydrogen-Bonding and Long-Range Interactions Involved in the Initial Attachment of Biofilm-Dispersed *Escherichia coli* and *Bacillus subtilis*

**F. Pinar Gordesli Duatepe**[1], Ayse Ordek[2], Gamze Nur Aspar[2]

[1]Department of Genetics and Bioengineering, Faculty of Engineering, Izmir University of Economics, 35330 Izmir, Turkey
[2]Bioengineering Graduate Program, Graduate School, Izmir University of Economics, 35330 Izmir, Turkey

pinar.gordesli@iue.edu.tr

Biofilms are surface-associated bacterial communities covered by a self-generated extracellular polymeric matrix that protects bacteria against various environmental stresses [1]. Biofilms are significant because of their role in the pathogenesis of many chronic infections and their ability to exhibit resistance to antimicrobial agents [1,2]. Biofilm development can be divided into three distinct stages: initial attachment of planktonic bacterial cells to a surface, growth of the cells into a sessile biofilm form, and dispersal of the cells from the biofilm [2]. The dispersal of the biofilm is the final stage of biofilm development that leads to the spread of the biofilm and hence the transmission of infection [2,3]. Studies have shown that the physiology of cells dispersed from biofilms is quite different from that of planktonic and biofilm cells [3]. Dispersed cells have also been shown to be highly virulent [3], and metabolically more active [4] compared to the planktonic cells. However, the initial attachment of biofilm-dispersed cells to surfaces, the first stage of biofilm development that takes place at the nanoscale, has not been systematically investigated therefore require further examination.

In general, the initial bacterial attachment to a surface is governed by long-range physicochemical interactions, often as described by the Derjaguin−Landau−Verwey−Overbeek (DLVO) theory, and short-range specific molecular interactions such as hydrogen bonds and ligand/receptor bonds [5-8]. The quantitative information on the overall interaction force between the bacterium and the surface can be directly obtained with high resolution using atomic force microscopy (AFM). Moreover, the application of Poisson statistical method to AFM adhesion data allows to decouple the overall interaction force into short-range specific and long-range nonspecific force components [5,7,8]. This method represents one of the only available ways to quantify hydrogen bonding between bacteria and surfaces from AFM data [5,7].

The goal of this study is to provide the necessary information on the fundamental components of the overall interaction forces mediating the initial attachment of biofilm-dispersed Gram-negative *Escherichia coli* and Gram-positive *Bacillus subtilis* cells. For this purpose, first *E. coli* and *B. subtilis* biofilms were grown on glass slides in continuous flow chambers for 24-h. Afterward, a dispersal agent, NO-donor sodium nitroprusside (SNP) was added to the medium bottles at a final concentration of 5 μM. Biofilm dispersion was induced by the continuous flow of the medium supplemented with 5 μM of SNP for 24-h at a rate of 0.4 ml/min (laminar flow) for each investigated. Finally, biofilm-dispersed *E. coli* and *B. subtilis* cells were collected from the waste bottles and directly prepared as samples for AFM measurements. The overall interaction forces (adhesion forces) between silicon nitride AFM tips and the surface molecules of biofilm-dispersed *E. coli* and *B. subtilis* were measured under water by AFM. The adhesion force is related to the number of bonds ruptured during the AFM pull-off event [7,8]. The adhesion forces were then decoupled into hydrogen bonding and long-range force components using the mean equals variance property of the Poisson distribution. Since there are no ligand/receptor bonds to be expected between silicon nitride and the bacterial surfaces in water, the short-range specific forces arise from hydrogen bonding in our system. The hydrogen bonding can arise from the interactions between the surface silanols of silicon nitride and the surface hydroxyl and/or amine groups of the outer membrane molecules of the bacterial cells in water [8].

Consequently, our results indicated that the nature of hydrogen-bonding and long-range forces were attractive for each investigated and, on average, the hydrogen-bonding forces were 2-fold stronger than the long-range forces. The hydrogen-bonding and long-range forces obtained for biofilm-dispersed *E. coli* (0.248 nN and 0.120 nN, respectively) were on average 5-fold higher than those obtained for biofilm-dispersed *B. subtilis* (0.05 nN and 0.02 nN, respectively). These findings together with those of planktonic cells available in the literature [5-8] may guide the design of new strategies aimed at eliminating the initial attachment of biofilm-dispersed Gram-negative and Gram-positive bacterial cells to inert surfaces from a biophysical perspective.

*Acknowledgement*

This study was financially supported by The Scientific and Technological Research Council of Turkey (TUBITAK) under Grant CAREER (118M404).

## References


[1] Donlan RM, Costerton JW. Clinical Microbiology Reviews 2002, 15, 167-193.
[2] Rumbaugh KP, Sauer K. Nature Reviews Microbiology 2020, 18, 571-586.
[3] Chua SL, Liu Y, Yam JK, et al. Nature Communications 2014, 5, 4462.
[4] Guilhen C, Forestier C, Balestrino D. Molecular Microbiology 2017, 105, 188-210.
[5] Abu-Lail NI, Camesano TA. Langmuir 2006, 22, 7296-7301.
[6] Carniello V, Peterson BW, van der Mei HC, Busscher HJ. Advances in Colloid and Interface Science 2018, 261, 1-14.
[7] Chen Y, Busscher HJ, van der Mei HC, Norde W. Applied Environmental Microbiology 2011, 77, 5065−5070.
[8] Gordesli FP, Abu-Lail NI. Environmental Science & Technology 2012, 46, 10089-10098.


## Figures

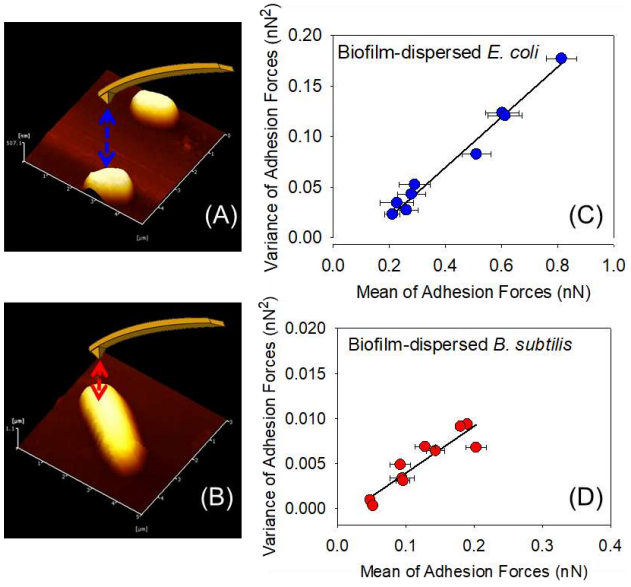


**Figure 1.** Dynamic fluid mode topographical images of (A) biofilm-dispersed *E. coli* and (B) biofilm-dispersed *B. subtilis* in water, and the representation of the measurement of overall interaction forces between silicon nitride AFM tips and the bacterial cells. (C) and (D) are the linear regressions to the scatter plots of mean versus variance of adhesion forces from which the hydrogen-bonding and long-range forces were determined through the use of Poisson statistical method.

# Protein-stabilized nanomaterials as novel MRI contrast agents

**Gabriela Guedes**[1], Kepa B. Uribe[1,2], Lydia Martínez-Parra[1], Jesús Ruiz-Cabello[1,3,4,5], Aitziber L. Cortajarena[1,3]

[1] Center for Cooperative Research in Biomaterials (CIC biomaGUNE), Basque Research and Technology Alliance, Parque Tecnológico de San Sebastian Paseo Miramón 194, 20014 Donostia-San Sebastian, Spain.
[2]Department of Biochemistry and Molecular biology, University of the Basque Country UPV/EHU, Leioa, 48940, Spain.
[3]Ikerbasque, Basque Foundation for Science, 48009 Bilbao, Spain.
[4]Ciber Enfermedades Respiratorias (Ciberes), 28029 Madrid, Spain.
[5]Departamento de Química en Ciencias Farmacéuticas, Universidad Complutense de Madrid, Madrid, 28040 Spain.

gguedes@cicbiomagune.es

Protein-stabilized nanomaterials recently emerged as materials of interest in the biomedical field due to the biocompatibility, stability, and ease of preparation,[1] presenting advantages over currently available diagnostic and therapeutic agents. Engineered metal-coordinating proteins combine the safety/biocompatibility with the diverse functionality of metal nanoparticles. Consensus tetratricopeptide repeat (CTPR) proteins are particularly notable for the robustness and mutational permissibility, due to the repeat nature of the protein, allowing the introduction of metal coordination sites without substantial impact on the structure.[2]

In the current project, cysteine- and histidine-based metal-binding sites were introduced into CTPR proteins for the coordination of Gd and Fe. These proteins were then used to generate protein stabilized nanoparticles (Prot-NPs) with tailored relaxivity properties (Figure 1), thereby allowing their exploration as Magnetic Resonance Imaging (MRI) contrast agents. Moreover, two different strategies were explored to target the Prot-NPs to specific pathologies. In a first approach, Prot-GdNPs were developed as T1-contrast agents, with the Gd particles stabilized on a cysteine-based scaffold that also contained an Hsp90 binding module. This binding module allowed the targeting of a cellular chaperone protein, Hsp90, that is overexpressed in several pathologies, *e.g.,* fibrosis and certain cancers. Likewise, protein stabilized iron oxide nanoparticles (Prot-IONPs) were also developed as contrast agents. The Prot-IONPs were grown on a histidine-based scaffold that was subsequently modified with alendronate to target calcifications in atherosclerotic plaques. This work serves as a proof-of-concept revealing the versatility and potential of the Prot-NPs in biomedical applications through the development of MRI contrast agents with targeting ability.

## References

[1] E. Porret, X. Le Guével, J. Coll, J. Mater. Chem. B, 8 (2020), 2216–2232.
[2] A. Aires, I. Llarena, M. Moller, J. Castro-Smirnov, J. Cabanillas-Gonzalez, A. L. Cortajarena, Angewandte Chemie, 131, 19 (2019), 6280-6285.

## Figures

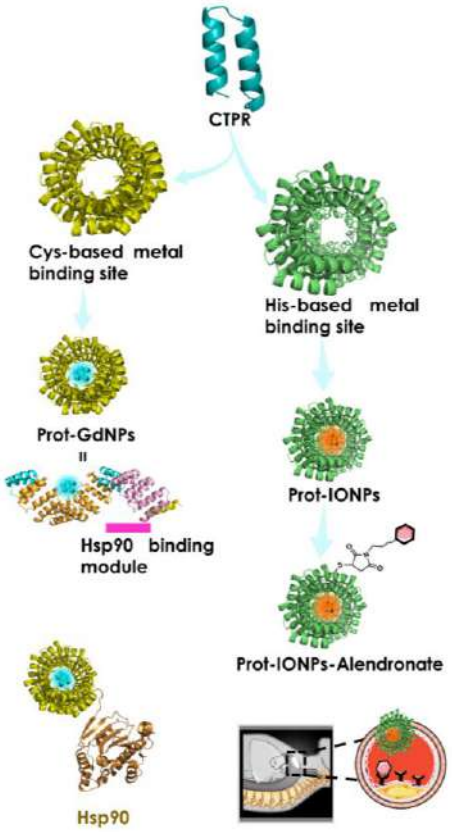


**Figure 1.** Designed CTPR proteins were used to generate custom Prot-NPs with tunable properties for use as targeted MRI contrast.

# $MoS_2$ Defect Healing for High-Performance Sensing of Polycyclic Aromatic Hydrocarbons and Mercury Ions

**Sara Gullace**[1], Fernando Jiménez Urbanos[1] and Paolo Samorì[1]

[1]Institut de Science et d'Ingénierie Supramoléculaires, 8 Allée Gaspard Monge, 67000 Strasbourg, France

gullace@unistra.fr

The increasing population, societal and industrial development represent major environmental problems. Nowadays various governmental agencies decided to pose limits for the maximum permitted levels of pollutants in water, soil and air. For example, among toxic chemicals, heavy metals such as mercury ions ($Hg^{2+}$) and polycyclic aromatic hydrocarbons (PAHs) are poisoning contaminants which could lead to serious health problems. The Environmental Protection Agency (EPA) defined as 10 nM and 0.2 ppb the maximum allowed levels of $Hg^{2+}$ ions and PAHs in drinkable water, respectively. For this reason, the development of fast and reliable sensors for air and water quality monitoring became a hot-topic in science. Low-dimensional materials have attracted great attention as ideal sensory materials, combining high surface-to-volume ratio with unique optical and electrical properties. [1] Among them, two-dimensional semiconductors, such as transition metal dichalcogenides (TMDCs) are characterized by physical and chemical properties that are hugely susceptible to environmental changes. TMDCs can be integrated in field-effect transistors (FETs), which can operate as high-performance chemical detectors of the (non-)covalent interaction with small molecules. Here, we have developed $MoS_2$-based FETs as platforms for PAHs sensing, relying on the affinity of the planar polyaromatic molecules for the basal plane of $MoS_2$ and the structural defects in its lattice. X-ray photoelectron spectroscopy (XPS) analysis, photoluminescence (PL) measurements and transfer characteristics in FETs showed a notable reduction in the defectiveness of $MoS_2$ and a p-type doping upon exposure to PAHs containing solutions, with a magnitude determined by the correlation between the ionization energies ($E_I$) of the PAH target and that of $MoS_2$. Naphthalene, endowed with the higher $E_I$ among the studied PAHs, exhibited the greatest output. Remarkably, we observed a log-log correlation between $MoS_2$ doping and naphthalene concentration in water in a wide range ($10^{-9}$-$10^{-6}$ M). Naphthalene concentrations as low as 0.128 ppb were detected (Figure 1a), being below the limits imposed by health regulations for drinking water. When performing several exposure/washing cycles, the sensor was also able to switch among two different doping levels. Furthermore, our $MoS_2$ devices can reversibly detect vapors of naphthalene both with an electrical and optical readout: overall, our device architecture could operate as a dual platform for the electrical sensing and Raman identification of the analyte. [2]

In another work, we have fabricated $MoS_2$-based FETs with a similar architecture and exploited them as platforms for $Hg^{2+}$ sensing, relying on the affinity of heavy metal ions for both point defects in TMDCs and sulfur atoms in the $MoS_2$ lattice. XPS characterization showed both a significant reduction of the defectiveness of $MoS_2$ when exposed to $Hg^{2+}$ ions with increasing concentration and a shift in binding energy of 0.2 eV suggesting a p-type doping of the 2D semiconductor. The efficient defect healing has been confirmed also by low-temperature PL measurements by monitoring the attenuation of defect-related bands after $Hg^{2+}$ exposure. Transfer characteristics in the $MoS_2$ FETs provided further evidence that Hg(II) acts as a p-dopant of $MoS_2$. Interestingly, we observed a strict correlation of the doping with the concentration of $Hg^{2+}$ ions, following a semi-log trend. Hg(II) concentrations as low as 1 pM can be detected (Figure 1b), being below the limits imposed by EPA regulations. Electrical characterizations also revealed that the sensor can be washed and used multiple times, efficiently switching among two different doping levels. Moreover, the developed devices displayed a markedly high selectivity for Hg(II) against other metal ions as ruled by soft/soft interaction among chemical systems with appropriate redox potentials. In conclusion, we propose a generally applicable approach to develop chemical sensing devices combining a highly sensitivity, selectivity and reversibility to meet technological needs. [3]

## References

[1] C. Anichini, W. Czepa, D. Pakulski, A. Aliprandi, A. Ciesielski, P. Samorì, Chemical Society Reviews, 47, 13, (2018), 4860-4908

[2] F. J. Urbanos‡, S. Gullace‡, and P. Samorì, ACS Nano, submitted

[3] F. J. Urbanos, S. Gullace, P. Samorì, Nanoscale, 13, (2021), 19682-19689

## Figures

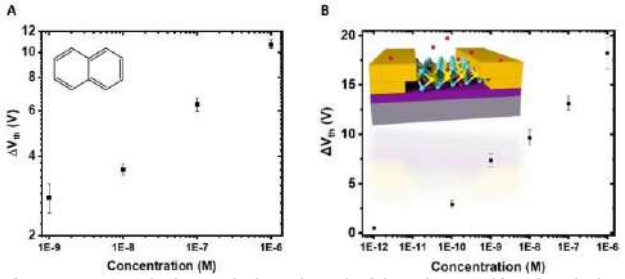


**Figure 1.** Variation of the threshold voltage ($\Delta V_{th}$) of the fabricated field effect transistors (FETs) as a function of **A**) naphthalene and **B**) mercury ions, in water. The inset shows a representative scheme of the interaction among Hg(II) ions and a $MoS_2$-based FET.

# Nanobiosensor devices for environmental quality assessment as containment systems

**Hernández-Albors, Alejandro**[1], Juarez, M.J.; Alcodori Ramos, Javier[1]; Prima, Helena[1]; González, Ernesto[1]; Fort-Escobar, Vicente[1]; Fito López, Carlos[1]

[1]ITENE Research Centre, Parque Tecnológico de Valencia, 46980 Paterna, Spain

alejandro.hernandez@itene.com

The quality of the environment, as well as the quality of the surroundings in which we live, has a relevant and significant influence on our health. In fact, this impact is known to be greater in children under 5 years of age and in people between 50 and 75 years of age. It is estimated that around 12 million people in the world die annually from living or working in highly polluted spaces and environments [1]. Environmental pollutants, which can range from chemical to microbiological agents, are responsible for the development of respiratory and cardiac diseases, as well as favouring the development of certain types of cancer. For example, in urban areas where industrial activity is high, access to clean water is very limited and soil degradation is notable due to the presence of chemical agents, the likelihood of developing these types of diseases is much higher **¡Error! No se encuentra el origen de la referencia.**. In addition, the recent pandemic has highlighted the value of tracking different areas to trigger early warnings, significantly shortening response times **¡Error! No se encuentra el origen de la referencia.**. Therefore, there is a clear need to develop devices capable of monitoring the presence of environmental pollutants, which can directly affect the quality of the living conditions and have a direct impact on our health. At present, diagnostic techniques for environmental analysis (classical chromatographic, spectroscopic and cell culture methods) are often expensive and laborious, require several sample preparation steps, use toxic chemicals and are time-consuming. In contrast, biosensors, that are analytical tools that combine materials and nanomaterials, such as carbon nanotubes, metal nanoparticles or graphene, with biological elements, such as antibodies, aptamers or enzymes, can provide real-time and robust responses, as well as being portable and cost-effective devices [4]. The construction of a biosensor must consider the complexity of the environmental sample. In this sense, the integration of biosensors with devices capable of sampling automatically, as well as the different pre-treatment steps necessary to guarantee the reliability of the analysis by means of the biosensor, are of special relevance.

In this work, will present the different approaches developed by ITENE in the field of environmental monitoring and based on the use of biosensors integrated with devices capable of automating both the sampling and its pre-treatment, as well as its detection, thus recording the levels of certain pollutants in environmental matrices such as water and air, in pseudo real time.

## References

[1] https://health.gov/healthypeople

[2] A Prüss-Ustün, J Wolf, C Corvalán, R Bos and M Neira,https://www.who.int/publications/i/item/9789241565196

[3] Zhang, X., Wu, J., Smith, L.M. et al., J Expo Sci Environ Epidemiol 32, 751–758 (2022). https://doi.org/10.1038/s41370-022-00442-9

[4] S. Rodriguez-Mozaz et al., Talanta 65 (2005) 291–297

## Figures


**Figure 1.** Environmental quality assessment, by using biosensor-based devices, in combination with other elements capable to sampling and pre-treating automatically, can offer significant advantages over with traditional methodologies, for monitoring the health of water, air and soil.

# Gold nanoshells with silica-coated magnetic cores for multimodal imaging and sensing

**Ondřej Kaman**[1,2], Duong Thuy Bui[1,3], Lenka Kubíčková[1], Jarmila Kuličková[1], and Vít Herynek[4]

[1] Institute of Physics, Czech Academy of Sciences Praha, Czech Republic
[2] Technische Universität Kaiserslautern, Germany
[3] University of Chemistry and Technology, Prague, Praha, Czech Republic
[4] First Faculty of Medicine, Charles University, Praha, Czech Republic

kaman@fzu.cz

Complex nanoparticles combining multimodal imaging with local sensing of physical properties or specific chemical species may lead to novel applications in biomedical research and diagnostics. However, reports that demonstrate the contrast effect of a single nanosized probe in several imaging modalities and its sensing performance at the same time are very scarce. Gold nanoshells with magnetic cores and specific organic functionalization may enable the development of such smart contrast agents with extended applicability. Their magnetic cores provide contrast effect in magnetic resonance imaging (MRI) or act as tracers in magnetic particle imaging (MPI). The gold nanoshells can be used as an exogenous contrast agent in photoacoustic imaging (PAI), and importantly, they enable surface-enhanced Raman spectroscopy (SERS). The SERS measurements can be employed either to analyze the local physical conditions based on suitable reporter molecules or to detect certain analytes based on molecular sensors. Such SERS-active molecules thus form an indispensable part of the organic functionalization, which can, however, comprise also other molecules convenient for imaging, e.g. a fluorescent tag.

The present contribution describes complex gold nanoshells with silica-coated Mn-Zn ferrite cores and an organic functionalization of two types. The functionalization of the first type is designed for pH sensing and involves a fluorescent tag as well. The performance of respective gold nanoshells is analyzed by $^1$H NMR relaxometry, fluorescence spectroscopy, proof-of-concept PAI study, and SERS study on aqueous suspensions of varying pH. The functionalization of the second type combines a urea-based receptor and an internal standard for sensing of fluoride anions.

The complex gold nanoshells were achieved by a multistep procedure (transmission electron micrographs of selected intermediates in Fig. 1): (i) hydrothermal synthesis of $Mn_{0.6}Zn_{0.4}Fe_2O_4$ nanoparticles with the mean crystallite size of 12 nm [1], (ii) encapsulation into silica by the Stöber process, (iii) electrostatic self-assembly of a polyelectrolyte multilayer (formed by alternating layers of poly(sodium 4-styrenesulfonate) and poly(diallyldimethylammonium chloride)) that alters the negative zeta potential of silica to positive values, (iv) adsorption of negatively charged ≈3 nm gold seeds, (v) growth of the gold seeds to coalescence by reduction of a soluble Au(III) precursor [2], and (vi) specific organic functionalization.

For the construction of the multimodal contrast agent capable of pH sensing, the gold surface was co-functionalized with 4-mercaptobenzoic acid (MBA) as a SERS-active pH sensor and 7-mercapto-4-methylcoumarin (MMC) as the fluorescent tag [3]. The $^1$H NMR relaxometry evidenced a very high transverse relaxivity of $r_2 \approx 900$ s$^{-1}$ mmol(f.u.)$^{-1}$ L (f.u. denotes the formula unit of the $Mn_{0.6}Zn_{0.4}Fe_2O_4$ ferrite), demonstrating its excellent properties as a negative contrast agent for $T_2$-weighted MRI. The PAI study (Fig. 2) revealed a strong contrast effect with the maximum photoacoustic signal at ≈700 nm, which corresponded to the maximum of the surface plasmon resonance in the UV-Vis spectrum. Finally, the SERS measurements showed a pH-dependent spectral response, which can be attributed to the different extent of protonation of the MBA reporter molecules (Fig. 3).

For the case study on the use of gold nanoshells for sensing of fluoride anions, the nanoshells were co-functionalized with the molecular sensor *N*-(4-thiophenyl)-*N'*-(4-nitrophenyl)urea, synthesized directly on the gold surface, and the internal standard 4-nitrothiophenol (NTP). The SERS study in acetonitrile solutions of tetrabutylammonium fluoride ($Bu_4NF$) (Fig. 4) showed that the spectral response of the urea sensor was dependent on the concentration of the fluoride in the range of $10^{-5}$–$10^{-1}$ mol L$^{-1}$ (Fig. 5). To facilitate the analysis, a model urea-based sensor was synthesized and Raman spectroscopy measurements free of gold nanostructures were carried out. The interpretation of the spectra and fluoride-induced effects was performed based on an extensive DFT study.

**Acknowledgement**

The participation of the first author in the conference is supported by the ESIF and MEYS (project FZU researchers, technical and administrative staff mobility - CZ.02.2.69/0.0/0.0/18_053/0016627). The experimental work was primarily supported by the Czech Science Foundation (project no. 19-02584S).

## References


[1] O Kaman, D Kubániová, K Knížek, L Kubíčková, J Kohout, and Z Jirák, J. Alloys Compd., 888 (2021) 161471.

[2] J Koktan, K Královec, R Havelek, J Kuličková, P Řezanka, and O Kaman, 520 (2017) 922

[3] DT Bui, R Havelek, K Královec, L Kubíčková, J Kuličková, P Matouš, V Herynek, J Kupčík, D Muthná, P Řezanka, and O Kaman, 12 (2022) 428.


## Figures

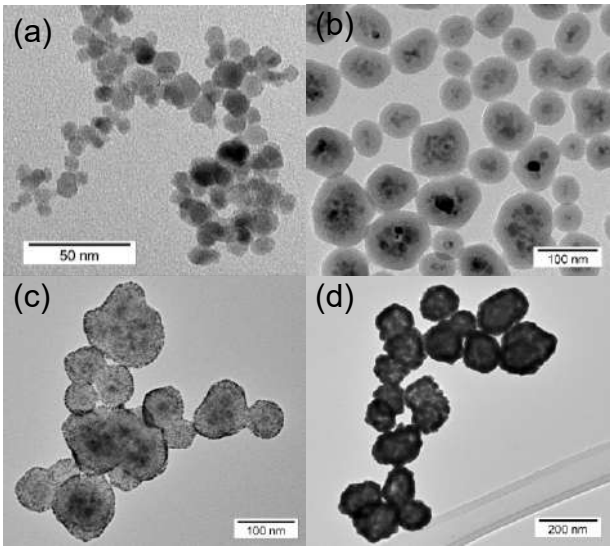


**Figure 1.** Transmission electron micrographs illustrating the main intermediates in the multistep synthesis of gold nanoshells with magnetic cores: (a) $Mn_{0.6}Zn_{0.4}Fe_2O_4$ ferrite nanocrystallites, (b) silica-coated nanoparticles, (c) the intermediate decorated with ultrafine gold seeds, and (d) the final gold nanoshells.

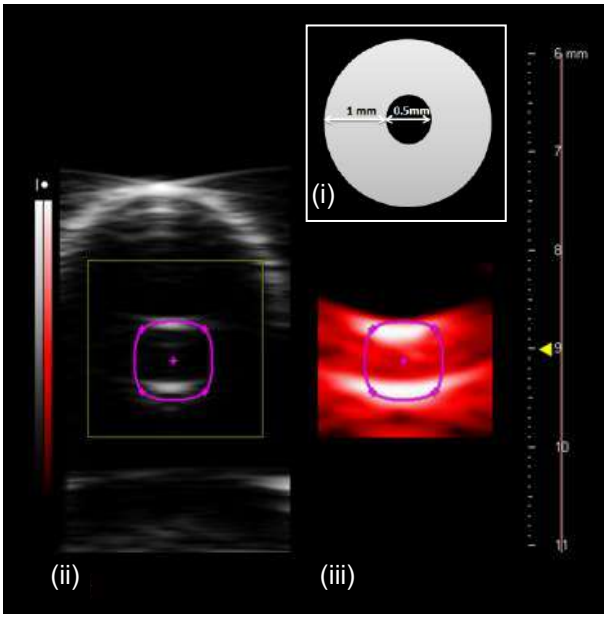


**Figure 2.** PAI study on an aqueous suspension of gold nanoshells, functionalized with MMC and MBA, in a silicone tube: (i) schematic cross-section of the tube filled with the suspension with a concentration of 0.64 mmol(f.u.) $L^{-1}$, where f.u. denotes $Mn_{0.6}Zn_{0.4}Fe_2O_4$, (ii) ultrasound image, (iii) photoacoustic image at 680-nm excitation.

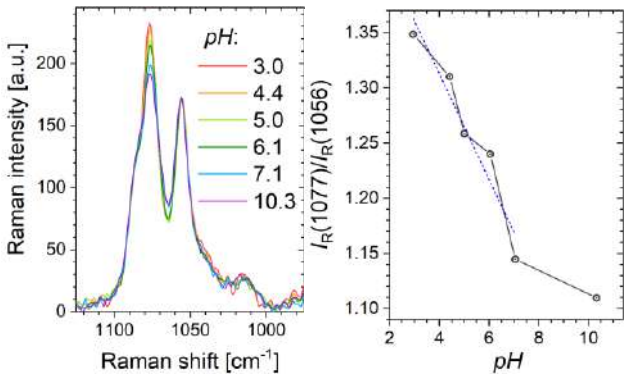


**Figure 3.** SERS study on pH sensing by the gold nanoshells functionalized with MMC and MBA. (a) Detail of the spectral region with the pH-dependent MBA band at 1077 $cm^{-1}$ and the MMC band at 1056 $cm^{-1}$, to which the spectra were normalized. (b) The dependence of the ratio of band intensities at 1077 $cm^{-1}$ and 1056 $cm^{-1}$ on pH, complemented by linear fit in the range of pH = 3–7.

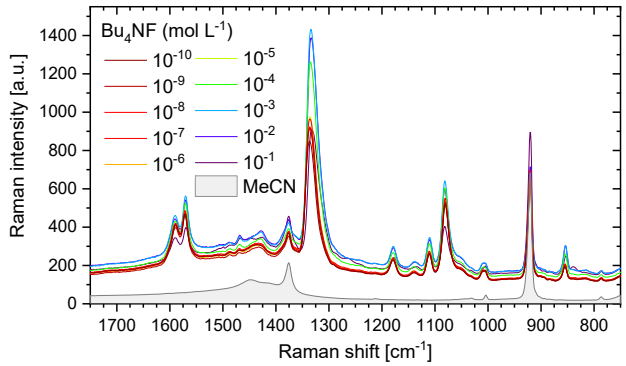


**Figure 4.** SERS spectra of gold nanoshells functionalized with the urea-based sensor and NTP and measured in acetonitrile with varying concentration of $Bu_4NF$.

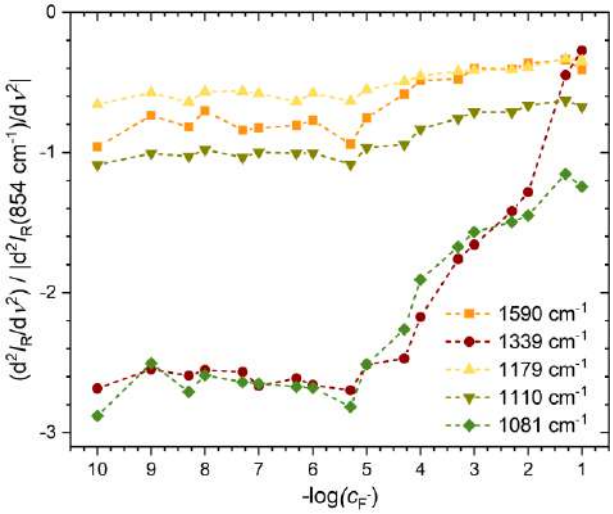


**Figure 5.** The evolution of intensities of selected bands in the second derivative with the addition of $Bu_4NF$, rescaled to achieve the unit intensity of the NTP band at 854 $cm^{-1}$.

# A low-cost, versatile and portable impedimetric biosensor for SARS-CoV-2 detection

**Soroush Laleh**[1,2], Bergoi Ibarlucea[3], Marlena Stadtmüller[4], Gianaurelio Cuniberti[3], Mariana Medina-Sánchez[1,2]

[1]Leibniz Institute for Solid State and Materials Research (IFW), Dresden, Germany
[2]Center for Molecular Bioengineering (B CUBE), Dresden University of Technology, Germany
[3]Institute of Materials Science and Max Bergmann Center of Biomaterials, Center for advancing electronics Dresden (cfaed), Technical university of Dresden, Dresden, Germany
[4]Universitätsklinikum Carl Gustav Carus Dresden, Dresden, Germany

s.laleh@ifw-dresden.de
m.medina.sanchez@ifw-dresden.de

Abstract

On March 11th 2020, Severe Acute Respiratory Syndrome coronavirus 2 (SARS-CoV-2) was declared as a worldwide pandemic by the World Health Organization (WHO) [1]. This virus is considered highly infectious and can lead to an acute respiratory disease, from mild to fatal, with an increase in severity linked to underlying medical conditions [2].

The gold standard for SARS-CoV-2 diagnosis is still Reverse Transcript Polymerase Chain Reaction (RT-PCR), which is a laboratory-based molecular diagnostic method. Although PCR provides a sensitive and specific detection of the viral load, it is quite costly and needs trained personnel and equipment. Typically PCR analysis takes also very long time for the sample transport, preparation and analysis (6-72 hours) [3]. Because of these reasons, it has already been reported that these techniques are unable to combat a highly infectious pathogens specifically in a state of low-resources, where the costs are high for mass screening and the high spread rate dictates the need for a fast early diagnosis [4]–[7].

Although there have been enormous efforts for developing Point of Care (POC) test devices that guarantee the so-called 'ASSURED' criteria (Affordable, Sensitive, Specific, User-friendly, Rapid and robust, Equipment-free and Deliverable to end-users) demanded by the WHO, there is still an urge to improve the existing platforms [8].

For instance, lateral flow immunoassays (LFIAs) tests as POC platform still suffer from low analytical performance [9]–[11] and there is still a controversy over their sensitivity and accuracy [12]–[15].

On the other hand, an early modelling study by Larremore et. al. highlighted the importance of performing continuous diagnosis of the disease for controlling the transmission of the virus, where even with an every-3day instantaneous testing scheme, the estimated infection transmission would be zero even if the tests are not so precise [16].

However, these LFIAs tests are only recommended to be used for individuals who are showing symptoms [17], [18], because it is challenging to detect the virus in carriers who host a reduced concentration and whose symptoms are not so predominant as before. For this reason, it is crucial to develop sensitive, cheap and portable sensors which reliably detect low viral loads.

Electrochemical biosensors are promising technologies for the POC devices, since they are cheap, compact, scalable, and user friendly. They are more sensitive compared to other POC devices like LFIA [8], [19]–[22], and they have the potential to be completely quantitative or semi-quantitative [23], [24]. In general, electrical measurement is performed employing an electrode that traces changes caused by the kinetic of a binding reaction, which indeed causes a change in electrochemical state of system (the electron transfer from the sample to the transducer) [25].

Although Differential Pulse Voltammetry (DPV) and Square Wave Voltammetry (SWV) have been adopted for detection of SARS-CoV-2 and tend to be faster in their response time, Electrochemical Impedance Spectroscopy (EIS) based biosensors are becoming more popular due to their versatility and label-free nature [26].

There are four major features in an electrochemical POC platform: 1. scalable, cheap, reliable and reproducible electrodes, 2. optimized and reliable preparation protocol, e.g. biofunctionalization steps, 3. automated or semi-automated sample handling and data acquisition, 4. reliable, sensitive, accurate and cheap readout. [25], [27]. Despite the astonishing improvements short time after the virus breakout, there are few works that combine more than two of these features at once for a POC.

The aim of this work is to develop an electrochemical biosensor platform based on EIS, which has the potential of satisfying all of these requirements. The proposed biosensor fabrication is very simple and straightforward, and involves no complicated technique or functionalization step. A microfluidic channel has been designed to make the sample handling and data acquisition in a semi-automated manner, and it is also integrated on a Card-Edge Printed Board Circuit (PCB) to make it more user-friendly and deliverable. The sensor chip was also used with both a desktop-portable electrochemical workstation and a mobile phone version, to demonstrate the capability of becoming a POC device.

First, we detected the Spike Glycoprotein of SARS-CoV-2 in physically relevant solution to characterize the developed biosensor and after optimizing the performance of the biosensor using Design of Experiment (DOE), a Limit of Detection (LOD) in fM range was achieved. Afterwards, the sensor performance was tested with nasopharyngeal

samples of patients, where it was able to detect the positive samples of patients with a CT (Cycle Threshold) as high as 27, which refers to low concentration of virus. Additionally, we demonstrated the versatility of this platform for being employed as a highly portable test device with smartphone-based readout, and also by integration of multiple electrodes for multiplexing and parallel analyte detection by simple connection to commercially available adapters. Figure 1 shows the concept and photos of the biosensor as well as its detection performance.

## References


[1] I. Santiago, ChemBioChem, (2020), pp. 2880–2889.

[2] W. Guan et al., N Engl J Med (2020) 382:1708-20.

[3] E. Morales-Narváez and C. Dincer, Biosens Bioelectron., (2020) 163, 112274..

[4] E. R. Adams et al., medRxiv, (2020) 20082099.

[5] P. K. Drain et al., Lancet Infect. Dis., (2021). 239–249.

[6] C. Sheridan, Nat. Biotechnol., (2020). 515–518.

[7] L. Xu, D. Li, S. Ramadan, Y. Li, and N. Klein, Biosens. Bioelectron., (2020) 112673.

[8] V. Vásquez and J. Orozco, Anal. Bioanal. Chem.,(2022) no. 0123456789.

[9] M. L. Everitt, A. Tillery, M. G. David, N. Singh, A. Borison, and I. M. White, Anal. Chim. Acta, (2021) 184–199.

[10] R. W. Peeling and P. Olliaro, Lancet Infect. Dis., (2021) 1052–1053.

[11] A. Scohy, A. Anantharajah, M. Bodéus, B. Kabamba-Mukadi, A. Verroken, and H. Rodriguez-Villalobos, J. Clin. Virol., (2020) 104455.

[12] F. Cerutti et al., J. Clin. Virol., (2020) 104654.

[13] P. de Michelena et al., J. Infect., (2022). e64–e66.

[14] P. Escribano et al., Clin. Microbiol. Infect.,(2022) 865–870.

[15] A. Osterman et al., Medical Microbiology and Immunology, (2021) 65–72.

[16] D. B. Larremore et al., Sci. Adv., (2021) 7 : eabd5393.

[17] M. Linares et al.," J. Clin. Virol., (2020). 104659.

[18] V. Schildgen, S. Demuth, J. Lüsebrink, and O. Schildgen, Pathogens, (2021) 10,38.

[19] S. Imran, S. Ahmadi, and K. Kerman, Micromachines, (2021),12, 174..

[20] N. Kumar, N. P. Shetti, S. Jagannath, and T. M. Aminabhavi, Chem. Eng. J., (2022) 132966.

[21] W. Yin Lim, B. Leong Lan, and N. Ramakrishnan, A Review.Biosensors, (2021) 11, 43.

[22] Z. Zhao et al., TrAC - Trends Anal. Chem., (2021) 116253, 2021.

[23] A. Merkoçi, C. Li, L. M. Lechuga, and A. Ozcan, Biosens. Bioelectron., (2021) 113046.

[24] M.Drobysh, Infection.Int. J. Mol. Sci., (2022) 23, 666.

[25] A. A. Ensafi, Electrochemical biosensors, Elsevier, (2019).

[26] R. Antiochia, Bioelectrochemistry, (2022)108190.

[27] R. Salahandish et al., Biosens. Bioelectron., (2022) 114459.


## Figures

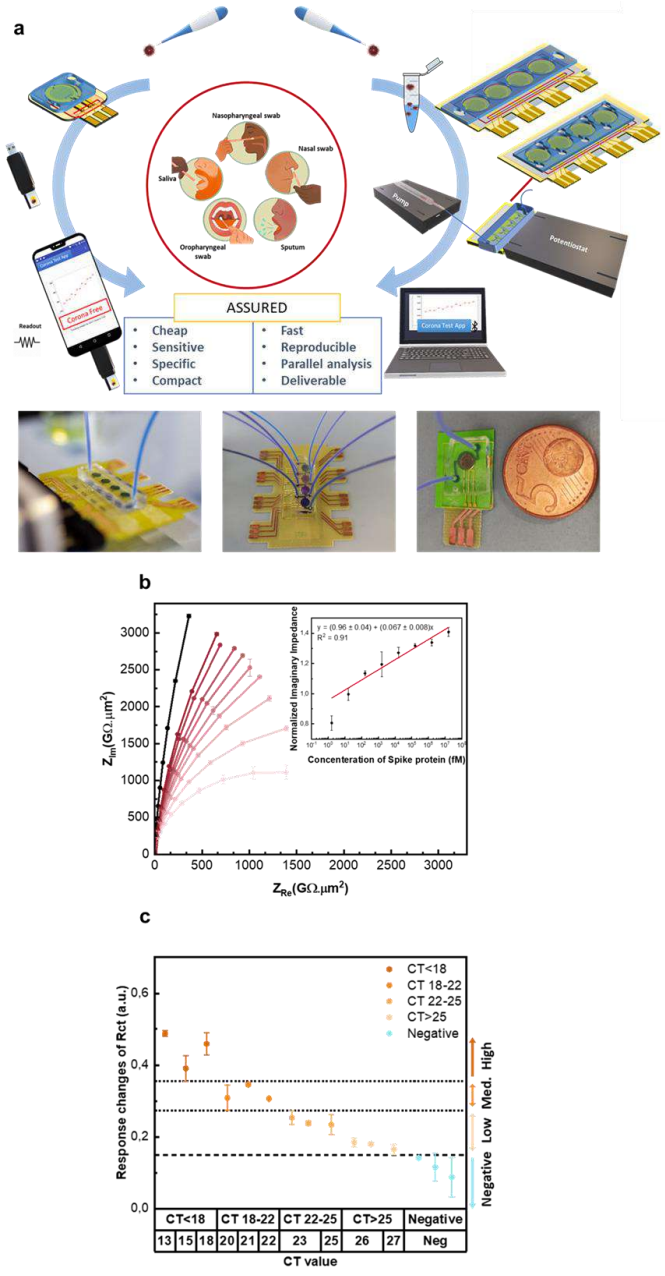


**Figure 1.** a) A schematic representing the concept of the proposed biosensor with a real image of fabricated sensors, b) Nyquist graph showing the response of biosensor with different concentration of SARS-CoV-2 Spike protein ranging from 1.6 fM to 1.6 nM, c) Changes of the charge transfer resistance with changes of Ct-value.

# Different size microdevices with nanostructured ZnO integrated for electrical cell stimulation

**Laura Lefaix**[1], Marc Navarro[1], Lucie Bacakova[2], Carme Noguès[3], Andreu Blanquer[3], Gonzalo Murillo[1]

[1]Instituto de Microelectrónica de Barcelona (IMB-CNM, CSIC), Barcelona, Spain
[2]Institute of Physiology of the Czech Academy of Sciences, Prague, Czech Republic
[3]Universitat Autònoma de Barcelona, Barcelona, Spain

* laura.lefaix@imb-cnm.csic.es

## Introduction

Electrical stimuli have been proved to induce different responses in cells. Among them, proliferation, differentiation and migration are the most studied and they can vary depending on the type of cell, duration and intensity of the stimulus. Other physiological processes that are due to electrical stimuli are nervous impulses and muscle contraction.

To study how cells respond to these electrical stimuli and activate cellular pathways, electronic devices are used to deliver these electrical signals to cells. A safe way to deliver the electrical signal is to use devices with piezoelectric materials integrated [1, 2]. This way, cables -generally used when working with MEAs and other electrode matrices- and highly energetic electromagnetic pulses -that alter the cells and their environment- can be avoided. Ultrasounds (US) can be used as a wireless way of communication with the piezoelectric devices; even if implemented its use as an implant inside of our body [2], where US in the biomedical range (MHz) could deliver the signal safely. The mechanical stress produced by the pressure of the sound wave generate an electric dipole along the surface in piezoelectric materials because of the reversible reorganization of the charges on the atoms of the material [1].

To prove everything stated above, microparticles smaller than a cell were fabricated using microfabrication techniques [3]. Later, a piezoelectric layer of nanostructured zinc oxide (ZnO) was grown on top of them through hydrothermal synthesis. Saos-2 osteosarcoma cells were cultured with the microdevices to analyse their cytocompatibility. Currently, we are working on the effect of the electric fields generated by the microdevices on cells by stimulating them using ultrasonic pulses [1, 2].

## Materials and methods

First, a microparticle array to be used as a template for the microdevices was designed following a microfabrication process in the clean room. Three different templates were designed: with microparticles of a size of 3 x 3 $um^2$, 6 x 10 $um^2$ and 12 x 18 $um^2$. In the microfabrication processs, the main steps were the metallization with a layer of aluminium nitride (AlN), the photolithography to define the particle and the etching to create the microparticles and their stand. The layer of AlN serves later as a seed layer to grow the piezoelectric ZnO in the form of nanosheets (NSs) through hydrothermal synthesis [4]. After this chemical synthesis, the microdevices were peeled-off, washed several times and suspended finally in ethanol, ready for its forthcoming use.

Secondly, a first approach to the biological characterization was performed by culturing the microdevices with Saos-2 human osteosarcoma cells. Microdevices of a 3 x 3 $um^2$ size were used. The experiments performed encompass a cytocompatibility test at days 1, 3 and 7, using calcein and ethium iodide; also, an internalization assay, where the cells were stained with phalloidine (actine fibers) and Hoechst dye (nuclei). Cells were observed at the confocal laser scanning microscope (CLSM) and, the microdevices in contact, quantified. In parallel, these cells were studied under the scanning electron microscope (SEM) to assess the positions taken. The intermediate size and bigger size microdevices were also tested for their cytocompatibility at day 3 and their internalization was also analysed after 24h without quantification.

Experiments stimulating these microdevices using ultrasonic pulses (ULTRASONIDO Sonic-Stimu Basic, Nu-Tek) are being performed on these Saos-2 cells and their cytocompatibility and calcium response using Fluo-4AM (calcium dye) under fluorescence microscope studied.

## Results and Discussion

Once the microfabrication process in the clean room was finished, we obtained microparticles fabricated in Figure 1A. As it can be seen in the image, discrete microparticles with different sizes anchored to the substrate though a fragile stand were fabricated. The sizes of the microparticles were measured, finally being of 3.58 ± 0.04 µm x 3.56 ± 0.05 µm (small), 6.68 ± 0.06 µm x 10.96 ± 0.05 µm (medium) and 13.45 ± 0.64 µm x 19.27 ± 0.27 µm (large). After the hydrothermal growth step, the microparticles were covered by the ZnO NSs layer, increasing the size of the microdevice around 2 µm (Figure 1B). The ZnO NSs thickness obtained was different depending on the microparticle size, changing from a 17 nm thickness in the small ones to around 23 nm in the medium and 32 nm in the

large ones. The whole process was highly reproducible and scalable.

After the peel-off step, the percentage of recovery of the microdevices was of 82% for the 3 x 3 $\mu m^2$ area and below a 30% for the medium size (29%) and large size microdevices (26%). However, millions of microdevices are recovered from a single processed wafer despite the lower obtention of intermediate and bigger size microdevices [3].

After adding the microdevices into the cell culture in a 2:1 (small), 1:1 (medium) and 0.5:1 (large) proportion, cell viability remained above 85% for all of them, with respect to the control that was 96.5%. The internalization of the microdevices, as expected, decreases as the size increases. For the small microdevices, that were studied the most extensively, three positions are taken: internalized, NSs top down and NSs bottom up.

According to the results, these microdevices can be considered cytocompatible. They can also achieve a position outside the cell membrane with the ZnO NSs facing the membrane, an interesting position to trigger the VGCCs in the membrane [1].

## Conclusions

Microfabrication techniques together with hydrothermal synthesis allowed to fabricate reproducible microdevices with different sizes and a piezoelectric layer of ZnO nanostructures. Their cytocompatibility was proved by culturing them with Saos-2 cells. The positions shown by the microdevices with respect to the cells were interesting to induce the electrical response in the cell. This is necessary for our upcoming work, as ultrasound actuation is currently being validated with promising expectations.

## Aknowledgements

This research was supported by La Caixa Foundation under the Junior Leader Retaining program (LCF/BQ/PR19/11700010) and continues to be supported by the Spanish State Research Agency (AEI) under the program Europe Excellence (EUR2020-112082). We also want to acknowledge all the staff at the IMB-CNM (CSIC), especially the clean-room engineers.

## References

[1] Murillo, G. et al., Adv. Mater 29, (2017) 1605048– 160555
[2] Marino, A. et al., ACS Nano 9, (2015) 7678-7689.
[3] Gómez-Martínez, R. et al. Small 6, (2010) 499– 502.
[4] Murillo, G. et al., Nano Energy 60, (2019) 817– 826.

## Figures

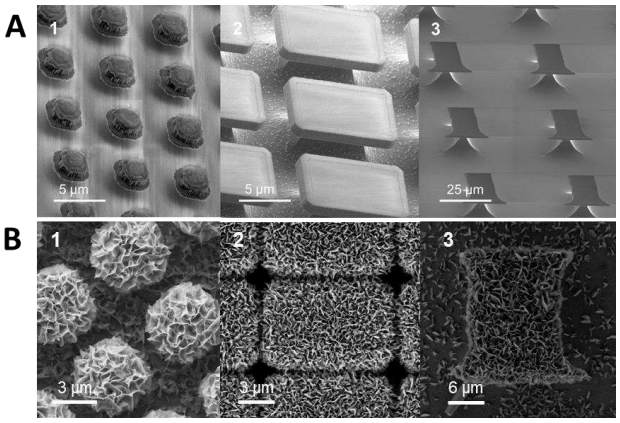


**Figure 1.** Microdevice fabrication. A) SEM image of the microparticle array: microparticles with 3 x 3 µm2 (1), 6 x 10 µm2 (2) and 12 x 18 µm2 (3) area. B) SEM images of the microdevices with the ZnO NSs piezoelectric layer.

# Inhaled amorphous drug nano-particle formulations of BTZ043 to improve tuberculosis treatment

**Feng Li**[1],
Franziska Marwitz[2], David Rudolph[3],
Lea Ann Dailey[1], Gabriela Hädrich[1]

[1] Department of Pharmaceutical Sciences, University of Vienna, Austria
[2] Research Center Borstel, Leibniz Lung Center, Priority Area Infections, Borstel, Germany
[3] Institute of Inorganic Chemistry, Karlsruhe Institute of Technology (KIT), Karlsruhe, Germany.

a12050445@unet.univie.ac.at

## Abstract

8-Nitrobenzothiazinones (BTZ) are a new class of anti-mycobacterial drugs with minimum inhibitory concentrations (MICs) as low as 2.3 nM [1] for drug-resistant *Mycobacterium tuberculosis* strains. However, due to poor solubility and metabolic instability, BTZs generally show poor oral bioavailability [2], which could significantly reduce treatment efficacy. The formulation of BTZ043 into amorphous drug nanoparticles is hypothesized to improve oral bioavailability via enhanced dissolution kinetics and also reduce the side effects.

In this study, amorphous BTZ043 nanoparticles were prepared via a solvent-antisolvent technique with a mean diameter of around 400 nm. The control group was comprised of BTZ043 crystals with a mean particle diameter of around 23 µm, which are representative of the current clinical formulation. Pharmacokinetic studies in healthy Balb/c mice demonstrated that the nanoparticle formulation increased the relative oral bioavailability ($F_{ref}$ %, Equation 1) of 384% in plasma compared to crystalline BTZ043. Inhalation administration of the BTZ043 nanoparticles further increased the relative plasma bioavailability of 862% compared to orally administered crystalline neat drug. Thus, the inhalation of amorphous drug nanoparticles is a promising approach to improve BTZ043 pharmacokinetics, thereby improving tuberculosis treatment with both oral and inhaled products.

## References

[1] Makarov V et al. Towards a new combination therapy for tuberculosis with next generation benzothiazinones. EMBO Mol Med. 2014 Mar;6(3):372-83.
[2] Gao C et al. Benzothiazinethione is a potent preclinical candidate for the treatment of drug-resistant tuberculosis. Sci Rep. 2016 Jul 13;6:29717.

## Figures

$$F_{rel}\% = \left( \frac{AUC_{nano} / Dose_{nano}}{AUC_{micro} / Dose_{micro}} \right) * 100$$

**Equation 1.** Calculation of relative bioavailability

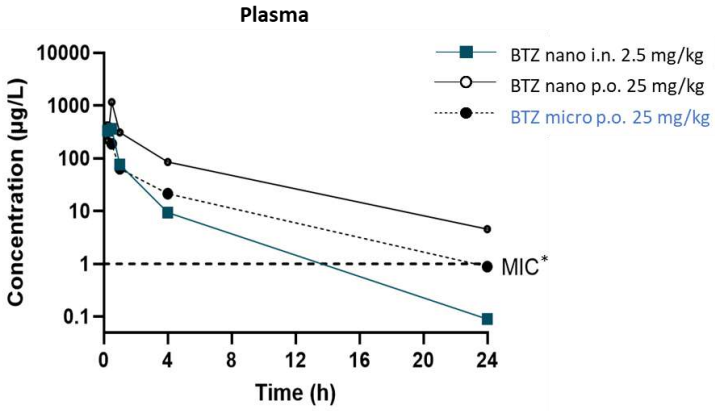


**Figure 1.** Plasma levels of BTZ043 observed in BALB/c mice

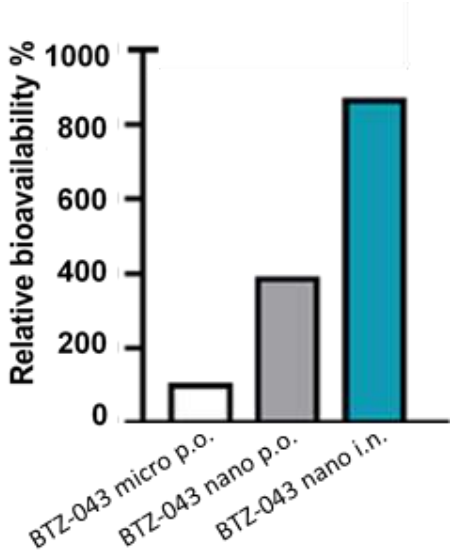


**Figure 2.** Relative bioavailability of BTZ-043 amorphous drug nanoparticle compared to oral administration in plasma.

# MRI tumour detection using metal-free radical dendrimers as contrast agents

**Vega Lloveras,**[1,2] **José Vidal-Gancedo,**[1,2] Songbai Zhang,[1] Luiz F. Pinto,[1] Silvia Lope,[3] Ana Paula Candiota[2,4,5]

[1]Institut de Ciència de Materials de Barcelona ICMAB–CSIC, Campus UAB s/n, 08193 Bellaterra, Spain
[2]CIBER de Bioingeniería, Biomateriales y Nanomedicina, CIBER-BBN, 08913 Bellaterra, Spain.
[3]Servei de Ressonància Magnètica Nuclear, Universitat Autònoma de Barcelona, 08193 Bellaterra, Spain
[4] Departament de Bioquímica i Biologia Molecular, Unitat de Bioquímica de Biociències, Edifici Cs, Universitat Autònoma de Barcelona, 08193 Bellaterra, Spain.
[5] Institut de Biotecnologia i de Biomedicina (IBB), Universitat Autònoma de Barcelona, Bellaterra, Spain

Contact@E-mail (vega@icmab.es; j.vidal@icmab.es)

Early detection of tumours is of vital importance to increase the survival ratio of patients. One of the most largely used clinical imaging procedures for the early diagnosis and follow-up of tumors is magnetic resonance imaging (MRI) thanks to its non-radiative and non-invasive character and its capacity of providing images of soft tissue anatomy in excellent detail, when assisted by contrast agents (CAs).

Nowadays, gadolinium-based contrast agents (GBCAs) are far the most widely used MRI contrast agents in clinical practice. GBCAs have historically been considered as safe but for more than a decade, a linear relationship between GBCA administration and the development of potentially lethal nephrogenic systemic fibrosis (NSF) has been recognized in patients with renal impairment.[1] Moreover, newer reports have emerged regarding the accumulation of residual Gd(III) ions in the brain, bones, skin, liver and kidneys of patients with normal renal function and intact blood–brain barrier (BBB).[2] For these reasons, it is critical to find alternative imaging probes to GBCAs to overcome their established toxicity.

Persistent organic radicals are promising alternatives since they also exhibit paramagnetic properties and can act as $T_1$ CAs like Gd-based CAs while being organic species, mitigating concerns about toxic metal accumulation. With the anchoring of many organic radicals on a dendrimeric macromolecule surface (radical dendrimers)[3] we can achieve an increase of the contrast capacity and protect the radicals from bioreduction, improving the behavior of isolated radicals.

We have successfully synthesized different generations of radical dendrimers fully soluble in water functionalized with nitroxide organic radicals in the periphery. We have demonstrated both *in vitro* and *in vivo* that they can provide similar or even higher contrast enhancement than GBCAs. Under *in vivo* conditions, radical dendrimers have been shown to provide suitable contrast enhancement on murine GL261 glioblastoma (GB) tumors, which was comparable to that of commercial Gd-based CAs, even at its 4 times lower administered dose[3j] (Figure 1). They have showed a selective accumulation in brain tumor tissues, which allows performing imaging acquisition over longer time frames (≥ 2.5 h) than with Gd chelates. No signs of toxicity have been detected and high stability of the radicals in biological media has been observed. All of these features allow us to suggest that radical dendrimers could be a viable alternative to metal-based MRI contrast agents, particularly on MRI analysis of glioblastoma.

## References

[1] M. Rogosnitzky S. Branch, Biometals, 2016, 29, 365-376.
[2] A. Ranga, Y. Agarwal, K. J. Garg, Indian J. Radiol. Imaging 2017, 27, 141−147.
[3] a) E. Badetti, V. Lloveras, K. Wurst, R.M. Sebastian, A.M. Caminade, J.P. Majoral, J. Veciana, J. Vidal-Gancedo, Org. Lett. 2013, 15, 3490−3493. b) E. Badetti, V. Lloveras, J.L. Muñoz-Gómez, R.M. Sebastián, A.M. Caminade, J.P. Majoral, J. Veciana, J. Vidal-Gancedo, Macromolecules, 2014, 47, 7717−7724. c) V. Lloveras, E. Badetti, K. Wurst, J. Vidal-Gancedo, Chem. Phys. Chem. 2015, 16, 3302−3307. d) V. Lloveras, E. Badetti, J. Veciana, J. Vidal-Gancedo, Nanoscale, 2016, 8, 5049−5058. e) V. Lloveras, F. Liko, L.F. Pinto, J.L. Muñoz-Gómez, J. Veciana, J. Vidal-Gancedo, Chem. Phys. Chem. 2018, 19, 1895−1902. f) V. Lloveras, F. Liko, J. Veciana, J.L. Muñoz-Gómez, J. Vidal-Gancedo, Chem. Mater. 2019, 31, 9400−9412. g) L.F. Pinto, V. Lloveras, F. Liko, S. Zhang, J. Veciana, J.L. Muñoz-Gómez, J. Vidal-Gancedo, ACS Applied Bio Materials 2020, 3, 369−376. h) S. Zhang, V. Lloveras, D. Pulido, F. Liko, L.F. Pinto, F. Albericio, M. Royo, J. Vidal-Gancedo, Pharmaceutics 2020, 12, 772-787. i) V. Lloveras, J. Vidal-Gancedo, Molecules 2021, 26, 1230. j) S. Zhang, V. Lloveras, S. Lope-Piedrafita, P. Calero, S. Wu, A. P. Candiota, J. Vidal-Gancedo, Biomacromolecules 2022, 23, 2767−2777.

## Figures

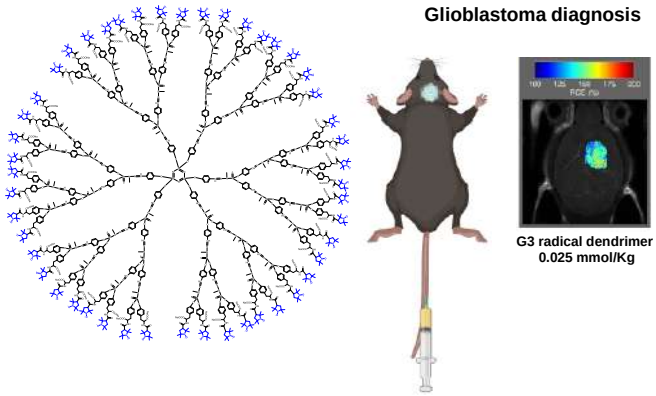


**Figure 1.** Left) Structure of the third generation of a radical dendrimer based on polyphosphorhydrazone dendrimer and proxyl organic radicals (in blue). Right) Color-code scale for relative contrast enhancement (RCE) of GL261 glioblastoma tumour-bearing mice with intravenous administration of the radical dendrimer.

# Guefoams: A new concept of filter media for water bacterial removal

**L.P. Maiorano**[1,2], M. Guidoum[2], M. Benkebiche[2], J.M. Molina[1,2]

[1]Inorganic Chemistry Department, University of Alicante, Alicante, Spain
[2]University Materials Institute of Alicante, University of Alicante, Alicante, Spain

lucila.maiorano@ua.es

Abstract

Open-pore foams are utilized in numerous applications, including medical implantology, catalysis, contaminant retention, heat dissipation, and energy absorption, among others. [1-4].
The replication method is one of the most widely used manufacturing strategies to produce open-pore foams, as it provides a great deal of design flexibility for both the porous architecture and the foam material. This technique is widely employed in the production of metallic, ceramic, and polymeric foams [5-12]. The process involves infiltrating a porous preform with a liquid precursor and then removing by dissolution or chemical reaction the template preform. The use of packed NaCl particulate beds as a leachable template in the production of ceramic materials and polymeric foams is particularly attractive due to its abundance, low cost, and simple disposal. However, its general application for this purpose is limited for the following reasons: (i) due to the high solubility of NaCl in water, water-based ceramic slurries dissolve part or all of the NaCl preform during infiltration , and (ii) due to the high wettability of many polymers on NaCl, their infiltration on NaCl-packed particle or sphere preforms results in a total filling of the pore space in a way that makes it impossible to dissolve the NaCl and obtain a foam material.
In this work, a method is proposed for the fabrication of foams and Guefoams (foams with guest phases located within their porous cavities without any chemical or physical bonding) with ceramic and polymeric matrices. To achieve this, the replication technique was modified by combining two templating agents. The first templating agent is sodium chloride particles or spheres, which are coated with paraffin (second templating agent) and sintered at low temperature (Figure 1). As a result, a self-standing preform with paraffin bridging the particles is obtained. The fully paraffin-coated preform is infiltrated with ceramic slurries or low solubility polymers in paraffin. When the matrix has been consolidated, the two templates can be easily eliminated. This method permits the fabrication of open-pore foam materials with a high degree of design flexibility in terms of both the foam material and its pore architecture (shape, size, and pore size distribution). The application of certain polymer matrix materials as antibacterial water filters was tested. These materials consisted of epoxy matrix Guefoams and activated carbon guest phases coated with iodine. E. coli and S. aureus were used in the tests as the bacteria. More than 99% of the bacteria were inhibited in a single pass through the filter, with the added benefit that the pressure drop imposed by the Guefoam material is significantly less than that of a bed of compacted particles of similarly modified activated carbon. In the field of bacteriological water purification, the results suggest that these materials are among the most promising alternatives.

## References

[1] G.J. Davies, Shu Zhen, Review Metallic foams: their production, properties and applications, Materials Science, 18 (1983) 1899-1911.

[2] J. Banhart, Manufacture, characterisation and application of cellular metals and metal foams, Progress in Materials Science, 46 (2001) 559-632.

[3] M. V. Twigg, J. T. Richardson, Theory and applications of ceramic foam catalysts, Chemical Engineering Research and Design, 80 (2002) 183-189.

[4] Q.Z. Wang, Compressive behaviors and energy-absorption properties of an open-celled porous Cu fabricated by replication of NaCl space-holders, Materials Processing Technology, 211 (2011) 363–367.

[5] C. San Marchi, A. Mortensen, Deformation of open-cell aluminium foam, Acta Materialia, 49 (2001) 3959-3969.

[6] C. Gaillard et al, Processing of NaCl powders of controlled size and shape for the microstructural tailoring of aluminium foams, Materials Science and Engineering A, 374 (2004) 250-262.

[7] Y. Conde et al, Replication processing of highly porous materials, Advanced Engineering Materials, 8 (2006) 795-803.

[8] R. Goodall et al, Spherical pore replicated microcellular aluminium: Processing and influence on properties, Materials Science and Engineering A, 465 (2007) 124-135.

[9] A. Bansiddhi, D.C. Dunand, Shape-memory NiTi foams produced by replication of NaCl space-holders, Acta Biomaterialia, 4 (2008) 1996-2007.

[10] M.A.A.M. Nor et al, Preparation and characterization of ceramic foam produced via polymeric foam replication method, materials processing technology, 207 (2008) 235-239.

[11] L. Stanev et al, Open-cell metallic porous materials obtained through space holders—Part II: Structure and Properties. A Review, Manufacturing Science and Engineering, 139 (2016) 050802.

[12] R. Yeetsorn, Fabrication of a ceramic foam catalyst using polymer foam scrap via the replica technique for dry reforming, ACS Omega, 7 (2022) 4202-4213.

## Figures

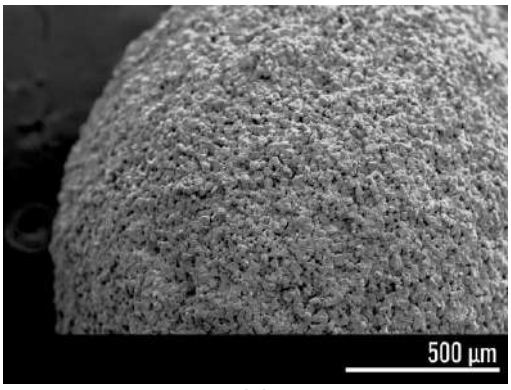


(a)

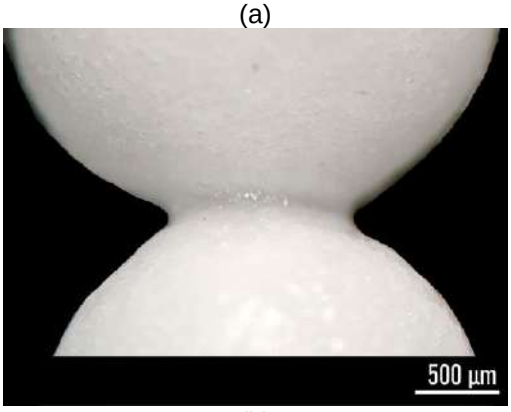


(b)

**Figure 1.** SEM image of the spherical NaCl particles prepared for the fabrication of leachable preforms; (b) photograph of the paraffin-coated NaCl spheres after the sintering process, showing the bonding bridges.

# Challenges of printing on Mussel-Inspired free-standing films as Artificial biosensing Skin

**Gabriel Maroli**[1,2],
Giulio Rosati[1], Salvio Suárez-García[1],
Massimo Urban[1], Patricia Batista Deroco[1,3],
Daniel Ruiz-Molina[1] and Arben Merkoçi[1,4]

[1]Catalan Institute of Nanoscience and Nanotechnology (ICN2), CSIC and BIST, Campus UAB, Bellaterra, 08193 Barcelona, Spain
[2]National Technological University (UTN-FRBA), Buenos Aires, Argentina
[3]Institute of Chemistry, University of Campinas (UNICAMP), Campinas, Sao Paulo, Brazil
[4]Catalan Institution for Research and Advanced Studies (ICREA), 08010 Barcelona, Spain

Arben.merkoci@icn2.cat

Printed sensors, both on flexible substrates and directly on the skin, have been shown to have great potential for developing wearables and point-of-care devices. For this reason, integrating sensors by printing methods into already developed mussel-inspired membranes as artificial skin for tissue regeneration is of great interest not only for sensing on the skin, but also for treating wounds.

However, printing on delicate materials such as artificial skin presents many challenges, especially when a common desktop printer is used. To print on these materials, they must be dry, making them fragile and brittle. Due to this, some of the inside components of the desktop printer, like the rollers and wheels for dragging the paper can easily damage and eventually break them apart. For tailoring some of these issues, can be may be beneficial to use more dedicated and advanced equipment, like research grade inkjet printers.

This work presents the comparison, advantages, and disadvantages of printing on mussel-inspired membranes using a Dimatix (Fujifilms DMP 280) research grade printer and an EPSON xp 15000 desktop printer. As a case study, the resistivity obtained from the inks has been compared and its possible application for the construction of RF antennas as well as for a temperature sensor on the skin.

## References

[1] MacNeil, S. Nature 2007, 445, 874-880.
[2] Rahmati, M. et al. Mater. Today Adv. 2020, 5, 100051.
[3] Ruiz-Molina, D. et al. Angew. Chem. 2019, 58, 696-714.
[4] Ershad, F. et al, Nat. Commun. 2020, 11, 3823.

## Figures

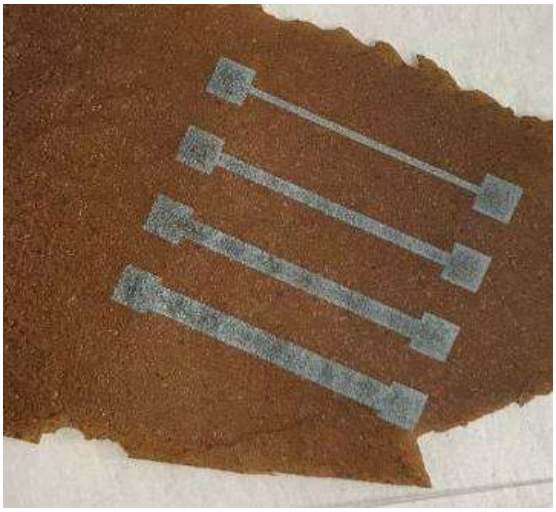

**Figure 1.** Silver tracks printed whit Epson printer on the mussel-inspired free-standing membrane

# Nanobiosensing of Small Molecules: Challenges and Prospects for Molecular Imprinting

**Jose Marrugo-Ramírez[1+]**
Nerea de Mariscal-Molina[1+], Giulio Rosati[1], Cecilia de Carvalho Castro e Silva[2], Lourdes Rivas[1], Emily Nguyen[1], Arben Merkoci[1,3]

[1] Nanobioelectronics & Biosensors Group, Catalan Institute of Nanoscience and Nanotechnology (ICN2), CSIC and BIST, Campus UAB, 08193 Bellaterra, Barcelona, Spain
[2] Graphene and Nanomaterials Research Center – MackGraphe, Campus UPM, 01302-907 São Paulo, SP, Brazil
[3] ICREA, Institució Catalana de Recerca i Estudis Avançats, Passeig Lluís Companys 23, Barcelona, Spain,

arben.merkoci@icn2.cat

Abstract

Biomedicine, environmental monitoring, and nanobiosensing are just some areas where molecularly imprinted polymers (MIPs) have shown their potential as synthetic receptors that can tell the difference between large and small molecules with high molecular specificity. Antibodies and enzymes, for example, have shown intrinsic issues with temporal stability and may be denatured under extreme conditions [1]. MIPs, however, are more robust in complex media, have better long-term stability, and a more straightforward and reproducible fabrication procedure. Nevertheless, there is a lack of publications in the literature investigating the quantitative analytical capabilities of MIPs in real-world applications. While there has been progress in commercializing biosensors based on MIPs [2,3], various issues must be investigated.

Researching the binding interactions between monomers and between the monomer and the template in a porogenic solvent is the most pressing issue in MIPs development since the template-monomer complex must form spontaneously and be stable. Using kynurenic acid as a model small molecule template, we investigated its ionic form in different matrices and its complexation with o-phenylenediamine. Additionally, further studies encompass an adaptation of the MIP layer onto nanomaterial-based electrodes due to their ease of tuning and fabrication. MIPs have been found to have greater sample loading capacity, sensitivity, and selectivity for small compounds than traditional immunoassays [4,5], making them appealing for quantitative small molecule biomarker detection.

## References

[1] Parisi, O.I, et al., J. Funct. Biomater, 13 (2022) 12.
[2] Ramanavicius, S., Jagminas, A., Ramanavicius, A., Polymers, 13 (2021) 974
[3] Lowdon, J. W. et al., Sensors and Actuators B: Chemical, 325 (2020) 128973.
[4] Ahmad, O. et al., Trends in Biotechnology, 37 (2019) 294-309
[5] Naseri, M.; Mohammadniaei, M.; Sun, Y.; Ashley, J., Chemosensors, 8 (2020) 32.

# Nanocasting template synthesis of porous persistent luminescent nanoparticles for PDT

**Mathilde Ménard**[1], Christophe Dorandeu[1], Sofia Dominguez-Gil[1], Nicolas Donzel[1], Jean-Olivier Durand[1], Frédérique Cunin[1], Aurélie Bessière[1]

[1]Institut Charles Gerhardt Montpellier, UMR 5253, CNRS, Montpellier, France

mathilde.menard@umontpellier.fr
aurelie.bessiere@umontpellier.fr

Persistent luminescent materials (PERL) possess the unique optical property to have a long-lasting afterglow that persists after the cessation of excitation. They are mostly made of bulk materials or micrometric powders synthesized by solid-state chemistry at high temperature. However, their nanoscale counterparts need softer chemistry synthesis pathways, like hydrothermal syntheses, leading frequently to a decrease in their PERL efficiency. Thus a post-synthesis annealing treatment is often necessary to increase their PERL properties but it has the major disadvantage to induce sintering effects. Therefore, we propose to use mesoporous silica nanoparticles as sacrificial hard-nano-template to synthesize porous PERL nanoparticles at high temperature. We choose $ZnGa_2O_4:Cr^{3+}$ as PERL material since it emits at 700 nm (red emission) [1] and it showed an exceptional potential as nano-probe for biomedical optical imaging [2]. However, the actual synthesis methods do not lead to porous $ZnGa_2O_4:Cr^{3+}$ nanoparticles thus limiting their biomedical applications. Indeed, additional synthesis steps are necessary to add porosity to the material like for example the addition of a porous silica shell. Therefore, we developed the synthesis of porous $ZnGa_2O_4:Cr^{3+}$ nanoparticles through a nanocasting synthesis strategy. First, the PERL precursors were impregnated into the mesoporosity of silica nanoparticles and then a thermal treatment was performed to crystalize the PERL material into the pores. Finally, the silica was dissolved to free the porosity of the as-obtained nano-PERL that can be then used for example for photosensitizers loading to perform deep PDT by persistent luminescence [3].

## References

[1] A. Bessière, et al., Optics Express, 19, 11, (2011), p 10131-10137
[2] T. Maldiney, et al., Nature Materials, 13, 4, (2014), p 418-426
[3] A. Bessière, et al., Nanophotonics, 10, 12 (2021), pp.2999-3029.

## Figures

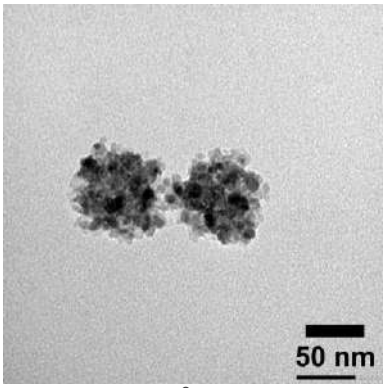


**Figure 1.** PERL $ZnGa_2O_4:Cr^{3+}$ nanoparticles synthesized via nanocasting

# NanoQSAR models on the toxicity of quantum dots

**Salvador Moncho**[1],
Eva Serrano-Candelas,[1] Rafael Gozalbes[1]

[1]ProtoQSAR, SL., CEEI Valencia, Parque Tecnológico de Valencia, 46980 Paterna, Spain

smoncho@protoqsar.com

QSARs (Quantitative Structure-Activity Relationships) are mathematical models relating the structure of molecules with a biological property or activity, through the use of statistical tools. They are used to predict properties and biological effects of new structures, quickly and at a very low cost in comparison to experimental approaches.

QSAR models for discrete organic molecules are widely used and can be accepted for regulatory purposes [1]. On the contrary, QSAR models on nanomaterials (NMs), commonly known as nanoQSARs, are still at an early stage. One of the challenges in this domain is the identification and description of what a particular NM is. Discrete molecules can be totally identified and characterized by their chemical structure, represented for example by the SMILES code, but this approach is insufficient for NMs, as a key component of their definition is the size and shape or the particles. Another particularity of NMs is the potential complexity of their chemical composition (Figure 1), as they could be formed by different parts: the core, a shell, impurities or dopants and ligands or coating.

As a direct consequence of the structural complexity of NMs, the development of QSAR models requires the codification of nanoform's information that exceeds the classical molecular descriptors. All these particularities should somehow be codified as NM descriptors that are the bases of the development of nanoQSAR models (in a similar way that molecular descriptors are fundamental for QSAR models).

After an extensive analysis of existing calculated and experimental features used to define and describe NMs in the literature, we propose a classification of the descriptors (Figure 2). Our classification differentiates between those descriptors that codify a direct and indirect description of the structure, and those that provide additional experimental knowledge. Direct descriptors provide information from the chemical composition of the core (a), the surface substituents (b) or the physical structure (c). Indirect descriptors codify information of experimental features that depend on the structure (d) or may cause changes in the structure (e). In addition, the classification includes features that do not describe the NM, but the conditions of the endpoint measurement (f).

Quantum dots (QDs) are a particular group of NMs which are characterized by their unique optical and electronic properties. Those nanoparticles present discrete electronic levels that lead to a UV-visible emission patterns which depend on the size of the particle (Figure 3). We have developed preliminary nanoQSAR models for the cytotoxicity of QDs, using a dataset compiled by Bilal et al. [2] and discussed the influence of the descriptors used in the performance of the models.

In this work we present the development of predictive models, as well as a discussion in the effect of different changes in the selected features, including calculated descriptors and experimental measurements.

## References

[1] R. Gozalbes, J.V. de Julián, IJQSPR, 3 (2018) 1-24.

[2] M. Bilal, E. Oh, R. Liu, J.C. Breger, I.L. Medintz, Y. Cohen, Small, 15 (2019) 1900510.

## Figures

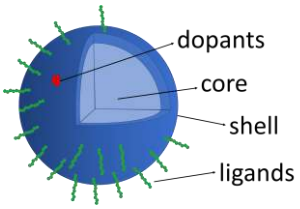


**Figure 1.** Schematic depiction of the parts of a complex nanoparticle

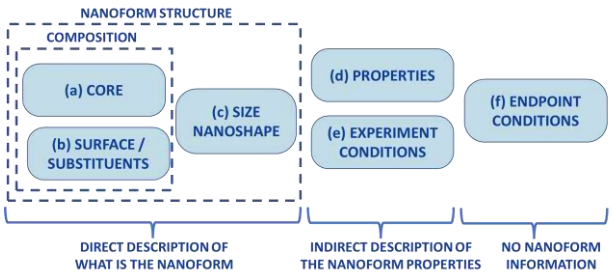


**Figure 2.** Classification of nanoQSAR descriptors

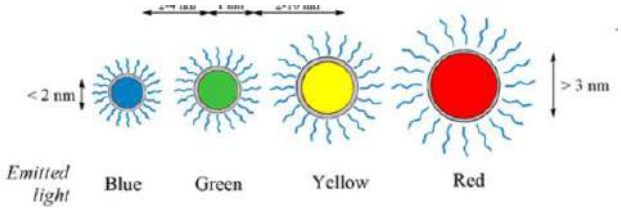


**Figure 3.** QDs light emission dependence on the size

# Tailoring carriers for specific applications by unveiling the role of individual components in pBAE/polynucleotide polyplexes: on road to rational formulations

**María Navalón[1],**
Aurora Dols[2], Santiago Grijalvo[3], Cristina Fornaguera[1], Salvador Borrós[1]

[1]Grup d'Enginyeria de Materials (Gemat), Institut Químic de Sarrià (IQS), Universitat Ramon Llull (URL), Barcelona, Spain
[2]Nanoscale bioelectrical characterization/IBEC, Barcelona, Spain
[3]Surfactants and Nanobiotechnology/IQAC-CSIC, Barcelona, Spain

marianavalonl@iqs.url.edu

## Introduction

Polynucleotide-based therapies steadily grow into transforming the whole (bio)medicine field as they show tremendous potential for prevention or treatment for a wide range of infectious diseases or genetic disorders.[1] Currently there are more than 2.400 clinical trials comprising gene therapies.[2] Remarkably, the first treatment applied worldwide, SARS-CoV-2 prophylactic vaccines, has only given a glimpse of the involved intricacies and revealed the untapped potential of polynucleotide-based therapies.[3,4] Despite their theoretical full potential, these therapies still find unsatisfactory clinical outcomes which is mainly related to the low chemical stability and poor bioavailability of polynucleotides in-vivo.[5]

Overcoming these drawbacks is accomplished by compartmentalizing the polynucleotides into designed nanocarriers (***Figure 1A***) programmed to deliver them into the specific tissue and intracellular compartment.[6] Genetically engineering viral vector emerged as a natural carrier for gene therapies as their ubiquitous ability to infect and transport the therapeutic nucleic acids across cellular barriers.[7] However, viral vectors are concerned in different aspects, such as safety, immunogenicity, insertional mutagenesis, low loading capacity and high production costs. These drawbacks triggered the development of nanotechnology-based non-viral delivery systems (***Figure 1B***), which on the one hand are modular to meet application requirements and on the other hand their production is cost-effective.[9]

Among non-viral carriers, poly(β-amino ester)s (pBAE) are an outstanding option as a carrier, due to their high building blocks versatility, high transfection efficacy, low toxicity and excellent biocompatibility and biodegradation profile[10]. Upon contact with polynucleotides, pBAEs condense into polymeric nanoparticles, (polyplexes), that protects the fragile cargo and transports it into the targeted tissue[11]. Additionally, pBAE building blocks contain hexyl monomers (C6) that provide certain hydrophobicity to the polymer, that allows freeze-drying of the polyplexes, a remarkable property for achieving long-term storage and ameliorated logistics of distribution.[9,12] Further functionalization of the pBAE vectors with short cationic oligopeptides (OM-pBAE), such as lysine (K), Arginine (R), and Histidine (H) (C6CK3, C6CR3 and C6CH3 respectively) are designed not only to increase their buffering capacity and ability to compact nucleic acids due to electrostatic interactions, but also to promote cellular internalization and nucleic acid transfection.[9]

As we previously described, C6CK3 promotes the plasmatic membrane crossing, C6CH3 assists in the endosomal scape development and C6CR3 gives an advantage to nuclear subcellular localization. Cationic peptides, however, increase the polyplex positive surface charge resulting in transfection promiscuity. Consequently, these pBAE-based polyplexes have low selectivity. Decreasing the surface charge and thus promiscuity is achieved by coating the polyplexes with Aspartic acid (D) functionalized pBAEs. In this sense, it is clear that careful combination of different OM-pBAEs is thus crucial for achieving an optimal functionality.[9,13]
Indeed, various OM-pBAEs combination have achieved optimal results *in-vitro* and *in-vivo*.[11] Despite these outstanding outcomes, the different pBAEs structure in the polyplexes and therefore their influence in the final properties is still unclear. These unknown characteristics involve a time-consuming experiments without specific and clear application due to the uncertainty of their target and uptake specificity, which are needful characteristics in order to achieve the medical needs.

Recently, we demonstrated the microstructure of C6CR3/pDNA polyplexes and an oligopeptide-dependence of time evolution of the cationic polyplexes using high resolution optical microscopy.[14,15] We aimed to understand the microstructure of polyplexes composed by mixtures of OM-pBAE and determine the role of individual components in the final formulation and create a library of OM- pBAE carriers based on a rational selection in function of the chased properties for an specific application.
For this purpose, we study six polyplex constructions with different compositions: KH, KHD, RH, RHD, RK and RKD, combining different OM-pBAEs (***Figure 1C***). We reveal the microstructure and physicochemical properties of the different polyplexes. Our results allow the rational

engineering of carriers for any required application and allows for the further development of pBAEs building blocks for the optimal delivery of polynucleotides.

## Experimental methods

Being assisted with advanced techniques such as Fluorescence Resonance Energy transfer (FRET), enhanced dark field spectral microscopy, Atomic Force Microscopy (AFM) and microscale thermophoresis (MST), we have been able to understand and therefore tailor the OM-pBAE carriers, by selecting the most accurate oligopeptide combination, based on the needs or interests requested for the specific application goal. Therefore, we have been able create a wide OM-pBAEs library for different application goals.

## Conclusions

Thanks to the mechanical and physicochemical properties given by each oligopeptide combination (***Table 1***), an OM-pBAE NPs library has been created. Thus, for the first time, we reveal properties that will allow tailoring the carriers by selecting the most accurate oligopeptide combination[16], based on the needs or interests requested for the specific application goal. Consequently, our results will boost future research on OM-pBAE to facilitate their transfer to clinical applications.

## References


1. Saji, V. S., Choe, H. C. & Yeung, K. W. K. Nanotechnology in biomedical applications: A review. *Int. J. Nano Biomater.* **3**, 119–139 (2010).
2. Jin, S. & Ye, K. Nanoparticle-Mediated Drug Delivery and Gene Therapy. *Biotechnol. Prog.* 32–41 (2007)
3. Papadopoulos, K. I., Wattanaarsakit, P., Prasongchean, W. & Narain, R. *Gene therapies in clinical trials*. *Polymers and Nanomaterials for Gene Therapy* (Elsevier Ltd., 2016).
4. Baden, L. R. *et al.* Efficacy and Safety of the mRNA-1273 SARS-CoV-2 Vaccine. *N. Engl. J. Med.* **384**, 403–416 (2021).
5. Kay, M. A. State-of-the-art gene-based therapies: The road ahead. *Nat. Rev. Genet.* **12**, 316–328 (2011).
6. Mendes, B. B. *et al.* Nanodelivery of nucleic acids. *Nat. Rev. Methods Prim.* **2**, 24 (2022).
7. Dosta, P., Segovia, N., Cascante, A., Ramos, V. & Borrós, S. Surface charge tunability as a powerful strategy to control electrostatic interaction for high efficiency silencing, using tailored oligopeptide-modified poly(beta-amino ester)s (PBAEs). *Acta Biomater.* **20**, 82–93 (2015).
9. Murali ramamoorth, A. narvekar. Non Viral Vectors in Gene Therapy- An Overview. *J. Clin. Diagnostic Res.* (2015) doi:10.7860/JCDR/2015/10443.5394.
10. Fornaguera, C. *et al.* mRNA Delivery System for Targeting Antigen-Presenting Cells In Vivo. *Adv. Healthc. Mater.* **7**, 1–11 (2018).
11. Karlsson, J., Rhodes, K. R., Green, J. J. & Tzeng, S. Y. Poly(beta-amino ester)s as gene delivery vehicles: challenges and opportunities. *Expert Opin. Drug Deliv.* **0**, (2020).
12. Cordeiro, R. A., Serra, A., Coelho, J. F. J. & Faneca, H. Poly(β-amino ester)-based gene delivery systems: From discovery to therapeutic applications. *J. Control. Release* **310**, 155–187 (2019).
13. Fornaguera, C., Castells-Sala, C., Lázaro, M. A., Cascante, A. & Borrós, S. Development of an optimized freeze-drying protocol for OM-PBAE nucleic acid polyplexes. *Int. J. Pharm.* **569**, 118612 (2019).
14. Segovia, N., Dosta, P., Cascante, A., Ramos, V. & Borrós, S. Oligopeptide-terminated poly(b-amino ester)s for highly efficient gene delivery and intracellular localization. doi:10.1016/j.actbio.2013.12.054.
15. Riera, R. *et al.* Tracking the DNA complexation state of pBAE polyplexes in cells with super resolution microscopy †. *Nanoscale* **11**, (2019).
16. Navalón-López M. et al. In preparation (2022)


## Figures

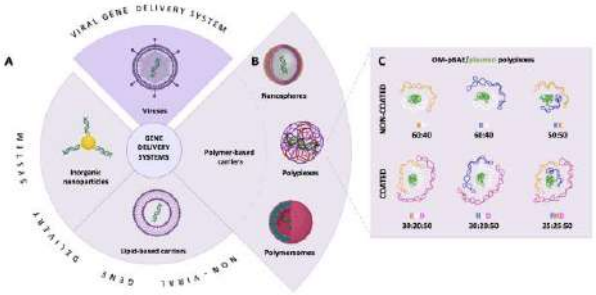


***Figure 1.*** **Gene delivery systems scheme.** A) Schematic classification of viral and non-viral gene delivery systems. B) Polymer-based nanocarriers subtypes. C) Poly (b aminoester) - pBAE/plasmid polyplexes constructions and its polymer/plasmid ratio used.

***Table 1. Scheme of the different NPs constructs properties and their possible applications***. In where "*" mean lowest values and "***" higher values.

| NPs Formulation | Z - potential | Size | EE | Adhesion | Binding Affinity | Stability | Applications |
|---|---|---|---|---|---|---|---|
| KH | *** | * | *** | ** | *** | * | Vaccination purposes, immunotherapy[15] |
| KHD | * | ** | ** | ** | ** | ** | Inhaled delivery and muscle regeneration purposes |
| RH | *** | * | * | *** | * | ** | Chronic diseases (cardiovascular, artheosclerosis, tumour treatment...) |
| RHD | * | *** | * | *** | ** | ** | Muscle regeneration purposes and inhaled delivery |
| RK | ** | * | * | ** | * | ** | Chronic autoimmune disease (diabetes) |
| RKD | * | ** | ** | *** | *** | ** | Dermo-cosmetic aims (retarding ageing) |

# NOVEL PIEZOELECTRONIC MICRODEVICE FOR ELECTRICAL CELL STIMULATION

**Marc Navarro**[1], Laura Lefaix[1], Gonzalo Murillo[1]

[1]Instituto de Microelectrónica de Barcelona (IMB-CNM, CSIC), Barcelona, Spain

marc.navarro@imb-cnm.csic.es

## Abstract

This paper reports a bioelectronic microdevice for electrical cell stimulation using ultrasound signals within the predefined medical frequency range. The microdevice size is comparable to a common human cell (around 1000 µm3). It is able to generate a local electric potential due to the actuation of a piezoelectric resonator that provides high-spatial resolution for the electrical stimulation. The electrical field generated by these microdevices is enough to open the voltage-gated calcium channels on the cell membrane, and therefore, electro-stimulate cells for future therapeutical applications.

## Background

Our previous work related to cell stimulation was reported in various articles in the last years [1], [2]. The fabrication of piezoelectric microdevices was presented in MEMS 2021[3]. This paper shows the design, simulation and on-going fabrication of novel cell-sized piezoelectric microdevices.
Previous attempts at electro-stimulating cells using piezoelectric materials in bone cells are reported using 2D ZnO nanosheets [1] and BNNTs in osteosarcoma cells (SaOS-2) using ultrasounds signals. The results show an enhanced expression of collagen type I (COL1). BNNTs also have been used in neuronal-like and human neuroblastoma cells with ultrasounds signals as mechanical stimuli. These results presented neurite sprout 30% greater than control [4]. Furthermore, using millimeter-sized piezoelectric devices and a neural interface platform, other authors have obtained promising results on neural activity monitoring and stimulation on in-vivo rodent models [6-8]. Lastly, the usage of ZnO nanosheets has also been studied in smooth and skeletal muscle cells demonstrating stimulation triggered by the nanogenerators only on smooth muscle cells [5].

## Methodology

Using silicon on insulator (SOI) wafers, the fabrication of the biomedical microdevices is divided in four stages. First, the deposition and etching of electrodes and piezoelectric material using sputtering and wet etching techniques. Then, the microdevices membrane is created using reactive ion etching (RIE) on the handle side of the wafers and, finally, the microdevices are released from the substrate using a patented procedure (WO2010112532A1). In the last step, the released microdevices are suspended in a biocompatible solution, ready to be applied to cell cultures or tissues as Figure 1 shows.

## Experimental Results

Using Finite Elements Modeling (FEM) software, COMSOL Multiphysics, the expected voltage output of the microdevices under biological media is ~40 V at 1.47 MHz as shown in Figure 2. A change on the dimensions of the microdevice will allow tunability in frequency spectrum. The fabrication process and device liberation is schematically shown in Figure 3. Previous work on microfabrication of piezoelectric devices is shown in Figure 4, showing the feasibility of the on-going fabrication process. The fabricated devices will be characterized by using a medical-frequency range ultrasound generator. The resonant frequency used to design the microdevices are in the range of 1 to 3 MHz. A cell culture of Saos-2 cells will be used in combination to the released microdevices to demonstrate the stimulation of the voltage-gated ion gates of the cell membrane.

## References

[1] Murillo, G. et al., Adv. Mater 29, (2017) 1605048–160555
[2] Kitsara, M. et al., Nanoscale 11, (2019) 8906-8917
[3] Lefaix, L. et al., MEMS21, (2021) 35
[4] Ciofani, G. et al., ACS Nano 4, (2010) 6267-6277
[5] Blanquer, A. et al., Int J Mol Sci 2, (2021) 432

## Figures

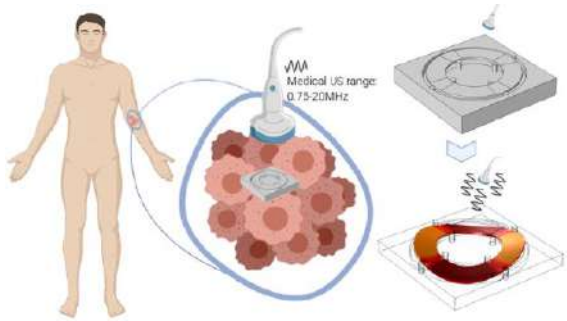


**Figure 1.** Final application of the presented novel microdevices for electrical cell stimulation.

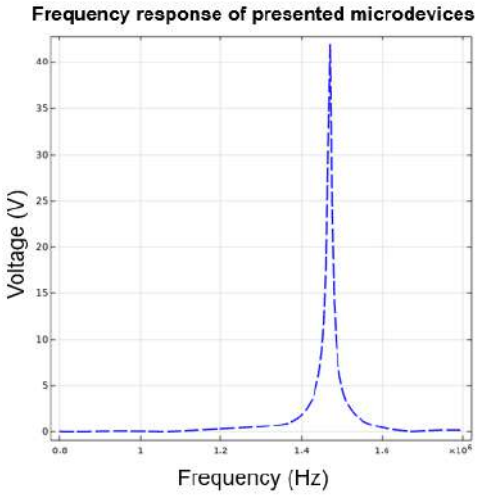


**Figure 2.** Simulated voltage frequency response of the novel proposed microdevices under biological media.

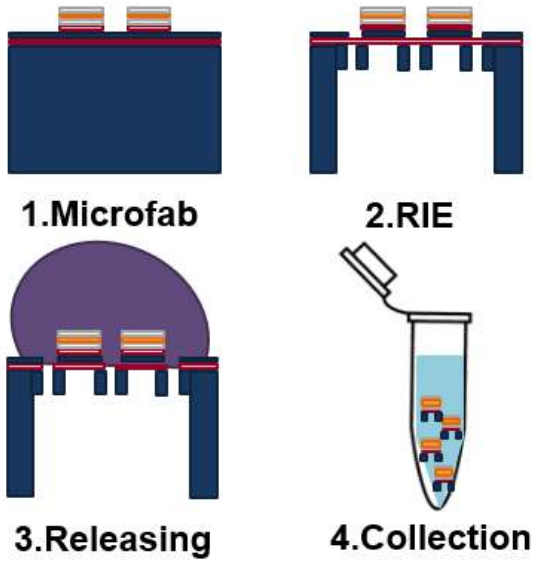


**Figure 3.** Simplified fabrication scheme of the novel piezoelectric bioelectronic microdevices.

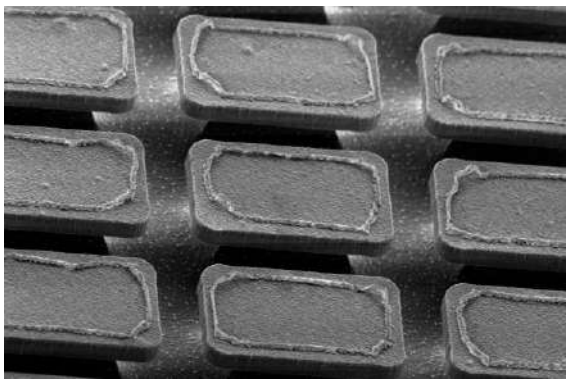

**Figure 4.** SEM of previous microfabrication work of piezoelectric bioelectronic microdevices.

# Effect of CeO2 NPs of varying Ce3+ and Ce4+ content on Chlamydomonas reinhardtii under high light stress

**Nisha Shabnam[1],** Dušan, Lazár[1]; Roman, Kouřil[1]; Jan, Filip[2]; Klára Cepe, Šafářová[2]; Pavel, Pospíšil[1]

[1] Department of Biophysics, Centre of the Region Haná for Biotechnological and Agricultural Research, Faculty of Science, Palacký University, 771 47 Olomouc, Czech Republic

[2] Regional Centre of Advanced Technologies and Materials, Czech Advanced Technology and Research Institute, Palacky University Olomouc, Olomouc, Czech Republic

shabnam251@gmail.com

Cerium oxide ($CeO_2$) nanoparticles (NPs) are well documented to have reactive oxygen species (ROS) scavenging properties. The potential of $CeO_2$ NPs to scavenge different types of ROS depends on the content of $Ce^{3+}$ and $Ce^{4+}$ [1]. The present study was designed to study the effect of $CeO_2$ NPs with varying ratio of $Ce^{3+}$ and $Ce^{4+}$ content under high light stress in *Chlamydomonas reinhardtii*. $CeO_2$ NPs of high and low $Ce^{4+}/Ce^{3+}$ content were synthesized and characterized using Transmission electron microscope (TEM), Scanning electron microscope (SEM) and X-ray diffraction (XRD). The high light induced decline in Fv/Fm (quantum yield of PS II activity) as well as the Chl *a* fluorescence transient of Chlamydomonas was unaffected by both types of $CeO_2$ NPs. Similar to high light, no effect of either $CeO_2$ NPs was noted on photosynthetic efficiency of Chlamydomonas under low light. Viability of cells also showed a similar trend. The effect of $CeO_2$ NPs on Chlamydomonas morphology, as well as interaction between the two was investigated through SEM. The ROS status of cells was evaluated by studying formation of protein radicals using immuno spin trapping technique. The findings of the present study will contribute to a better understanding of effect of nanoparticles on algae and other microbes in aquatic environment and call for environment assessment.

## References

[1] Wu H, Tito N, Giraldo JP. ACS Nano. 11 (2017) 11283-97.

[2] Pulido-Reyes G, Rodea-Palomares, I, Das, S, Sakthivel, TS, Leganes F, Rosal, R, Seal, S, Fernández-Piñas, F. Sci. Rep. 5 (2015) 15613

# Boron clusters-based systems for molecular imaging and BNCT

**Rosario Núñez**[1], Mahdi Chaari1, Justo Cabrera-González1, Albert Ferrer-Ugalde1, Gerard Tobias1, Clara Viñas1, Francesc Teixidor[1], Carme Nogués,2 Jordi Llop,3

[1]Institut de Ciència de Materials de Barcelona (ICMAB-CSIC), Campus UAB, Bellaterra, Barcelona, Spain
[2]Departament de Biologia Cel·lular, Fisiologia i Immunologia. Universitat Autònonma de Barcelona (UAB), Bellaterra, Barcelona, Spain
[3]CICbiomaGUNE, Basque Research and Technology Alliance (BRTA), Donostia-San Sebastián, Guipúzcoa, Spain

rosario@icmab.es

Icosahedral boron clusters or borohydride clusters, carboranes and metallacarboranes, do not exist in nature and are purely abiotic, man-made compounds. The structure of boron cluster compounds differs from that of organic ones, as they have a polyhedral cage-like structure, which consists of different numbers of vertices occupied by boron atoms or heteroatoms to usually form an icosahedral. They are highly thermally and chemically stable. This stability results from the 3-dimensional aromaticity of boron cluster compounds, in which σ bonds are delocalized, as opposed to delocalized π bonds of the 2-dimensional aromaticity of organic compounds [1]. Their unique properties as rigidity, chemical stability, 3D aromaticity, low toxicity, as well as their hydrophilicity, hydrophobicity, or amphiphilicity (depending on the structure), and the ability to form dihydrogen and σ-hole bonding, give them the ability to interact with biological molecules in a different way than organic compounds and make them useful in biomedical applications as pharmacophores, especially in the design of boron carriers for Boron Neutron Cancer Therapy (BNCT).[2]

Furthermore, due to their unique structural and electronic properties, boron clusters are excellent entities when applying them to tailor the fluorescence emission of any fluorophore group.[3],[4] Then, more recently, the interest has been focused on developing boron rich photoluminescence systems by linking different light emitting fluorophores to neutral and anionic boron clusters. The main goal has been to design new boron-based molecules and materials as theranostic agents for diagnosis (bioimaging) and boron carriers for BNCT. In the last decade, our group have developed boron cluster-based molecules as fluorescent probes for in vitro fluorescent bioimaging, by linking different neutral or anionic boron clusters: $C_2B_{10}H_{12}$, $[B_{12}H_{12}]^{2-}$, $[3,3'\text{-}M(C_2B_9H_{11})_2]^-$ (M = Co, Fe) to diverse fluorophores. We have used well-known fluorophores as BODIPY, *aza*BODIPY, anthracene, or fluorescent organotin complexes. All of them have shown exceptional cellular uptake and intracellular boron release that together with their fluorescent properties and biocompatibility make these compounds good candidates for cell tracking and boron delivery systems.

BODIPY-anionic boron cluster conjugates bearing $[B_{12}H_{12}]^{2-}$ and $[3,3'\text{-}Co(1,2\text{-}C_2B_9H_{11})_2]^-$ (COSAN) and $[3,3'\text{-}Fe(1,2\text{-}C_2B_9H_{11})_2]^-$ did not show cytotoxicity at low concentration (5 µg B/ml). All these compounds were well internalised by Hela cells, being the BODIPY-COSAN derivative the one that showed an exceptional cellular uptake and intracellular boron release. These properties together with its fluorescence, biocompatibility and high boron content make this compound potential candidate for cell labelling agents towards medical diagnosis and boron carrier for BNCT(Figure 1).[5]

Apart from previous BODIPY derivatives bearing anionic boron clusters, our group has also developed neutral BODIPY- and aza-BODIPY-carborane conjugates bearing C-substitued *ortho*- and *meta*-carborane clusters.[6] HeLa cells were incubated with our set of BODIPYs that exhibited different behaviour regarding cellular uptake and subcellular distribution. The differences seem to be originated in their unlike static dipole moments and partition coefficients, which depend on the type of cluster isomer (o- or m-) linked to the BODIPY and that modulate the ability of these molecules to interact with the lipophilic microenvironments in cells. It can be highlighted that the *m*-carborane derivatives with a higher lipophilicity were much better internalized by cells than their *ortho*-analogues. These behaviour was also observed in anthracenyl-containing iodo-*m*-carborane derivatives, that were internalised by HeLa cells by endocytosis and accumulated in the cytoplasm, which allowed their cellular imaging by confocal microscopy.[7]

Organotin compounds are based on 4-hydroxy-N'-((2-hydroxynaphthalen-1-yl)methylene)benzohydrazidato that was derivatized with $[B_{12}H_{12}]^{2-}$ and COSAN.[8] These compounds showed luminescence properties in solution with $\Phi_F$ values in the range from 24% to 49%. Mouse melanoma B16F10 cells were incubated with 10 µg/mL of the different compounds for 2 h and then analysed by confocal laser microscopy. Noticeable different staining effect was observed depending on the type of boron cluster; compounds bearing the COSAN anion showed an important fluorescence in the cytoplasm, whereas those bearing $[B_{12}H_{12}]^{2-}$ produced extraordinary nucleoli and cytoplasmic staining. The remarkable fluorescence staining properties of these organotin compounds in B16F10 cells make them excellent candidates for in vitro fluorescent bioimaging.

Besides previous luminescent materials, our group has also prepared carbon-based nanomaterials which consists of graphene oxide functionalized in the surface by monoiodinated

cobaltabis(dicarbollide).[9] We have efficiently developed a new nanomaterial (GO-I-COSAN, Fig. 2) based on graphene oxide (GO) functionalized with radiolabeled COSAN (I-COSAN) and demonstrated that our nanomaterial can potentially act as a theranostic agent for diagnosis (radioimaging) and therapy (anticancer agent for BNCT). TEM analyses confirm the internalisation of the nanomaterial by cells and its accumulation in the cytoplasm, without causing changes neither in the size nor in the morphology of cells. The GO-I-COSAN does not show cytotoxicity in vitro for HeLa cells, with a cell viability greater than 90 %. Furthermore, GO-I-COSAN is ingested by *C. elegans* resulting in a survival rate of around 100 %, revealing the absence of toxicity in vivo for the worms and supporting the results observed in the in-vitro studies. Radiolabeling of the material with the positron emitter $^{124}$I was achieved via isotopic exchange of the I-COSAN to obtain [$^{124}$I]I-COSAN followed by its grafting onto GO. Biodistribution studies by Positron Emission Tomography (PET) indicate accumulation of the nanomaterial in the liver at early time, as well as accumulations in lungs and kindness. The nanomaterial shows radiochemical stability in vivo and relative long circulation time. Taking into account that long-circulating nanomaterials tend to accumulate in tumors to a certain extent due to enhanced permeability and retention (EPR) effect, it is reasonable to assume that our nanomaterial would show important tumor uptake, resulting in a high concentration of boron atoms in the tumor tissue, which is a requirement for BNCT. Notably, a favorable biodistribution profile suggests the potential use of this nanomaterial as a theranostic agent for in vivo bioimaging and boron carriers for BNCT.

## References


[1] a) J. Poater, M.Sola,C.Viñas, F. Teixidor, Angew. Chem. Int. Ed., 2014, 53, 12191. b) Poater J, Viñas C, Bennour I, Escayola S., Sola, M., Teixidor F. J. Am. Chem. Soc. 2020, 42, 9396.

[2] a) C. Viñas, Future Med. Chem., 2013; 5, 617. b) C. Viñas, R. Núñez, I. BennourI, F. Teixidor. Curr Med Chem 2019, 26, 4935. c) Boron-Based Compounds, eds. E. Hey-Hawkins and C. Viñas, John Wiley & Sons Ltd, Chichester, UK, 2018. d) K. Hu, Z. Yang, L. Zhang, L. Xie, L. Wang, H. Xu, L. Josephson, S. H. Liang and M.-R. Zhang, Coord. Chem. Rev., 2020, 405, 213139.

[3] R. Núñez, M. Tarrés, A. Ferrer-Ugalde, F. Fabritzi de Biani, F. Teixidor, *Chem. Rev*., 2016, 116(23), 14307.

[4] a) A. Ferrer-Ugalde, A. González-Campo, C. Viñas, J. Rodríguez-Romero, R. Santillan, N. Farfán, R. Sillanpää, A. Sousa-Pedrares, R. Núñez and F. Teixidor. Chem. Eur. J., 2014, 20, 9940. b) J. Cabrera-González, C. Viñas, M. Haukka, S. Bhattacharyya, J. Gierschner and R. Núñez., Chem. Eur. J., 2016, 22, 13588. c) M. Chaari, Z. Kelemen, J. Giner-Planas, F. Teixidor, D. Choquesillo-Lazarte, A. Ben Salah, C. Viñas and R. Núñez. J. Mater. Chem. C, 2018, 6, 11336.

[5] M. Chaari, N. Gaztelumendi, J. Cabrera-González, P. Peixoto-Moledo, C. Viñas, E. Xochitiotzi-Flores, N. Farfán, A. Ben Salah, C. Nogues, R. Núñez, Bioconjugate Chem., 2018, 29, 1763.

[6] C. Bellomo, M. Chaari, J. Cabrera-González, M. Blangetti, C. Lombardi, A. Deagostino, C. Viñas, N. Gaztelumendi, C. Nogués, R. Núñez and C. Prandi, Chem. Eur. J., 2018, 24, 15622. b) P. Labra-Vázquez, R. Flores-Cruz, A Galindo-Hernández, J. Cabrera-González, C. Guzmán-Cedillo, A. Jiménez-Sánchez, P. G. Lacroix, R. Santillan, N. Farfán and R. Núñez, Chem. Eur. J., 2020, 26, 16530.

[7] M. Chaari, Z. Kelemen, D. Choquesillo-Lazarte, F. Teixidor, N. Gaztelumendi, C. Viñas, C. Nogues and R. Nuñez, Biomat. Sci. 2019, 7, 5324.

[8] B. M. Muñoz-Flores, J. Cabrera-González, C. Viñas, A. Chávez-Reyes, H. V. R. Dias, V. M. Jiménez-Pérez, R. Núñez, Chem. Eur. J., 2018, 24, 5601.

[9] A. Ferrer-Ugalde, S. Sandoval, K. Reddy Pulagam, A. Muñoz-Juan, A. Laromaine, J. Llop, G. Tobias and R. Núñez. ACS Appl. Nano Mater., 2021, 4, 1613.


## Figures

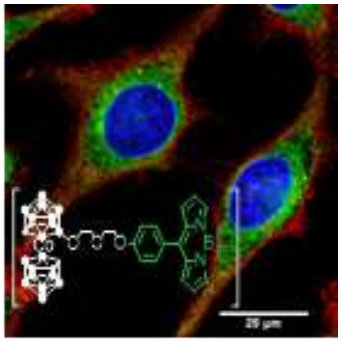

**Figure 1.** Confocal image of HeLa Cells incubated with Bodipy-Cosane conjugates after incubation for 2 hours.

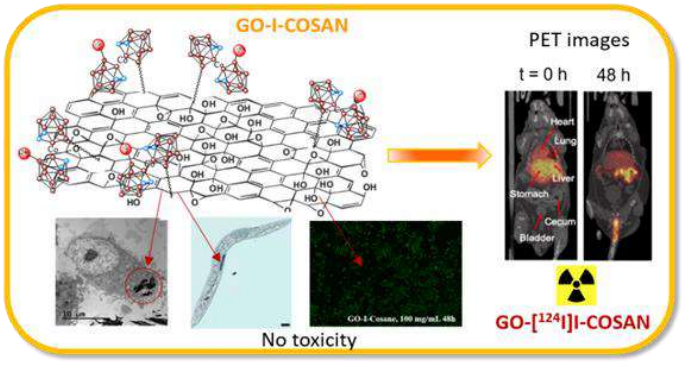


**Figure 2.** Representation of GO functionalised with radiolabelled GO-[124I]I-COSAN including TEM and PET images.

# Bioactivity of PDGF-BB-loaded NLCs after sterilization with gamma or beta radiation

**ORDOYO-PASCUAL, Jorge** [1,2,3], RUIZ-ALONSO, Sandra [1,2,3], GALLEGO, Idoia [1,2,3], GARCIA-VILLEN, Fátima [1,2,3], SAENZ-DEL-BURGO, Laura [1,2,3], PEDRAZ, Jose Luis [1,2,3]

[1]NanoBioCel Group, Laboratory of Pharmaceutics, School of Pharmacy, University of Basque Country (UPV/EHU), Vitoria-Gasteiz, Spain.
[2]Biomedical Research Networking Center in Bioengineering, Biomaterials and Nanomedicine (CIBER-BBN), Vitoria-Gasteiz, Spain.
[3]Bioaraba Health Research Institute, NanoBioCel Research Group, Vitoria-Gasteiz, Spain.

jorge.ordoyo@ehu.eus

## 1. Introduction

Growth factors are cytokines that stimulate cell proliferation, differentiation and/or activation. Despite this, they are very sensitive to chemical and enzymatic degradation [1]. To protect them, they can be encapsulated within drug delivery systems, such as nanostructured lipid carrier (NLCs), which also enable controlled pharmacokinetics [2]. As the final objective of this nanoparticle system is the administration to the patient, one of the main requirements is sterility. The use of gamma and beta radiation is considered one of the most efficient techniques for the reduction of microorganisms [3].

In the present study, PDGF-BB growth factor, which is related to cell proliferation and migration, was encapsulated in NLCs. Then, the nanoparticles were submitted to gamma or beta radiation at two different doses. Sterilization was verified by a sterility test and the changes that each of the radiations might provoke in the biologic effect of the released factor was studied.

## 2. Materials and methods

### 2.1. NLCs preparation

To obtain the NLCs, an o/w emulsion was formed using the hot melt homogenization technique. Subsequently, the final product was lyophilized.

### 2.2. NLCs sterilization

NLCs were irradiated with gamma or beta radiation. The doses to be irradiated were 12 kGy and 25 kGy in both cases but there are methodological differences. Gamma radiation is more penetrating than beta radiation, with a longer exposure time (up to hours). In contrast, with beta radiation it is a few minutes.

### 2.3. Sterility test

To verify that the nanoparticles were correctly sterilized, we followed the test from the Royal European Pharmacopoeia. Sterilized NLCs were added to two different media, Fluid Thioglycollate Medium and Tryptic Soy Broth. Next, they were cultured at 32±2°C and 22±2°C respectively, for 14 days.

### 2.4. Bioactivity assay

A wound healing assay was performed with human mesenchymal stem cells. Photos were taken every 20 minutes for 48 hours to observe the wound closure using a Cytation (BioTek, Winooski, United States). Images were subsequently analyzed.

## 3. Results and Discussion

The sterility test was performed to check if the different doses of the two types of radiation were sufficient for achieving sterility of the NLCs. The results collected in Figure 1 show that at a dose of 25 kGy, both gamma and beta radiation were able to assure sterility. In contrast, when doses of 12 kGy were applied, beta radiation was able to kill all microorganisms and spores. However, when gamma radiation was used, microbial growth was observed. In Tryptic Soy Broth, the appearance of turbidity in the medium was observed, which indicates the growth of aerobic bacteria and fungi. Therefore, the 12 kGy dose of gamma radiation is not sufficient for achieving sterile NLCs.

One of the possible risks of using radiation is that it might affect the bioactivity of the factor encapsulated within the NLCs. For this reason, a bioactivity study was carried out to verify that there was no loss of activity of the released factor. Figure 2 shows the images collected from the bioactivity assay were differences can be observed among the images obtained at 48 hours. The wound of non-irradiated PDGF-BB and the one of PDGF-BB released from irradiated NLCs at the lower dose (12 kGy, both types of radiations) was very similar, achieving a complete confluence and closure of the wound. In contrast, PDGF-BB released from NLCs irradiated with 25 kGy did not completely close the wound, although it achieves a greater effect when beta radiation is used.

To analyze these images, a graph showing percentage of wound closure as a function of time is plotted and shown in Figure 3. When gamma radiation was used (Figure 3A), the 25 kGy dose showed no improvement in wound closure compared to baseline. Indicating that the dose is too aggressive for the factor, losing its activity. The

12 kGy dose was able to close the wound, as was the factor released by non-irradiated NLCs, although there was slight factor damage, as the rate of closure was lower in the case of irradiated NLCs.

In the case of beta radiation (Figure 3B), both the factor released from non-irradiated NLCs, as well as those irradiated with 12 kGy and 25 kGy, showed a greater effect than that of the basal condition. With a dose of 12 kGy, the curve was the same as when the nanoparticles were not irradiated, suggesting that dose does not modify the activity of the factor. In contrast, when the 25 kGy dose is used, there is a slight decrease in confluence in the wound. This fact might indicate that the higher dose slightly affects the activity of PDGF-BB.

### 4. Conclusions

It was observed that in both types of radiation, when sterilizing with 25 kGy dose, the activity was always lower than with 12 kGy, since the treatment is more aggressive. In addition, the data reflect that gamma radiation causes a greater loss of activity. This could be due to longer irradiation times, which means a higher temperature rise.

Therefore, the best option in order to achieve sterilized encapsulated PDGF-BB in NLCs might be to irradiate them with 12 kGy of beta radiation. In this way, we manage to sterilize the nanoparticles without affecting their biological activity.

### 5. Acknowledgements

This project was supported by the Basque Country Government (Grant IT1448-22), and by the TriaAnkle european project (Horizon 2020, TRI-ankle 952981-2). This research was also supported by CIBER (CB06/01/1028, ISCIII, Ministerio de Ciencia e Innovación). Authors wish to thank the intellectual and technical assistance from the ICTS “NANBIOSIS,” U10 of the CIBER-BBN at the University of the Basque Country (UPV/EHU).

## References

[1] Catarina A, João S, Moreira N, Manuel J, Lobo S, Almeida H. Springer, 2020.
[2] Scioli Montoto S, Muraca G, Ruiz ME. Frontiers in Molecular Biosciences, 2020.
[3] Della Schiava N, Pedroli F, Thetpraphi K, Flocchini A, Le M, Lermusiaux P, et al. Scientific Reports, 2020.

## Figures

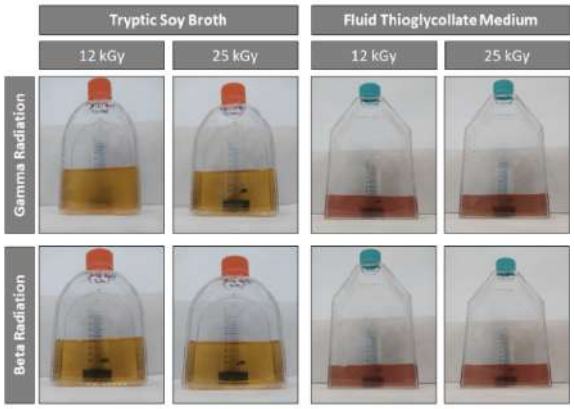


**Figure 1.** Sterility test, performed for 14 days.

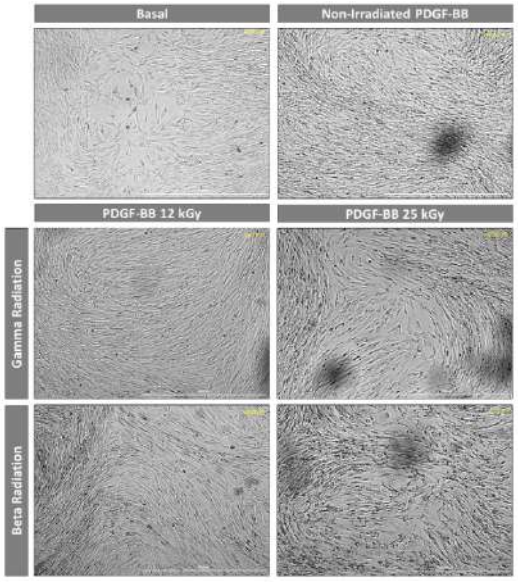


**Figure 2.** Images of the wound healing assay at 48 hours on human mesenchymal stem cells.

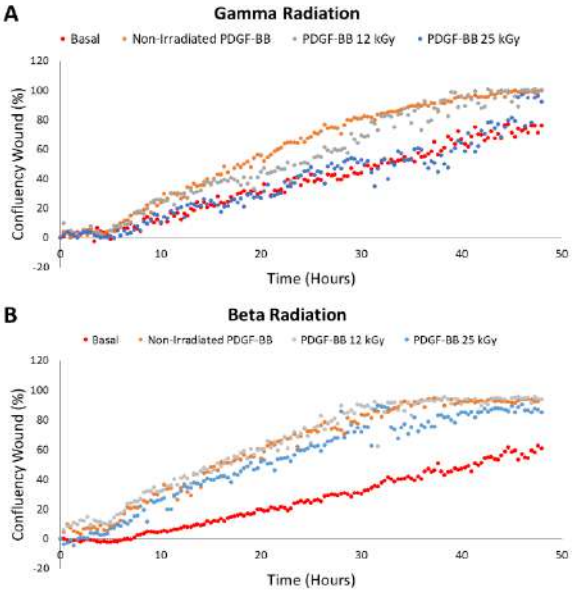


**Figure 3.** Wound healing assay plots, Confluency wound (%) vs. time. **A.** Gamma radiation. **B.** Beta radiation.

# Safe and efficient modular nanovectors for gene/drug delivery in precision medicine

**Ilaria Elena Palamà**[1], Gabriele Maiorano[1], Clara Baldari[2], Alessandra Invidia[2], Barbara Cortese[3], Loris Rizzello[4,5], Gianluca De Rinaldis[2], Annamaria Russo[2], Andrea Giglio[2], Giuseppe Gigli[1,2]

[1]Nanotechnology Institute, CNR-NANOTEC, Monteroni street - 73100 Lecce, Italy.
[2]Dep. of Mathematics and Physics, University of Salento, Monteroni street - 73100 Lecce, Italy
[3]Nanotechnology Institute, CNR-NANOTEC, c/o La Sapienza University, P.le A. Moro- 00185 Rome, Italy
[4]Department of Pharmaceutical Sciences (DISFARM), University of Milan, G. Balzaretti 9 Street, 20133 Milan, Italy
[5]National Institute of Molecular Genetics (INGM), Francesco Sforza 35 Street, 20122 Milan, Italy

ilaria.palama@nanotec.cnr.it

A combinatorial approach based on cells engineered to express/silence specific genes and innovative delivery of pharmacological active molecules could pave the way for remarkable therapeutic solutions in cancer, rare and neurodegenerative diseases.
In this frame, thanks to their ability to improve drug efficiency within single administrations, properly engineered nanovectors show a controlled drug release at the action site by reducing side effects, additionally, nanovectors can be used to genetically modify cells thus avoid safety issues of viral vectors.
In this context, we have developed several modulable nanosystems such as enzyme-responsive polyelectrolyte capsules [1], polyelectrolyte complexes [2] and core/shell polymeric nanoparticles for drug/gene delivery in cancer cells [3-9].
These nanosystems are based on the proper employment of both FDA approved synthetic and natural polymers, and loaded with drugs/natural compounds and/or nucleic acids for application in oncology and neurodegenerative diseases.
High drug loading efficiency and sustained release over time is obtained, such as good transfection efficacy of different primary/immortalized human cells. In addition, these nanoparticles showed the ability to penetrate into 3D spheroids, thus allowing to target inner cells and to achieve transfection and/or drug release. Additionally, thanks to their biomimetic properties [10], the developed nanovectors are able to target specific cells.

## References

[1] I. E. Palamà et al., Nanomedicine, (2010), 5, 3, 419-431
[2] I. E. Palama, et al., Nanomedicine, (2014), 9, 14, 2087-2098
[3] B. Cortese, et al., Pharmaceutics, (2018), 10, 2
[4] C. Guido, et al., Materials Advances, (2021), 310-321
[5] C. Guido et al., Diagnostics, (2022), 12, 1,. 173
[6] G. Maiorano et al., Pharmaceutics, (2022) 14, 7
[7] B. Cortese, et al., Cancers (2019), 11, 9
[8] M. Zangoli, et al., ACS Appl Bio Mater (2019)
[9] F. Monti, et al., Adv Healthc Mater (2021)
[10] C. Guido, et al., Bioengineering (2020), 7, 3

# 4D-printed multifunctional microcarriers for passive and active cargo delivery

**Fatemeh Rajabasadi**[1], Silvia Moreno[2], Kristin Fichna[2], Azaam Aziz[1], Dietmar Appelhans[2], Oliver G. Schmidt[3,4], and Mariana Medina-Sánchez*[1,5]

[1]Leibniz Institute for Solid State and Materials Research, Dresden, Germany
[2]Leibniz Institute for Polymer Research, Dresden, Germany
[3]Research Center for Materials, Architectures and Integration of Nanomembranes (MAIN), Chemnitz University of Technology, Germany
[4]School of Science, Dresden University of Technology, Germany
[5]Center for Molecular Bioengineering (B CUBE), Dresden University of Technology, Germany

f.rajabasadi@ifw-dresden.de
*m.medina.sanchez@ifw-dresden.de

Abstract

Nowadays, remote controllable soft and smart microrobots have facilitated less-invasive medical operations due to their unique capability to adapt and perform multiple functions. Microrobots are categorized based on their propulsion mechanisms into the chemical, physical, or biohybrid ones.[1] Biohybrid microrobots are the ones who propel by means of motile cells or microorganisms as they take advantage of the taxis and cell-interaction abilities of the living components.[2]

From the wide range of motile cells and microorganisms, bacteria and sperm cells are shown to be efficient moving in complex fluids and environments, even against flow, being suitable for various in vivo medical operations.[3-5]

For example, genetically modified Magnetococcus marinus “MC-1”, known as magnetotactic bacteria (MTB), has been widely used for targeted drug delivery.[6-8] They not only can be steered by external magnetic fields because of existing the magnetosomes but also can be tracked via magnetic resonance imaging (MRI).[9]

On the other hand, sperm cells are optimized to swim in various viscous environments inside the female reproductive tract without inducing any immunoreaction or inflammation. Moreover, recently, studies showed that sperm have high drug loading-capability for targeting various gynecological cancers, in particular cervical and ovarian cancer.[10,11] Naturally, sperm cells respond to different physical and chemical changes in their surroundings. For example chemotaxis (tendency to swim toward a higher concentration of extracellular signals), thermotaxis (tendency to swim towards a temperature gradient), thigmotaxis (tendency to swim near the surface), and rheotaxis (swimming against the fluid flow), which can be considered together with the additional functionalities provided by the synthetic microstructures for engineering sperm-based microrobots to be able to target the disease location by either local taxis or external control.[12-14]

Our group was the pioneer of sperm-hybrid micromotors in both development of in vitro/in vivo assisted fertilization applications and targeted drug delivery approaches.[15-18] Primarily, the capture, guidance and release of single sperm cell was successfully demonstrated.[11] Then, the influence of different parameters like sperm morphology and tail beating amplitude, as well as, the temperature and viscosity of the surrounding fluid on sperm-hybrid microrobots’ performance was investigated.[15,16] To improve sperm release different strategies have been developed such as using either thermo-responsive rolled-up microtubes, or by bending arm microstructures.[17,18]

The aim of the current work is to assist sperm cells reaching the fertilization site in a case of oligospermia (when the sperm count is <20 million sperm per mL). Currently, there are two different ways to treat this male infertility problem in the clinics. One is in vitro fertilization (IVF) and the other is intracytoplasmic sperm injection (ICSI). In IVF the preselected sperm cells (millions of them) are introduced with the retrieved oocytes and in ICSI only one sperm cell is picked up and directly injected into the oocyte for the fertilization. Although, the fertilization rates are quite high, there is a challenge to increase the embryo implantation rates.[19] This problem might be caused by the oxidative stress on gametes outside the natural environment (female reproductive tract) during retrieval, washing, selection, and incubation which affect their quality. To address this challenge, here, we introduced 4D-printed multifunctional sperm-hybrid microcarriers to transport a high number of sperm cells inside female reproductive tract while assisting them by local capacitation and facilitating the digestion of the cumulus complex that surrounds the oocyte.

4D-printed microcarriers are fabricated with a non-stimuli-responsive polymer (IPS photoresist) and a thermo-responsive hydrogel poly(N-isopropylacrylamide) (PNIPAM) via two-photon polymerization (TPP).[20] Thermo-responsive hydrogels like PNIPAM are undergo reversible phase transition from a swollen hydrophilic state at temperatures below its lower critical solution temperature (LCST) to a collapsed hydrophobic state at temperatures above its LCST, which can be beneficial to make an adoptive gates in our microcarriers.[21-23] Hereby, PNIPAM not only used for triggering sperm cell release at specific temperature but also considered to expel heparin (specific protein caused sperm hyperactivation) at the same time, for future in vivo assisted fertilization scenarios. Moreover, microcarriers are functionalized with hyaluronidase-loaded polymersomes (HYAL-Psomes) to locally mediate the hyaluronic acid (HA) degradation found in the oocyte-cumulus complex.[24]

Conclusively, our presented sperm-hybrid microcarriers are able to: (i) capture, transport and release multiple motile sperm cells, to increase the chances of fertilization, (ii) release heparin at the certain time to in-situ capacitate/hyperactivate sperm cells, and (iii) mediate degradation of HA (found in the cumulus complex matrix, one of the natural biological barrier) to assist sperm penetration into the oocyte, by the HYAL-Psomes previously immobilized on the microcarrier's surface **(Figure 1)**.[25]

## References


[1] M. Medina-Sánchez, O. G. Schmidt, Nature (2017), 545, 406.
[2] S. Martel, Biomed. Microdevices (2012), 14, 1033.
[3] O. Yasa, et al., Adv. Mater. (2018), 30, 1804130.
[4] J. Zhuang, M. Sitti, Sci. Rep. (2016), 6, 32135.
[5] J. Han, et al., Sci. Rep. (2016), 6, 28717.
[6] D. Akin, et al., Nat. Nanotechnol. (2007), 2, 441.
[7] S. Taherkhani, et al., ACS Nano (2014), 8, 5049.
[8] S. Martel, et al., Appl. Phys. Lett. (2006), 89, 233904.
[9] K. Schmidt, et al., Nat. Commun. (2020), 11, 5618.
[10] V. Magdanz, et al., Adv. Mater. (2017), 29, 1606301.
[11] L. Schwarz, et al., Reproduction (2020), 159, R83.
[12] M. Medina-Sánchez, et al., Ther. Deliv. (2018), 9, 303.
[13] V. Kantsler, et al., Elife (2014), 3, e02403.
[14] Z. Zhang, et al., Sci. Rep. (2016), 6, 23553.
[15] V. Magdanz, et al., Adv. Funct. Mater. (2015), 25, 2763.
[16] F. Striggow, et al., Small (2020), 16, 2000213.
[17] V. Magdanz, et al., Adv. Mater. (2016), 28, 4084.
[18] H. Xu, et al, ACS Nano (2018), 12, 327.
[19] S. Bartnitzky, et al., D·I·R Annual German IVF-Registry, (2021).
[20] F. Rajabasadi, et al., Prog. Mater. Sci. (2021), 120, 100808.
[21] Han, et al., Sci. Rep. (2018), 8, 1963.
[22] Y. Okada, F. Tanaka, Macromolecules (2005), 38, 4465.
[23] L. D. Zarzar, et al., Angew. Chemie (2011), 123, 9528.
[24] M. Ergüven, T. İrez, Fertil. Steril. (2020), 114, e352.
[25] F. Rajabasadi, et al., Adv. Mater. (2022), (in press).


## Figures

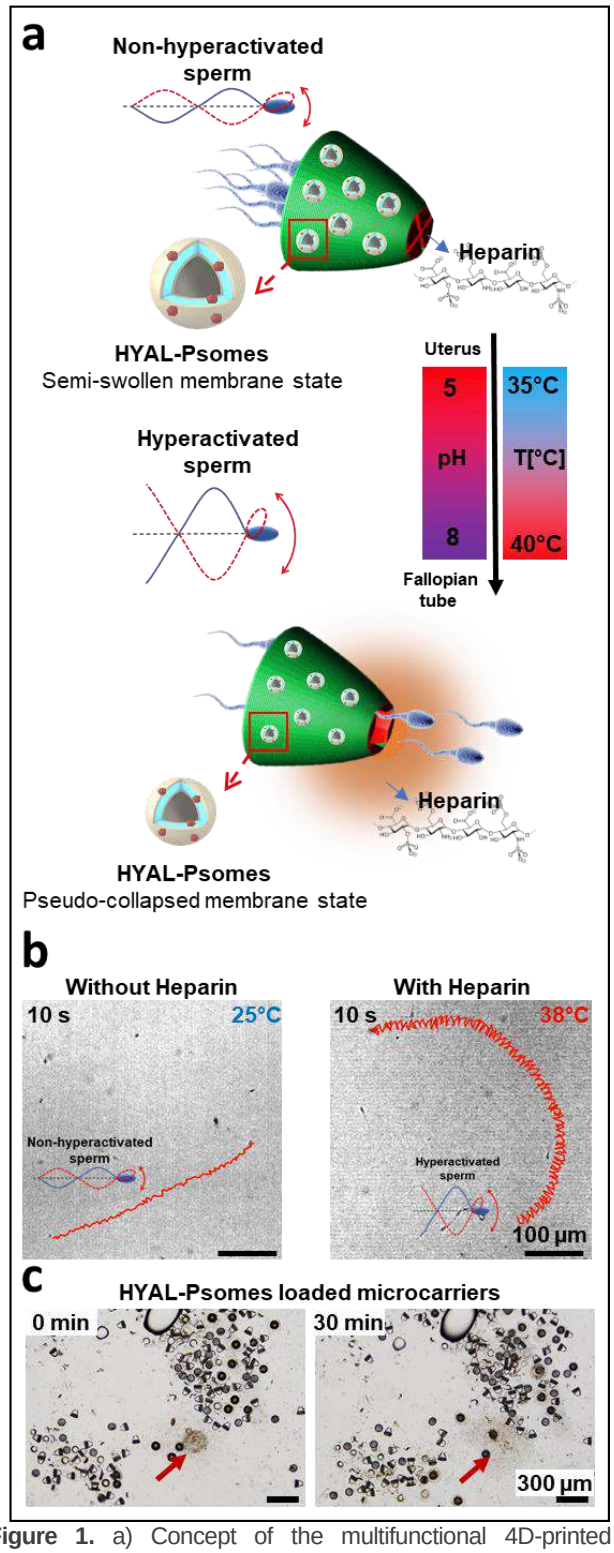


**Figure 1.** a) Concept of the multifunctional 4D-printed microcarrier with heparin (used for sperm hyperactivation) and hyaluronidase-loaded polymersomes (used for cumulus cell removal), and the expected natural stimuli (pH and temperature varying from the uterus to the fertilization site) for active (motile sperm cell) and passive (heparin and hyaluronidase) cargo release. b) Sperm hyperactivation in presence of heparin with circular motion pattern. c) Locally cumulus cell removal by HYAL-Psomes loaded microcarriers, the arrow indicates the location of oocyte surrounded by cumulus cells. Adopted from [25].

# Design of active targeted PLGA-$SO_3$ nanoparticles encapsulating PARP and PD-L1 inhibitors for BRCA-mutated breast cancer therapy

**Daniel Rodriguez Ajamil**[1],
Shani Koshrovski-Michael[1], Pradip Dey[1], Ronit Satchi-Fainaro[1,2]

[1] Department of Physiology and Pharmacology, Sackler School of Medicine, Tel Aviv University, Tel Aviv 69978, Israel.

[2]Sagol School of Neurosciences, Tel Aviv University, Tel Aviv 69978, Israel.

E-Mail: danielra151920@gmail.com

Breast cancer (BC) is the most frequently diagnosed cancer and the second most common cause of cancer mortality in women worldwide. Approximately 15% of all BC are triple negative (TNBC), among them, 30% are BRCA1- or BRCA2-mutated. These tumors are highly aggressive and invasive. Recently, inhibition of poly(ADP-ribose)polymerase-1 (PARP1), a DNA repair enzyme, was shown to induce “synthetic lethality” in BRCA-mutated cancer cells prolonging PFS (Progression Free Survival) . This led to the FDA approval of PARP inhibitors (PARPi) for the treatment of BRCA-mutated BC. Despite their promise, resistance mechanisms to PARPi often develop affecting drug availability, (de)PARylation enzymes, restoration of Homologous Recombination (HR) or restoration of replication fork stability. Moreover, PARPi have been shown to have an impact on cancer-associated immunity, and their combination with immune checkpoint therapy (ICT) has been explored in clinical trials. Therefore, we aimed to rationally-design a nanomedicine combining PARPi with a programmed death-ligand 1 (PD-L1) inhibitor, a small molecule immunosuppressive checkpoint ligand inhibitor developed in our lab. We postulated that co-delivery of these therapeutic agents would result in enhanced therapeutic efficacy in BRCA-mutated cancers. First, we assessed the anti-proliferative effect of several PARPi and selected Talazoparib, as it was shown to be the most potent**.** In addition, as a side effect, we observed increased expression of PD-L1 following treatments with Talazoparib on EMT6 murine BRCA-mutated BC cell line. This was subsequently abrogated following treatment with our PD-L1i small molecule. Furthermore, our PD-L1i small molecule limited EMT6 spheroids proliferation, migration and sprouting when grown in co-culture with activated splenocytes.

Additionally, since the enhanced permeability and retention (EPR) effect varies between tumor types, we synthesized one non-targeted and three targeted NPs with sulfonated moieties that actively target P-Selectin, an adhesion molecule expressed in our 3D EMT6 spheroid models. These nanocarriers were characterized (Figure 1) and evaluated for their biocompatibility and capability to internalize 3D cell culture models to determine the best candidate. The selected candidate demonstrated optimized targeting and tumor internalization features, while retaining their anti-tumor cytotoxic activity. Here, we focus on the rational design and physico-chemico-biological characterization of precision nanomedicines combining PARPi with immunotherapy to treat this aggressive BC. Based on our previous experience with several drug combinations, we hypothesize that the proposed nanocarriers will increase the half-life of the encapsulated drugs, selectively target them to release the active compounds at the tumor site while reducing their side effects following the proposed mechanism (Figure 2). We plan to exploit this nano-based therapy in other BRCA-mutated cancer types such us pancreatic and ovarian.

**References:**


[1] C. Denkert, et al., The Lancet 2017, 389 (10087), 2430-2442.

[2] A. Turk, et al., Cancer 2018, 124 (12), 2498-2498.

[3] H. Sato, et al., Nature Communications, 2017, 8 (1), 1751-1751.

[4] Ferber, Tiram, et al., eLife, 2017, 6, e25281.

[5] Acúrcio RC, et al. J Immunother Cancer 2022;10: e004695.


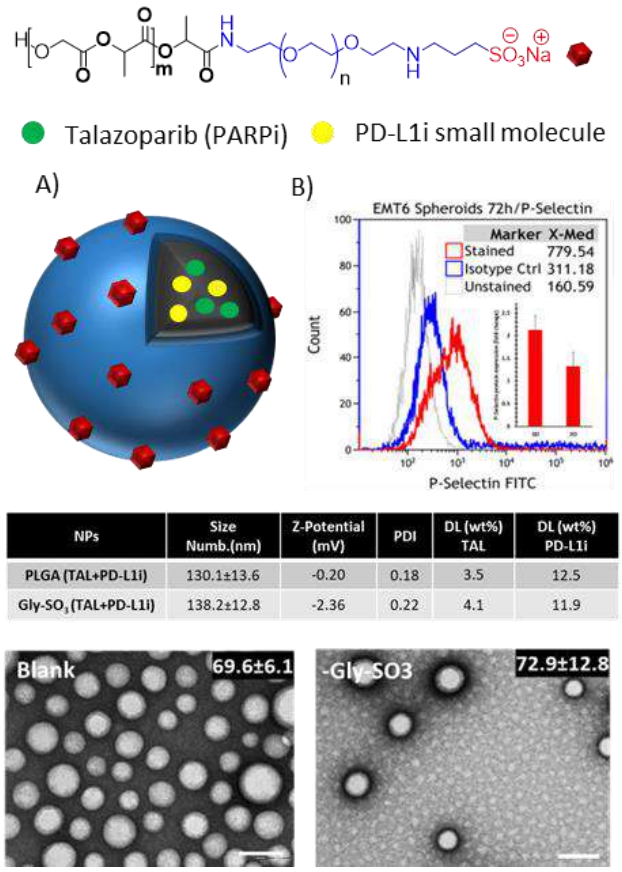


| NPs | Size Numb.(nm) | Z-Potential (mV) | PDI | DL (wt%) TAL | DL (wt%) PD-L1i |
|---|---|---|---|---|---|
| PLGA (TAL+PD-L1i) | 130.1±13.6 | -0.20 | 0.18 | 3.5 | 12.5 |
| Gly-$SO_3$ (TAL+PD-L1i) | 138.2±12.8 | -2.36 | 0.22 | 4.1 | 11.9 |




**Figure 1.** PLGA-PEG-$SO_3$ NPs. A) Rational design of P PLGA-PEG-$SO_3$ NPs. B) P-Selectin protein expression in EMT6 cellular models. C) PLGA-PEG-$SO_3$ NPs physico-chemical characterization: Hydrodynamic radius (Size number); Z-Potential; Polydispersity Index (PDI); Drug Loading (DL); Transmission Electron Microscopy (TEM) Imaging.

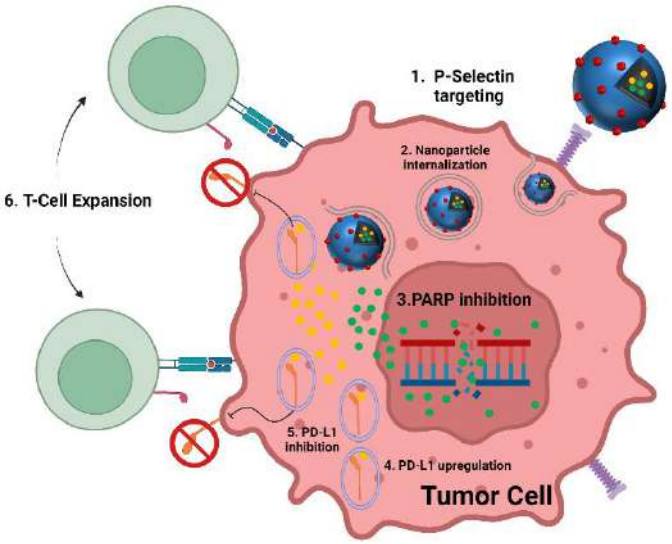


**Figure 2.** Mechanism of action of PLGA-PEG-$SO_3$ NPs encapsulating PARP and PD-L1i

# *In Vitro* Cytotoxicity of Upconverting Tm/Er Co-Doped Layered Perovskite and their Nanosheets

**Özge Sağlam**[1,2], Bensu Günay[2], Ece Sarıyar[2], Ugur Unal[3], Zeynep Firtina Karagonlar[2,4]

[1]Department of Mechanical Engineering, İzmir University of Economics, Sakarya Cad. 156, İzmir 35330, Turkey

[2] Division of Bioengineering, Graduate School, İzmir University of Economics, Sakarya Cad. 156, İzmir 35330, Turkey

[3] Department of Chemistry, Koç University, Rumelifeneri Yolu 34450 Sarıyer, İstanbul, Turkey

[4]Department of Genetics and Bioengineering, İzmir University of Economics, Sakarya Cad. 156, İzmir 35330, Turkey
ozge.saglam@ieu.edu.tr

In this study, the upconversion properties of $Tm^{3+}/Er^{3+}$ co-doped Ruddlesden-Popper type $K_2Ln_2Ti_3O_{10}$ (Ln: La, Tm, Er) layered perovskites and their exfoliated two-dimensional (2D) materials were reported [1,2]. The host lattice of the layered perovskite was preferred to study for the exfoliation procedure because of its low phonon energy. The excitation of co-doped $K_2Ln_2Ti_3O_{10}$ by a 980 nm NIR laser diode resulted in green and red visible emissions and a NIR emission corresponding to the $^4S_{3/2}\rightarrow{}^4I_{15/2}$ with $^2H_{11/2}\rightarrow{}^4I_{15/2}$ and $^4F_{9/2}\rightarrow{}^4I_{15/2}$ of the $Er^{3+}$ transitions and $^3H_4\rightarrow{}^3H_6$ transition of the $Tm^{3+}$, respectively. According to the CIE chromaticity diagram the pure green and red emissions of the materials were obtained by tuning the activator and sensitizer amount in the host lattice of the layered perovskite. The 2D nanosheets derived by chemical exfoliation of the layered perovskites depicted an intense NIR emission with weak red and green emissions. The single oxide nanosheets had approximately 1.8 nm thickness and 2 µm lateral size. Moreover, MTT assay and Calcein/PI staining were performed to evaluate the cytotoxicity of non-doped and $Tm^{3+}/Er^{3+}$ co-doped $K_2Ln_2Ti_3O_{10}$ perovskites and their 2D nanosheets on HEK293 and HepG2 cell lines. Even if the cell viability decreased with increasing concentration, both assays showed good cell viability at even 100 µg/mL. In addition to the intense luminescence and optical features of the 2D materials, the nanomaterials also demonstrated lower cytotoxicity than their bulk forms. This study was supported by the Scientific and Technological Research Council of Turkey (TÜBİTAK; Grant number 117M512).

## References

[1] Gunay B., Sarıyar E, Unal U, Karagonlar ZF, Sağlam Ö., Colloids and Surfaces A: Physicochemical and Engineering Aspects, 612 (2021) 126003

[2] Günay B., Süer Ö., Döğer H., Arslan Ö., Unal U., Sağlam Ö., Colloids and Surfaces A: Physicochemical and Engineering Aspects 649 (2022) 129502

## Figures

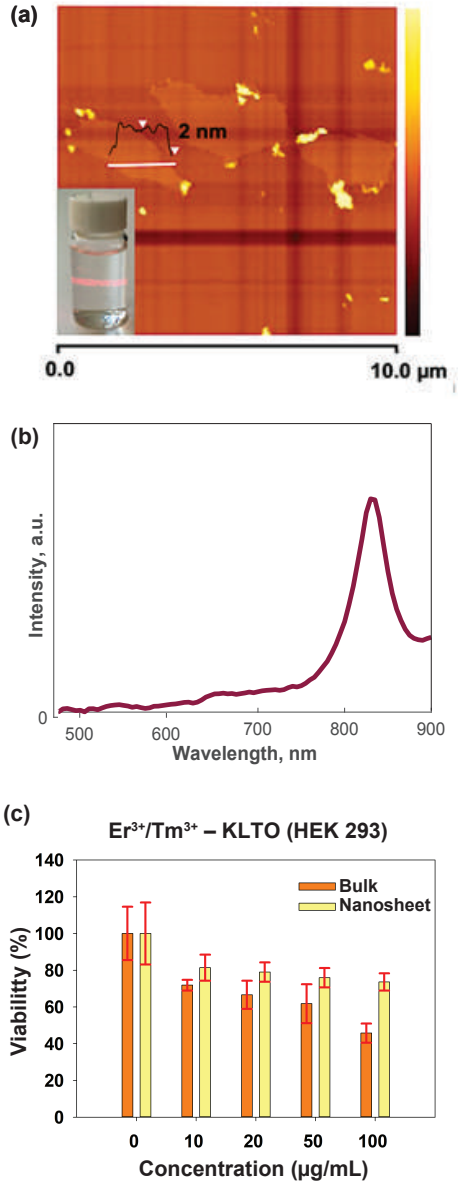


**Figure 1.** (a) AFM image with a height profile. The inset shows the Tyndall effect of the nanosheet solution (b) The upconversion emission spectrum of the exfoliated nanosheets derived from $K_2Ln_2Ti_3O_{10}$ co-doped with 20% $Er^{3+}$+ 2.5% $Tm^{3+}$ (c) Cytotoxicity analyzes of $K_2Ln_2Ti_3O_{10}$ co-doped with 20% $Er^{3+}$+ 2.5% $Tm^{3+}$ and their nanosheets for HEK 293 cell lines.

# Upgrading nanobiosensing platforms: comparison between different inkjet printed biosensors for detection of Neutrophil Gelatinase Associated Lipocalin-2 (NGAL)

**Massimo Urban**[1],
Giulio Rosati[1], Arben Merkoçi[1,2]

[1]Catalan Institute of Nanoscience and Nanotechnology (ICN2), Edifici ICN2, Campus UAB, 08193 Bellaterra, Barcelona, Spain
[2]Catalan Institution for Research and Advanced Studies (ICREA), Passeig de Lluís Companys, 23, 08010 Barcelona, Spain

massimo.urban@icn2.cat
arben.merkoci@icn2.cat

Efforts have been put by the research community into developing and using different nanomaterials for biosensing applications[1]. Nanobiosensors take advantage of the unique proprieties of the nanomaterials to enhance the response, sensitivity and performance of the analytical device[2]. Each different component of the biosensor play a unique role into the overall performance of the device, and all the elements have to cooperatively work and interact together, in harmony going from the analyte to be detected to the readout interphase. This large variety of interactions readily give a perspective of the level of complexity and the technological requirements for fabricating reliable biosensors.

Advancement in the biotechnology of the receptors, introducing aptamers and selection techniques like SELEX, or applying new discoveries to the biosensing field, such as CRISPR-Cas family, resulted in a fast progresses in the area[3,4].

With the advent and rapid growth in the field of nanomaterials, more effort has been put into engineering and tune the proprieties of the transducing element of the sensor opening endless possibilities and combinations, with different receptors and transducing mechanisms. Upgrading already established platforms, introducing new features and materials with complementary properties, is the key, to push the reliability, performance and qualities of the devices.

Here we show a possible approach using a consumer inkjet printer, comparing different transduction mechanisms and different materials for the detection of Neutrophil Gelatinase Associated Lipocalin-2 (NGAL), as a case study. Inkjet printing may be one ideal candidate for fast prototyping and the continuous upgrade of nanobiosensing platforms, thanks to its versatility, available choices for materials, and combinations of layout and substrates[5].

## References

[1] Holzinger M. et al., *Front. Chem. 2,* (2014), 1.
[2] Quesada-González D., Merkoçi A., *Biosens. Bioelectron. 73,* (2015), 47.
[3] Downs A. M., Plaxco K. W., *ACS sensors* (2022), DOI 10.1021/acssensors.2c01428.
[4] Broto M., et al, *Nat. Nanotechnol.* 17, (2022), 1120–1126
[5] Rosati G. et al, *Biosens. Bioelectron. 196*, (2022), 113737.

# Surface modification of stainless steel by low-pressure plasma

**Metka Benčina** [1,2], Ita Junkar [1], Matic Resnik [1], Janez Kovač [1], Aleš Iglič [2,3]

[1] Department of Surface Engineering, Jožef Stefan Institute, Ljubljana, Slovenia,
[2] Laboratory of Physics, Faculty of Electrical Engineering, University of Ljubljana, Ljubljana, Slovenia
[3] Laboratory of Clinical Biophysics, Faculty of Medicine, University of Ljubljana, Ljubljana, Slovenia
metka.bencina@ijs.si

Surface modification of stainless steel (SS) used for biomedical applications is important because it affects corrosion resistance, biocompatibility and antibacterial characteristics. For instance, chemical composition and surface oxide layer on stainless steel, which can be altered by various surface treatment techniques, play an important role in its corrosion resistance. Cr is an important constituent of SS as it enables the spontaneous formation of the passive surface oxide layer, which acts as a barrier between the metal and biological environment. Also, the ion release is affected by the Cr content of the oxide film; it has been shown that with the increase in Cr/(Cr+Fe) ratio in the oxide layer, the metal ion release into physiological media decreases [1,2].

In the present contribution low pressure radio frequency plasma was used to modify the surface of SS 316L and the Cr content in the newly formed oxide layer was examined. The following plasma parameters were applied:

- Sample 1 (S1): $H_2$ plasma treatment at pressure 40 Pa lasted for 40 s; $H_2$ + $O_2$ treatment at pressure 50 Pa lasted for 20 s
- Sample 2 (S2): $H_2$ plasma treatment at pressure 40 Pa lasted for 40 s, $H_2$ + $O_2$ treatment at a pressure 50 Pa lasted for 120 s.

The amount of Cr in the surface oxide layer was investigated by Secondary ion mass spectrometry (SIMS) and X-ray photoelectron spectroscopy (XPS) as described in Ref. 3. The amount of Cr was higher (9.7 at. %) on the surface of S1 than on the surface of S2 (8.2 at. %). The Cr/Fe ratio was 2,04 for S1 and 1,11 for S2. Figure 1 shows different signal for CrO and FeO in untreated, plasma-treated S1 and S2 depending on the depth; SIMS profile revealed that the top surface layer of the plasma-treated surface of S1 is prevailingly covered by CrO, while the surface of S2 is mainly covered by FeO. Although CrO is already found on SS 316L surface in an untreated state, the thickness of the layer seems to increase after plasma exposure.

The results indicate that plasma treatment could increase the corrosion resistance of SS due to high Cr-content in the surface oxide layer. In further studies the corrosion resistance analysis will be performed.

## References

[1] Herting, G., Wallinder, I. O., & Leygraf, C. (2006). Factors that influence the release of metals from stainless steels exposed to physiological media. Corrosion Science, 48(8), 2120-2132.
[2] Herting, G., Wallinder, I. O., & Leygraf, C. (2007). Metal release from various grades of stainless steel exposed to synthetic body fluids. Corrosion Science, 49(1), 103-111.
[3] Resnik, M., Benčina, M., Levičnik, E., Rawat, N., Iglič, A., & Junkar, I. (2020). Strategies for improving antimicrobial properties of stainless steel. Materials, 13(13), 2944.

## Figures

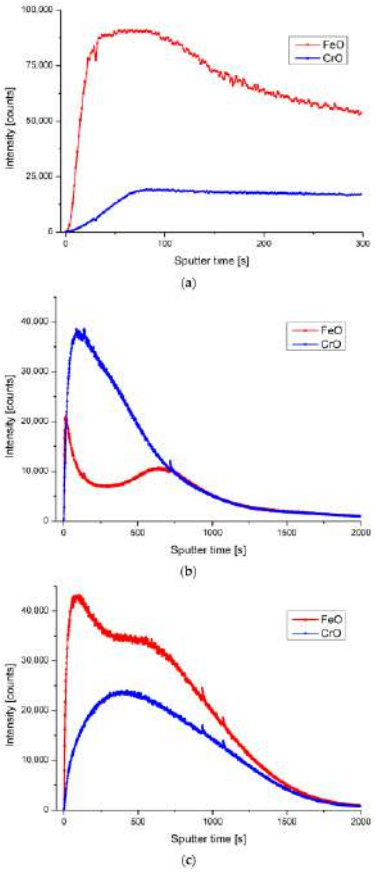


**Figure 1.** SIMS analysis of SS 316L, (a) untreated, (b) plasma treated with prevailing CrO, (c) plasma treated with prevailing FeO.

# Label-free sensor for the near real-time detection of prostate cancer

**Josep Maria Cantons Pérez**[1], Akash Bachhuka[1] and Lluis F. Marsal[1]

[1]Department of Electronics, Electric and Automatic Engineering, Universitat Rovira I Virgili, Tarragona, Spain
josepmaria.cantons@estudiants.urv.cat, lluis.marsal@urv.cat and akash.bachhuka@urv.cat

Cancer is a disease that occurs when a group of cells in our body start growing in a non-controlled way. There are more than 200 types of cancer, depending on their origin. Among these, prostate cancer was reported to have the most cases in Spain in 2021 [1]. To date, the gold standard non-invasive test for the detection of prostate cancer is the prostate-specific antigen (PSA) test which unfortunately has a high false positive rate (75%). Therefore, this study was aimed to fabricate a proof-of-concept (POC) device that can overcome the disadvantages of the current PSA test for the early detection of prostate cancer. To fabricate this POC device, the optical and geometric properties of nanoporous anodic alumina (NAA) [2] [3] [4] were combined with the optical properties of gold nanoclusters (AuNCs). In addition, endoglin (ENG-105) was used as the target protein for the early detection of prostate cancer [5]. The POC device was optimized at various conditions: a) NAA pore size- 35 and 75 nm [6] [7] (Figure 1), b) immobilization of gold nanoclusters- with and without the addition of NHS and EDC, c) the incubation time for both gold nanoclusters and endoglin protein, d) adding different blocking buffers- Ethanolamine and Bovine Serum Albumin (BSA). NAA samples with larger pores (75 nm) showed a higher photoluminescence (PL) signal for biomarker detection than NAA samples with small pores (35 nm) [8] [9]. The POC device showed sensitivity for the endoglin detection range in fg/ml to ug/ml (Figure 2). However, non-specific binding was observed in the case of the control antibody. Although this pilot study demonstrates the potential of the proposed POC device, further optimization is required to overcome the non-specific binding.

## References

[1] Cancer: new cases diagnosed by type Spain 2021 | Statista [Internet]. Statista. 2022. Available from: https://www.statista.com/statistics/779054/number-from-new-cases-from-cancer-by-kind-in-spain/#professional.

[2] Choudhari K, Choi C, Chidangil S, George S. Nanomaterials. 2022, 12(3):444

[3] Amouzadeh Tabrizi M, Ferré-Borrull J, Marsal L.F. Sensors and Actuators B: Chemical. 2020, 304:127302.

[4] Ferré-Borrull J., Xifré-Pérez E., Pallarès J., Marsal L.F. Springer Series in Materials Science, 2015, vol 219, pages 185-217, Losic, D., Santos, A. (eds) Springer.

[5] Meyer A, Gorin M. Nature Reviews Urology. 2019, 16(6):331-332.

[6] Santos A, Balderrama V, Alba M, Formentín P, Ferré-Borrull J, Pallarès J et al. Advanced Materials. 2012, 24(8):1050-1054.

[7] Santos A, Ferré-Borrull J, Pallarès J, Marsal L.F. Physical status solidi (a). 2010, 208(3):668-674.

[8] Santos A, Vojkuvka L, Alba M, Balderrama V, Ferré-Borrull J, Pallarès J, Marsal L.F. Physical status solidi. (a) 2012, 209(10), 2045-2048.

[9] G. Macias, L. P. Hernández-Eguía, J. Ferré-Borrull, J. Pallares, and L. F. Marsal. ACS Appl. Mater. Interfaces, 2013, vol. 5, no. 16, pp. 8093–8098.

## Figures

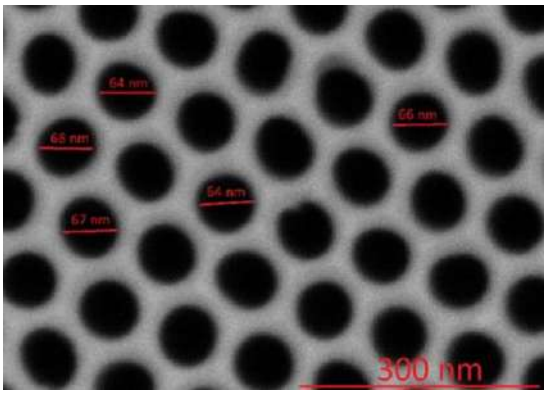


**Figure 1.** NAA sample anodized with 0.3M oxalic acid after a pore widening treatment.

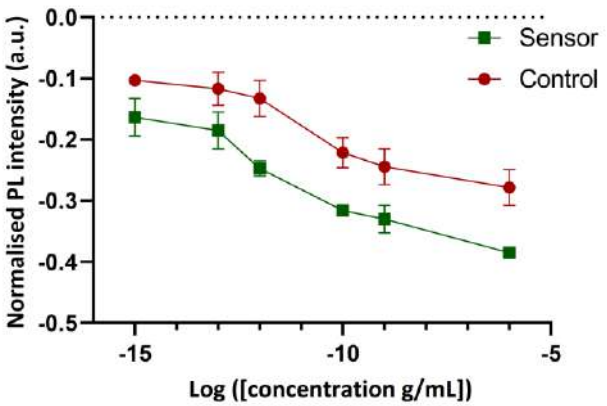


**Figure 2.** Photoluminescence response of the sensor for different endoglin concentrations.

# Alginate/collagen porous scaffolds coated with conductive poly(3,4-ethylenedioxythiophene) nanoparticles for small-diameter tissue-engineered blood vessels

**Emilio Castro**[1,2], Èlia Bosch-Rué[1,2], Sara Estruch-Sotoca[1], Román A. Pérez[1,2]

[1]Bioengineering Institute of Technology, Universitat Internacional de Catalunya, Sant Cugat del Vallès, 08195 Barcelona, Spain
[2]Basic Sciences Department, Universitat Internacional de Catalunya (UIC), Sant Cugat del Vallès, 08195 Barcelona, Spain

ecastro@uic.es

Abstract

Cardiovascular disease (CVD) involving narrowing or obstruction of blood vessels remains the leading cause of morbidity and mortality today, despite advances made in the development of artificial vascular grafts. Although large-diameter tissue-engineered blood vessels (TEBVs) emerged some years ago as a successful alternative therapy to autologous vascular grafts to treat CVD, functional small-diameter TEBVs (ø ≤ 6 mm) have not yet been achieved [1].

Using a triple coaxial nozzle, alginate, collagen and a sacrificial polymer were directly extruded obtaining the scaffold of a TEBV mimicking the microarchitecture of native blood vessels [2], with an outer diameter of 1599 ± 21 µm and a wall thickness of 265 ± 23 µm. After extrusion, the samples were first immersed in an aqueous solution of ammonium persulfate (APS) and secondly in a hexane solution, establishing a coating of different molar concentrations of conductive poly(3,4-ethyldenedioxythiophene) (PEDOT) nanoparticles (average diameter of 50 nm) on the outer layer of the scaffolds to promote cell adhesion and stimulation [4,5].

Double-layered conduits developed by direct extrusion showed high homogeneity and reproducibility. Moreover, it was found that liophylization of samples was not necessary after extrusion as it was not favorable for acquiring good conduit properties. The two best molar concentration ratios of PEDOT to APS were found to be 4:2 and 8:2, which proved to increase the swelling rates of pure Alg/Col scaffolds while significantly decreasing their degradation process and increasing the mechanical properties.

The improved surface roughness caused by these nanoparticles increased the hydrophilicity of the scaffolds (the higher the PEDOT molar concentration ratio, the lower the water contact angle), which favored cell adhesion in both concentrations of PEDOT/Alg/Col scaffolds. The conductive polymer increased the mechanical properties (burst pressure increased from 1.13 ± 0.05 bar in pure Alg/Col scaffolds to 3.38 ± 0.08 bar in 4PEDOT/Alg/Col scaffolds) and the electrical conductivity (PEDOT/Alg/Col hydrogels with a molar concentration ratio of 4 presented the highest electrical conductivity, 122.18 ± 1.32 µS/cm) of the scaffolds, allowing cell survival. The obtained structures were seeded with human aortic smooth muscle cells (hASMC) on the outermost layer. The PEDOT layer on the surface of the scaffolds induced a rough topography that allowed hASMCs to adhere and proliferate on the outer layer of the samples.

In summary, conductive porous conduits were developed by uniformly assembling PEDOT on the surface of Alg/Col scaffolds through in situ interfacial polymerization. The hydrophilic hydrogel was then characterized, sterilized and hASMCs were seeded. The combination of the natural polymers together with these conductive nanoparticles encompassed the advantages of both, obtaining a potentially exceptional scaffold for vascular regeneration [6]. These results suggest that this method might be suitable for stimulating smooth muscle cells (SMCs) with this small-diameter TEBV in the future. Being able to bioengineer this type of functional artificial arteries would not only represent an advance as small-diameter vascular substitutes for grafts, but also for vascularizing artificial organs.

## References

[1] Qiao Zhang, Èlia Bosch-Rué, Román A. Pérez, and George A. Truskey, APL Bioengineering 5 (2021) 021507.
[2] E. Bosch-Rué, Luis M. Delgado, F. Javier Gil, and Roman A. Perez, Biofabrication 13 (2021) 015003.
[3] Shuping Wang, Changkai Sun, Shui Guan, Wenfang Li, Jianqiang Xu, Dan Ge, Meiling Zhuang, Tianqing Liu, and Xuehu Ma, J. Mater. Chem. B 5 (2017) 4774.
[4] Chao Xu, Shui Guan, Shuping Wang, Weitao Gong, Tianqing Liu, Xuehu Ma, and Changkai Sun, Materials Science and Engineering C 84 (2018) 32.
[5] Shuping Wang, Shui Guan, Zhibo Zhu, Wenfang Li, Tianqing Liu, and Xuehu Ma, Materials Science and Engineering C 71 (2017) 308.

[6] Ismael Babeli, Guillem Ruano, Jordi Casanovas, Maria-Pau Ginebra, Jose García-Torres and Carlos Alemán, J. Mater. Chem. C 8 (2020) 8654.

## Figures

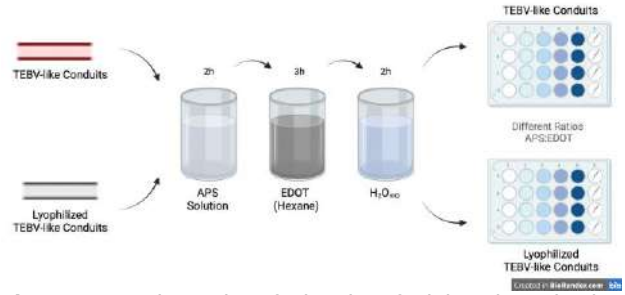


**Figure 1.** Schematic of the interfacial polymerization procedure to obtain conductive PEDOT/Alginate/Collagen scaffolds. Image created using BioRender.

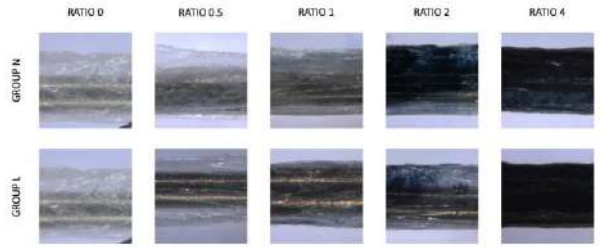


**Figure 2.** Optical images of the two groups of polymerized PEDOT/Alg/Col conductive scaffolds at different molar concentration ratios of APS to EDOT. Group N, lyophilized exclusively after the interfacial polymerization in situ, and Group L, lyophilized before and after the incorporation of nanoparticles.

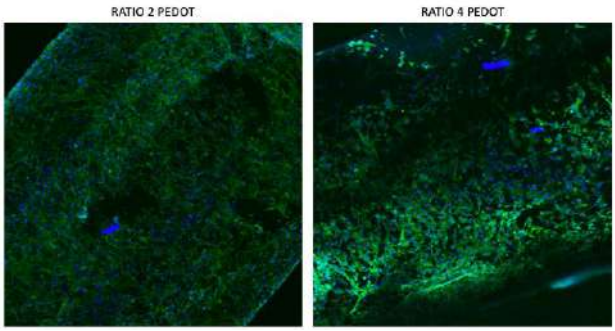


**Figure 3.** Confocal microscopy images of hASMCs seeded in the conduits with two different PEDOT ratios (2 and 4). Actin filaments stained in green (Phalloidin), and the nucleus stained in blue (DAPI).

# Urease-powered polymeric nanomotor containing STING agonist for immunotherapy of bladder cancer

**Hyunsik Choi**[1,3],
Samuel Sánchez[1,2], Sei Kwang Hahn[3]

[1]Institute for Bioengineering of Catalonia (IBEC), C/ Baldiri Reixac, 10-12, Barcelona, Spain
[2]Institució Catalana de Recerca i Estudis Avançats (ICREA), Passeig Lluís Companys, 23, Barcelona, Spain
[3]Department of Materials Science and Engineering, Pohang University of Science and Technology (POSTECH), 77 Cheongam-ro, Nam-gu, Pohang, Gyeongbuk 37673, Korea

hchoi@ibecbarcelona.eu

Most non-muscle invasive bladder cancer (NMIBC) have been treated with transurethral resection of bladder cancer and following intravesical injection of immune therapeutics [1,2]. However, delivery efficiency of the agents is very low because the intravesically injected agents have faced several biological circumstances including clearance from the periodic urination, blockage of penetration to the bladder wall by glycogaminoglycan (GAG) layer [3]. Here, we report the urease-powered nanomotor containing agonist of stimulator of interferon genes (STING) for rapid and efficient activation of immune cells in bladder wall by overcoming these biological circumstances. After confirmation of successful fabrication of nanomotor by transmission electron microscopy, dynamic light scattering analysis, UV-vis spectrometer and urease activity test, we analyzed the motion of nanomotors in range of urea concentration (0~200 mM) with *in vitro* swarming behavior. We demonstrated the *in vitro* uptake mechanism of nanomotor into dendritic cells and activation of dendritic cells. After intravesical injection, we confirmed that the nanomotors showed enhanced penetration into bladder wall and prolonged retention in bladder even after several urination. Furthermore, with bladder cancer bearing mice, we investigated the anti-tumor effect of nanomotor containing STING agonist (almost 0 % of bladder cancer after 14 d), recruitment of activated T cells and mRNA expression in bladder. Taken together, we confirmed the feasibility of urease powered nanomotor as a next-generation platform for bladder cancer treatment

## References

[1] Bas W. G. van Rhijn, et al., European Urology, 3 (2009) 430-442.
[2] Caroline Pettenati, et al., Nature Review Urology, 15 (2018) 615-625
[3] Choi, et al., ACS Nano, 14 (2020) 6683-6692

## Figures

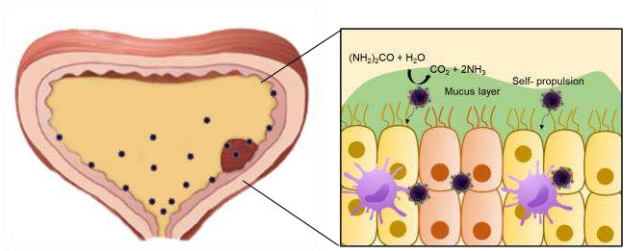


**Figure 1.** Schematic illustration for the intravesical delivery of STING agonist containing urease-powered nanomotors for activation of immune cell in bladder wall.

# Au decorated self-ordered Al nanoconcavities as a SERS platform

Gohar Ijaz Dar, Elisabet Xifre-Perez, **Lluís F. Marsal**

Department of Electrical Electronic Engineering and Automation, Rovira i Virgili University, Avda. Països Catalans 26, 43007, Tarragona,Spain

E-mail: lluis.marsal@urv.cat

Surface-enhanced Raman scattering (SERS) has attracted extensive interest due to its promising applications in chemical/biological sensing and biomedical diagnostics. In nanotechnology, we mimic the fascinating honeycomb configuration on Aluminum (Al) substrate and its adaptable functionalizations utilizing Au sputtering process [1,2]. Herein, we demonstrate the synthesis of the Al Nano bowl morphology with the deposition of Au nanoarray patterned by a sputtering technique. Al templates were synthesized through a two-step anodization process using phosphoric acid. First, a self-ordered pore structure of anodic alumina (AAO) was fabricated through hard anodization (HA) of Al templates using phosphoric acid (195 V) [3]. The second step of anodization was performed with the same parameters of temperature and voltage for 3 h. To acquire the nano bowled morphology on the surface of the Al template as shown in Figure 1(a), the AAO samples were immersed in the stirring assertive mixture of chromium trioxide (0.2 M) and phosphoric acid (0.42 M) for 2 h at 70 ºC. Then Au was sputtered (200 sec) on the resultant Al concavities for further functionalization shown in Figure 1(b). The size of the resultant nanoparticles relies on the sputtering time and thickness of the Au film as followed by Al template morphology [4]. When the Au-coated honeycomb-like nanoarrays will treat to thermal annealing, the Au layer initiates to act with the topography of synthesized nano concavities. This work reveals the efficient strong mechanism to assemble the Au nanoparticles onto dense electrochemically synthesized nanoarrays having a honeycomb-like structure with high spatial resolution. Their plasmonic properties are determined experimentally over a wide range from visible to NIR region, demonstrating to be an efficient substrate for highly sensitive applications, especially for SERS. These interstitial spots were considered to owe concentrated electromagnetic fields conjugated with intense localized surface plasmon resonance [5]. For the occurrence of interparticle plasmon coupling, separation distance among the particles should be less, which will resultantly lead to a significant increment of near field intensity as well SERS or an increase of LSPR refractive index sensitivity [6].

## References

[1] Josep Ferré-Borrull, Josep Pallarès, Gerard Macías, and Lluis F. Marsal, *Materials*,7 (2014): 5225-5253.

[2] Gayathri Rajeev , Elisabet Xifre-Perez, Beatriz Prieto Simon, Allison J. Cowin, Lluis F. Marsal, and Nicolas H. Voelcker, *Sensors and Actuators B: Chemical* 257 (2018): 116-123.

[3] Abel Santos, Lukáš Vojkuvka, Josep Pallarés, Josep Ferré-Borrull, and Llius F. Marsal. *Journal of Electroanalytical Chemistry,* 632(2009): 139-142.

[4] Gerard Macias, Laura P. Hernández-Eguía, Josep Ferré-Borrull, Josep Pallares, and Lluís F. Marsal, *ACS applied materials & interfaces*, 16 (2013): 8093-8098.

[5] Laura P. Hernández-Eguía, Josep Ferré-Borrull, Gerard Macias, Josep Pallarès, and Lluís F. Marsal, *Nanoscale Research Letters*, 1 (2014): 1-8.

[6] Zewen Zuo, Lianye Sun, Yongbin Guo, Lujun Zhang, Junhu Li, Kuanguo Li, and Guanglei Cui, *Nano Research* 15 (2022): 317-325.

## Figures

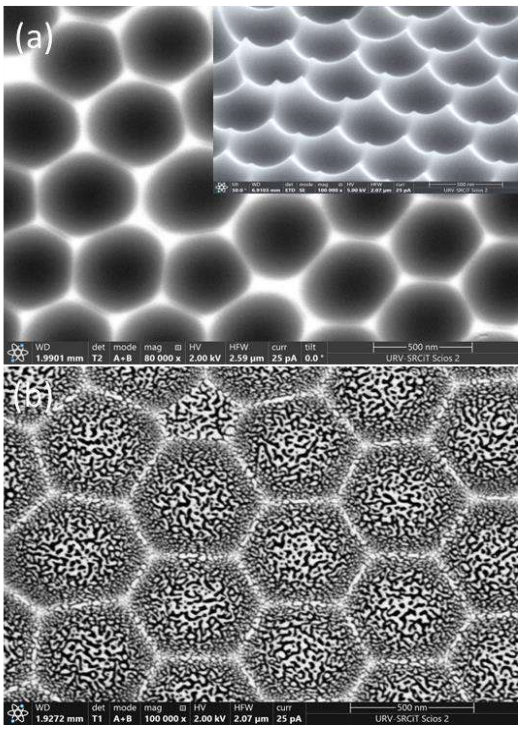


**Figure 1.** FESEM images (a) Top and tilted view of Al concavities and inset the tilted image of nano bowled structure without Au sputtering. (b) Al nano bowled template with Au sputtering of 200 sec.

## Acknowledgment

This project has received funding from the European Union's Horizon 2020 research and innovation programme under the Marie Skłodowska-Curie grant agreement No. 945413.

# Fluorouracil - layered double hydroxides nanocomposites obtained through LDH-LDO-LDH structural conversion

Gabriela Bruja-Sorodoc[1,2], Alina Ibanescu[1,3], Doina Lutic[1,2], **Brindusa Dragoi[1,2]**

[1]Regional Institute of Oncology, 2-4 General Henri Mathias Berthelot, 700483 Iasi, Romania
[2]Faculty of Chemistry, „Alexandru Ioan Cuza" University of Iasi, 11 Carol I Blvd., 700506, Iasi, Romania
[3]"Cristofor Simionescu" Faculty of Chemical Engineering and Environmental Protection, Gh. Asachi Technical University, Dimitrie Mangeron Bvd., 700050 Iasi, Romania

brindusa.dragoi@yahoo.com

## Introduction

In the last several decades, but mainly in the last 10+ years, nanocarrier formulation of anticancer drugs has strongly stimulated the research, becoming a key topic in cancer nanotechnology [1]. Layered double hydroxides (LDH) with two dimensional structure are among the nanocarreirs holding promise for oncologic applications due to their low toxicity, particular structure and morphology, relatively high specific surface areas, anion exchange capacity, positive Zeta potential, to name only a few of their attracting physico-chemical properties [2]. Their unique structure, consisting of compact layers embedding inorganic cations separated by a space accommodating anions and water, make them a generous platform for developing an extremely large number of nanodrugs for cancer, but not limited to (Figure 1).

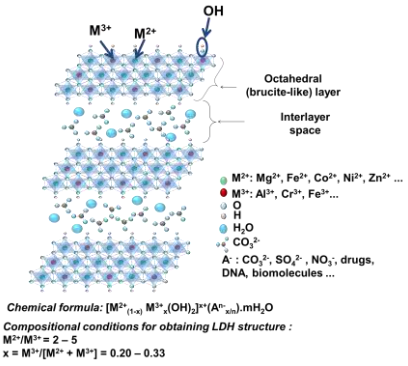


**Figure 1.** Schematic structure of LDH

Essentially, the layers contain cations ($M^{2+}$ and $M^{3+}$), each of them being surrounded by six OH groups forming octahedra linked together by the edges [3]. The trivalent cations in the layers bring a positive charge, which is beneficial for both hosting organic anionic molecules, such as drugs, in the space between the layers and for interaction with the negatively charged phospholipids in the cell membrane. Such materials can be conveniently synthesized by several methods [4]. However, the appropriate method has to be selected depending on the desired properties. The most employed methods to synthesis organic-inorganic LDH hybrids, are coprecipitation at low and high suprasaturation, anion exchange and reconstruction. *Coprecipitation* implies the addition of two solutions, one containing the metallic precursors and the other one the precipitation agent to a solution containing the drug at controlled pH, temperature, stirring, time, and aging conditions. The *anion exchange* supposes putting into contact a pre-synthesized LDH with a solution of the drug to be encapsulated. In this case, the inorganic anion between the layers is replaced by the drug. Finally, the late approach, *reconstruction* implies three main stages, that is, *(i)* synthesis of LDH, *(ii)* thermal degradation through calcination at high temperatures (usually 400 - 450 °C for 4 - 6 h) when the layered double oxides (LDO) are formed, followed by *(iii)* rehydration of LDH to recover their initial structure. In this case, the drug to be incorporated is dissolved in the solution used for rehydration of LDO and incorporated during this step. This unique LDH-LDO-LDH structural conversion is based on the so called "*memory effect*" of these exciting materials. While the first two methods do not allow to reach the maximum loading degree due to the presence of the inorganic anions ($Cl^-$, $NO_3^-$ and or $CO_3^{2-}$), the reconstruction occurring in the absence of those inorganic anions has all the premises to incorporate the highest amount of drug that the gallery space *in tandem* with the amount of $M^{3+}$ cation can accommodate.

## Originality

In this work, we studied the ability of a $MgOAl_2O_3$-LDO obtained from the corresponding MgA-LDH to accommodate fluorouracil (FU). FU is a heterocyclic aromatic organic compound with a structure similar to that of the pyrimidine molecule and is one of the most used anticancer drug for a large pallet of malign tumors [5]. Herein, we were particularly interested in seeing how the rehydration time impacts both *(i)* the degree of crystallinity and thus the recover of the initial order of the materials and *(ii)* the amount of FU sealed off between the reorganized layers. Also, how the drug molecule is placed between the octahedral layers, as an indication of the amount of drug that can be loaded in the LDH, was also in our area of interest.

## Experimental

**Synthesis** *Step 1*: The starting material, MgAl-LDH with Mg/Al molar ratio of 3/1 was synthesized by co-precipitation under low suprasaturation method at 25 °C. A solution containing the metal nitrates (1 M) and an alkaline solution ([NaOH] = 2 M) were simultaneously added in an automated double jacked reactor from Syrris, which allowed to carefully control the temperature, pH and stirring. The suspension was vigorously stirred and maintained at the desired pH (~10) by adjusting the flow rates of the solutions. The final suspension was aged under stirring at 90 °C for 14 h. The white precipitate was filtered, washed with deionized water and then dried at 80 °C for 24 h. The sample was denoted as $NO_3$-LDH. *Step 2*: To obtain $MgOAl_2O_3$-LDO, the obtained MgAl-LDH was calcined at 400 °C with a

rate of 1 °C.min$^{-1}$ for 6 h under stagnant air in an oven. The sample was denoted as LDO. *Step* 3: Reconstruction of MgAl-LDH from $MgOAl_2O_3$-LDO while incorporating FU between the layers was performed by using an Al/FU molar ratio of 1.6. The rehydration was performed in a round bottom flask and using decarbonated water. The suspension (pH ~8) was gentle stirred at 25 °C for 24 and 72 h. The samples are denoted as FU-LDH-24 and FU-LDH-72 for a treatment performed for 24 and 72 h, respectively. **Physico-chemical characterization** The samples were characterized by XRD, $N_2$ physisorption, and FTIR in order to assess the structure, texture, and interlayer composition. In order to evaluate the amount of FU in the sample (loading degree), both samples were dissolved in strongly acidic media (HCl + $HNO_3$) aiming at returning the cations into solution while releasing the entire amount of FU previously enclosed in the solid. The concentration of was determined by the UV-Vis spectrometry based on the typical absorption of FU at 266 nm and using a calibration curve.

**Results and discussion**

Figure 2 illustrates the XRD patterns of all samples, that is, original LDH, the calcined form and the organic-inorganic LDH hybrids reconstructed based on the "memory effect".

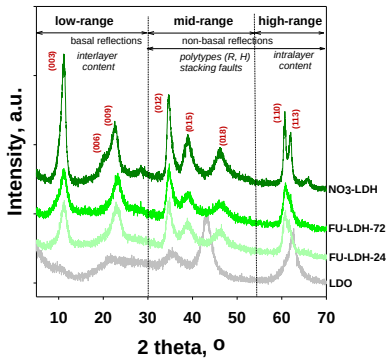


**Figure 2.** XRD patterns of samples.

The XRD pattern of $NO_3$-LDH displays the typical reflections, that is, basal reflections ((003) and 006)) and non-basal reflection ((012), (015), (018), (110) and (113)) typical for a LDH material. Moreover, the shape of the peaks plus the well-shaped (110) and (113) reflections clearly show a high-quality crystalline material. The thermal treatment at 400 °C for 6 h was enough to completely break the high order of the materials, effect reinforced by the disappearance of the LDH reflection and appearance of the typical reflection of the mixed oxides in the pattern of LDO. The rehydration of the oxides-based sample in the presence of FU solution for 24 and 72 h led indeed to the reorganization of the samples in the 2D structural arrangement of LDH. Yet, the crystallinity is much lower as compared to the parent material, but even high enough according to the shape of the peaks. Interestingly, the position of the first basal reflection is not shifted at lower values of 2 theta, but it is placed at almost the same value as in the case of initial LDH for both samples. Because the reconstruction took place in the presence of FU and not other anions were in the solution, it is hypothesized that the FU molecule was taken by the reconstructing layers and placed in a flat position instead of perpendicular against to the layers. Indeed, the FTIR spectra show clear evidence of the presence of FU inside the samples mainly based on the vibrations at 1654, 1246 and 807 cm$^{-1}$ belonging to $\nu C^4=O$, $\nu C$-F and $\delta N_1$- H, respectively. No clear indication on the amount of FU in the sample was provided by the FTIR spectra. The evaluation of the amount of FU by UV-Vis in the solution obtained upon acidic dissolution of solid samples provided a loading degree of 12.36 and 10.50% for FU-LDH-24 and FU-LDH-24, respectively. Comparing these values with that obtained for FU included in the same parent $NO_3$-LDH by anion exchange, which was of only 3.52%, the improvement by reconstruction approach is obvious.

**Conclusion**

To sum up, the LDH-LDO-LDH structural conversion led to materials of reasonable quality in terms of crystallinity irrespective of rehydration time when compared to the parent material obtained by coprecipitation. On the other hand, the results revealed that the amount of FU was slightly influenced by the time of treatment, longer time decreasing the loading degree by ~2%. However, irrespective of the amount incorporated, the FU occupied a parallel position against the brucite-like sheets in the interlayer space, which does not allow to additionally increasing the amount of FU as a perpendicular position would entail. Yet, when compared with the anionic exchange, it can be stated that indeed reconstruction proved to be a much more efficient approach in terms of FU amount and efficient exploitation of the interlayer gallery.

**Acknowledgments**: This work was supported by a H2020 grant – ERA-Chair, no 952390 and a grant of the Ministry of Education and Re-search, CNCS/CCCDI - UEFISCDI, project number PN-III-P3-3.6-H2020-2020-0105/35/2021

## References

[1] What Is Cancer Nanotechnology? Grobmyer S.R., Iwakuma N., Sharma P., Moudgil B.M. in Cancer Nanotechnology Methods and Protocols, Grobmyer S.R., Moudgil B.M., Humana Press, Springer, 2021.

[2] Park D.-H., Choi G., Choy, J.-H., Photofunctional Layered Materials. Bio-Layered Double Hydroxides Nanohybrids for Theranostics Applications; Yan, D., Wei, M., Eds.; Springer International Publishing: Switzerland, 2015.

[3] Cavani F., Trifiro F., Vaccari A., Catal. Today, 11 (1991) 173.

[4] Klemkaite K., Prosycevas I., Taraskevicius R., Khinsky A., Kareiva A., Cent. Eur. J. Chem., 9 (2011) 275.

[5] Zhang N., Yin Y., Xu S.-J., Chen W.-S., Molecules, 13 (2008) 1551.

# Co-axial 3D bioprinting for Biomimetic Multifibre Skeletal Muscle-based Bioactuators

**Judith Fuentes**[1]
Rafael Mestre[1], Maria Guix[1], Ibtissam Ghailan[1], Samuel Sánchez[1,2]

[1] Institute for Bioengineering of Catalonia (IBEC), The Barcelona Institute of Science and Technology, 08028, Barcelona, Spain
[2] Institució Catalana de Recerca i Estudis Avancats (ICREA), Barcelona, Spain

jfuentes@ibecbarcelona.eu

**Abstract**

Recent advances in three-dimensional (3D) bioprinting and tissue engineering have opened new possibilities in the fabrication of bioengineered muscle models able to mimic the complex hierarchical organization and functional properties from the native tissues [1]. The combination of skeletal muscle tissue and artificial elements has led to a wide variety of innovative solutions to create bio-hybrid robotic systems and bioactuators [2] that offer the opportunity to study processes of interest in the biomedical field, such as muscle development and regeneration. However, one key problem in tissue engineering is the poor oxygen and nutrients supply in the inner regions of the printed scaffold, leading to a reduced cell viability.

In our work, we explored co-axial 3D bioprinting [3] as a novel strategy towards overcoming the nutrient diffusion problem by creating individual, non-fused fibers with defined thickness. Therefore, we aim to develop a 3D bioengineered skeletal muscle bioactuator with biomimetic design in terms of structure and functionality. In comparison with conventional 3D-bioprinting, where a single syringe containing the cell-laden bioink is used, in co-axial 3D-bioprinting an outer layer of sacrificial material (pluronic acid in this study) allows a physical confinement on the inner layer (i.e bioink), obtaining thin independent printed fibers that can be hierarchically organized (Figure 1). Such technique is generally implemented in the fabrication of vascular systems [4]. The use of bioprinting techniques allow the fabrication of bioengineered muscle-based actuators that present highly aligned myotubes with contractile capabilities. However, the formation of thinner and individual fibers obtained by co-axial 3D-printing resulted in an enhanced diffusion of nutrients during the muscle maturation process, improving cell differentiation and obtaining stronger bioactuators which present an increased force output in comparison with the actuators fabricated by using conventional printing.

After exploring the potential of 3D bioprinting for fabricating 3D bioengineered skeletal muscle bioactuators, our interests are currently focused on exploiting the regenerative capabilities of muscle tissue to integrate self-healing properties to living actuators [5] and create more biomimetic in vitro muscle models for biomedical applications.

## References

[1] Mestre, R., Patiño, T., Barceló, X., Anand, S. Pérez-Jiménez, A., Sánchez, A. Adv. Mater. Technol. (2019). [4, 1800631].
[2] Guix, M., Mestre, R. Patiño, T., De Corato, M., Fuentes, J., Zarpellon, G., Sánchez, S. Sci. Robot. (2021). [6, eabe7577].
[3] Patent #EP203825971 filled, “Printing system for obtaining biological fibers”.
[4] Millik, S. C., Dostie, A. M., Karis, D. G., Smith, P. T., McKenna, M., Chan, N., Curtis, C. D., Nance, E., Theberge, A. B., & Nelson, A. Biofabrication. (2019). [11(4), 045009].
[5] Raman, R., Grant, L., Seo, Y., Cvetkovic, C., Gapinske, M., Palasz, A., Dabbous, H., Kong, H., Perez Pinera, P., Bashir, R. (2017). Adv. Healthc. Mater. Millik, S. C., Dostie, A. M., Karis, D. G., Smith, P. T., McKenna, M., Chan, N., Curtis, C. D., Nance, E., Theberge, A. B., & Nelson, A. Biofabrication. (2019). [11(4), 045009].

## Figures

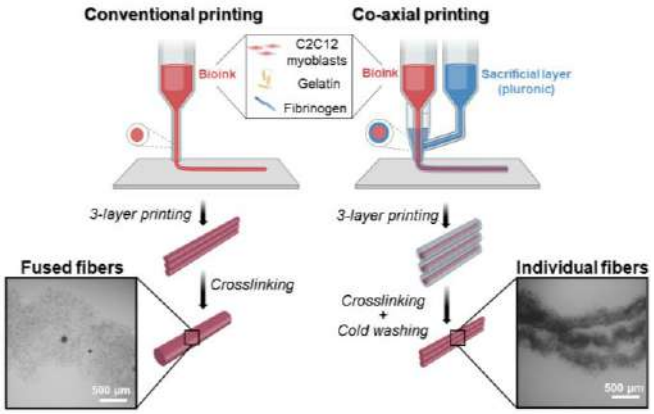


**Figure 1.** Schematic of the two 3D bioprinting techniques used: conventional printing and co-axial printing.

# Hybrid composite coatings for osteostimulating implants in osteoporosis

**Yordan S. Handzhiyski**[1], Ralitsa T. Mincheva[1], Gjorgji Atanasov[1] Anna I. Kozelskaya[2], Elena Soldatova[2], Sergei I. Tverdokhlebov[2], and Margarita D. Apostolova[1]

[1]Roumen Tsanev Institute of Molecular Biology - BAS, Acad. G. Bonchev Str., Bl. 21, 1113 Sofia, Bulgaria
[2]Tomsk Polytechnic University, 30 Lenin Avenue, 634050 Tomsk, Russian Federation

folie@abv.bg

Additive manufacturing is incrementally deployed in the field of materials science of medical implants, as it allows the fabrication of individualized and highly complex implant structures. Due to high biocompatibility, titanium and titanium alloys are the material of choice for bone regeneration. However, these implants exhibit significant drawbacks - lack of rapid osteo- and angiogenesis and the presence of inflammatory processes.

In the present study, 2D and 3D implants were prepared with the coatings obtained by micro-arc oxidation (MAO) and electrolytes containing Ca, P, Sr, and Mg. The layers were coated with biodegradable polymers containing an anti-osteoporotic and pro-angiogenic drug to improve biocompatibility. Depending on electrolyte solution and MAO process parameters, a different coating thickness, various crystallite phase compositions, and significantly diverse biocompatibility were obtained. This approach proves a difference in deposited film thickness compared to the commonly employed one. The physicochemical properties and morphology of the fabricated MAO coating were investigated in detail. Biocompatibility of the three different coatings has been verified by endothelial cells (EA.hy 926), MG-63 cells (bone fibroblast, osteosarcoma), and adult human adipose-derived mesenchymal stem cells by investigation of cell adhesion, proliferation, and osteogenic differentiation. The relatively large MAO surfaces provided many attachment points for cell growth. It should be noted that by using various MAO modes and electrolytes with different compositions, it was possible to control the porosity of the coatings and thereby control the loading and the releasing of drugs from the layer. The porous morphology of the MAO coatings enhanced the binding of the implant and bone tissue, thus contributing to bone tissue regeneration.

Acknowledgment: This project was supported by Bulgarian Science Fund (Grant Agreement KP-06-Russia/20).

# Silver modified surfaces for photothermal therapy

**Lucie Hochvaldova**[1], Lucie Válková[2], Karolína Simkovičová[1], Kateřina Plecho[1], Libor Kvítek[1], Hana Kolářová[2] and Aleš Panáček[1]

[1]Palacky University, Department of Physical Chemistry, Faculty of Science, Olomouc, Czech Republic
[2]Palacky University, Department of Biophysics, Faculty of Medicine and Dentistry, Olomouc, Czech Republic

lucie.hochvaldova@upol.cz

Photothermal therapy seems to be one of the promising tools in the treatment of various cancerous diseases. In this case, cancer cells were killed by high local temperatures, which were induced by laser irradiation of the nanoparticles coated on the well surface. If the surface is illuminated by laser of suitable wavelength, which corresponds to the position of the nanoparticle absorption maximum, the conversion of energy to heat is enhanced and leads to local hyperthermia and causes irreversible cell damage. The main goal of this research was to prepare nanoparticles, whose position of the absorption maximum could be tuned easily and would be in resonance with the wavelength of the used laser.

Nanoparticles with a wide range of sizes, shapes, therefore plasmonic/optical properties were synthesized by two step reduction process, where the ratio between reducing and stabilizing agent had the main impact on the nanoparticle final properties. Nanoparticles with the absorption maximum of desired wavelength (with respect to the used laser) were deposited on 96-well microtitration plate (by electrostatic layer-by-layer deposition) and used to evaluate anti-tumor efficacy in photothermal therapy.

This work was supported by the students grant DSGC-2021-0120 "Light-assisted in vitro therapy using plasmonic materials" funded under the OPIE project "Improvement of Doctoral Student Grant Competition Schemes and their Pilot Implementation", reg. no. CZ.02.2.69/0.0/0.0/19_073/0016713.

## References

[1] Mistrik, M., Skrott, Z., Muller, P., Panacek, A., Hochvaldova, L., Chroma, K., Buchtova, T., Vandova, V., Kvitek, L. & Bartek, J. (2021). Microthermal-induced subcellular-targeted protein damage in cells on plasmonic nanosilver-modified surfaces evokes a two-phase HSP-p97/VCP response. *Nature Communications*, *12*(1).

[2] Malá, Z., Žárská, L., Bajgar, R., Bogdanová, K., Kolář, M., Panáček, A., Binder, S. & Kolářová, H. (2021). The application of antimicrobial photodynamic inactivation on methicillin-resistant S. aureus and ESBL-producing K. pneumoniae using porphyrin photosensitizer in combination with silver nanoparticles. *Photodiagnosis and Photodynamic Therapy*, *33*.

## Figures

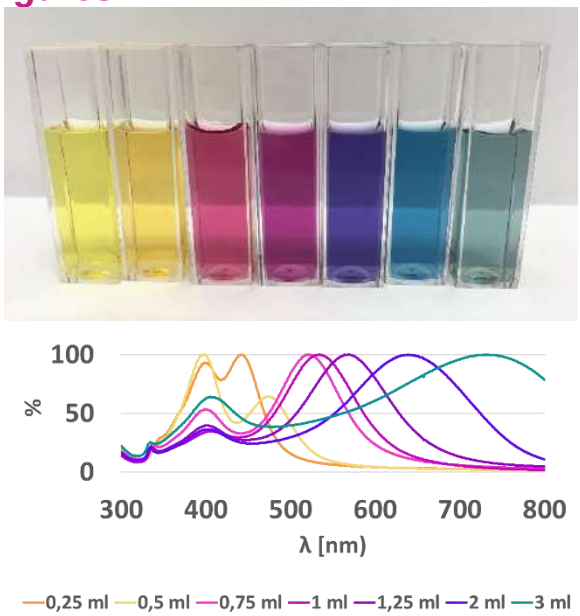


**Figure 1a.** Water dispersion of silver nanoparticles prepared by stabilization with different amount of citrate and their absorption spectra **(Figure 1b)**.

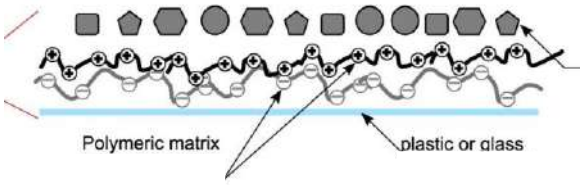


**Figure 2.** Formation of the plasmon layer on the cultivation surface (- PAA, + chitosan & AgNPs of various shapes)

**Figure 3.** Poster in PDF

# Fabrication and Characterisation of Lactate Releasing PLGA Particles for cardiac regeneration

**Christopher James**[1,2], Barbara Blanco, PhD[1,2], Soledad Perez-Amodio, PhD,[1,2,3] Prof. Elisabeth Engel Lopez[1,2,3]
[1]Institute of Bioengineering Catalunya (IBEC), The Barcelona Institute of Science and Technology, Barcelona, Spain
[2]CIBER en Bioingenieria, Biomateriales y Nanomedicina, CIBER-BBN, Madrid, Spain
[3] IMEM-BRT group, Departament de Ciència i Enginyeria de Materials, Universitat Politecnica de Catalunya, Barcelona, Spain
Contact@E-mail (Arial 9)

Background

Lactate is known to be utilised as a fuel and regulator in a range of cellular processes including immune tolerance, memory function, ischaemic tissue injury, cancer growth, metastasis, and wound healing.[1] Systemic or local delivery of lactate in mice with ischemic wounds increased reparative angiogenesis through endothelial progenitor cell recruitment and deposition of extracellular matrix leading to accelerated wound healing and reduced skeletal muscle atrophy.[2] Recent work by our group also showed that lactate promoted neuronal stem cell/progenitor maintenance and cardiomyocyte cell cycle progression.[3,4] Here we set out to fabricate particles that release sufficient lactate to initiate such responses.

Materials and methods

Utilising a well-defined synthesis method, water-oil-water emulsion, we fabricated poly(lactic-co-glycolic) (PLGA) particles loaded with lactate and characterised their properties such as size and lactate release. Tuning the polymer length and the ratio of lactic to glycolic acids within the PLGA used to synthesise particles, as well as the method for fabrication (e.g., polymer concentration, ultrasonication intensity and time) used has allowed tuning of their size and biodegradation rate, and so their lactate release profile.[5] A cryoprotector was used to prevent particle aggregation during the freeze-drying process and the degradation products were assessed for cytotoxicity in cardiomyoblast (H9c2) and endothelial cells (HUVEC).

Results

In this study PLGA particles with sizes between 200 and 300 nm that release up to 5 mM of lactate per mg have been achieved, reaching biological active concentrations . The degradation products of the particles showed no cytotoxicity.

Acknowledgements

Financial support for the BIOCARDIO project was received in the form of a grant from the Spanish Ministry of Economy and Competitiveness (MINECO/FEDER, RTI2018-096320-B-C21), and the EuroNanoMed3 project nAngioDerm funded through the Spanish Ministry of Science and Innovation (ref. PCI2019-103648).

## References

[1] Sun, S., Li, H., Chen, J. & Qian, Q., APS: Physiology, 32:6 (2017) 453-463
[2] Porporato, P. E. et al., Angiogenesis 15 (2012) 581–592
[3] Álvarez, Z. et al., Biomaterials 35 (2014) 4769–4781
[4] Ordoño, J., Pérez-Amodio, S., Ball, K., Aguirre, A. & Engel, E., Biomaterials Advances, 139 (2022) 213035
[5] Ochi, M., Wan, B., Bao, Q. & Burgess, D. J., Int J Pharm 599 (2021) 120450

## Figures

**Figure 1.** Fabrication of PLGA particles, with 5 steps to control their size, and so degradation and lactate release. (1) Polymer concentration + molecular weight (high (HMw) vs low (LMw)), (2) Lactide monomer concentration, (3) PVA concentration, (4) Intensity of ultrasonication, and (5) Duration of sonication.

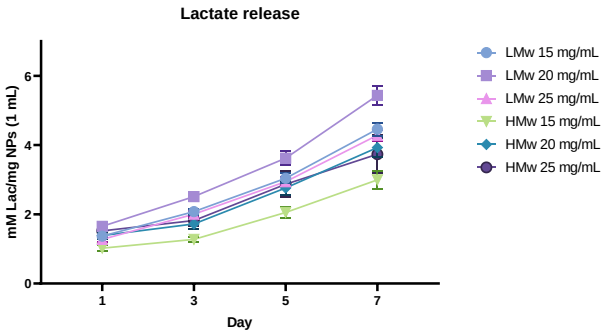


**Figure 2.** Lactate release of PLGA nanoparticles loaded with lactide monomer over 7 days.

# Environmental monitoring of pathogens by semi-automated biosensors

**Juárez, M.J**[1], Hernández-Albors, Alejandro[1]; Alcodori-Ramos, Javier[1]; Fort-Escobar, Vicente[1]; Fito-López, Carlos[1]

[1]ITENE Research Centre, Albert Einstein St., No.1, Paterna (Valencia), Spain

mariajose.juarez@itene.com

The Covid-19 disease alert has evidenced the continuous exposure of human to pathogens and the health risk they represent. Microorganisms can be located not only in airborne samples, as in the case of Sars-CoV-2 and other respiratory pathogens such as *Legionella* [1], as well as in wastewater that can contaminate the sea, or even in the food we consume daily. The detection and monitoring of pathogens in different environments allows the control of their exposure and rapid decision making in alert situations, reducing, therefore, their potential health risk [2].

A useful strategy to carry out these screenings has been shown to be the use of nanobiosensors because these devices usually offer a lower response time than traditional methods, more versatility, high sensitivity and low cost, which makes them accessible to most of the contamination-sensitive areas [3]. Despite the good sensitivity of these devices, environmental samples often have a quite low pathogen concentration [4], being necessary in most cases a preconcentration system or advanced high sensitivity and expensive instrumentation to achieve its detection.

In this context, ITENE research centre has developed new automated systems that allow the sampling and preconcentration of air environmental samples, with a high collection efficiency (100 L/min), and of wastewater, decreasing 100-fold the detection limit, in a short time. These systems also facilitate sample conditioning for compatibility with bioreceptors. Furthermore, easy-to-use and automatable biosensors with good analytical sensitivity have also been developed for the determination of Sars-CoV-2 and *Escherichia coli (E. coli)* in air and water samples, respectively. These biosensors have been optimized to increase the sensitivity of the determination and minimize the cost and time of the assay.

Developed biosensors have been integrated with the sampling and pretreatment systems and were validated in environments of interest. In the case of the Sars-CoV-2 biosensor, the device was installed in rooms of diagnosed patients in the reference hospital of València, Hospital Universitario y Politécnico La Fe. In this study, it was observed that 30% of the samples collected were positive. Regarding the determination of *E. coli* in wastewater, Samples with *E. coli* values higher than 100 CFU/mL collected at different locations of the treatment plant showed a positive result with the developed biosensor.

These results show the validity of the methodology in environmental monitoring of pathogens and its applicability to different industries and pathogens.

## References

[1] Allegra, S., Leclerc, L., Massard, P. A., Girardot, F., Riffard, S., & Pourchez, J. *Scientific reports*, *6*(1), (2016) 1-8.

[2] Nnachi, R. C., Sui, N., Ke, B., Luo, Z., Bhalla, N., He, D., & Yang, Z. *Environment international*, (2022).107357.

[3] Kaya, H. O., Cetin, A. E., Azimzadeh, M., & Topkaya, S. N. *Journal of Electroanalytical Chemistry*, *882*, (2021). 114989.

[4] Borges, J. T., Nakada, L. Y. K., Maniero, M. G., & Guimarães, J. R. Environmental Science and Pollution Research *28* (30) (2021), 40460-40473.

## Figures

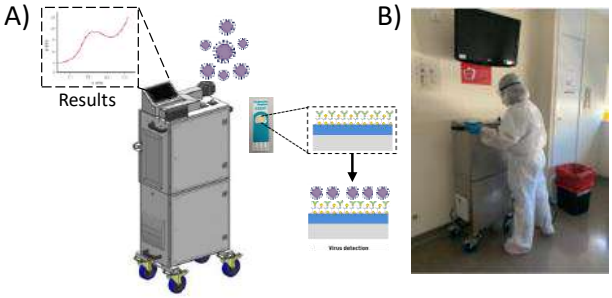


**Figure 1.** A) Scheme of integrated sampling and pretreatment systems and electrochemical biosensor for airborne detection. B) Photo of the validation in hospital environments.

# Stretch-growth and cell therapy: a novel combinatorial approach for treating spinal cord injuries

**F. Merighi[1]**,
S. De Vincentiis[1], M. Baggiani[1],
A. Zanelli[1], Mariachiara di Caprio[2],
M. Costa[3], M. Mainardi[3], M. Onorati[1], V. Raffa[1]
[1] Department of Biology, University of Pisa, Italy
[2]Laboratory of Biology, Scuola Normale Superiore, Pisa
[3]Neuroscience Institute, National Research Council, Pisa
francesca.merighi@phd.unipi.it

Abstract
Spinal Cord Injury is a pathological condition with devastating physical and socio-psychological consequences [1], but effective treatments are lacking due to the complex pathophysiology. Recent investigations in the field of regenerative medicine show the therapeutic potential of neuroepithelial stem (NES) cells to treat this type of injury [2], while advancement in nanotechnologies enables the development of novel nanomedical tools. Previous studies investigated the use of magnetic nanoparticles (MNPs) and magnetic field to induce stretch-growth (SG), i.e. the stimulation of axonal outgrowth by mechanical stimuli [3][4][5]. The purpose of this work is to validate a novel combinatorial approach to treat spinal cord injuries based on the use of SG and cell therapy. Indeed, the success of stem cell-based therapies depends on the capacity to promote axonal growth, which is necessary to reconstitute lost neural circuits. Our data concern mechanically induced stretch growth of MNP-labelled human-derived differentiating neurons both in vitro and microinjected in the ex vivo model of mouse spinal cord (SC) organotypic slices. Our data demonstrate that we can manipulate elongation and guidance of the neurites of stretched NES cells both in vitro and in the SC tissue. We are also developing an innovative platform of cortico-spinal assembloids to model the cortico-spinal tract (CST) in vitro. After performing an injury of the assembloids, these will be used to test the effective regenerative potential of our approach in a human 3D cytoarchitectural context.

## References

[1] Ahuja, C.S. et al., Nature Reviews Disease Primers, 2017, 3.
[2] Dell'Anno et al., Nature Communications, 2018, 9(1)
[3] Raffa,V. et al., Biophys J, 2018, 15(10)
[4] De Vincentiis, S. et al., Journal of Neuroscience, 2020, 40(26) 4997
[5] De Vincentiis, S. et al., Int J Mol Sci, 2020, 21(21)

## Figures

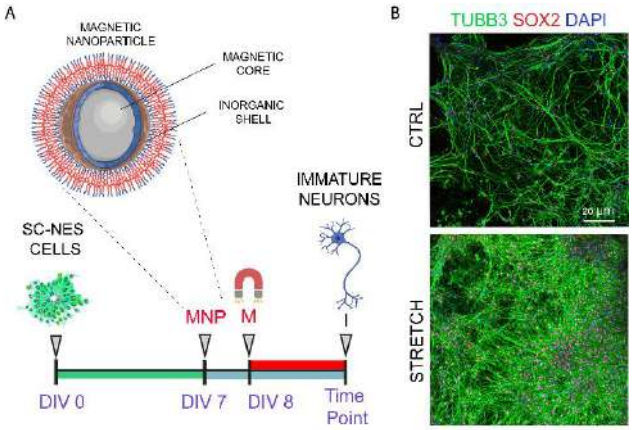


**Figure 1.** (A) Schematic representation of stretch growth protocol: SC-NES cells are labelled with MNPs at DIV 7 of differentiation; at DIV 8 external magnetic field is applied. Cells are fixed at specific time points: DIV 10 for short term assay; DIV 60 for long term assay. (B) Representative images of DIV 60 neurons in control (upper image) and stretch (lower image) condition.

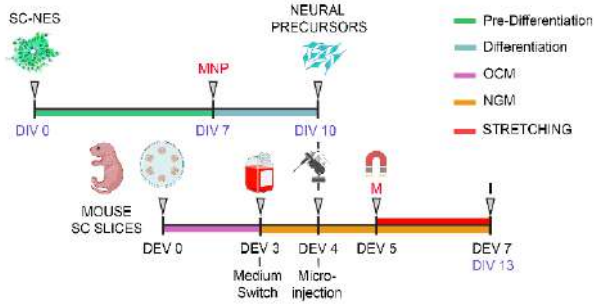


**Figure 2.** Schematic representation SC-NES cell transplantation protocol into mouse spinal cord organotypic slices. Cells are labelled with MNPs prior to transplantation. The external magnetic field is applied for two days (short term assay), then cells are fixed for further analysis.

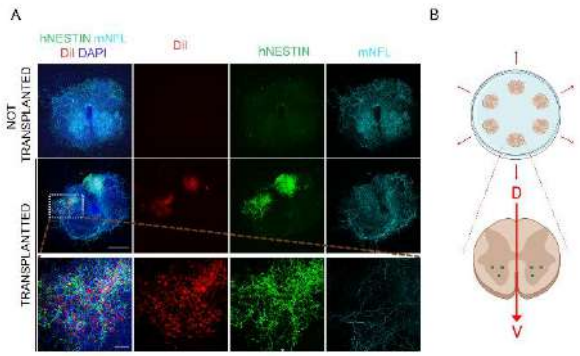


**Figure 3**. (A) Immunofluorescence staining for human-NESTIN (green) to detect human SC-NES cell-derived neural precursors transplanted into the mouse spinal cord organotypic slices. (B) Co-culture organization design: up to 6 SC slices are placed concentrically with the dorso-ventral axis (red arrow) in the radial direction (centrifugal) and human SC-NES cells are microinjected in the ventral horns (3 injections per horn- green dots).

# Nanoporous Anodic Alumina-based Portable Optical Sensor for the Detection of Hg+ ions

**Sachin Mishra**, Eugeni Garcia, Akash Bachhuka, Lluís F. Marsal

Department of Electrical Electronic Engineering and Automation, Rovira i Virgili University, Spain

E-mail: sachin.mishra@urv.cat, lluis.marsal@urv.cat

Mercury is used extensively in various industries such as gold and coal mining and electrical equipment, batteries, semiconductors, and medical appliances. The unique mercury compounds are also naturally emitted into the atmosphere from volcanoes, forest fires, and the weathering of rocks. Although it has its advantages for some industries, it is toxic and dangerous for human health and ecosystems [**1**]. In addition, organic mercury is harmful to peripheral nerves like skin nerves or solid bone nerves related to the central dogma of the nervous system of humans. Due to the complexity and continuous use of mercury in industry, the rapid detection of mercury is warranted to control and monitor its concentration [**2**]. The typical detection techniques used to sense ionic mercury are atomic absorbing spectroscopy (AAS) and gas chromatography (GC) [**3**]. However, these techniques are expensive, time-consuming, and require expert personnel. To overcome these problems, we propose to fabricate a portable device by combining the optical properties of anodic porous alumina (NAA) and gold nanoclusters (AuNCs) for selective and fast detection of mercury [**Figure 1**]. AuNCs have a very high affinity and selectivity to mercury because $Au^{+}$ can selectively sense $Hg^{+2}$ through metallophilic interactions between the electrons in “d” orbitals. A higher photoluminescence (PL) intensity for mercury ions detection was observed for NAA with larger pores size (75 nm) compared to smaller pores (35 nm) [**4-7**]. Besides, AuNCs had the same stability and PL intensity for samples with/without NHS/EDC coupling. The sensing performance of the system was assessed through several tests, establishing its sensing performance and chemical selectivity. The sensor device showed sensitivity for Hg detection range in mM to µM [**Figure 2**] [**8, 9**]. The label-free merit of detection of the proposed sensor platform paves the way for future applications in heavy metal ion sensing.

## References

[1] UNEP Chemicals Branch. In UNEP Global Mercury Assessment 2013: Sources, Emissions, Releases and Environmental Transport; UNEP: Geneva, Switzerland, 2013.

[2] Zhang, L.; Chang, H.; Hirata, A.; Wu, H.; Xue, Q. K.; Chen, M. ACS Nano 7, 4595−4600, 2013.

[3] Gras, Ronda; Luong, Jim; Shellie, Robert A. 2018, 2, 5, 471–478.

[4] A. Santos, J. Ferré-Borrull, J. Pallarès, and L. F. Marsal, Phys. Status Solidi A 208(3), 668–674, 2011.

[5] A. Santos, L. Vojkuvka, M. Alba, V. S. Balderrama, J. Ferré-Borrull, J. Pallarès, and L. F. Marsal, Phys. Status Solidi A 209(10), 2045-2048, 2012.

[6] Santos, Abel; Macías, Gerard; Ferré-Borrull, Josep; Pallarès, Josep; Marsal, Lluís F., ACS Applied Materials & Interfaces, 4(7), 3584–3588, 2012.

[7] Santos. A, Deen, M J, Marsal, L F., Nanotechnology, 26, 042001, 2015.

[8] Tabrizi. M. A., Ferré-Borrull, J., Marsal, L. F., Biosensors and Bioelectronics,137, 2019, 279-286.

[9] Tabrizi. M. A., Ferré-Borrull, J., Marsal, L. F., Sensors and Actuators B: Chemical 304, 127302, 2020.

## Figures

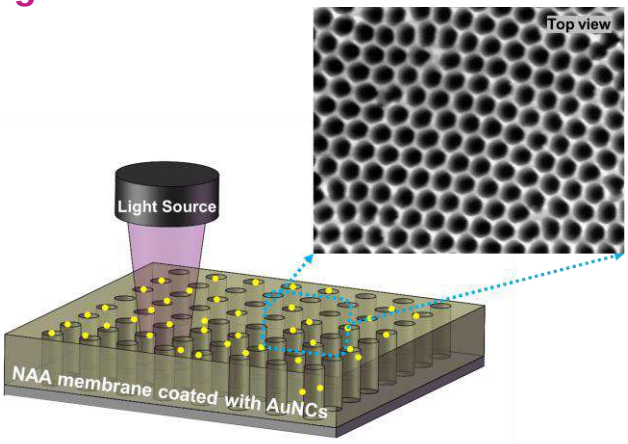


**Figure 1.** NAA surfaces with AuNCs for the selective detection of mercury.

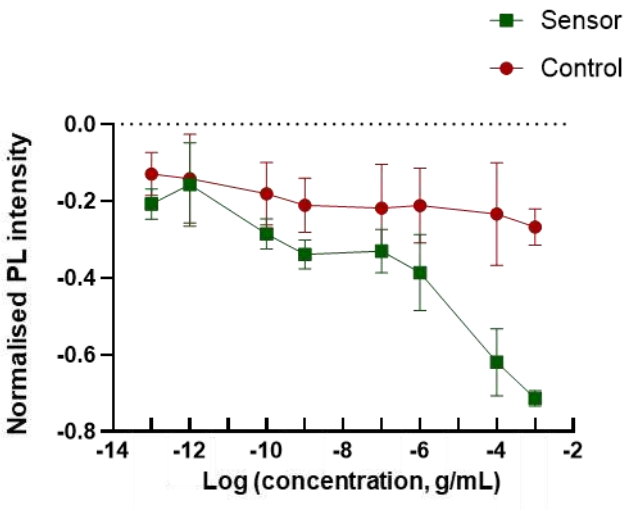


**Figure 2**: Normalized photoluminescence intensity of mercury ions (**green**) and control zinc ions (**red**) at 600nm wavelength.

# Conductive Biohybrid Skeletal Muscle Tissue

**Brenda G. Molina**[1,2,3*], Judith Fuentes[3], Carlos Alemán[1,2,3] and Samuel Sánchez [3,4]

1 Departament d'Enginyeria Química, EEBE, Universitat Politècnica de Catalunya, C/ Eduard Maristany 10-14, Ed. I2, 08019, Barcelona, Spain
2 Barcelona Research Center for Multiscale Science and Engineering, Universitat Politècnica de Catalunya, C/ Eduard Maristany 10-14, Ed. C, 08019, Barcelona, Spain
3 Institute for Bioengineering of Catalonia (IBEC), The Barcelona Institute of Science and Technology, Baldiri Reixac 10-12, 08028 Barcelona, Spain
4 Institució Catalana de Recerca i Estudis Avançats (ICREA), Passeig de Lluís Companys 23, Barcelona, 08010 Spain

*bmolina@ibecbarcelona.eu

**Abstract**

Electrical stimulation (ES) has been successfully used in medicine for several applications, among them, ES is used to influence cells proliferation, migration, differentiation and self-healing. [1-3] However, it is highly challenging to transmit electrical signals to cells in 3D structures due to its limited electrical conductivity. Therefore, to overcome this drawback it has been reported that including conductive materials in tissue engineering enhanced the electrostatic interaction between cells and the substrate, improving ES effect. [4,5]
For that reason, we present a research project where a 3D printed tissue engineering has been growth in the presence of conductive polymer nanoparticles. More specifically, poly(3,4-ethylenedioxythiophene) nanoparticles (PEDOT NPS) were incorporated into a C2C12 mouse myoblast biohybrid skeletal muscle and incubated during 14 days. After time, the PEDOT NPS effect was studied trough morphological, chemical and biocompatibility evaluation. Meanwhile, the impact of ES in C2C12 muscle tissue, with and without PEDOT NPS, was evaluated by the contraction force from the biohybrid muscle stimulated with 10, 15 or 20 V. Results suggest that the incorporation of conductive nanoparticles did not affects C2C12 cells viability, while the contraction force increase between 23-48%, in comparison to the non-conductive system, leading to more efficient and stronger Biohybrid Skeletal Muscle Tissue, which are a fundamental element in Biohybrid Robotic Systems.

**Keywords:** 3D Bioprinting, conductive polymer, C2C12 mouse myoblast, skeletal muscle electrostimulation, …

## References

[1] Park, H.; Bhalla, R.; Saigal, R.; Radisic, M.; Watson, N.; Langer, R. and Vunjak-Novak, G. Tissue Eng Regen Med, 2, 2008; 279–28.
[2] Akiyama, Y.; Nakayama, A.; Nakano, S.; Amiya, R. and Hirose, J. Cyborg and Bionic Systems 2021, Article ID 9820505, 12 p.
[3] Lin, JW., Huang, YM., Chen, YQ. et al. Cell Death Discov. 7, 2021; 35
[4] Kim, D.; Shin, M.; Choi, J-J. and Choi, J-W. *ACS Sens.* 7, **2022**, 740−747.
[5] Wang, Y.; Wang, Q.; Luo, S.; Chen, Z.; Zheng, X.; Kankala, R. K.; Chen, A. and Wang, S. *Regenerative Biomaterials* **2021**, 1–11.

## Figures

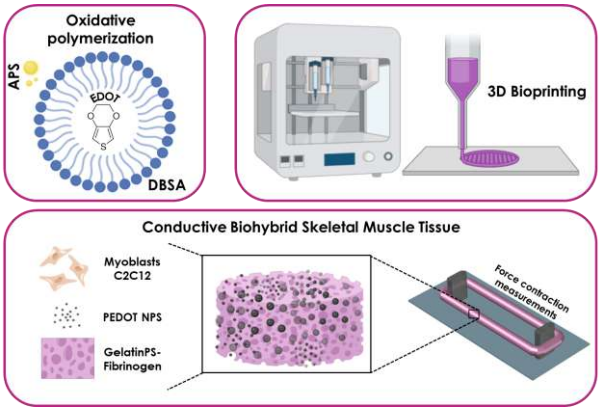


**Figure 1.** Schematic rout of the Conductive Biohybrid Skeletal Muscle Tissue synthesis.

# Effect of temperature, vacuum, and process duration on the freeze-dry of PEGylated Solid Lipid Nanoparticles

**David A. Narváez-Narváez**[1], Ronny Vargas[1], Anna Nardi-Ricart[1], Encarna Garcia-Montoya[1], Pilar Pérez-Lozano[1], Josep M. Suñé-Negre[1], Cristina Hernández-Munain[2], Carlos Suñé[2], Marc Suñé-Pou[1]

[1]University of Barcelona, Avda. Joan XXIII, 27-31, 08028 Barcelona, Spain
[2]Institute of Parasitology and Biomedicine "López Neyra" (IPBLN-CSIC), PTS, 18016 Granada, Spain

dnarvana20@alumnes.ub.edu

## Introduction

In the last three decades, the development of several nanostructures with the potential to provide controlled drug release and targeted delivery of active agents has gained great interest. Thus, the use of nanoparticles (NPs) has become a promising tool to establish new therapeutic routes for clinical use, such as gene and RNA therapies.

One of the types of nanoparticles that has become more important in recent years are Solid Lipid Nanoparticles (SLN), thus being one of the most promising mechanisms for gene therapy. Cationic solid-lipid nanoparticles (cSLNs) are biodegradable and biocompatible non-viral lipid-based nanoparticles with a positive surface charge, capable of forming SLN complexes with DNA/RNA.

However, complex, and difficult-to-scale manufacturing processes, high cost, and low transfection efficiency, compared to viral vectors, continue to hamper the widespread use of nanotechnology for clinical purposes in humans, and greater efforts are needed to improve these issues.

In this sense, one of the great challenges in the field is to achieve adequate colloidal stability of nanoparticles (NPs) over time. To achieve this goal, the freeze-drying process is the main technique used, since NP-based formulations are currently available in liquid suspensions and require very cold temperatures to prevent particle aggregation and/or fusion (COVID-19 vaccines), which limits its transportation and storage [1].

Nonetheless, both processes, the complexity of the lyophilization and the development of NPs, are highly challenging, due to the lack of universal rules and the low colloidal stability that NPs have. In addition, the lyophilization cycle (freezing, primary drying, and secondary drying) generates stressful conditions for NPs, especially the freezing step, which drastically affects their physicochemical properties, such as particle size and polydispersity index.

It is essential to establish the correct parameters, such as temperature, vacuum, and process duration to achieve good lyophilization results to avoid nanoparticle aggregation [2]. Therefore, this study seeks to evaluate the effect of the parameters mentioned above on two different PEGylated cSLNs based on cholesteryl-oleate matrix core, which have demonstrated their efficacy and safety *in vitro* [3] and thus develop an optimal, reproducible, and successful freeze-drying process.

In this poster, the impact of the lyophilization process on the physicochemical characteristics of two different formulations incorporating different types of PEG excipients will be presented and compared.

## Materials and methods

**PEG-cSLNs production**
The following materials were used to synthesize the nanoparticles: poloxamer 188, octadecylamine, stearic acid, cholesteryl oleate, ultrapure water, and two different PEGylated excipients (Myrj 52 and Myrj Tefose 1500). PEG-SLNs were prepared using an oil-in-water emulsion technique based on the hot microemulsification method.

**Freeze-drying of PEG-cSLNs**
The glass transition temperature (Tg) was determined by Differential Scanning Calorimetry (DSC) before lyophilizing the PEG-cSLNs to establish the appropriate parameters for the process. The SLNs were freeze-dried using a trehalose solution (5%, w/v) as a cryoprotectant, and were performed in a pilot LyoLab C85 20 (Coolvacuum, Barcelona, SPAIN) freeze-drying system.

We performed two main experiments involving temperature (ºC), vacuum (mbar), and process duration (hours). The first corresponds to three different assays modifying temperature and duration in the primary drying (ramps) with a previous fast and constant freezing step. In the second, we tested different vacuum values also in the primary drying with the best conditions previously obtained, thus the correct parameters for a quality freeze-drying process can be established.

**Physicochemical characterization of PEG-cSLNs**
The physicochemical properties of both suspended nanoparticles in aqueous medium and freeze-dried SLNs reconstituted with 4 ml of MiliQ Water were

analyzed. Particle size (PSD) and polydispersity index (PdI) were determined by dynamic light scattering on a Zetasizer Nano ZS90 (Malvern Instruments, UK). The surface charge (zeta-potential) of all formulations was measured by laser Doppler microelectrophoresis using a Zetasizer Nano-Z (Malvern Instruments, UK).

**Table 1.** Polydispersity index (PdI), particle size (Size), zeta potential (ZP), and size difference (Diff. S) between the suspended (S) SLNs vs. unfiltered (UF) and filtered (F) SLNs of PEG Tefose 1500.

| PEG | Vacuum (mbar) | SLNs | PdI | Size (nm) | ZP (mV) | Diff. S vs. UF/F |
|---|---|---|---|---|---|---|
| Tefose 1500 | 0,3 | S | 0,184 | 196,4 | 34 | |
| | | UF | 0,321 | 203,3 | NA | 6,9 |
| | | F | 0,217 | 196,4 | 44,8 | 0 |

## Results and Discussion

The results showed that the optimization and standardization of the freeze-drying process are crucial to avoid irreversible SLNs aggregation, due to the unavoidable stress produced in the freeze-drying cycle. The adjustment of the several parameters that the process has, is very important to protect the nanoparticles from both the low temperatures and the extreme vacuum that is required for the lyophilization to take place (Table 1).

It is well known that the most aggressive step in the process is freezing due to the formation of ice crystals that exert mechanical stress on the molecules. To avoid crystal formation, we performed a quick freezing in the three temperature ramps carried out with the two PEG-cSLNs.

Thus, the implementation of temperature ramps in the primary drying, which is the most transcendental step in the freeze-drying process, contributes to avoid the nanoparticle agglomeration and therefore the increase in particle size (Figure 1). It is important to know the glass transition temperature (Tg) of the samples since it is recommended that the temperature established in the primary drying be below Tg.

The parameters (temperature and process duration) of the temperature ramp # 3 resulted in being the most suitable procedure to lyophilize the SLNs, indicating a minimum increase in particle size, which means that the agglomeration of nanoparticles was low. This ramp with a vacuum of 0,3 mbar proved to be the best freeze-drying cycle to maintain the physicochemical properties of the SLNs similar to those in suspension (Figure 2).

However, in all assays, the reconstituted freeze-dried SLNs were filtered through 43–48 µm filter papers to remove all agglomerates found in the resuspension medium. This implies that the lyophilization process is not yet fully standardized, so other changes to the procedure will be tested to achieve optimal freeze-drying.

## Conclusions

It was not possible to correctly resuspend the lyophilized nanoparticles, and both PEG formulations had to be filtered to remove any agglomerates that might exist. Nevertheless, a freeze-drying cycle was established that turned out to be effective in obtaining resuspended SLNs with acceptable physicochemical characteristics. This indicates that the optimization of the lyophilization process is not yet fully standardized, so it is necessary to carry out tests involving a reduction in freezing time, to test different types of cryoprotectants and/or lyoprotectants, as well as different concentrations, and if necessary, carry out tests to evaluate different concentrations of the surfactant used in the formulations.

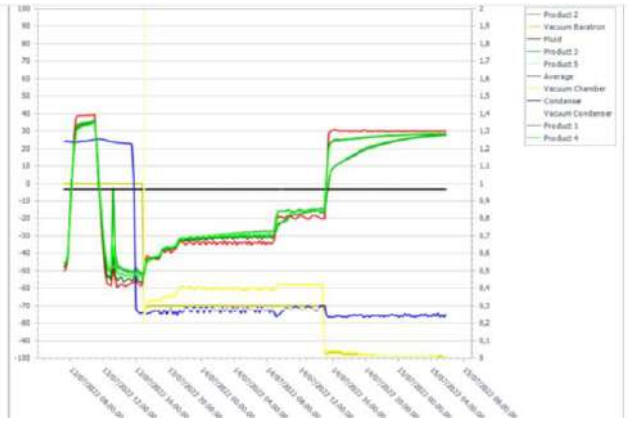

**Figure 1.** Freeze-drying graph of ramp # 3. Product 3 and Product 2 correspond to both PEGs: Myrj 52 and PEG Tefose 1500 respectively. Freezing (-55 ºC, 2 h), Primary drying (-45 ºC, 2 h; -40 ºC, 2 h; -35 ºC, 2 h; -30 ºC, 12 h; -15 ºC, 8 h), vacuum (0,3 mbar), Secondary drying (25 ºC, 16 h).

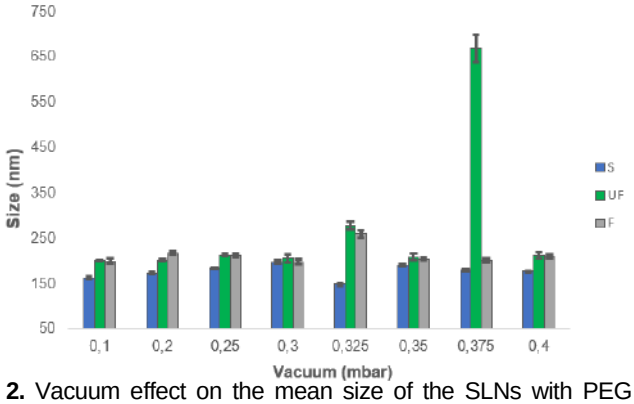


**Figure 2.** Vacuum effect on the mean size of the SLNs with PEG Tefose 1500 at different pressures. The blue bars indicate SLNs suspended in water; the green bars indicate SLNs unfiltered; the grey bars indicate SLNs filtered.

## References

[1] Luo WC, O'Reilly Beringhs A, Kim R, Zhang W, P, et al. Eur J Pharm Biopharm. 2021;169:256–67.
[2] Trenkenschuh E, Savšek U, Friess W. Int J Pharm. 2021;606:120929.
[3] Suñé-Pou M, Limeres MJ, Nofrerias I, Nardi-Ricart A, et al. Colloids Surfaces B Biointerfaces. 2019;180:159–67.

# Quantum Mechanical Model for Long-Range Electron Transport in Solid-State Protein Junctions

**Eszter Papp**[1], Gábor Vattay[1], Carlos Romero-Muñiz[2], Linda A. Zotti[3], Jerry A. Fereiro[4], Mordechai Sheves[5], David Cahen[5]

[1]Department of Physics of Complex Systems, Eötvös Loránd University, H-1053 Budapest, Egyetem tér 1-3., Hungary
[2]Departamento de Física Aplicada I, Universidad de Sevilla, E-41012 Seville, Spain
[3]Departamento de Física Teórica de la Materia Condensada and IFIMAC, Universidad Autónoma de Madrid, E-28049 Madrid, Spain
[4]School of Chemistry, Indian Institute of Science Education and Research Thiruvananthapuram, Thiruvananthapuram- 695551 Kerala, India
[5]Department of Molecular Chemistry and Materials Science, Weizmann Institute of Science, 76100 Rehovot, Israel

eszter.papp@ttk.elte.hu

Solid-state electronic junctions of biological macromolecules – from DNA to functionally more diverse proteins – have become of increasing interest given several truly astonishing properties, such as efficient transport of electrons over longer than expected distances[1]. That transport often shows no significant or minimal change when the junctions are cooled to 10 Kelvin or even lower[2].

The potential to incorporate proteins as active elements in electronic devices has thus prompted numerous experimental and theoretical studies to understand the current flow through proteins in solid-state junctions and how to control it. With the rising interest came the awareness that the theoretical description of the electron transport mechanism through these junctions is very challenging because different conductance regimes have been observed depending on the experimental conditions. This situation led to an ongoing debate, highlighting the lack of well-tested theoretical models capable of describing all the different behaviors these systems show.

According to our model[3], for junctions based on ultra-thin films of two types of electron transfer proteins, the conductance at sufficiently low temperatures is no longer dominated by electrons activated from the HOMO to LUMO orbitals. Instead, electrons from the electrode can tunnel into spatially close, localized states of the protein and then, within the protein, descend – in energy – to low-lying states, such as the LUMO and LUMO+1. Electrons escaping from LUMO+1 modulate the conductance with a temperature-dependent contribution with an Arrhenius-like factor.

We could extract the corresponding activation energies and, using advanced DFT calculations[4,5], get the relevant energy differences that match the activation energies well, implying the mechanism's validity.

While our Landauer-based model reproduces the experimental temperature-current results, it is more important and convincing that it explains, for the first time, the empirical observation of how just one of the contacts defines the behavior of the complete junction.

## References

[1] Bostick, Christopher D., et al. "Protein bioelectronics: A review of what we do and do not know." *Reports on Progress in Physics* 81.2 (2018): 026601.

[2] Kayser, Ben, et al. "Solid-state electron transport via the protein azurin is temperature-independent down to 4 K." *The journal of physical chemistry letters* 11.1 (2019): 144-151.

[3] Papp, Eszter, et al. "A Landauer Formula for Bioelectronic Applications." *Biomolecules* 9.10 (2019): 599.

[4] Romero-Muniz, Carlos, et al. "Ab initio electronic structure calculations of entire blue copper azurins." *Physical Chemistry Chemical Physics* 20.48 (2018): 30392-30402.

[5] Romero-Muñiz, Carlos, et al. "Mechanical deformation and electronic structure of a blue copper azurin in a solid-state junction." *Biomolecules* 9.9 (2019): 506.

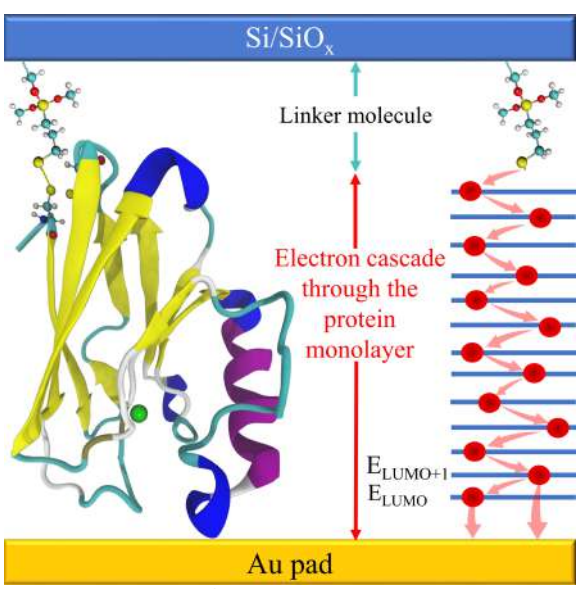


**Figure 1.** Illustration of the solid-state protein junction and the proposed mechanism.

# Investigating high entropy nanoparticles as signal transducers in point-of-care lateral flow immunoassays

**Thuong Phan Xuan**[1],
Ben Breitung[2]
Lea Ann Dailey[1]

[1]Department of Pharmaceutical Technology and Biopharmacy, University of Vienna, Austria
[2]Institute of Nanotechnology, Karlsruhe Institute of Technology (KIT), Germany

phanxuant90@univie.ac.at

## Abstract

Lateral flow immunoassay is by far one of the most successful analytical platforms applied in point-of-care diagnostic test due to it simplicity, rapidity and cost effectiveness. It should be noticed that the treatment outcome can be significantly improved if the time of diagnosis is reduced.

In 2007, $Fe_3O_4$ nanoparticles were reported to possess peroxidase-like activity.[1] Later, a point-of-care test based on $Fe_3O_4$ nanoparticles was developed for rapid detection of Ebola virus.[2] It was also demonstrated that replacing $Fe^{2+}$ ion by other ions ($Co^{2+}$, $Mn^{2+}$, $Ni^{2+}$, $Zn^{2+}$, $Mg^{2+}$, $Cu^{2+}$)[3,4] allowed a tailored peroxidase-like activity or even offered a new enzyme-mimicking activity, e.g. catalase.

High entropy nanoparticles are defined as materials containing 5 or more metal cations with a maximized configurational entropy and have been extendedly studied as catalysts in energy-related areas. However, there is limited report of their utility in biomedical sciences.

In our research, several high entropy oxide nanoparticles were prepared by ball milling and their peroxidase-like activity was determined. It turned out that the samples did possess enzyme-like activity and some of them showed a higher activity, compared to reference $Fe_3O_4$ nanoparticles. Their catalytic activity depends on different metal compositions distributed in A sites and B sites of spinel structure. The materials displayed a better thermostability than native horseradish peroxidase. Furthermore, selective materials were bioconjugated with rabbit IgG antibody. The result showed that the conjugation step was successfully done and the conjugates preserved their activity in nELISA assay. This may suggest the potential of high entropy nanoparticles for lateral flow assay.

## Figures

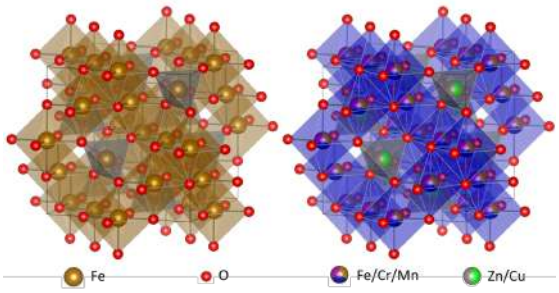


**Figure 1.** Crystal structure of $Fe_3O_4$ nanoparticles and high entropy oxide nanoparticles $(ZnCu)(FeCrMn)_2O_4$

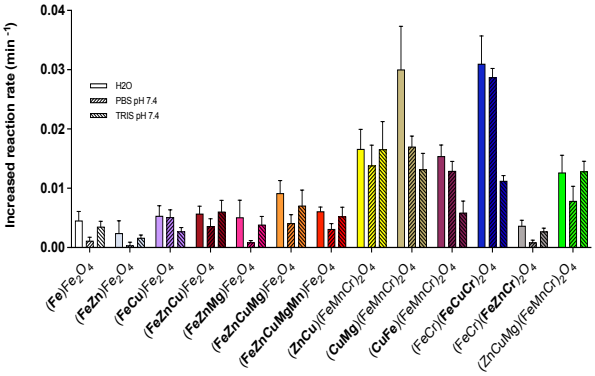


**Figure 2.** Catalytic activity towards TMB/$H_2O_2$ in different mediums

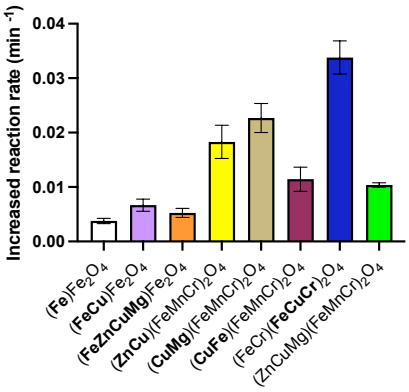


**Figure 3.** Catalytic activity of IgG conjugates in nELISA format

## References

[1] Gao, L. et al. Intrinsic peroxidase-like activity of ferromagnetic nanoparticles. Nat Nanotechnol **2**, 577–583 (2007).
[2] Duan, D. et al. Nanozyme-strip for rapid local diagnosis of Ebola. Biosens Bioelectron **74**, 134–141 (2015).
[3] Vetr, F., Moradi-Shoeili, Z. & Özkar, S. Oxidation of o-phenylenediamine to 2,3-

diaminophenazine in the presence of cubic ferrites MFe2O4 (M = Mn, Co, Ni, Zn) and the application in colorimetric detection of H2O2. Appl Organomet Chem **32**, (2018).

[4] Su, L. et al. The peroxidase/catalase-like activities of MFe2O4 (M=Mg, Ni, Cu) MNPs and their application in colorimetric biosensing of glucose. Biosens Bioelectron **63**, 384–391 (2015).

# Investigating plasma protein adsorption for 5-fluorouracil-encapsulating liposomes

**Amărandi Roxana-Maria**[1], Marin Luminița[2], Drăgoi Brîndușa[1]

[1]TRANSCEND Research Center, Regional Institute of Oncology Iași, Str. General Henri Mathias Berthelot 2-4, Iași, Romania
[2]"Petru Poni" Institute of Macromolecular Chemistry of Romanian Academy, Aleea Grigore Ghica Voda, nr. 41A, Iași, Romania

rpomohaci@iroiasi.ro

5-Fluorouracil (5-FU) is one of the most prescribed small molecule drugs for the treatment of several tumors, including colorectal, breast, liver and pancreatic cancer [1]. However, it has a short half-life (<30 min), and its administration is usually recommended in high doses over long periods of time, which can lead to severe systemic side effects induced by its cardiac, neural, gastrointestinal and hematological toxicities. While numerous approaches have been proposed to minimize the side effects of 5-FU treatment, nanotechnological drug delivery systems have shown the most promising results in improving 5-FU's therapeutic index, although encapsulation efficiencies are low and rapid leakage is known to occur [2].
Liposomes possess several advantages as drug delivery vehicles, including prolonged circulation kinetics, passive targeting properties, as well as the possibility to encapsulate both hydrophobic and hydrophilic drugs [3]. The stability and fate of liposomes in biological environments are affected by a wide variety of factors, including lipid composition, size, surface charge, as well as the nature of their biomolecular partners, which can ultimately influence therapeutic efficiency. As with any nanostructure, upon entering a biological environment, liposomes are surrounded by a dynamic biomolecular coating of proteins, known as protein corona, which evolves over time and controls particle fate and transport properties [4] (Figure 1). As recent studies emphasize that lipid composition is one of the most influencing factors of protein corona formation on the liposomal surface [5,6], the aim of the present study is to investigate the protein adsorption behavior of 5-FU-encapsulating liposomes with various compositions. The ultimate goal of our ongoing investigation is to define an optimal 5-FU-encapsulating liposomal formulation with a rationally controlled protein adsorption pattern which ensures increased liposome circulation time and reduced *in vivo* immune recognition.

## Experimental

*Liposome preparation*

Liposomes were generated through thin-film hydration (TFH) [7], followed by sonication and extrusion, with 5-FU loading by passive encapsulation. The lipids used in this investigation were Egg PC, DPPC and DSPC, either monocomponent or containing 40 mol% cholesterol.

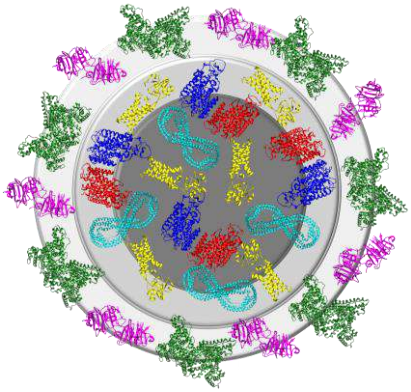

**Figure 1.** General structure of a liposomal protein corona. Liposome is colored in dark grey, hard protein corona with proteins with high affinity for the liposomal surface is colored medium grey, and soft protein corona with proteins with low affinity for the liposomal surface is colored light grey. Different proteins are shown as ribbon representations.

In brief, lipids were dissolved in chloroform, which was evaporated under reduced pressure. Lipid films were kept under vacuum and the system was flushed with $N_2$ to remove traces of organic solvent. Dry lipid films were hydrated with 10 mM PBS (pH 7.4) or 10 mM 5-FU in 10 mM PBS (pH 7.4). The final lipid concentration in the hydration solution was 7.5 mM. Liposomal suspensions were sonicated for 15 min at 26 kHz and extruded 11 times through 200 nm pore size polycarbonate membranes using a Mini-Extruder (Avanti), at a temperature greater than the phase transition temperature of the used lipid. Unentrapped drug was removed by dialysis at 4°C in 125 volumes of 10 mM PBS using a 12-14 kDa molecular weight cutoff dialysis membrane. All prepared formulations were stored at 4°C.

*Vesicle characterization*

Liposome size was measured through dynamic light scattering (DLS) using an Amerigo instrument (Cordouan Technologies). Zeta potential was measured using the same instrument through Laser Doppler Electrophoresis (LDE).
5-FU concentration was determined at 266 nm, on a Shimadzu UV 1900i UV-Vis spectrophotometer, using a standard curve which was linear in the 0.83-100 μM 5-FU range ($R^2$=0.9996). Encapsulation efficiencies (EE %) were calculated after removal of unencapsulated drug, while drug intravesicular concentrations were approximated assuming no lipid loss, with liposomes being regarded as spherical and monodisperse, with a mean bilayer thickness of 4.47 nm for monocomponent liposomes and 4.8 nm for cholesterol-containing formulations [8]. Mean cross sectional areas considered for the used lipids were 0.64 $nm^2$ for DPPC, 0.671 $nm^2$ for DSPC and 0.27 $nm^2$ for cholesterol [9]. Drug release behavior of liposomal formulations was investigated through dialysis at 37°C under continuous stirring.

*Plasma protein adsorption*

Liposomes were incubated with rat plasma for 1 h at 37°C in a 3:1 ratio (v/v) under continuous stirring. The liposome-protein corona complexes were recovered after centrifugation for 10 min at 10,000 x g at 4°C and then washed three times with cold 10 mM PBS in order to remove unbound or loosely bound proteins (soft protein corona). The adsorbed proteins (hard protein corona) were separated by one-dimensional SDS-PAGE and stained with Coomassie Brilliant Blue.

## Results

*Characterization of liposomal formulations*

Mean vesicle diameters were in the expected range for all generated liposomal formulations, around 200 nm (Table 1). As expected, drug encapsulation efficiency was low for all tested liposomal formulations, the highest encapsulation efficiency being obtained for DPPC:Chol 60:40 mol% (Table 1). Estimated intravesicular concentrations of 5-FU were similar to ones observed by other groups [7].

**Table 1.** Liposomal formulation characteristics

| Formulation | Mean vesicle diameter (nm) | EE (%) | Estimated intravesicular 5-FU concentration (mM) |
|---|---|---|---|
| Egg PC | 174 | 6.58 | 14.82 |
| Egg PC:Chol 60:40 mol% | 186 | 5.97 | 16.46 |
| DPPC | 240 | 9.32 | 17.41 |
| DPPC:Chol 60:40 mol% | 205 | 10.19 | 29.59 |

*Plasma protein adsorption*

Liposome corona formation upon plasma incubation was first confirmed through DLS measurements. Thus, the mean hydrodynamic diameter of 5-FU-containing liposomes increased upon plasma incubation by at least a few nanometers, and varied greatly among formulations. At the same time, the zeta potential of plasma-incubated liposomal suspensions decreased in all cases, a phenomenon which is known to occur due to the overall negative charge of plasma proteins at physiological pH [6].

SDS-PAGE experiments confirmed both protein corona formation on the surface of all tested liposomal formulations, as well as different interaction strengths between proteins and the liposomal surface. As expected, protein adsorption patterns were influenced by liposomal composition, with both the main lipid constituent and cholesterol presence impacting protein preference for the liposomal surface. No difference was observed between formulations encapsulating 5-FU and the same formulations without drug, suggesting that protein adsorption patterns are not influenced by 5-FU presence. Most likely, the drug is completely distributed inside liposomes, leaving the external surface identical with that of homologous liposomes without 5-FU.

Following incubation, several protein bands which were not present in the supernatant could be observed for some liposomal formulations, suggesting the successful depletion of specific protein species from the plasma. In addition, several protein bands corresponding to abundant proteins in the plasma could be identified (e.g. serum albumin), suggesting that not only the type, but also protein plasma concentration plays a role in liposomal protein corona formation. Protein bands which appear only in the supernatant likely correspond to proteins which do not associate strongly with liposomes and do not contribute to hard protein corona formation.

## Conclusions

Several liposomal formulations of 5-FU were successfully prepared through TFH, followed by sonication and extrusion. Although encapsulation efficiency was low, estimated intravesicular 5-FU concentrations were in the millimolar range for all generated liposomal formulations.

The plasma protein adsorption patterns identified in our study demonstrate that lipid composition has a major impact on the preference of plasma constituents for the nanovehicle surface. Our work in this direction will be continued with the identification of the differentially adsorbed proteins through LC-MS, as well as measuring 5-FU concentration in plasma following incubation.

## Acknowledgements

This work was supported by a grant of the Romanian Ministry of Research, Innovation and Digitalization, CNCS - UEFISCDI, project number PN-III-P1-1.1-PD-2021-0786, within PNCDI III and a H2020 grant-ERA-Chair, no. 952390.

## References

[1] Longley DB, Harkin DP, Johnston PG, Nat. Rev. Cancer, 3 (2003) 330-338
[2] Petaccia M, Condello, et al., MedChemComm 6 (2015) 1639-1642
[3] Torchilin VP, Nat. Rev. Drug Discov, 4 (2005) 145-160
[4] Bozzuto G, Molinari A., Int. J. Nanomedicine, 10 (2015) 975-99
[5] Bigdeli A, Palchetti S et al., ACS Nano, 10 (2016) 3723-3737
[6] Palchetti S, Caputo D, Digiacomo L, Capriotti AL, Coppola R, Pozzi D, Caracciolo G, Pharmaceutics, 11 (2019) 31
[7] da Costa CAM, Moraes AM, Acta Scientiarum. Technology, 25 (2003) 53-61
[8] Gallová J, Uhríková D et al., Eur. Biophys. J., 40 (2011) 153-163
[9] Armstrong CL, Marquardt D et al., PLoS One, 8 (2013) e66162

# Functionalized and targeted nanoformulations: combined therapy against colorectal cancer tumor cells

**J. Prados**[1,2,3], C. Melguizo[1,2,3], A. Cepero[1,2,3], L. Gago[1,2], Y. Jabalera[4], G. Iglesias[4], R. Ortiz[1,2,3], C. Jiménez-López[4], C. Luque[1,2,3], G. Perazzoli[1,3], M. Peña[1,2,3], A. Ortigosa[1,2,3], R. Vergara[1,3], M.A Chico[1,2,3], L. Cabeza[1,3]

[1]Institute of Biopathology and Regenerative Medicine (IBIMER), Center for Biomedical Research (CIBM), University of Granada, 18100 Granada, Spain.
[2] Department of Anatomy and Embryology, Faculty of Medicine, University of Granada, 18071 Granada, Spain.
[3]Instituto Biosanitario de Granada (ibs. GRANADA), 18014 Granada, España.
[4]Department of Microbiology, Sciences School, University of Granada, Campus de Fuentenueva, 18002 Granada, Spain

jcprados@ugr.es

**Introduction.** Oxaliplatin (OXA) is one of the most widely used chemotherapy drugs, both alone and in combination [1], for the treatment of colorectal cancer (CRC). However, OXA induces many side effects, such as peripheral neuropathy [2]. Therefore, it is necessary to develop new strategies that allow greater targeting of treatments. In this context, CRC cancer stem cells (CSCs) may show high expression of LGR5 which has been related to the initiation of tumor growth, the resistance to chemotherapy and radiotherapy, and aggressiveness [3]. The synthesis of nanoformulations to selectively target CSCs or CRC cells through specific markers constitutes a new research field with a promising future [4]. Specifically, magnetoliposomes (MLPs) are a type of nanocarrier with multiple properties, such as controlled release of antitumor agents, active targeting by monoclonal antibody binding, and high bioavailability. Our objetive was to analyse in vitro effect of OXA-loaded MLPs directed against LGR5 (MLPs-OXA-LGR5).

**Methods.** OXA-loaded MLPs directed against LGR5 (MLPs-OXA-LGR5) were generated and characterizated. Protein expression of the LGR5 was analyzed by western blot in CRC cell lines. CCR CSCs were generated and their markers analyzed by q-PCR. Cytotoxicity experiments were performed using the sulforhodamine B assay. All methods were carried out following our own experience [5].

**Results and conclusion.** The MLP-OXA-LGR5 nanoformulations showed high stability and could be tested in vitro using different CRC cell cultures. Analysis of LGR5 in T-84 and MC38 CRC cell lines showed high expression. CRC CSCs, classically associated with chemoresistance, showed controversial results. Specifically, MLP-OXA-LGR5 showed a greater cytotoxic effect than the OXA-free drug in T84 and MC38 CRC cell lines. The control (empty MLP) showed no effect on cell culture. MLP-OXA-LGR5 may be a promising strategy to selectively eliminate LGR5+ cells from CRC. Further in vitro and in vivo studies are needed to validate the selective antitumor effect.

## References

[1] Kibudde S, Begg W. Pan Afr Med J. 2022 Jun 22;42:141. doi: 10.11604/pamj.2022.42.141.31234. eCollection 2022.

[2] Prutianu I, Alexa-Stratulat T, Cristea EO, Nicolau A, Moisuc DC, Covrig AA, Ivanov K, Croitoru AE, Miron MI, Dinu MI, Ivanov AV, Marinca MV, Radu I, Gafton B. World J Clin Cases. 2022 Apr 6;10(10):3101-3112. doi: 10.12998/wjcc.v10.i10.3101.

[3] Descarpentrie J, Araúzo-Bravo MJ, He Z, François A, González Á, Garcia-Gallastegi P, Badiola I, Evrard S, Pernot S, Creemers JWM, Khatib AM. Cancers (Basel). 2022 Feb 25;14(5):1195. doi: 10.3390/cancers14051195.

[4] Ortíz R, Quiñonero F, García-Pinel B, Fuel M, Mesas C, Cabeza L, Melguizo C, Prados J. Cancers (Basel). 2021 Apr 24;13(9):2058. doi: 10.3390/cancers13092058.

[5] Garcia-Pinel B, Jabalera Y, Ortiz R, Cabeza L, Jimenez-Lopez C, Melguizo C, Prados J. Pharmaceutics. 2020 Jun 24;12(6):589. doi: 10.3390/pharmaceutics12060589.

# Complement Activation Dramatically Accelerates Blood Plasma Fouling On Antifouling Poly(2-hydroxyethyl methacrylate) Brush Surfaces

**Tomáš Riedel**[1,*]
Andres de los Santos Pereira[1]
Johanka Táborská[1]
Zuzana Riedelová[1]
Ognen Pop-Georgievski[1]
Pavel Májek[2]
Klára Pečánková[2]
Cesar Rodriguez-Emmenegger[3,4]

[1]Institute of Macromolecular Chemistry Czech Academy of Sciences, Heyrovského nám. 2, Prague, Czech Republic
[2]Institute of Hematology and Blood Transfusion,U Nemocnice 1, Prague 128 00, Czech Republic
[3]Institute for Bioengineering of Catalonia (IBEC), The Barcelona Institute of Science and Technology (BIST), Carrer de Baldiri Reixac, 10, 12, 08028 Barcelona, Spain
[4]Institució Catalana de Recerca i Estudis Avançats (ICREA), Passeig Lluís Companys 23, 08010 Barcelona, Spain

riedel@imc.cas.cz

Non-specific protein adsorption (fouling) triggers a number of deleterious events in the application of biomaterials. Antifouling polymer brushes successfully suppress fouling,[1] however for some coatings an extremely high variability of fouling for different donors remains unexplained.[2] The authors report that in the case of poly(2-hydroxyethyl methacrylate) (poly(HEMA)) this variability is due to the complement system activation that causes massive acceleration in the fouling kinetics of blood plasma. Using plasma from various donors, the fouling kinetics on poly(HEMA) is analyzed and correlated with proteins identified in the deposits on the surface and with the biochemical compositions of the plasma. The presence of complement components in fouling deposits and concentrations of C3a in different plasmas indicate that the alternative complement pathway plays a significant role in the fouling on poly(HEMA) through the “tick-over” mechanism of spontaneous C3 activation. The generated C3b binds to the poly(HEMA) surface and amplifies complement activation locally (Figure 1). Heat-inactivated plasma prevents accelerated fouling kinetics, confirming the central role of complement activation. The results highlight the need to take into account the variability between individuals when assessing interactions between biomaterials and blood plasma, as well as the importance of the mechanistic insight that can be gained from protein identification.[3]

## Acknowledgement

This work was supported by the Czech Science Foundation (project no. 20-10845S).

## References

[1] C. Rodriguez Emmenegger, E. Brynda, T. Riedel, Z. Sedlakova, M. Houska, A. B. Alles, Langmuir. 25 (2009), 6328-33.
[2] A. de los Santos Pereira, C. Rodriguez-Emmenegger, F. Surman, T. Riedel, A. B. Alles, E. Brynda, RSC Advances, 4 (2014), 2318-21.
[3] T. Riedel, A. de los Santos Pereira, J. Táborská, Z. Riedelová, O. Pop-Georgievski, P. Májek, K. Pečánková, C. Rodriguez-Emmenegger, Macromol. Biosci., 22 (2022), 2100460.

## Figures

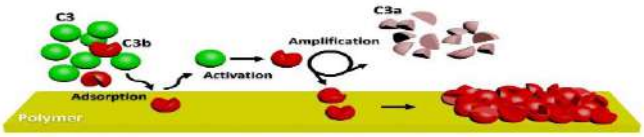


**Figure 1.** Proposed scheme of C3 activation on the poly(HEMA) surface. Spontaneously generated C3b molecules in the blood plasma adsorb on the surface and trigger the alternative complement pathway leading to a massive generation of C3b that fouls the surface.

# Synergistic effect of swarms of enzyme-powered nanomotors for enhancing the diffusion of macromolecules

**Noelia Ruiz-González**[1], Marta Guri[1], Juan C. Fraire[1,2], Tania Patiño[3], Samuel Sánchez[1,4]*

[1]*Institute for Bioengineering of Catalonia (IBEC), The Barcelona Institute of Science and Technology (BIST), Baldiri i Reixac 10-12, 08028 Barcelona, Spain*

[2]*Laboratory of General Biochemistry and Physical Pharmacy, Faculty of Pharmacy, Ghent University, Ottergemsesteenweg 460, 9000 Ghent, Belgium*

[3]*Eindhoven University of Technology, 5612 AZ Eindhoven, The Netherlands*

[4]*Institució Catalana de Recerca i Estudis Avancats (ICREA), Passeig Lluís Companys 23, 08010 Barcelona, Spain*

nruiz@ibecbarcelona.eu

In the last decades, the development of nanoparticles that can increase the efficiency of clinical treatments has been studied. The use of passive nanoparticles has been reported to have low efficacy due to the need for overcoming the biological barriers present in the human body[1] .One way of tackling this problem is by developing the so-called “active” nanoparticles[2–4] , which interact with the media and change its rheology, reducing its viscosity. These viscous media are a challenge for the field of nanomedicine as passive particles are retained and trapped in the complex network, reducing their ability to move and reach the target site[5,6]. However, the development of enzyme-powered nanomotors that can interact with these biological barriers and allow them to move within these fluids has not been well-studied yet. Actually, the study of the motion of nanomotors has been mainly performed in aqueous media. Nevertheless, most of the fluids present in our body are viscoelastic media such as synovial fluid present in the joints, mainly composed of hyaluronic acid[6]. Here, we show that the combination of enzyme-powered nanomotors based on hyaluronidase and urease enzymes in different troops can interact with the complex media, reducing the viscosity of both simulated synovial fluid and ex vivo synovial fluid from sheep. Our results show enhanced diffusion of both macromolecules and urease nanomotors when synovial fluid was previously treated with hyaluronidase nanomotors. These results pave the way for the use of nanomotors for joint injury treatment, improving therapeutic effectiveness, and achieving faster and more efficient delivery of therapeutic agents than traditional methods.

## References

[1] Narum, S. M., Le, T., Le, D. P., Lee, J. C., Donahue, N. D., Yang, W., & Wilhelm, S. (2020). Passive targeting in nanomedicine: fundamental concepts, body interactions, and clinical potential. Nanoparticles for biomedical applications (pp. 37-53). Elsevier.

[2] Walker, D., Käsdorf, B. T., Jeong, H. H., Lieleg, O., & Fischer, P. (2015). Enzymatically active biomimetic micropropellers for the penetration of mucin gels. Science Advances, 1(11), e1500501.

[3] Ma, X., Hortelão, A. C., Patino, T., & Sanchez, S. (2016). Enzyme catalysis to power micro/nanomachines. ACS nano, 10(10), 9111-9122.

[4] Hortelão, A. C., Patiño, T., Perez-Jiménez, A., Blanco, À., & Sánchez, S. (2018). Enzyme-powered nanobots enhance anticancer drug delivery. Advanced Functional Materials, 28(25), 1705086.

[5] Wilhelm, S., Tavares, A. J., Dai, Q., Ohta, S., Audet, J., Dvorak, H. F., & Chan, W. C. (2016). Analysis of nanoparticle delivery to tumours. Nature reviews materials, 1(5), 1-12.

[6] Mitchell, M. J., Billingsley, M. M., Haley, R. M., Wechsler, M. E., Peppas, N. A., & Langer, R. (2021). Engineering precision nanoparticles for drug delivery. Nature Reviews Drug Discovery, 20(2), 101-124.

# Catalase-powered nanomotors disrupt and cross an *in vitro* mucus model

**Meritxell Serra-Casablancas**[1,2], Carles Prado[1,2], Valerio Di Carlo[1], Samuel Sánchez[1,3]

[1]Institute for Bioengineering of Catalonia (IBEC), C/ Baldiri Reixac, 10-12, Barcelona, Spain
[2]University of Barcelona – Faculty of Pharmacy, Av. de Joan XXIII, 27-31, Barcelona, Spain
[3]Institució Catalana de Recerca i Estudis Avançats (ICREA), Passeig Lluís Companys, 23, Barcelona, Spain

mserra@ibecbarcelona.eu

Cancer chemotherapies used in the clinic have poor bioavailability and severe off-target effects, mainly due to their systemic administration. Drugs can be administered locally to a specific organ or area of the body to increase their concentration in the target and reduce side effects, although this approach is hampered by biological barriers such as mucus. Goblet cells, found in the intestine or lung, secrete mucus to create a protective layer that prevents microorganisms, allergens, and other particles from reaching cells and damage them [2]. However, this natural protection system acts as an obstacle to delivering localized therapy [3]. Here we show how catalase-powered nanomotors can disrupt and cross mucus secreted from cells, in the presence of hydrogen peroxide, thanks to the oxygen bubbles produced by the enzyme and to their active motion. This strategy can overcome current treatment limitations by increasing the number of particles that reach their target, thus having the potential to act as drug delivery systems.

## References

[1] J. V. Fahy and B. F. Dickey, The New England Journal of Medicine, 2010
[2] X. Murgia, et al., Advanced Drug Delivery Reviews, 2018

## Figures

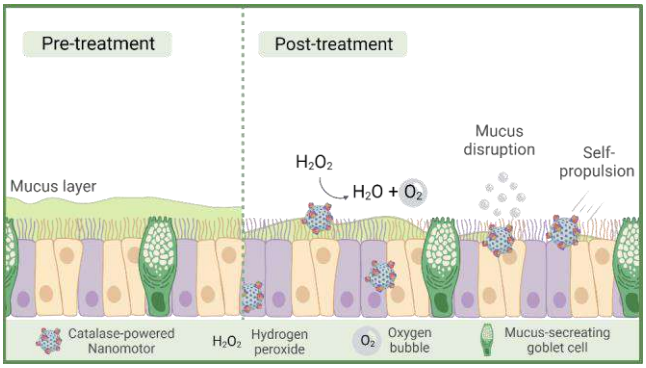


**Figure 1.** Graphical representation of the mucus disruption and crossing capacity of the catalase-powered nanomotors

# Effect of chemically modified nanodiamonds on 3D human atherosclerotic plaques model

**Rositsa Tsekovska**[1], Ralitsa Mincheva[1], Gjorgji Atanasov[1], Yordan Handzhiyski[1], Sascha Balakin[2], Alexandra Parichenko[2], Anita Stoppel[2], Natalia Beshchasna[2], Jörg Opitz[2] and Margarita D. Apostolova[1]

[1]Roumen Tsanev Institute of Molecular Biology - BAS, Acad. G. Bonchev Str., Bl. 21, 1113 Sofia, Bulgaria
[2] Fraunhofer Institute for Ceramic Technologies and Systems IKTS, Maria-Reiche Strasse 2, 01109 Dresden, Germany

rcekovska@gmail.com

Atherosclerosis is the major underlying cause of cerebrovascular and cardiovascular diseases [1]. It is considered that this disease is linked to hypercholesterolemia and the accumulation of inflammatory cells in the artery wall. Inflammation is involved in the atherosclerotic process by recruiting leucocytes, promoting plaque growth, and inducing plaque destabilization. Formation of the plaque usually continues over decades, starting with early lesions formation, which may occur in early adolescence. The disease progression depends on many factors, such as gender, genetics and some well recognized risk factors- obesity, diabetes, hypertension, smoking, aging, etc. [2]. The development of advanced atherosclerosis is a slow progressive process that starts in childhood and remains asymptomatic for many decades, with complications such as myocardial infarction, stroke, or peripheral ischemia usually occurring in later life [3]. In the last decades, stenting became an effective minimally invasive therapy for reducing coronary artery blockage and achieved great success. However, in-stent restenosis is still a clinical problem, and no effective treatment for removing atherosclerosis plaque in human vessels exists.

This study aimed to develop a new generation of unique cardiovascular stents through the innovative double-layer coating. A hybrid biodegradable nanocomposite sub-coating layer serving for anti-plaque effect with a chemical functionalized Fe@C or nanodiamonds (NDs) containing lipophilic organic groups to promote the reverse cholesterol transport.

NDs have been proposed for various biomedical applications, including bioimaging, biosensing, and drug delivery, owing to their physical-chemical properties and biocompatibility. Different surface functionalization methods have been developed, varying the ND's surface properties and rendering the possibility to attach biomolecules to interact with biological targets. The NDs used in this study were functionalized in three steps, shown in Figure 1. Following the physical-chemical characterization of arylated NDs, their cytotoxicity was analyzed in vitro as a significant concern for future clinical translation. This study used rapid, sensitive, and reproducible 2D and 3D models for nanotoxicity tests. We optimize the conditions for using the 3D atherosclerotic plaque model and analyze the toxicity in the presence of NDs. NDs were observed by laser confocal fluorescence microscopy and fluorescence lifetime imaging. Using the 3D human atherosclerotic plaque model for a safety evaluation and treatments with NDs-based nanolabel will be discussed.

Acknowledgments: This project was supported by Bulgarian Science Fund (ERA-NET-Russia Plus KP-06-DO 02/3).

## References

[1] Soufi M., Sattler A.M., Maisch B., Schaefer J.R. Herz 27 (2002) 637-648.
[2] Biros E., Karan M., Golledge J. Curr. Genomics 9 (2008) 29-42.
[3] Blanco-Colio L.M., Martin-Ventura J.L., Vivanco F., Michel J.B., Meilhac O., Egido J. Cardiovasc. Res. 72 (2006) 18-29.

## Figures

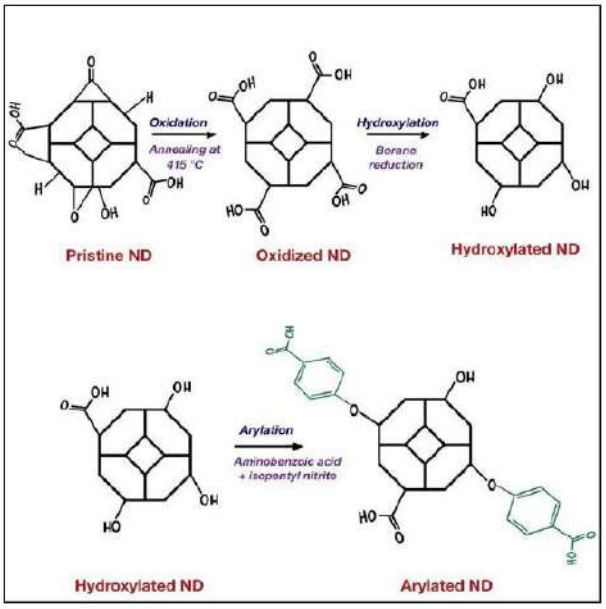


**Figure 1.** NDs surface functionalization steps. 1 - The NDs oxidation by thermal annealing at 415 ºC, 2 - Hydroxylation by using borane reduction treatment, 3 - Arylation by addition of aminobenzoic acid and isopentyl nitrite.

# Lipid nanoparticles functionalization strategies to cross the blood-brain-barrier

**Ronny Vargas**[1,2], David Narváez- Narváez[1], Cristina Moreno-Castro[3], Anna Nardi-Ricart[1], Pilar Pérez-Lozano[1], Encarna García-Montoya[1], Josep María Suñé-Negre[1], Cristina Hernández-Munain[3], Carlos Suñé[3], Marc Suñé-Pou[1]

[1]University of Barcelona, Av. de Joan XXIII, 27-31, Barcelona, Spain
[2]Universidad de Costa Rica, Ciudad Universitaria Rodrigo Facio, San José, Costa Rica
[3]Instituto de Parasitología y Biomedicina "López-Neyra" (IPBLN-CSIC), Av del Conocimiento 17, Granada, 18016, Spain

Contact@: ronny.vargas_m@ucr.ac.cr

Brain diseases are a mayor public health concern worldwide [1,2]. The blood-brain-barrier (BBB) acts as a protective shield, preventing the direct exposure of the central nervous system (CNS) to pathogens and toxic substances [1]. While keeping the homeostatic environment of the brain, the BBB also prevents delivery of therapeutic substances. Therefore, it becomes an obstacle to treat many brain diseases [3-5]. This limitation becomes more critical with the shift in therapeutics from small molecules to macromolecules [1]. On the other hand, the BBB counts with several transport mechanisms for endogenous substances to satisfy the high metabolic requirements of the brain [6]. Nanotechnology-based drug delivery strategies have become an opportunity to take advantage of those mechanisms and target the CNS without compromising the BBB structure or functionality [4,5]. The modification of lipid nanoparticles (LNP) and other nanocarriers with surface moieties such as antibodies or peptides allows the stimulation and exploitation of transport mechanisms expressed in BBB [6,7]. A systematic review was carried out to compile the functionalization strategies used in academic works, and to evaluate which studies have provided more evidence on the effectiveness of brain targeting. This is part of a research project that aims to deliver small interfering ribonucleic acid (siRNA) through the BBB, with LNP. Figure 1 shows the schematization of the bibliographic review. In the screening phase other reviews and other pharmaceutical preparations instead of LNP were excluded. Experimental designs targeting the BBB through nasal route and research articles in which the nanoparticle crossing of the BBB was not objectively assessed (either using *in vitro* or *in vivo* models), were also excluded. Figure 2 shows the therapeutic goal of each of the 79 research papers included in the review. The largest group were applications for several types of brain cancer (29 research papers). Notably, eight studies worked on applications for Alzheimer's disease and only one publication had the final objective of developing treatments for Parkinson's disease. This relatively low academic production within this subject contrasts with the general academic interest and epidemiologic prevalence of Parkinson's disease [8]. Table 1 shows the active pharmaceutical ingredients incorporated to the LNP. There were 11 research works developed for no specific disease. These studies correspond to empty LNP developed as a model for brain delivery. Furthermore, Figure 3 shows the modification strategies used to facilitate the passage through BBB. An important group of papers did not identify a functionalization strategy (25), while another five use PEG or surfactant as a functionalization strategy (compared to the rest of formulations, these five could also be consider as LNP without active targeting modification). This is consequent with some literature reporting that unmodified LNP could cross the BBB due to its size and lipophilic nature [9]. The need for further modification could rely on an enhanced effect and specific targeting inside the BBB. Among the studies that included a surface modification, the most used were antibodies (10), proteins (12) and peptides (15). Figure 4 shows the distribution of the most used peptides. Finally, the evaluation strategies applied to determinate BBB crossing are classified in Table 2. The approach to incorporating controls among studies was not the same, specifically with respect to the inclusion of loaded/empty and functionalized/unfunctionalized combinations. Some authors did not include any comparisons in the study. Considering that the BBB crossing has been demonstrated without the need for any modification, the inclusion of controls is crucial to objectively determine the success of a given strategy. Despite the differences on evaluation strategies, composition and physical properties among the reviewed articles, the systematic review allowed us to identify:

- Therapeutic fields that represent research opportunities for brain delivery.
- The diversity of functionalization strategies and the predominance of peptide-based modification.
- Methodological practices that could provide greater robustness to experimental designs on the delivery of LNP through BBB.

This compilation of scientific literature in the field is an important input for research projects on LNP delivery across the BBB, and consequently, a contribution to the chain of development that would bring therapeutic solutions for brain diseases.

## References


[1] M. Nowak, M. E. Helgeson, and S. Mitragotri, Adv. Ther., vol. 3, no. 1, p. 1900073, 2020,

[2] T. D. Brown, N. Habibi, D. Wu, J. Lahann, and S. Mitragotri, ACS Biomater. Sci. Eng., vol. 6, no. 9, pp. 4916–4928, 2020,

[3] G. Tosi, J. T. Duskey, and J. Kreuter, Expert Opin. Drug Deliv., vol. 17, no. 1, pp. 23–32, 2019,

[4] S. Ding et al., Mater. Today, vol. 37, no. August, pp. 112–125, 2020,

[5] M. Á. Elena Ortega, Santos Blanco, Adolfina Ruiz and S. P. and M. E. M. Peinado, 2020.

[6] G. Z. Jin, A. Chakraborty, J. H. Lee, J. C. Knowles, and H. W. Kim, J. Tissue Eng., vol. 11, 2020,

[7] J. J. Mulvihill, E. M. Cunnane, A. M. Ross, J. T. Duskey, G. Tosi, and A. M. Grabrucker, Nanomedicine, vol. 15, no. 2, pp. 205–214, 2020,

[8] M. J. Armstrong and M. S. Okun, JAMA, vol. 323, no. 6, pp. 548–560, Feb. 2020,

[9] I. Singh, R. Swami, D. Pooja, M. K. Jeengar, W. Khan, and R. Sistla, J. Drug Target., vol. 24, no. 3, pp. 212–223, Mar. 2016,


## Figures & Tables

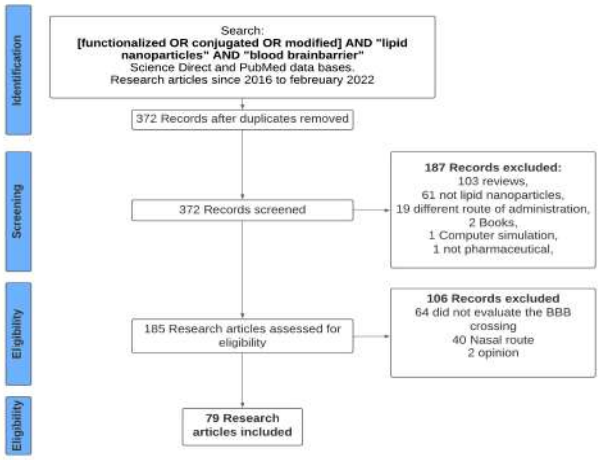


**Figure 1.** Flow diagram of the systematic review.

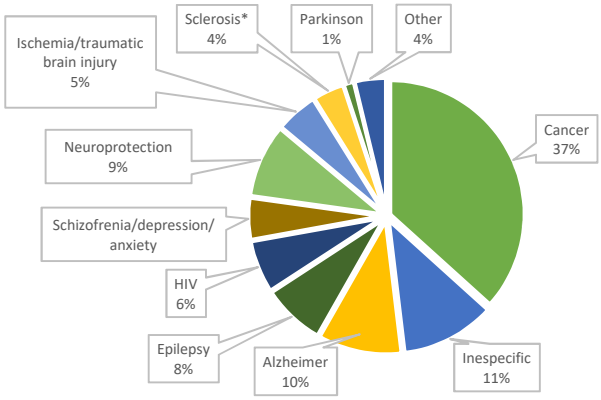


**Figure 2.** Therapeutic objective of the research articles included in the review. *Note: includes multiple and amyotrophic lateral sclerosis.

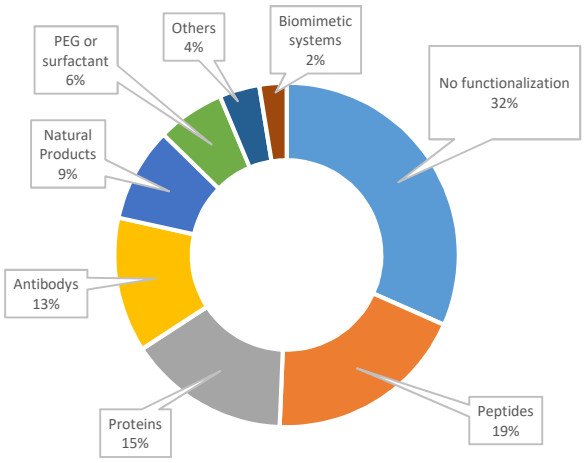


**Figure 3.** Lipid nanoparticle modification strategies to cross the blood-brain-barrier.

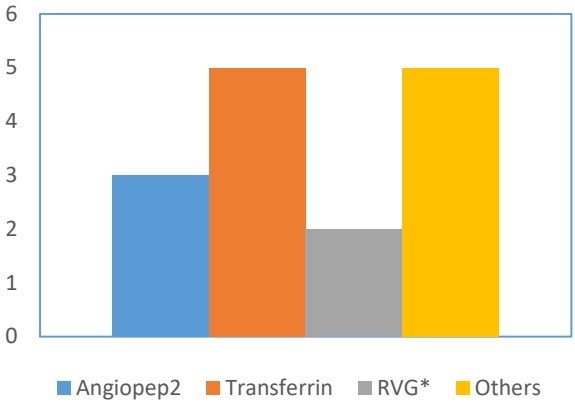


**Figure 4.** Peptide-based functionalization strategies to cross the BBB. *Note: rabies virus glycoprotein.

**Table 1.** Active pharmaceutical ingredients most commonly delivered for the therapeutic objectives described in Figure 2.

| Drug | Number of papers[1] |
|---|---|
| Curcumin | 7 |
| Docetaxel, Resveratrol | 5 |
| Doxurrubicin, Etoposide | 4 |
| Quercitine | 3 |
| Dimetil fumarate, Nevirapine, Placitaxel | 2 |

Note: 1- There are 34 more drugs appear in 34 different papers.

**Table 2.** Evaluation strategies for BBB crossing.

| Type of study | Number of papers |
|---|---|
| *In vitro* studies | 34 |
| *In vivo* studies | 35 |
| *In vivo + in vitro* studies | 10 |

# Towards hemocompatible surfaces: Interactive coating directs blood to fight against thrombi

**Lena Witzdam**[1,2,3], Fabian Obstals[2,3], Manuela Garay-Sarmiento[2,4], Jonas Quandt[2,3], Nina Yu. Kostina[1], Oliver Grottke[5], Cesar Rodriguez-Emmenegger*[1,2,6]

[1] Institute for Bioengineering of Catalonia (IBEC), Barcelona, Spain
[2] DWI – Leibniz Institute for Interactive Materials e.V., Aachen, Germany
[3] Institute of Technical and Macromolecular Chemistry, RWTH Aachen University, Aachen, Germany
[4] Chair of Biotechnology, RWTH Aachen University, Aachen, Germany
[5] Department of Anesthesiology, University Hospital of the RWTH Aachen University, Aachen, Germany
[6] Institució Catalana de Recerca i Estudis Avançats (ICREA), Barcelona, Spain
lwitzdam@ibecbarcelona.eu

The contact of blood with the artificial surface of medical devices inevitably causes the activation of coagulation leading to a number of serious complications. In nature, the lining of healthy endothelium is capable of sensing and maintaining a tightly regulated equilibrium, called hemostasis that prevents hemorrhages and excessive coagulation. In this work, we developed a coating system that mimics the fundamental hemostatic regulation exerted by endothelium. In its dormant state the coating is stealth to blood components and prevents activation of coagulation. However, the presence of a clot turn the coating into an active state in which it directs blood to digest the clot. The coating consists of ultra-low fouling poly(N-hydroxypropyl methacrylamide-co-carboxybetaine methacrylamide) brushes on which tissue plasminogen activator (tPA) is immobilized. We exploited the allosteric activation of tPA by fibrin clot as a positive feedback mechanism to reversibly switch the coating into its active state/dormant state, that coupled with an amplification mechanism, transformed sufficient amount of endogenous plasminogen into plasmin to locally digest fibrin clots. Impressively, the amplification mechanism allowed that only few nanograms of immobilized tPA could orchestrate the complete digestion of macroscopic clots while prohibiting the adhesion of blood components, molecules, and cells and displaying no cytotoxicity. We envision that the extremely low density of tPA required in this coating system and the safety of this approach make this strategy a promising route towards the improvement of the hemocompatibility of blood contacting medical devices.

## References

[1] F. Obstals, L. Witzdam, M. Garay-Sarmiento, N. yu. Kostina, J. Quandt, S. Singh, O. Grottke, C. Rodriguez-Emmenegger, ACS Appl. Mater. Interfaces, 13 (2021) 11696-11707.

## Figures

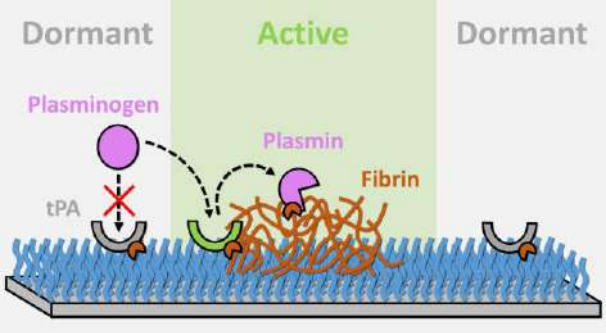


**Figure 1.** Fibrinolytic coating system developed in the present study. Polymer brushes are decorated with tPA. The coating can detect the presence of a fibrin clot by its binding to tPA. This lead to the activation of tPA and the fibrinolytic system. Afterwards tPA returns to its dormant state [1].

Edited by

PHANTOMS FOUNDATION
Alfonso Gómez 17
28037 Madrid, Spain
www.phantomsnet.net

AMERICAN ELEMENTS

THE ADVANCED MATERIALS MANUFACTURER®

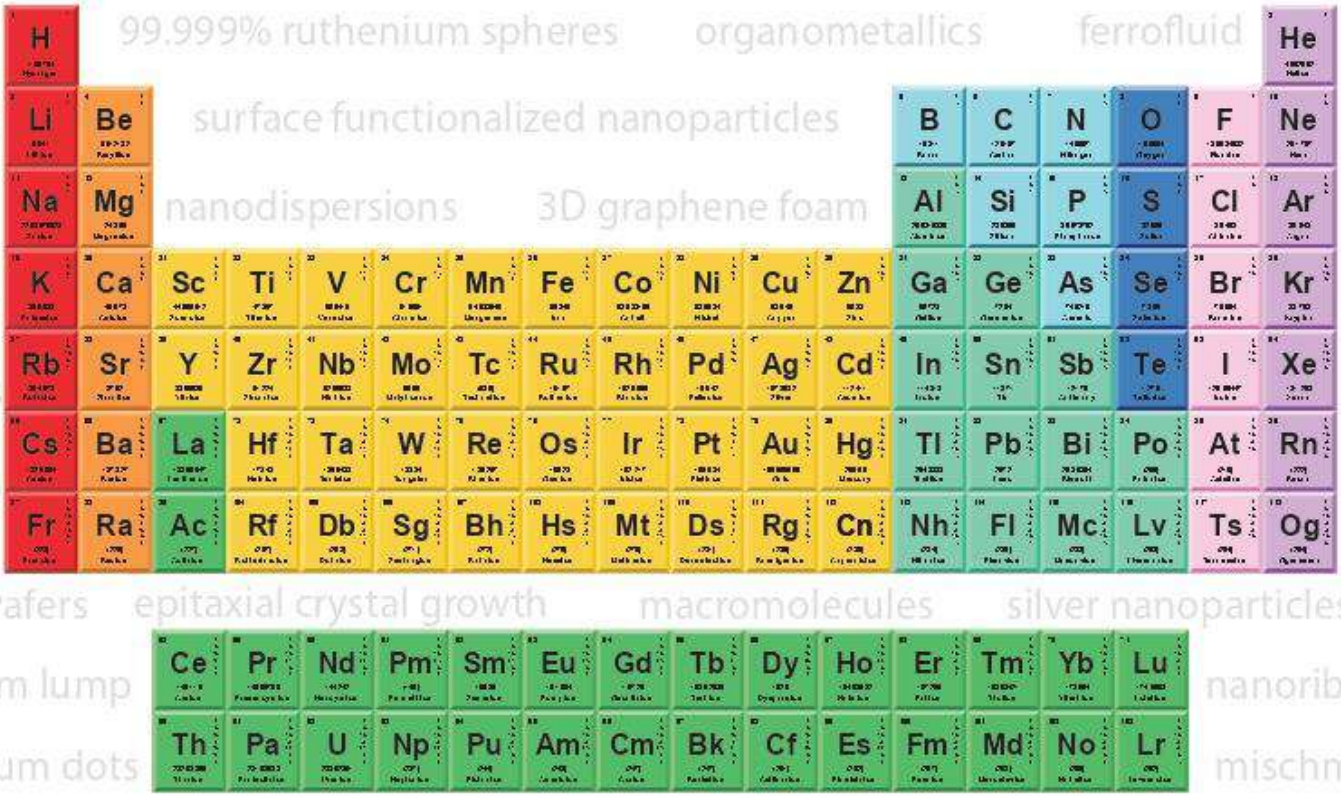


# Now Invent.™

The Next Generation of Material Science Catalogs

As one of the first, and currently the world's largest, catalog of nanoparticles and nanotubes, expect to find essentially every nanoscale metal, alloy & compound that nature and current technology allows.

***American Elements Opens a World of Possibilities..... Now Invent!***

www.americanelements.com